TECHNICAL REPORTS SERIES NO. 468

Cyclotron Produced Radionuclides: Physical Characteristics and Production Methods

IAEA
International Atomic Energy Agency

CYCLOTRON PRODUCED RADIONUCLIDES: PHYSICAL CHARACTERISTICS AND PRODUCTION METHODS

The following States are Members of the International Atomic Energy Agency:

AFGHANISTAN
ALBANIA
ALGERIA
ANGOLA
ARGENTINA
ARMENIA
AUSTRALIA
AUSTRIA
AZERBAIJAN
BANGLADESH
BELARUS
BELGIUM
BELIZE
BENIN
BOLIVIA
BOSNIA AND HERZEGOVINA
BOTSWANA
BRAZIL
BULGARIA
BURKINA FASO
CAMEROON
CANADA
CENTRAL AFRICAN REPUBLIC
CHAD
CHILE
CHINA
COLOMBIA
COSTA RICA
CÔTE D'IVOIRE
CROATIA
CUBA
CYPRUS
CZECH REPUBLIC
DEMOCRATIC REPUBLIC OF THE CONGO
DENMARK
DOMINICAN REPUBLIC
ECUADOR
EGYPT
EL SALVADOR
ERITREA
ESTONIA
ETHIOPIA
FINLAND
FRANCE
GABON
GEORGIA
GERMANY
GHANA
GREECE
GUATEMALA
HAITI
HOLY SEE
HONDURAS
HUNGARY
ICELAND
INDIA
INDONESIA
IRAN, ISLAMIC REPUBLIC OF
IRAQ
IRELAND
ISRAEL
ITALY
JAMAICA
JAPAN
JORDAN
KAZAKHSTAN
KENYA
KOREA, REPUBLIC OF
KUWAIT
KYRGYZSTAN
LATVIA
LEBANON
LIBERIA
LIBYAN ARAB JAMAHIRIYA
LIECHTENSTEIN
LITHUANIA
LUXEMBOURG
MADAGASCAR
MALAWI
MALAYSIA
MALI
MALTA
MARSHALL ISLANDS
MAURITANIA
MAURITIUS
MEXICO
MONACO
MONGOLIA
MONTENEGRO
MOROCCO
MOZAMBIQUE
MYANMAR
NAMIBIA
NEPAL
NETHERLANDS
NEW ZEALAND
NICARAGUA
NIGER
NIGERIA
NORWAY
PAKISTAN
PALAU
PANAMA
PARAGUAY
PERU
PHILIPPINES
POLAND
PORTUGAL
QATAR
REPUBLIC OF MOLDOVA
ROMANIA
RUSSIAN FEDERATION
SAUDI ARABIA
SENEGAL
SERBIA
SEYCHELLES
SIERRA LEONE
SINGAPORE
SLOVAKIA
SLOVENIA
SOUTH AFRICA
SPAIN
SRI LANKA
SUDAN
SWEDEN
SWITZERLAND
SYRIAN ARAB REPUBLIC
TAJIKISTAN
THAILAND
THE FORMER YUGOSLAV REPUBLIC OF MACEDONIA
TUNISIA
TURKEY
UGANDA
UKRAINE
UNITED ARAB EMIRATES
UNITED KINGDOM OF GREAT BRITAIN AND NORTHERN IRELAND
UNITED REPUBLIC OF TANZANIA
UNITED STATES OF AMERICA
URUGUAY
UZBEKISTAN
VENEZUELA
VIETNAM
YEMEN
ZAMBIA
ZIMBABWE

The Agency's Statute was approved on 23 October 1956 by the Conference on the Statute of the IAEA held at United Nations Headquarters, New York; it entered into force on 29 July 1957. The Headquarters of the Agency are situated in Vienna. Its principal objective is "to accelerate and enlarge the contribution of atomic energy to peace, health and prosperity throughout the world".

TECHNICAL REPORTS SERIES No. 468

CYCLOTRON PRODUCED RADIONUCLIDES: PHYSICAL CHARACTERISTICS AND PRODUCTION METHODS

INTERNATIONAL ATOMIC ENERGY AGENCY
VIENNA, 2009

COPYRIGHT NOTICE

Sales and Promotion, Publishing Section
International Atomic Energy Agency
Wagramer Strasse 5
P.O. Box 100
1400 Vienna, Austria
fax: +43 1 2600 29302
tel.: +43 1 2600 22417
email: sales.publications@iaea.org
http://www.iaea.org/books

Printed by the IAEA in Austria
February 2009
STI/DOC/010/468

IAEA Library Cataloguing in Publication Data

Cyclotron produced radionuclides : physical characteristics and production methods. — Vienna : International Atomic Energy Agency, 2009.
p. ; 24 cm. — (Technical reports series, ISSN 0074–1914 ; no. 468)
STI/DOC/010/468
ISBN 978–92–0–106908–5
Includes bibliographical references.

1. Radioisotopes in medical diagnosis. — 2. Cyclotrons. I. International Atomic Energy Agency. II. Series: Technical reports series (International Atomic Energy Agency) ; 468.

IAEAL 08–00552

FOREWORD

Radioisotopes find applications in nearly all the countries of the world, contributing significantly to the improvement of health care and industrial output, as well as safety. Globally, the number of medical procedures involving the use of isotopes is constantly growing, and these procedures require an increasing number of different isotopes. In industry, isotope uses are very diverse, but their relative importance in the various sectors differs greatly. However, in general, isotopes are required where they are more efficient than the alternatives or have no substitute.

The IAEA has been helping Member States in the development of technologies for the production, radiochemical processing, safe transport and applications of radioisotopes. IAEA publications, such as Radioisotope Production and Quality Control, published in 1971, were the reference publications used by many developing Member States for establishing their radioisotope production programmes. A recent publication, Manual for Reactor Produced Isotopes, published in 2003, elaborated on the production and radiochemical processing of 48 important reactor produced radioisotopes.

The IAEA published a directory on cyclotrons used for isotope production in 1998, and revised versions were published in 2002 and 2006, which documented the cyclotrons available in Member States. The last 15 years have seen the installation of a large number of new cyclotrons for isotope production. Many of these are dedicated to the production of a single isotope or a small group of isotopes. However, the majority of them have spare capacity for the production of many other useful isotopes, and this capability needs to be explored. The IAEA has been extending support in various forms to Member States to acquire or enhance the technology they have for the production of isotopes using cyclotrons. The publication of reports covering different aspects of radioisotope production using cyclotrons has been one activity that has been identified which needs further input and support.

In 2004, a group of consultants identified the need for a publication similar to the Manual for Reactor Produced Isotopes covering those isotopes that are of both current and potential interest. Consequently, 49 isotopes were identified, and 20 of these were further grouped in terms of their higher utility. It was decided to produce a report covering all the relevant information needed for the production of the above isotopes; the level of information corresponds to the extent of each isotope's utility and the need for it. Consequently, this report covers data on nuclear decay characteristics such as half-life, mode of decay, energy and abundance, nuclear reactions and the excitation functions of the selected isotopes. The nuclear data given in this report are adapted from either the database of the IAEA and/or that of Brookhaven National

Laboratory. For the most commonly used isotopes, additional data on target preparation, radiochemical processing, recovery of enriched targets and radiochemical specifications are also provided.

The IAEA is grateful to the consultants who prepared this report and to the reviewers for their valuable contributions. One of the consultants, D.J. Schlyer (USA), edited the scientific content of this report. The IAEA officers responsible for this report were M.R.A. Pillai and M. Haji-Saeid of the Division of Physical and Chemical Sciences.

EDITORIAL NOTE

CONTENTS

Chapter 1

PRINCIPLES OF PRODUCTION OF RADIOISOTOPES USING CYCLOTRONS

1.1. INTRODUCTION

The development of nuclear technology was one of the most significant achievements of the twentieth century. The pioneering work of Marie and Pierre Curie in uncovering substances with previously unrecognized properties, for which they coined the term radioactive, opened up many new fields of opportunity. The Curies' discovery was the result of Marie Curie's belief that the ore pitchblende contained another, more active, substance than uranium. Within a few months of starting to analyse pitchblende in 1898, Marie Curie had isolated two previously unknown elements. She named the first polonium, after her native Poland; the second she called radium, in response to its intense radioactivity. Practical applications in scientific research for radioisotopes followed from these discoveries in the period from 1920 to the early 1930s. However, the few naturally occurring radioisotopes that were available severely limited the scope of what was possible. The full potential was not realized until radioisotopes could be produced artificially.

The first major advance occurred in 1934 with the invention of the cyclotron by Ernest Lawrence in Berkeley, California. With this machine being used to accelerate deuterons to very high speeds, it became possible to create the nuclear instability that we now know is a prerequisite for radioactivity. By directing a beam of fast moving deuterons at a carbon target, Lawrence induced a reaction that resulted in the formation of a radioisotope with a half-life of 10 min.

Particle accelerators and, in particular, cyclotrons, were very important in the preparation of radioisotopes during the years from 1935 to the end of World War II. After World War II, reactors were used to produce radioactive elements, and the use of accelerators for this purpose became less common. (For a discussion of reactor produced radioisotopes see the IAEA's Manual for Reactor Produced Radioisotopes [1.1].) As the techniques for using radiotracers became more sophisticated, it became clear that reactor produced radionuclides could not completely satisfy the growing demand and, therefore, accelerators were needed to produce new radioisotopes that could be used in new ways in both industry and medicine. Most of these applications use radionuclides at tracer concentrations to investigate some process or phenomenon.

In industry, these applications have taken the form of embedding the tracer into a system, or actually directly inducing radioactivity in the system by charged particle or neutron activation. The IAEA publication, Radiotracer Applications in Industry — A Guidebook, provides an overview of recent research on the use of radiotracers in a variety of applications [1.2].

The major uses of radionuclides are in applications to medicine or what has become known as nuclear medicine. Although nuclear medicine traces its clinical origins back to the 1930s, the invention of the gamma scintillation camera by American engineer Hal Anger in the 1950s brought major advances in nuclear medical imaging and rapidly increased the use of radioisotopes in medicine. The medical uses of radionuclides can be broken down into two general categories: imaging and radiotherapy. Imaging can be further divided into single photon emission computed tomography (SPECT) and positron emission tomography (PET).

The production of radionuclides for use in biomedical procedures, such as diagnostic imaging and/or therapeutic treatments, is achieved through nuclear reactions in reactors or from charged particle bombardment in accelerators. In accelerators, the typical charged particle reactions utilize protons, although deuterons and helium nuclei ($^{3}He^{2+}$ and alpha particles) play a role.

One clear advantage that accelerators possess is the fact that, in general, the target and product are different chemical elements. This makes it possible to:

(a) Find suitable chemical or physical means for separation;
(b) Obtain high specific activity (SA) preparations, owing to the target and product being different elements;
(c) Produce fewer radionuclidic impurities by selecting the target material, particle and energy window for irradiation.

1.2. CYCLOTRONS FOR RADIOISOTOPE PRODUCTION

The production of radionuclides with an accelerator requires that particle beams be delivered with two specific characteristics. The beams must have sufficient energy to bring about the required nuclear reactions, and sufficient beam current to give practical yields.

The first cyclotron dedicated to medical applications was installed at Washington University in St. Louis, in 1941, where radioactive isotopes of phosphorus, iron, arsenic and sulphur were produced. During World War II, a cyclotron in Boston also provided a steady supply of radionuclides for medical purposes. In the middle 1950s, a group at Hammersmith Hospital in London

put into operation a cyclotron wholly dedicated to radionuclide production. The major change occurred in the early and middle 1960s, when the work carried out on hot atom chemistry (e.g. the in situ chemistry of nucleogenic atoms occurring in a target being bombarded) laid the foundation for the synthesis of organic compounds labelled with positron emitters. A 1966 article by Ter-Pogossian and Wagner focused on the use of ^{11}C [1.3, 1.4]. As the field of nuclear medicine has progressed, the number of available types of particle accelerators with varying characteristics dedicated to radionuclide production for nuclear medicine has also expanded. The major classes of accelerators are the positive and negative ion cyclotrons. More recent innovations include superconducting magnet cyclotrons, small low energy linacs, tandem cascade accelerators and low energy linacs.

Cyclotrons come in many sizes depending on the function for which they are intended. Some examples are shown in Fig. 1.1. The cyclotron shown in Fig. 1.1(a) is a deuteron machine designed to produce only ^{15}O for PET studies. The machine shown in Fig. 1.1(b) is the 500 MeV cyclotron at TRIUMF in Vancouver, Canada, where a wide variety of radionuclides are produced and other experiments are carried out.

The basic characteristics of all cyclotrons are the same. There is an ion source to produce ions, an acceleration chamber to accelerate them and a magnet to contain the ions on a circular path. The construction of a typical modern cyclotron is shown in Fig. 1.2.

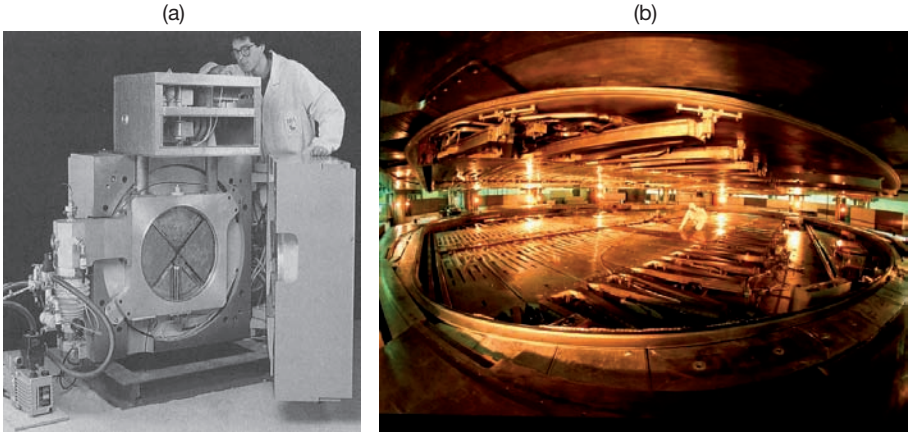

FIG. 1.1. Comparison of cyclotrons: (a) a small single isotope machine; (b) a large multi-purpose research machine.

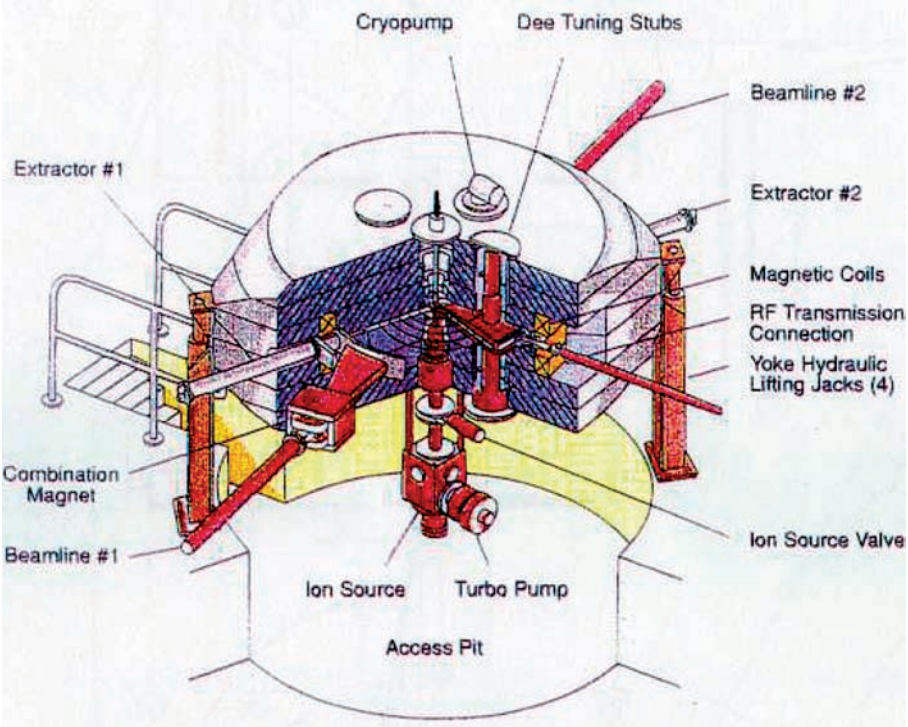

FIG. 1.2. Internal working parts of a modern cyclotron.

1.3. NUCLEAR REACTIONS

As an energetic charged particle passes through any material, there is some probability that it will interact with a nucleus along its path. The particle may be scattered off the nucleus or, if the energy is high enough when they collide, they may combine to form a compound nucleus that may decompose along one of several channels, leading to a new nucleus. The incoming particle must have sufficient energy to overcome two potential barriers. The first barrier is the electrostatic repulsion between the positively charged particles and the positively charged nucleus. This is referred to as the Coulomb barrier. The second depends on whether the reaction is exothermic or endothermic, and is referred to as the Q value. The Q value is the mass difference between the compound nucleus and the incoming particles. If a reaction occurs, the compound nucleus is usually highly excited because the absorbed particle brings along both a part of its kinetic energy and the mass difference energy.

1.3.1. Coulomb barrier

In the classic sense, a reaction between a charged particle and a nucleus cannot take place if the centre of mass energy of the two particles is less than the Coulomb barrier. In the case that applies to the production of radionuclides with a cyclotron, this implies that the charged particle must have an energy greater than the electrostatic repulsion, which is given [1.5] by the following equation:

$$B = Zze^2/R \tag{1.1}$$

where

B	is the barrier to the reaction;
Z and z	are the atomic numbers of the two species;
e	is the electric charge; and
R	is the separation of the two species (cm).

The values of the Coulomb barrier for the four major particles used in cyclotrons (p, d, ^{3}He, ^{4}He) are plotted in Fig. 1.3 as a function of the Z value of the material. These reactions take place at energies well below this barrier, due to the effects of quantum tunnelling.

1.3.2. *Q* value

In any nuclear reaction, the total energy must be conserved, which means that the total energy including the rest mass of the reactants must be equal to the total energy including the rest mass of the products. Any increase in kinetic energy must be accompanied by an equal decrease in the rest masses. The Q value of a nuclear reaction may be either positive or negative. If the rest masses of the reactants exceed the rest masses of the products, the Q value of the reaction is positive, with the decrease in rest mass being converted into a gain in kinetic energy. The energy equivalent of the mass deficit Q is given by:

$$Q\ (\text{MeV}) = 931.4\Delta M \tag{1.2}$$

where

$$\Delta M = (m_p + M_T) - (m_q - M_R)$$

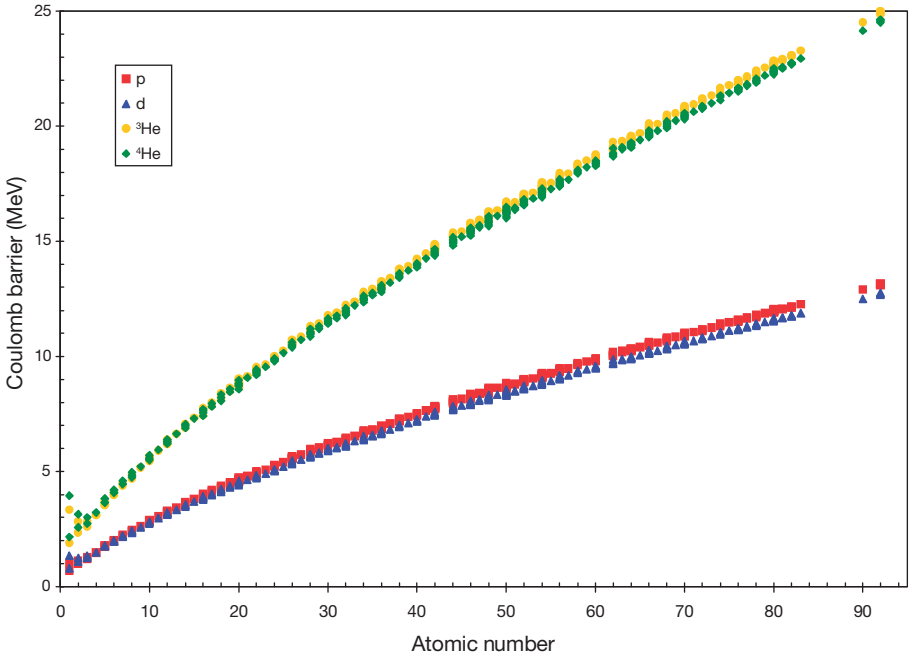

FIG. 1.3. Plot of the Coulomb barrier as a function of the atomic number of the nucleus for the four major particles used in cyclotrons.

in which

m_p is the particle mass;
M_T is the target mass;
M_R is the product mass; and
m_q is the emitted particle mass.

If $Q < 0$ the reaction is called endoergic, and if $Q > 0$ the reaction is said to be exoergic. If the reaction is endoergic, then an energy of an amount greater than this must be supplied in order for the reaction to proceed. The threshold will be the Coulomb barrier plus this difference. Owing to the conservation of momentum, only a fraction of the kinetic energy is available to compensate for the mass deficit. If the reaction is exoergic, the threshold energy will just be the Coulomb barrier. In reality, as a result of quantum mechanical tunnelling, nuclear reactions start to occur when the tails of the energy distributions overlap, and so they will occur at energies below the Coulomb barrier. An

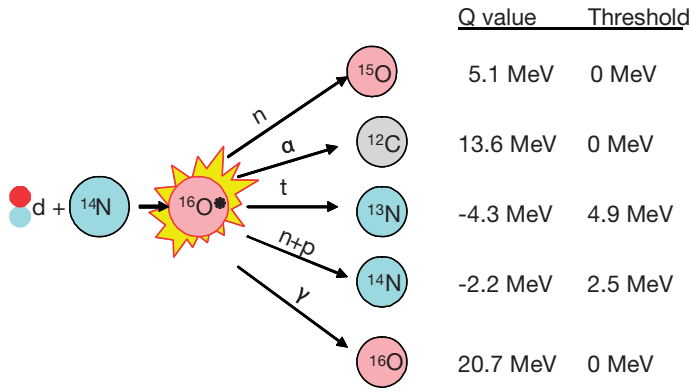

FIG. 1.4. Q values and thresholds of nuclear decomposition for the reaction of a deuteron with a ^{14}N nucleus after forming the compound nucleus ^{16}O.

example of the possible reaction pathways is shown in Fig. 1.4, along with their corresponding Q and threshold values. As opposed to chemical reactions, the energy changes in a nuclear reaction are large enough that changes in the mass of the reactants and products are observable.

The calculation of the Q and threshold values E_{THR} from the mass excess (Δ) data of all reaction partners in Fig. 1.4 is shown in Table 1.1. The numerical values of Δ were taken from the AME 2003 Atomic Mass Evaluation Tables [1.6].

TABLE 1.1. CALCULATION OF Q AND THRESHOLD VALUES FROM MASS EXCESS DATA

Reaction	$^{14}N(d, n)^{15}O$		$^{14}N(d, \alpha)^{12}C$		$^{14}N(d, t)^{13}N$		$^{14}N(d, np)^{14}N$		$^{14}N(d, \gamma)^{16}O$	
Δ_T	^{14}N	0.003074	^{14}N	0.003074	^{14}N	0.003074	^{14}N	0.003074	^{14}N	0.003074
Δ_p	d	0.014102	d	0.014102	d	0.014102	d	0.014102	d	0.014102
Δ_q	n	0.008665	^4He	0.002603	^3H	0.016029	n	0.008665	γ	0.000000
							p	0.007825		
Δ_R	^{15}O	0.003065	^{12}C	0.0	^{13}N	0.005739	^{14}N	0.003074	^{16}O	–0.005085
Q (u)	0.005446		0.014573		–0.004592		–0.002388		0.022261	
Q (MeV)	5.07		13.57		–4.28		–2.22		20.73	
E_{THR}	0.00		0.00		4.89		2.54		0.00	

1.3.3. Nuclear reaction cross-section

The nuclear reaction cross-section represents the total probability that a compound nucleus will be formed and then decomposes along a particular channel. This is often called the excitation function. This function determines the amount of a radionuclide that may be made on a given cyclotron, and the levels of contamination of other radioisotopes that can be present in the target material. In the 'touching spheres' model of nuclear reactions, we can visualize two spheres coming towards each other. If the spheres touch, then there will be a reaction, and if they do not touch, there will not be a reaction. In this visualization, the reaction probability is proportional to the cross-sectional area of the two spheres. The total reaction cross-section is given by the following equation:

$$\sigma_R = \pi r_0^2 (A_p^{1/3} + A_T^{1/3})^2 \tag{1.3}$$

where $r_0 \approx 1.6$ fm.

The unit of this measure is the barn, where 1 b = 1×10^{-24} cm^2. The expression 'barn' comes from the fact that the probability for a neutron to interact with a target is proportional to the area of the nucleus, which compared with the size of the neutron appears to be as large as a barn.

The nuclear reaction cross-section represents the total probability that a compound nucleus will be formed and that it will decompose through a particular channel. A nuclear reaction will not occur except by tunnelling effects if the minimum energy is below that needed to overcome the Coulomb barrier and a negative Q value of the reaction. Particles with energies below this barrier have a very low probability of reacting. The energy required to induce a nuclear reaction increases as the Z value of the target material increases. For many low Z materials, it is possible to use a low energy accelerator, but for high Z materials, it is necessary to increase the particle energy [1.7]. An example of the cross-section for the ^{14}N(d, n)^{15}O reaction is shown in Fig. 1.5. Note that the Q value for this reaction is positive and the threshold is zero, but that the cross-section is very small below about 1 MeV.

1.4. CALCULATION OF RADIOISOTOPE YIELD

The rate of radionuclide production is dependent on a number of factors, including the magnitude of the reaction cross-section as a function of energy, the incident particle energy, the thickness of the target in nuclei per cm^2, which will determine the exit particle energy, and the flux (related to beam current) of

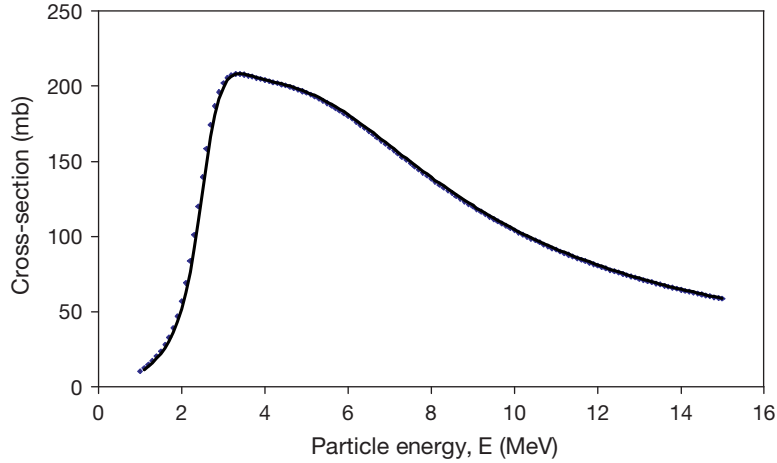

FIG. 1.5. Excitation function for the $^{14}N(d, n)^{15}O$ reaction.

incoming particles. In the simplest case, where the cross-section is assumed to be constant, the rate of production is given by:

$$R = n_T I\sigma \tag{1.4}$$

The cross-section is always a function of energy, as has been shown in the previous section. If we use this more exact expression, then the equation becomes:

$$R = n_T I \int_{E_s}^{E_0} \frac{\sigma(E)}{\mathrm{d}E/\mathrm{d}x}\,\mathrm{d}E \tag{1.5}$$

where

R is the number of nuclei formed per second;
n_T is the target thickness in nuclei/cm^2;
I is the incident particle flux per second and is related to the beam current;
σ is the reaction cross-section, or probability of interaction, expressed in cm^2 and is a function of energy;
E is the energy of the incident particles;

x is the distance travelled by the particle; and

$\int_{E_s}^{E_0}$ is the integral from the initial energy to the final energy of the incident particle along its path.

As the particle passes through the target material, it loses energy due to the interactions of the particle with the electrons of the target. This is represented in the above equation by the term dE/dx (also called the stopping power).

Returning to the expression for the cross-section, it can be seen that n_T is given by the following expression:

$$n_T = \frac{\rho x}{A_T}\zeta \tag{1.6}$$

where

n_T is the target thickness in nuclei/cm^2;
A_T is the atomic weight of the target material in grams;
ρ is the density in g/cm^3;
ζ is Avogadro's number; and
x is the distance the particle travels through the material.

If the target material is a compound rather than a pure element, then the number of nuclei per unit area is given by the following expression:

$$N_G = \frac{F_A C \zeta}{A_A} \tag{1.7}$$

where

N_G is the number of target nuclei per gram;
F_A is the fractional isotopic abundance;
C is the concentration by weight;
ζ is Avogadro's number; and
A_A is the atomic mass number of nucleus A.

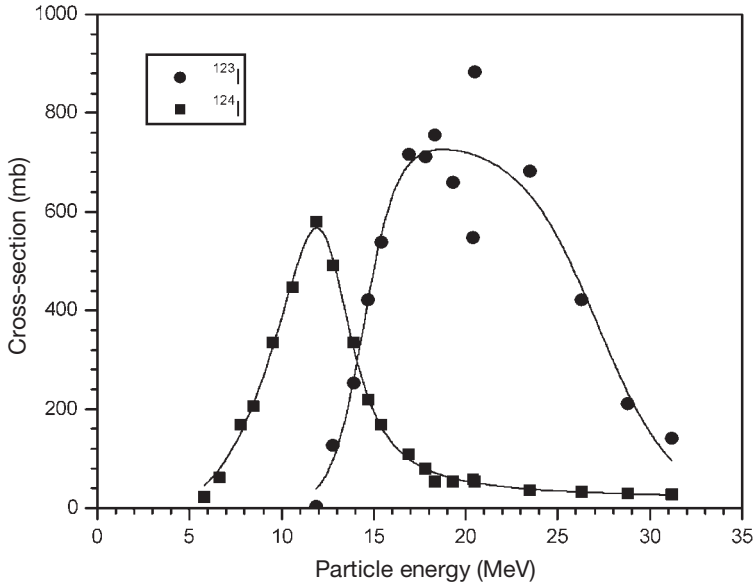

FIG. 1.6. Nuclear reaction cross-sections for production of ^{123}I and ^{124}I from ^{124}Te.

The above equations lead to one of the basic facts of radioisotope production. It is not always possible to eliminate the radionuclidic impurities even with the highest isotopic enrichment and the most precise energy selection. An example of this is given in Fig. 1.6 for the production of ^{123}I with a minimum of ^{124}I impurity [1.8–1.11].

As can be seen from Fig. 1.6, it is not possible to eliminate the ^{124}I impurity from the ^{123}I because the ^{124}I is being made at the same energy. All that can be done is to minimize the ^{124}I impurity by choosing an energy where the production of ^{124}I is near a minimum. In this case, proton energies higher than about 20 MeV will give a minimum of ^{124}I impurity.

1.4.1. Saturation factor

As soon as radioisotopes have been produced, they start to decay. This leads to the following expression, where the overall rate of production is then:

$$-\frac{\mathrm{d}n}{\mathrm{d}t} = n_{\mathrm{T}} I \int_{E_I}^{E_0} \frac{\sigma(E)}{\mathrm{d}E/\mathrm{d}x}\mathrm{d}E - \lambda N \tag{1.8}$$

where

λ is the decay constant and is equal to $\ln 2/t_{1/2}$;
t is the irradiation time in seconds; and
N is the number of radioactive nuclei in the target.

The term $\mathrm{d}E/\mathrm{d}x$ in the above expression is often referred to as the total stopping power. At a particular energy E, it can be represented as $S_T(E)$ in units of $\mathrm{MeV \cdot cm^2 \cdot g^{-1}}$ and is given by the following expression:

$$S_T(E) = \frac{\mathrm{d}E}{\mathrm{d}x} \tag{1.9}$$

where

$\mathrm{d}E$ is the differential loss in energy; and
$\mathrm{d}x$ is the differential distance travelled by the particle.

The loss of energy, $\mathrm{d}E$, in MeV of the particle crossing the slab, is then given by:

$$\mathrm{d}E = S_T(E)\rho\mathrm{d}x \tag{1.10}$$

where ρ is the density of the material in units of $\mathrm{g/cm^3}$, and the thickness of the slab $\rho\mathrm{d}x$ (in $\mathrm{g/cm^2}$) can be expressed as a function of $\mathrm{d}E$:

$$\rho\mathrm{d}x = \frac{\mathrm{d}E}{S_T(E)} \tag{1.11}$$

If this equation is integrated, including the stopping power to account for energy loss during the transit of the particle through the target material and assuming that the beam current is the same as the particle flux (which is true only for particles with a charge of +1), then the yield of a nuclear reaction is given by:

$$Y_{EOB} = \frac{N_A I}{A_T}(1 - \mathrm{e}^{-\lambda t})\int_{E_E}^{E_I} \sigma_T(E)\frac{\mathrm{d}E}{S_T(E)} \tag{1.12}$$

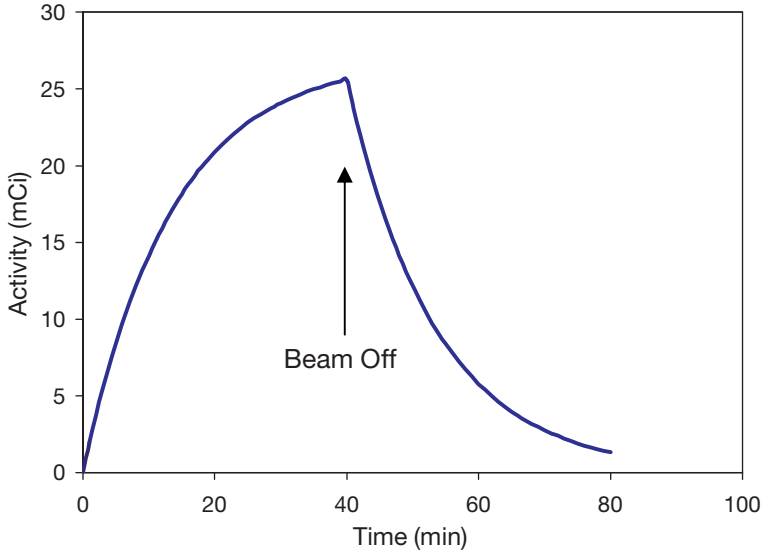

FIG. 1.7. Saturation factor of the irradiation of ^{13}C to produce ^{13}N, showing the production of the radionuclide and its decay after the beam has been turned off.

The term $1 - e^{-\lambda t}$ is often referred to as the saturation factor, and accounts for the competition of the production of nuclei due to the particle reaction and the radioactive decay of the nuclei that have been produced. An example using ^{13}N is shown in Fig. 1.7. The beam is turned on at time zero and turned off 40 min after the start of bombardment.

If an infinitely long irradiation that makes the saturation factor tend to the value 1 is assumed, then we have what is referred to as the saturation yield. This quantity is shown as a function of energy in Fig. 1.8 for the $^{14}N(d, n)^{15}O$ reaction.

1.4.2. Nomenclature

The nomenclature for nuclear reactions as it is usually used throughout this report needs to be defined. If a ^{13}C nucleus is irradiated with a proton beam to produce a nucleus of ^{13}N with a neutron emitted from the compound nucleus, this reaction will be written as $^{13}C(p, n)^{13}N$. In a similar manner, if a ^{20}Ne nucleus is bombarded with a deuteron beam to produce a nucleus of ^{18}F with the concomitant emission of an alpha particle, this reaction sequence will be abbreviated as $^{20}Ne(d, \alpha)^{18}F$.

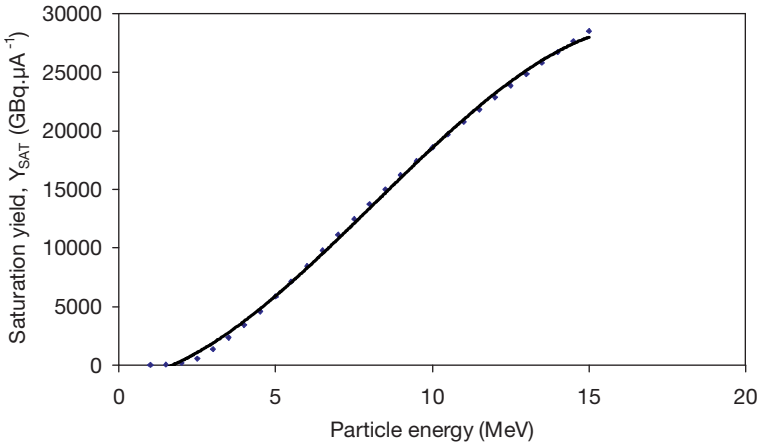

FIG. 1.8. Saturation yield for the $^{14}N(d, n)^{15}O$ reaction.

1.5. CYCLOTRON TARGETRY

There are literally several hundreds of radioisotopes that can be produced with charged particle accelerators. The cyclotron is the most frequent choice, but the linac and other accelerators may become more common with the development of smaller, more reliable, machines. The goal of cyclotron targetry is to introduce the target material into the beam, keep it there during the irradiation and remove the product radionuclide from the target material quickly and efficiently. The specific design of the target is what allows this goal to be achieved. The efficiency of radionuclide production will depend to a great extent on having a good design for the cyclotron target. For production of radionuclides, the target material may be either a gas, liquid or solid. Targets are, consequently, designed to accommodate the material being irradiated. The design of the target will also depend on whether the target is placed inside (internal) or outside (external) the cyclotron.

Figure 1.9 shows an example of a gas target used for producing radionuclides. One can see the area for containment of the gas in the beam, a water cooling jacket, helium cooling flow in the front foil and a vacuum isolation foil leading to the cyclotron vacuum chamber or beam line.

These general features are evident on most cyclotron targets, although the form will be different, depending on the chemical and physical characteristics of the target material.

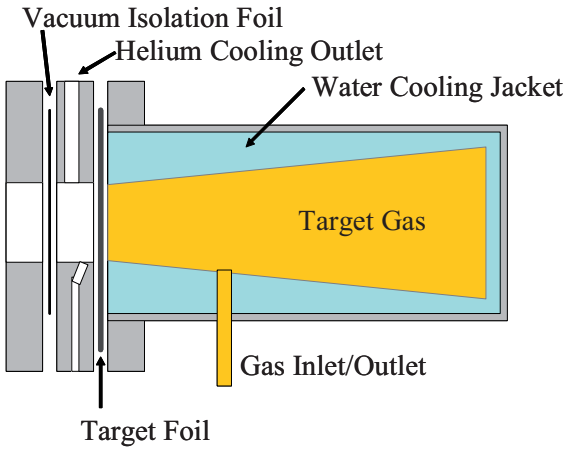

FIG. 1.9. Schematic diagram of a typical cyclotron target used with gases.

1.6. LABORATORY FACILITIES FOR RADIOISOTOPE PRODUCTION

1.6.1. Laboratory design

The design of a good radiochemistry laboratory takes into account the flow of work as the radionuclides are prepared, irradiated, recovered, purified, quality checked and packaged for transport [1.12, 1.13]. As a result of these activities, the laboratory facility should contain areas for each. There should be a target preparation area where solid targets are prepared. There will be a cyclotron vault for irradiation of samples. The cyclotron may have several target stations where different types of target may be irradiated. There will be a target processing area, which is usually contained in a shielded enclosure known as a 'hot cell'. These hot cells shield the operator from the high levels of radioactivity present. The purification of the radionuclide or the conversion of a radionuclide into a radiopharmaceutical is usually carried out in these hot cells. There will be a quality control (QC) area, where the purity of the radionuclides or radiopharmaceuticals is checked.

A typical radiochemistry laboratory designed for the preparation of PET radiotracers is shown in Fig. 1.10.

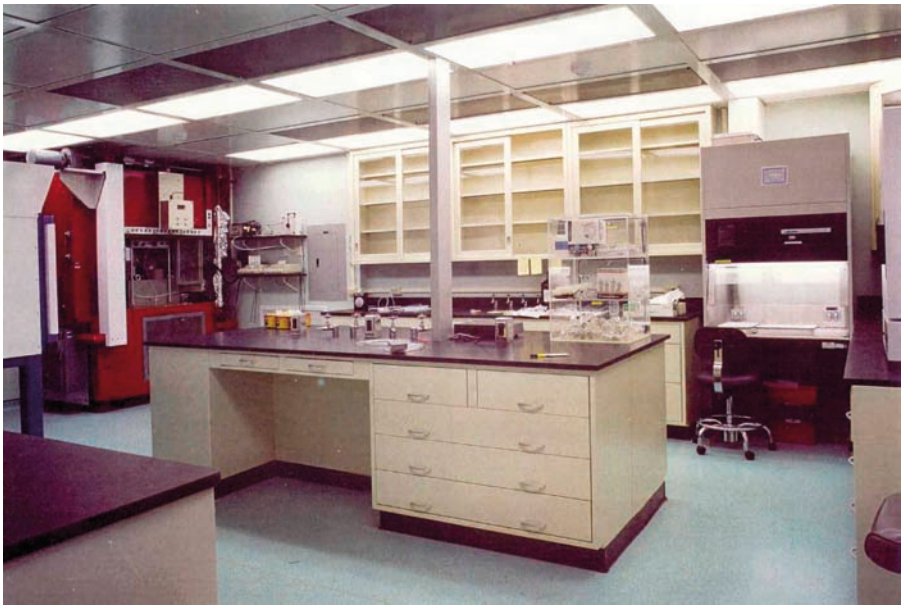

FIG. 1.10. A typical radiochemistry laboratory just after completion. (Note that the laminar flow hood on the right for the preparation of sterile vials and the red hot cell on the left where the syntheses are carried out.)

The hot cell is the central feature of any laboratory dealing with high levels of radioactivity. It is usually built with thick lead or steel walls that shield the operator from the radioactivity. A typical hot cell is shown in Fig. 1.11.

1.6.2. Airflow

Airflow in the facility is a critical parameter. It is essential that radioactive material (dust, airborne radioactivity, etc.) is not drawn from the areas with high levels of contamination to the areas of low contamination. The air in the cyclotron vault can contain some radioactive dust or small particles. If the air pressure gradient is in the direction of the hot lab, then some of this material may be drawn into the lab and may contaminate the samples being produced. In the case of PET radiotracers, the contamination could well be long lived material.

1.6.3. Radiation level gradient

In a similar fashion to the pressure gradient, there should also be a radiation field gradient. With the cyclotron turned off, the highest level of

FIG. 1.11. Hot cell with leaded glass window that can be lowered for working inside when radioactivity is not present.

radiation will be around the targets. The radioactivity from the targets will be transferred into the hot cells, processed and then transferred to the dispensing and QC units. At each step along this path, the amount of radioactivity being handled is less. The ideal situation is when the facility is set up in such a way that the staff and materials follow this gradient and do not have to pass through a low radiation area on their way from one high radiation area to another. The ideal situation is illustrated in Fig. 1.12.

1.6.4. Workflow

A great deal of consideration should be given to the workflow within the facility. It is important to minimize radiation exposure and to increase efficiency by providing a smooth flow to the processing unit. This can be done by ensuring that the area for each step in the processing is in close proximity to that for the step before. Another approach is to use a shielded transport system for moving the dose along without human contact. A passage in a wall can be an effective means of moving material from one area to another, while minimizing the chance for spread of contamination.

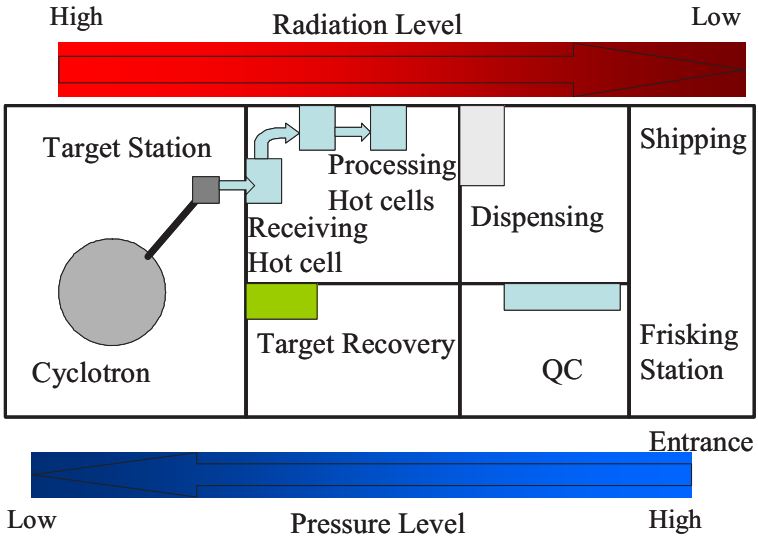

FIG. 1.12. Ideal pressure and radiation gradients in a cyclotron facility.

1.7. PACKAGES AND TRANSPORTATION OF RADIOISOTOPES

Radioactive material is packaged to ensure that radiation levels at the package surface do not exceed the levels set by national or international regulations. This ensures that carriers, the public and the environment are not exposed to radiation levels that exceed recognized safe limits.

Different packages for use in shipping are required for various types, forms, quantities and levels of radioactivity. There are four basic package types. These are:

(1) Excepted packages;
(2) Industrial packages;
(3) Type A packages;
(4) Type B packages.

Most radionuclides for nuclear medicine are shipped in type A packages. They are typically constructed of steel, wood or fibreboard, and have an inner containment vessel made of glass, plastic or metal surrounded with packing material made of polyethylene, rubber or vermiculite. Type A packages and their radioactive contents must meet standard testing requirements designed to ensure that the package retains its containment integrity and shielding under

FIG. 1.13. A typical container for transport of low level radioactive materials such as medical radionuclides.

normal transport conditions. Type A packages must withstand moderate degrees of heat, cold, reduced air pressure, vibration, impact, water sprays, being dropped, penetration and stacking. Type A packages are not, however, designed to withstand the forces of an accident. The consequences of a release of the material from one of these packages would not be significant, since the quantity of material in these packages is so limited. A typical container with the appropriate markings is shown in Fig. 1.13.

Although the package required for transporting radioactive material is based on the activity 'inside' the package, the label required on the package is based on the radiation hazard 'outside' the package. Radioactive material is the only hazardous material that has three possible labels, depending on the relative radiation levels external to the package. In addition, the labels for radioactive material are the only ones that require the carrier to write some information on the label. The information is a number called the transport index (TI), which, in reality, is the highest radiation level at 1 m from the surface of the package. The three labels are commonly called White I, Yellow II and Yellow III, referring to the colour of the label and the Roman numeral prominently displayed. A specific label is required if the surface radiation limit and the limit at 1 m distance satisfy the requirements given in Table 1.2.

TABLE 1.2. DIFFERENT TYPES OF LABEL USED FOR RADIOACTIVE PACKAGES

Label	Surface radiation level		Radiation level at 1 m
White I	Does not exceed 5 μSv/h		Not applicable
Yellow II	Does not exceed 500 μSv/h	and	Does not exceed 10 μSv/h
Yellow III	Exceeds 500 μSv/h	or	Exceeds 10 μSv/h

Since the TI is the radiation level at 1 m, it is clear that a White I label has no TI. A Yellow II label must have a TI no greater than 1, while a Yellow III label may have a TI greater than 1.

1.8. CONCLUSION

The expansion in the number of cyclotrons during the last ten years has been driven by: the advent of advances in medical imaging instrumentation (PET, SPECT and more recently PET/CT); the introduction of user friendly compact medical cyclotrons from several companies that manufacture cyclotrons; and recent decisions in the developed world that some PET radiopharmaceuticals are eligible for reimbursement by government or insurance companies. It is expected that this rapid growth will continue and that the demand for new radionuclides that can be applied in industry, as well as medicine, will continue to expand. With this expansion, there will be a greater need for cyclotrons and the radionuclides they can produce.

REFERENCES TO CHAPTER 1

[1.1] INTERNATIONAL ATOMIC ENERGY AGENCY, Manual for Reactor Produced Radioisotopes, IAEA-TECDOC-1340, IAEA, Vienna (2003).

[1.2] INTERNATIONAL ATOMIC ENERGY AGENCY, Radiotracer Applications in Industry — A Guidebook, Technical Reports Series No. 423, IAEA, Vienna (2004).

[1.3] TER-PERGOSSIAN, M.M., Cyclotron produced short-lived radioactive isotopes, Am. J. Roentgenol. Radium Ther. Nucl. Med. **96** (1966) 737–743.

[1.4] TER-PERGOSSIAN, M.M., WAGNER H.N., Jr., A new look at the cyclotron for making short-lived isotopes, Semin. Nucl. Med. **28** (1998) 202–212 (reprint of a classic 1966 article in Nucleonics).

[1.5] EVANS, R.D., The Atomic Nucleus, McGraw-Hill, New York (1955).
[1.6] UNITED STATES NATIONAL NUCLEAR DATA CENTER, 2003 Atomic Mass Evaluation (2003), http://www.nndc.bnl.gov/masses/
[1.7] DECONNINCK, G., "Introduction to radioanalytical physics", Nuclear Methods Monographs No. 1, Elsevier Scientific Publishing, Amsterdam (1978).
[1.8] GUILLAUME, M., LAMBRECHT, R.M., WOLF, A.P., Cyclotron production of ^{123}Xe and high purity ^{123}I: A comparison of tellurium targets, Int. J. Appl. Radiat. Isot. **26** (1975) 703–707.
[1.9] LAMBRECHT, R.M., WOLF, A.P., "Cyclotron and short-lived halogen isotopes for radiopharmaceutical applications", Radiopharmaceuticals and Labelled Compounds (Proc. Int. Conf. Copenhagen, 1973), Vol. 1, IAEA, Vienna (1973) 275–290.
[1.10] CLEM, R.G., LAMBRECHT, R.M., Enriched ^{124}Te targets for production of ^{123}I and ^{124}I, Nucl. Instrum. Methods Phys. Res. A **303** (1991) 115–118.
[1.11] QAIM, S.M., Target development for medical radioisotope production at a cyclotron, Nucl. Instrum. Methods Phys. Res. A **282** (1989) 289–295.
[1.12] JACOBSON, M.S., HUNG, J.C., MAYS, T.L., MULLAN, B.P., The planning and design of a new PET radiochemistry facility, Mol. Imag. Biol. **4** (2002) 119–127.
[1.13] SCHYLER, D.J., "Laboratory and cyclotron requirements for PET research", Chemists' Views of Imaging Centers (EMRAN, A.N., Ed.), Plenum Press, New York and London (1995) 123–131.

Chapter 2

PHYSICAL CHARACTERISTICS AND PRODUCTION DETAILS OF ISOTOPES

Table 2.1 lists the radioisotopes that have been used as tracers in the physical and biological sciences. While the list is not exhaustive, it does contain a wide variety. The list is provided alphabetically. However, there is a subset (in bold) of radioisotopes for which more detailed information is provided. This subset represents those radioisotopes that are more widely used.

TABLE 2.1. THE RADIOISOTOPES THAT HAVE BEEN USED AS TRACERS IN THE PHYSICAL AND BIOLOGICAL SCIENCES

Isotope	Isotope	Isotope
Actinium-225	**Fluorine-18**	**Oxygen-15**
Arsenic-73	**Gallium-67**	**Palladium-103**
Arsenic-74	**Germanium-68**	**Sodium-22**
Astatine-211	Indium-110	**Strontium-82**
Beryllium-7	**Indium-111**	Technetium-94m
Bismuth-213	Indium-114m	**Thallium-201**
Bromine-75	Iodine-120g	Tungsten-178
Bromine-76	Iodine-121	Vanadium-48
Bromine-77	**Iodine-123**	Xenon-122
Cadmium-109	**Iodine-124**	Xenon-127
Carbon-11	Iron-52	**Yttrium-86**
Chlorine-34m	Iron-55	Yttrium-88
Cobalt-55	**Krypton-81m**	Zinc-62
Cobalt-57	Lead-201	Zinc-63
Copper-61	Lead-203	Zirconium-89
Copper-64	Mercury-195m	
Copper-67	**Nitrogen-13**	

The information provided for all radioisotopes includes:

— Isotope;
— Half-life;
— Nuclear reactions;
— Excitation function;
— Bibliography.

In addition to the above, the more detailed information for the isotopes shown in bold in Table 2.1 includes:

— Uses;
— Decay mode;
— Thick target (TT) yield;
— Target materials;
— Target preparation;
— Target processing;
— Enriched materials recovery;
— Specifications.

The cross-sections have been taken from IAEA-TECDOC-1211, Charged Particle Cross-section Database for Medical Radioisotope Production: Diagnostic Radioisotopes and Monitor Reactions, and from the IAEA or from US National Nuclear Data Center (NNDC) databases.

2.1. ACTINIUM-225

Half-life: 10.0 d.

Alpha emission products of ^{225}Ac

This table is also continued on the next page.

Fraction	Energy (MeV)	Fraction	Energy (MeV)
0.001000	5.553000	0.029000	5.722600
0.001300	5.444000	0.044000	5.636200
0.002300	5.286000	0.086000	5.791000
0.003780	5.450400	0.100000	5.731000

Fraction	Energy (MeV)	Fraction	Energy (MeV)
0.011000	5.608000	0.181000	5.792000
0.012000	5.579000	0.516000	5.829000
0.014000	5.681000		

Electron emission products of ^{225}Ac

Fraction	Energy (MeV)	Fraction	Energy (MeV)
0.009672	0.056113	0.023100	0.021348
0.011440	0.058248	0.046410	0.031948
0.012800	0.055761	0.048015	0.044261
0.015000	0.064261	0.064380	0.019861
0.015795	0.080911	0.067200	0.007361
0.021532	0.007263	0.130900	0.017961
0.022866	0.033848	0.221640	0.008900

Photon emission products of ^{225}Ac

Fraction	Energy (MeV)	Fraction	Energy (MeV)
0.001000	0.253500	0.003200	0.073830
0.001100	0.452400	0.003200	0.111500
0.001300	0.145000	0.004600	0.188000
0.001400	0.195690	0.005500	0.062900
0.001500	0.082900	0.006500	0.099550
0.001600	0.094900	0.007100	0.150090
0.001900	0.123800	0.007660	0.097500
0.001900	0.154000	0.009257	0.165160
0.002000	0.138200	0.010156	0.083230
0.002800	0.108400	0.016815	0.086100
0.002900	0.087380	0.017000	0.099800
0.003100	0.157250	0.212950	0.012000

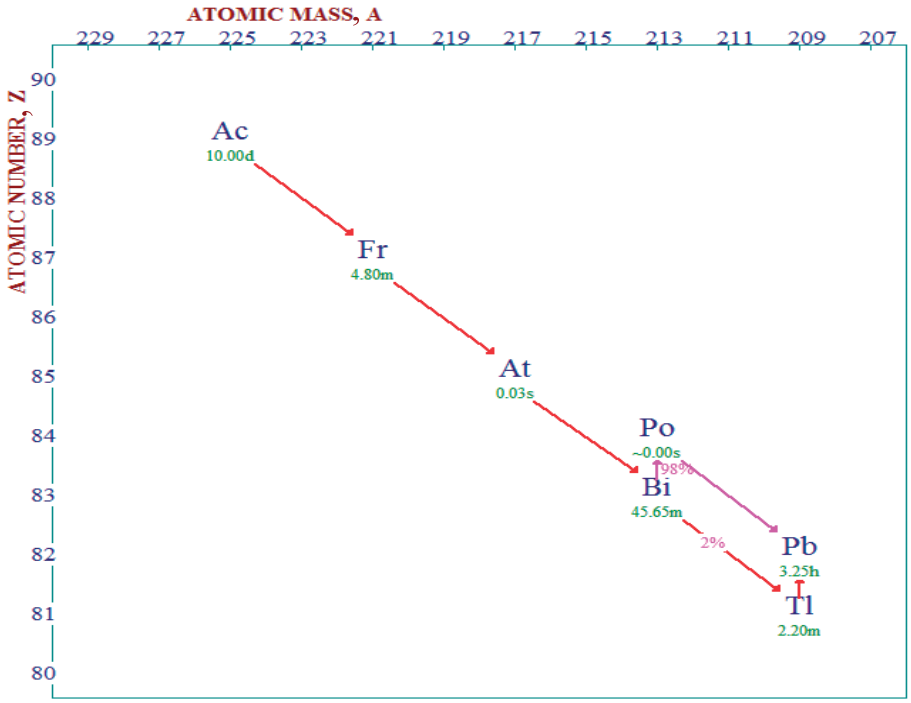

FIG. 2.1.1. Decay scheme of ^{225}Ac.

Decay scheme

The decay scheme of ^{225}Ac is shown in Fig. 2.1.1.

Nuclear reactions

There is only one favourable reaction for the production of ^{225}Ac on an accelerator: ^{226}Ra(p, 2n)^{225}Ac.

Excitation function

The excitation function for the ^{226}Ra(p, 2n)^{225}Ac reaction is shown in Fig. 2.1.2.

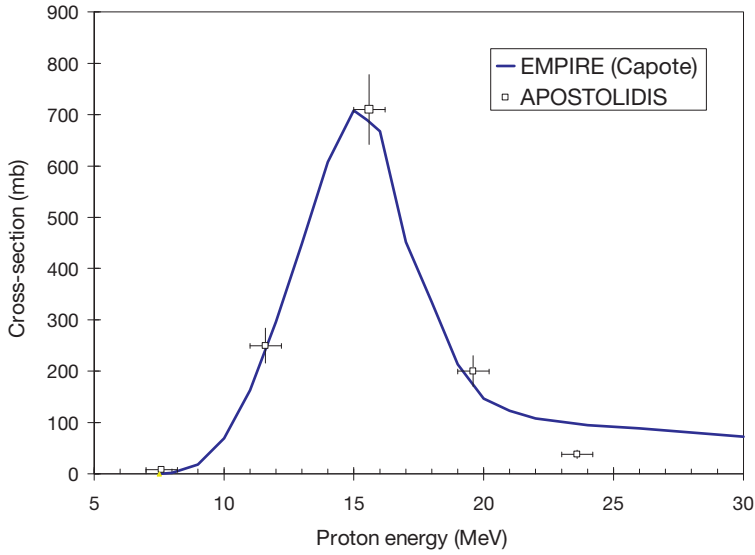

FIG. 2.1.2. Excitation function for the $^{226}Ra(p, 2n)^{225}Ac$ reaction.

BIBLIOGRAPHY TO SECTION 2.1

APOSTOLIDIS, A.C., et al., Cyclotron production of Ac-225 for targeted alpha therapy, Appl. Radiat. Isot. **62** (2005) 383–387.

INTERNATIONAL ATOMIC ENERGY AGENCY, Nuclear Data for the Production of Therapeutic Radionuclides,
http://www-nds.iaea.org/radionuclides/index.html

KENNEL, S.J., MIRZADEH, S., Vascular targeted radioimmunotherapy with ^{213}Bi — An α-particle emitter, Nucl. Med. Biol. **25** (1998) 241–246.

McDEVITT, M.R., FINN, R.D., SGOUROS, G., MA, D., SCHEINBERG, D.A., An $^{225}Ac/^{213}Bi$ generator system for therapeutic clinical applications: Construction and operation, Appl. Radiat. Isot. **50** (1999) 895–904.

MIRZADEH, S., Generator-produced alpha-emitters, Appl. Radiat. Isot. **49** (1998) 345–349.

2.2. ARSENIC-73

Half-life: 80.3 d.

Electron emission products of ^{73}As

Fraction	Energy (MeV)	Fraction	Energy (MeV)
0.029500	0.013263	0.603000	0.011849
0.036100	0.053257	0.751000	0.042334
0.089300	0.013083	0.875890	0.008560
0.109000	0.052023	3.196900	0.001190
0.278000	0.002160		

Photon emission products of ^{73}As

Fraction	Energy (MeV)	Fraction	Energy (MeV)
0.000888	0.013263	0.132560	0.011000
0.019297	0.001190	0.303290	0.009855
0.103000	0.053437	0.592370	0.009886

Nuclear reactions

There are two reactions for the production of ^{73}As, the first using protons and the second using alpha particles.

These tables are also continued on the next page.

^{nat}Ge(p, x)^{73}As	
Energy (MeV)	TT yield (μCi/μA·h)
7	1
10.9	3.2
14	9
17.5	24.4

^{nat}Ge(α, x)^{73}As	
Energy (MeV)	TT yield (μCi/μA·h)
10.8	0.8
24.2	1.8
32.6	4.5
39.8	6.6

$^{nat}Ge(p, x)^{73}As$	
Energy (MeV)	TT yield (μCi/μA·h)
21.1	45.4
22.2	54.6

$^{nat}Ge(\alpha, x)^{73}As$	
Energy (MeV)	TT yield (μCi/μA·h)
44	9.0

Note: 1 Ci = 37 GBq.

Excitation functions

The excitation functions for $^{nat}Ge(p, x)^{73}As$ and $^{76}Se(p, \alpha)^{73}As$ are shown in Figs 2.2.1 and 2.2.2, respectively.

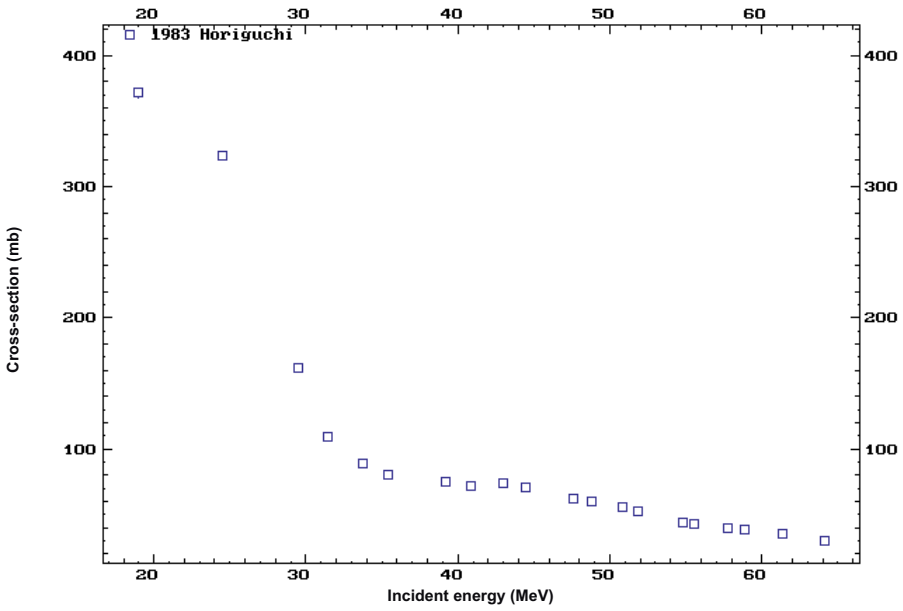

FIG. 2.2.1. Excitation function for the $^{nat}Ge(p, x)^{73}As$ reaction.

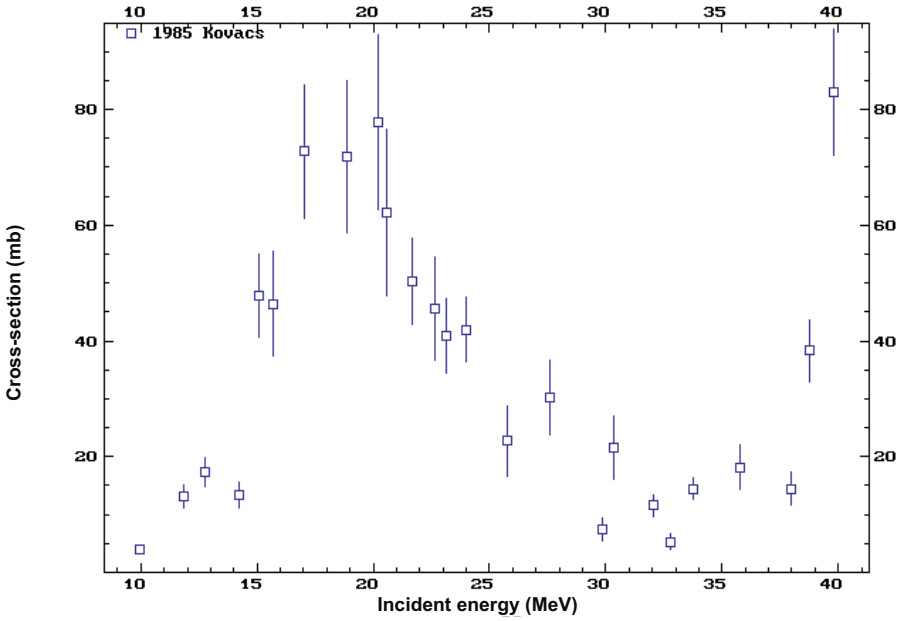

FIG. 2.2.2. Excitation function for the $^{76}Se(p, \alpha)^{73}As$ reaction.

BIBLIOGRAPHY TO CHAPTER 2.2

BASILE, D., et al., Excitation functions and production of arsenic radioisotopes for environmental toxicology and biomedical purposes, Int. J. Appl. Radiat. Isot. **32** (1981) 403–410.

DMITRIEV, P.P., MOLIN, G.A., The yields of As-73 and As-74 in nuclear reactions with protons, deuterons and alpha particles, Sov. At. Energy (Engl. Transl.) **41** (1976) 657–661.

HORIGUCHI, T., KUMAHORA, H., INOUE, H., YOSHIZAWA, Y., Excitation function of Ge(p, xnyp) reactions and production of ^{68}Ge, Int. J. Appl. Radiat. Isot. **34** (1983) 1531–1535.

KOVÁCS, Z., BLESSING, G., QAIM, S.M., STÖCKLIN, G., Production of ^{75}Br via the ^{76}Se(p, 2n)^{75}Br reaction at a compact cyclotron, Int. J. Appl. Radiat. Isot. **36** (1985) 635–642.

2.3. ARSENIC-74

Half-life: 17.8 d.

Beta emission products of ^{74}As

Fraction	Maximum energy (MeV)	Average energy (MeV)
0.000250	0.084200	0.022100
0.155000	0.718320	0.242900
0.188000	1.353100	0.530900

Positron emission products of ^{74}As

Fraction	Maximum energy (MeV)	Average energy (MeV)
0.000165	0.336100	0.147600
0.030000	1.540400	0.701100
0.266000	0.944520	0.408000

Electron emission products of ^{74}As

Fraction	Energy (MeV)	Fraction	Energy (MeV)
0.146410	0.008560	0.434280	0.001190

Photon emission products of ^{74}As

Fraction	Energy (MeV)	Fraction	Energy (MeV)
0.000921	1.194100	0.050698	0.009855
0.002621	0.001190	0.099020	0.009886
0.002873	1.204300	0.154350	0.634780
0.005506	0.608400	0.592330	0.511000
0.022158	0.011000	0.598530	0.595880

Nuclear reactions

The production reactions for ^{74}As are:

(a) ^{74}Ge(d, 2n)^{74}As;
(b) ^{74}Ge(p, n)^{74}As;
(c) ^{nat}Ga(α, x)^{74}As.

Excitation function

The excitation function for the ^{nat}Ge(p, x)^{74}As reaction is shown in Fig. 2.3.1.

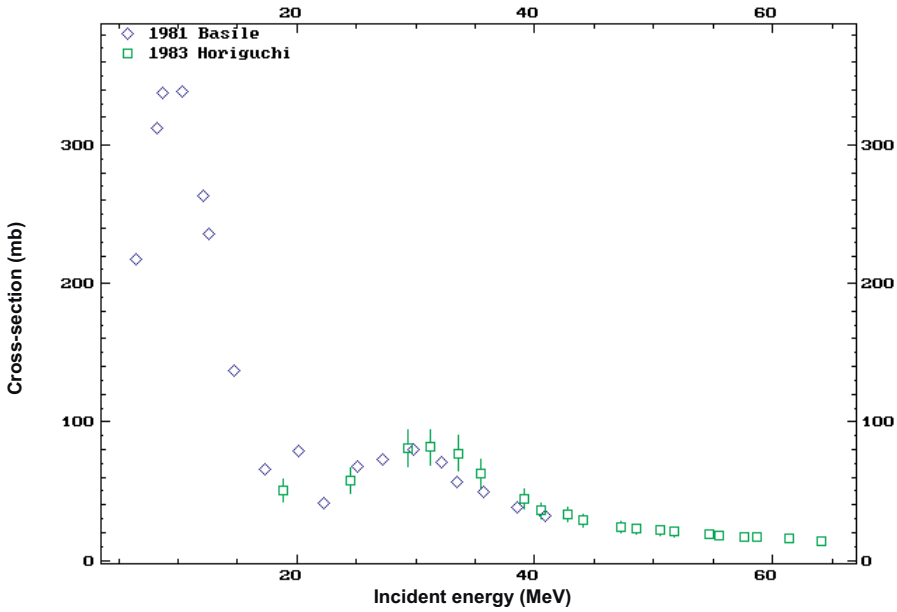

FIG. 2.3.1. Excitation function for the ^{nat}Ge(p, x)^{74}As reaction.

BIBLIOGRAPHY TO SECTION 2.3

BASILE, D., et al., Excitation functions and production of arsenic radioisotopes for environmental toxicology and biomedical purposes, Int. J. Appl. Radiat. Isot. **32** (1981) 403–410.

DMITRIEV, P.P., MOLIN, G.A., The yields of As-73 and As-74 in nuclear reactions with protons, deuterons and alpha particles, Sov. At. Energy (Engl. Transl.) **41** (1976) 657–661.

HORIGUCHI, T., KUMAHORA, H., INOUE, H., YOSHIZAWA, Y., Excitation function of Ge(p, xnyp) reactions and production of ^{68}Ge, Int. J. Appl. Radiat. Isot. **34** (1983) 1531–1535.

LEVKOVSKIJ, V.N., in Activation Cross Sections for the Nuclides of Medium Mass Region (A = 40–100) with Medium Energy (E = 10–50 MeV) Protons and Alpha Particles: Experiment and Systematics, Inter-Vesi, Moscow (1991).

2.4. ASTATINE-211

Half-life: 7.2 h.

Uses

Because of the high linear energy transfer (LET) associated with alpha particles, alpha emitters have long been thought to have therapeutic potential (See representative articles in the bibliography to this section). Astatine-211, because of its alpha energy of 5.7 MeV, is a very attractive isotope for cancer therapy. It has been used to attach to antibodies, proteins, drugs and inorganic colloids. The main problem is getting the astatine to remain attached to the molecule under physiological conditions. It should be pointed out that there is a potential radionuclidic contaminant (^{210}At) that must be minimized because of its decay product (^{210}Po), which is a pure alpha emitter and chemically binds to the bone marrow.

Decay mode

Astatine-211 decays via electron capture (59%) and alpha emission (41%). The decay product of the electron capture, ^{211}Po, decays by alpha emission (100%). Thus, every decay of ^{211}At results in an alpha particle.

Alpha emission products of ^{211}At

Fraction	Energy (MeV)
0.000045	5.1959
0.418	5.870

Alpha emission products of ^{211}Po

Fraction	Energy (MeV)
0.00544	6.568
0.00557	6.892
0.989	7.450

Electron emission products of ^{211}At

Fraction	Energy (MeV)	Fraction	Energy (MeV)
0.013462	0.059700	0.261490	0.008330

Photon emission products of ^{211}At

Fraction	Energy (MeV)	Fraction	Energy (MeV)
0.000044	0.685160	0.127020	0.07686
0.002455	0.687000	0.197270	0.011100
0.095480	0.089800	0.212760	0.079290

Photon emission products of ^{211}Po

Fraction	Energy (MeV)	Fraction	Energy (MeV)
0.000032	0.328200	0.005380	0.897830
0.005219	0.897830	0.005380	0.569670

Decay scheme

The decay scheme of ^{211}At is shown in Fig. 2.4.1.

Note that the daughter from the alpha decay of ^{211}At is radioactive, ^{207}Bi ($t_{½}$ = 32.2 a). However, because of the half-life differences, the photon intensities from ^{207}Bi will be less than 10^{-5} relative to the amount of ^{211}At.

Excitation functions

The excitation functions for ^{209}Bi(α, 2n)^{211}At and ^{209}Bi(α, 3n)^{210}At are shown in Figs 2.4.2 and 2.4.3, respectively.

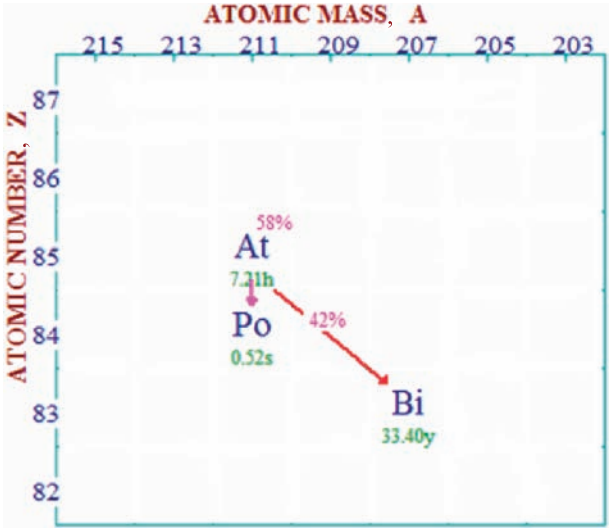

FIG. 2.4.1. Decay scheme of ^{211}At.

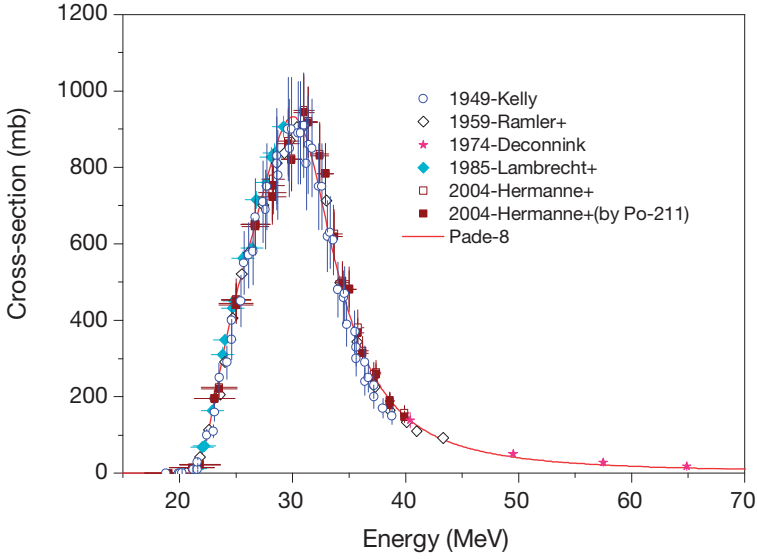

FIG. 2.4.2. Excitation function for the $^{209}Bi(\alpha, 2n)^{211}At$ reaction.

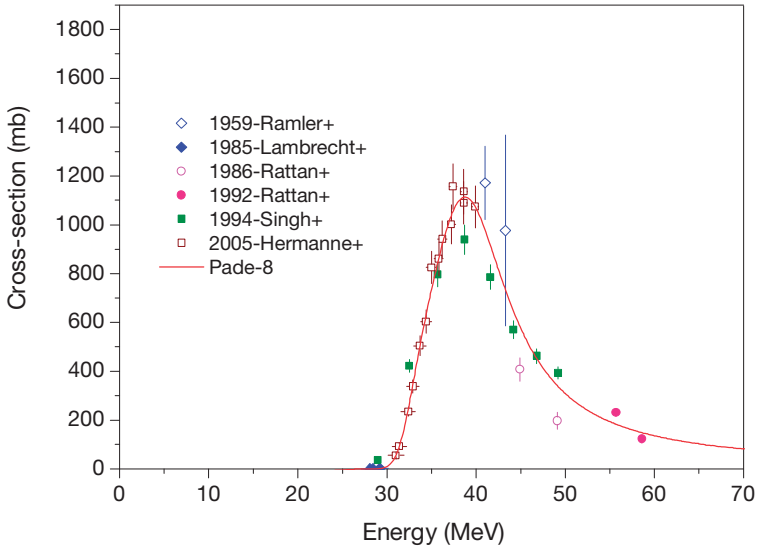

FIG. 2.4.3. Excitation function for the $^{209}Bi(\alpha, 3n)^{210}At$ reaction.

Thick target yields of ^{209}Bi(α, 2n)^{211}At

As can be seen from the excitation function, the yield of ^{211}At is very sensitive to the bombarding energy; thus, a theoretical calculation is not warranted. The table below compiles some of the results in the literature, which show a fairly wide range. Each publication in the reference list to this section has details regarding the target backing, and whether an internal or external beam was used; thus, the reader is encouraged to consult the literature to learn the details from the respective authors in order to obtain a perspective.

Thick target yields for production of ^{211}At

Alpha energy (MeV)	TT yield (mCi/μA·h)	Reference
28	41	[2.4.1]
28–29	16.3	[2.4.2]
29.1	30	[2.4.3]
29.5	38	[2.4.4]

Target material

The target material of choice is high purity bismuth metal.

Target preparation

Just as in the yield variation, there is a fairly wide range of target preparation procedures. However, the consensus is that an aluminium backing is preferred because of its ease of handling and adequate thermal properties. It should be noted that bismuth has a relatively poor thermal conductivity and a low melting point.

Bismuth can be melted onto the backing, pressed or vacuum evaporated. Because of the physical properties of bismuth, as thin a layer as possible is recommended. Thus, the target should be operated at a slant so as to take advantage of the increased target thickness while maintaining a thin profile. The aluminium backing should be water cooled. It should be noted that copper has been tried, but with lower yields than those with aluminium.

Target processing

The standard method for removing ^{211}At from the bismuth target matrix is by dry distillation at 650°C in a quartz oven. A dry nitrogen, argon or oxygen carrier gas is used to carry the ^{211}At out of the still. The distilled astatine is trapped in a polyetheretherketone® (PEEK) tubing cooled to –77°C with a mixture of ethanol and dry ice. The trapped astatine can be recovered with a small volume of organic solvent.

While there are reports of possible wet chemical methods being used to isolate astatine from bismuth targets, there are no publications with reliable results describing this approach.

Enriched materials recovery

Natural bismuth is monoisotopic ^{209}Bi. There is no need to recover the target material.

Specifications

As indicated below, the major contaminant is ^{210}At/^{210}Po. Since there are no stable isotopes of astatine, the SA will approach the theoretical values. However, as in all radiochemical processes, there is always the necessity of removing or minimizing pseudo-carriers, which may be in the form of another halogen in this case.

The primary concern is the amount of ^{210}At/^{210}Po as a radionuclidic impurity, because its decay product (^{210}Po) is a pure alpha emitter and binds chemically to bone marrow. The level of impurity acceptable will have to be decided by the local authorities. However, Henriksen et al. [2.4.3] suggested that at 29.1 MeV the relative atomic content of ^{210}At at end of bombardment (EOB) is approximately 0.023%.

For assay purposes, the following table contains relevant decay properties for the 210 chain.

Decay properties of the 210 chain

Nuclide	Half-life	Decay mode	Gamma energy (keV)	Per cent
At-210	8.1 h	EC	245.3	79.5
			1181.4	99.4
			1483.3	46.5
Po-210	138.4 d	α	803	0.00121

Note: Table adapted from Ref. [2.4.5].

REFERENCES TO SECTION 2.4

[2.4.1] LARSEN, R.H., WEILAND, B.W., ZALUTSKY, M.R., Evaluation of an internal cyclotron target for the production of ^{211}At via the ^{209}Bi(α, 2n)^{211}At reaction, Appl. Radiat. Isot. **47** (1996) 135–143.

[2.4.2] SCHWARZ, U.P., et al., Preparation of ^{211}At labeled humanized anti-tac using ^{211}At produced in disposable internal and external bismuth targets, Nucl. Med. Biol. **25** (1998) 89–93.

[2.4.3] HENRIKSEN, G., MESSELT, S., OLSEN, E., LARSEN, R.H., Optimisation of cyclotron production parameters for the ^{209}Bi(α, 2n)^{211}At reaction related to biomedical use of ^{211}At, Appl. Radiat. Isot. **54** (2001) 829–834.

[2.4.4] LEBEDA, O., JIRAN, R., RÁLIŠ, J., ŠTURSA, J., A new internal target system for production of ^{211}At on the cyclotron U-120M, Appl. Radiat. Isot. **63** (2005) 49–53.

[2.4.5] LARSEN, R.H., et al., Alpha-particle radiotherapy with ^{211}At-labelled monodispersed polymer particles, ^{211}At-labelled IgG proteins, and free ^{211}At in a murine intraperitoneal tumor model, Gynecol. Oncol. **57** (1995) 9–15.

BIBLIOGRAPHY TO SECTION 2.4

ANDERSSON, H., et al., Radioimmunotherapy of nude mice with intraperitoneally growing ovarian cancer xenograft utilizing ^{211}At-labelled monoclonal antibody MOv18, Anticancer Res. **20** (2000) 459–462.

GROPPI, F., et al., Optimisation study of alpha-cyclotron production of At-211/Po-211g for high-LET metabolic radiotherapy purposes, Appl. Radiat. Isot. **63** (2005) 621–631.

HADELY, S.W., WILBUR, D.S., GRAY, M.A., ATCHER, R.W., Astatine-211 labeling of an antimelanoma antibody and its Fab fragment using N-succinimidyl p-Asatobenzoate: Comparison in vivo with the p-[^{125}I]iodobenzoylconjugate, Bioconjug. Chem. **2** (1991) 171–179.

HERMANNE, A., et al., Experimental study of the cross-sections of alpha-particle induced reactions on ^{209}Bi, Appl. Radiat. Isot. **63** (2005) 1–9.

INTERNATIONAL ATOMIC ENERGY AGENCY, Charged Particle Cross-section Database for Medical Radioisotope Production: Diagnostic Radioisotopes and Monitor Reactions, IAEA-TECDOC-1211, IAEA, Vienna (2001).

IMAM, S.K., Advancements in cancer therapy with alpha emitters: A review, Int. J. Radiat. Oncol. Biol. Phys. **51** (2001) 271–278.

LAMBRECHT, R.M., MIRZADEH, S., Astatine-211 — Production, radiochemistry and nuclear data, J. Labelled Compd. Radiopharm. **21** (1985) 1288–1289.

LAMBRECHT, R.M., MIRZADEH, S., Cyclotron isotopes and radiopharmaceuticals XXXV: Astatine-211, Int. J. Appl. Radiat. Isot. **36** (1985) 443–450.

LARSEN, R.H., et al., ^{211}At-labelling of polymer particles for radiotherapy: Synthesis, purification and stability, J. Labelled Compd. Radiopharm. **33** (1993) 977–986.

LINDEGREN, S., BÄCK, T., JENSEN, H.J., Dry-distillation of astatine-211 from irradiated bismuth targets: A time-saving procedure with high recovery yields, Appl. Radiat. Isot. **55** (2001) 157–160.

PALM, S., et al., In vitro effects of free ^{211}At, ^{211}At-albumin, and ^{211}At-monoclonal antibody compared to external photon irradiation for two human cancer cell lines, Anticancer Res. **20** (2000) 1005–1012.

RAMLER, W.J., WING, J., HENDERSON, D.J., HUIZENGA, J.R., Excitation functions of bismuth and lead, Phys. Rev. **114** (1959) 154–162.

UNITED STATES NATIONAL NUCLEAR DATA CENTER,
http://www.nndc.bnl.gov/

VAIDYANATHAN, G., ZALUTSKY, M.R., Targeted therapy using alpha emitters, Phys. Med. Biol. **41** (1996) 1915–1931.

WILBUR, D.S., et al., Preparation of and evaluation of para-[^{211}At]astatobenzoyl labeled anti-renal cell carcinoma antibody A6H F(ab0)2 in vivo distribution comparison with para-[^{125}I]iodobenzoyl labeled A6H F(ab0)2, Nucl. Med. Biol. **20** (1993) 917–927.

ZALUTSKY, M.R., et al., Radioimmunotherapy of neoplastic meningitis in rats using an α-particle-emitting immunoconjugate, Cancer Res. **54** (1994) 4719–4725.

2.5. BERYLLIUM-7

Half-life: 53.4 d.

Photon emission products of ^{7}Be

Fraction	Energy (MeV)
0.104200	0.477590

Nuclear reactions

Beryllium-7 can be a contamination hazard as it is made in accelerators that have boron nitride exposed to the beam. The $^{10}B(p, \alpha)^{7}Be$ reaction has a significant cross-section at low energy. The following nuclear reactions produce ^{7}Be:

— $^{3}He(\alpha, \gamma)^{7}Be$
— $^{6}Li(d, n)^{7}Be$
— $^{7}Li(p, n)^{7}Be$
— $^{10}B(p, \alpha)^{7}Be$
— $^{16}O(p, x)^{7}Be$.

Excitation functions

The excitation functions for ^{7}Be are shown in Figs 2.5.1–2.5.5.

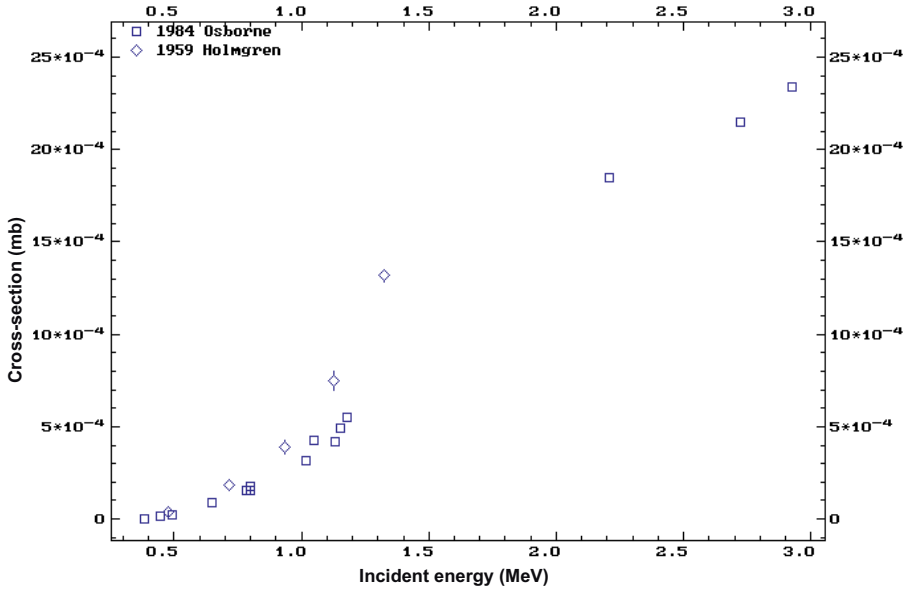

FIG. 2.5.1. Excitation function for the $^{3}He(\alpha, \gamma)^{7}Be$ reaction.

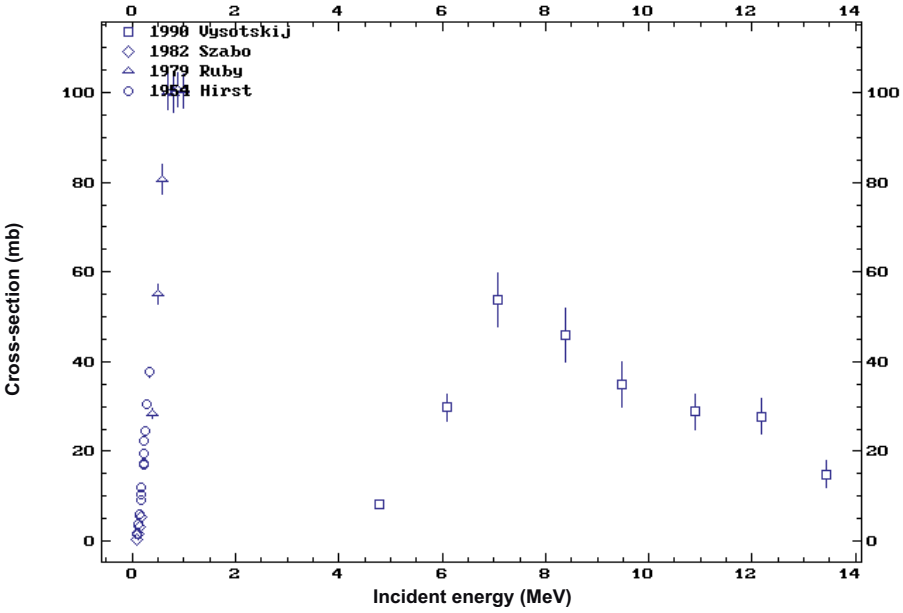

FIG. 2.5.2. Excitation function for the $^{6}Li(d, n)^{7}Be$ reaction.

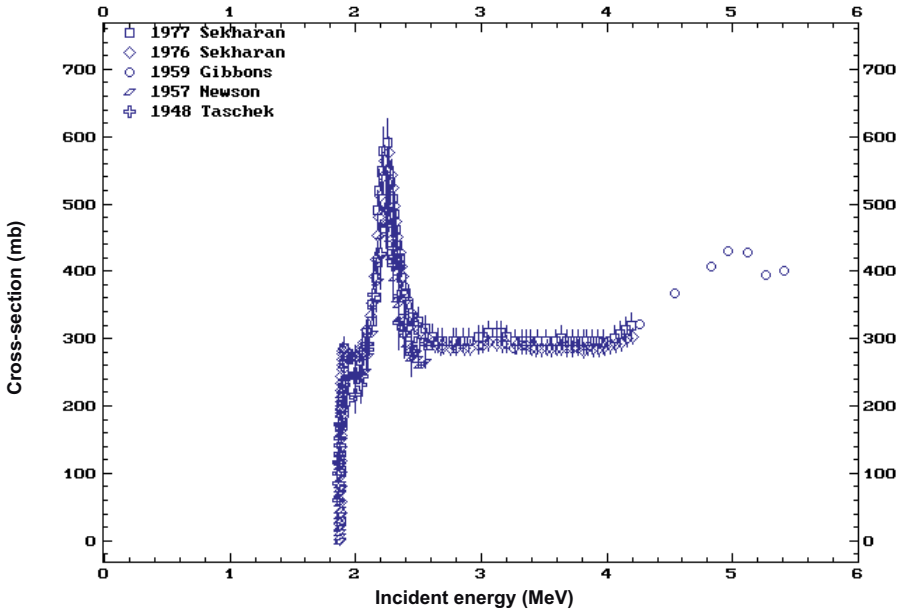

FIG. 2.5.3. Excitation function for the $^{7}Li(p, n)^{7}Be$ reaction.

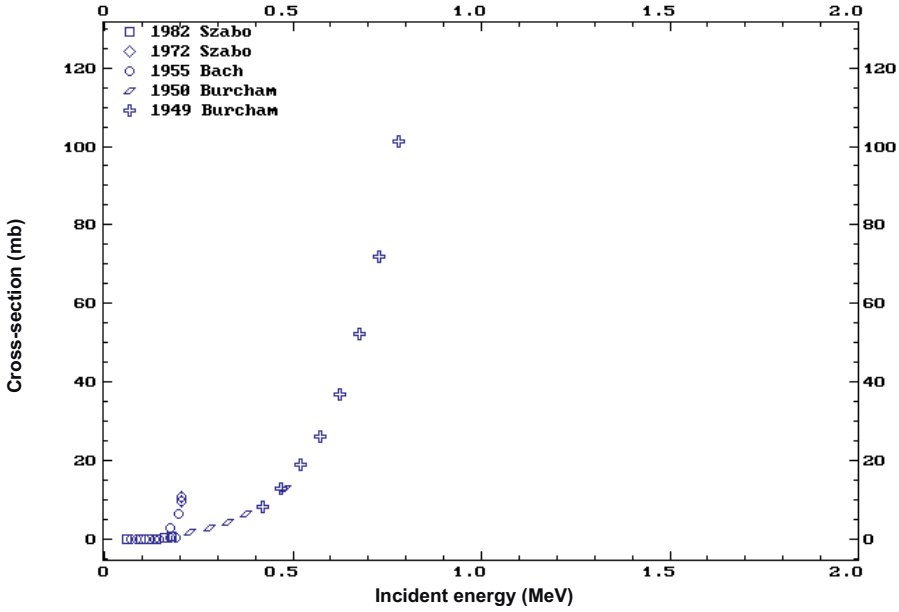

FIG. 2.5.4. Excitation function for the $^{10}B(p, \alpha)^{7}Be$ reaction.

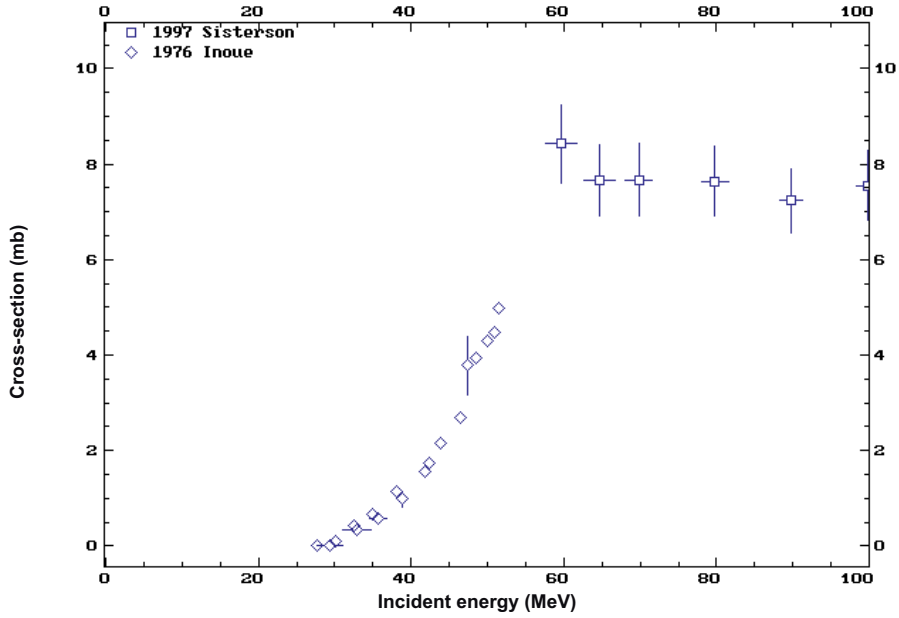

FIG. 2.5.5. Excitation function for the $^{16}O(p, x)^{7}Be$ reaction.

BIBLIOGRAPHY TO SECTION 2.5

DITRÓI, F., et al., Investigation of the charged particle nuclear reactions on natural boron for the purposes of the thin layer activation (TLA), Nucl. Instrum. Methods Phys. Res. B **103** (1995) 389–392.

DITRÓI, F., TAKÁCS, S., TÁRKÁNYI, F., MAHUNKA, I., Study of the $^{nat}C(^3He, 2\alpha)^7Be$ and $^9Be(^3He, \alpha n)^7Be$ nuclear reactions and their applications for wear measurements, Nucl. Instrum. Methods Phys. Res. B **103** (1995) 412–414.

ENGLAND, J.B.A., REECE, B.L., A study of the (^{3}He, ^{7}Be) reaction in ^{12}C, Nucl. Phys. **72** (1965) 449–460.

GIBBONS, J.H., MACKLIN, R.L., Total neutron yields from light elements under proton and alpha bombardment, Phys. Rev. **114** (1959) 571–580.

HOLMGREN, H.D., JOHNSTON, R.L., $^3H(\alpha, \gamma)^7Li$ and $^3He(\alpha, \gamma)^7Be$ reactions, Phys. Rev. **113** (1959) 1556–1559.

INOUE, T., TANAKA, S., Production of ^{7}Be from proton bombardment of light elements, J. Inorg. Nucl. Chem. **38** (1976) 1435–1427.

OSBORNE, J.L., et al., Low-energy behavior of the $^3He(\alpha, \gamma)^7Be$ cross section, Nucl. Phys. A **419** (1984) 115–132.

ROBERTSON, R.G.H., et al., Cross section of the capture reaction $^3He(\alpha, \gamma)^7Be$, Phys. Rev. C **27** (1983) 11–17.

SEKHARAN, K.K., LAUMER, H., KERN, B.D., GABBARD, F., A neutron detector for measurement of total neutron production cross sections, Nucl. Instrum. Methods **133** (1976) 253–257.

2.6. BISMUTH-213

Half-life: 60.55 min.

Uses

The therapeutic potential of the bismuth radionuclide, ^{213}Bi, has been demonstrated in patients with leukaemia. Bismuth-213 emits alpha radiation, which is delivered to bone marrow, spleen and blood via a monoclonal antibody conjugate. The chemical basis for alpha radioimmunotherapy with

^{213}Bi is the formation of a conjugate that contains a bifunctional chelate. Bismuth-213 is derived from the alpha decay of ^{225}Ac.

Decay scheme

The decay scheme of ^{213}Bi is shown in Fig. 2.6.1.

Alpha emission products of ^{213}Bi

Fraction	Energy (MeV)	Fraction	Energy (MeV)
0.001598	5.549000	0.020002	5.870000

Beta emission products of ^{213}Bi

Fraction	Maximum energy (MeV)	Average energy (MeV)
0.007000	1.127200	0.376000
0.010600	0.319820	0.090000
0.320000	0.979580	0.319000
0.640000	1.420000	0.491000

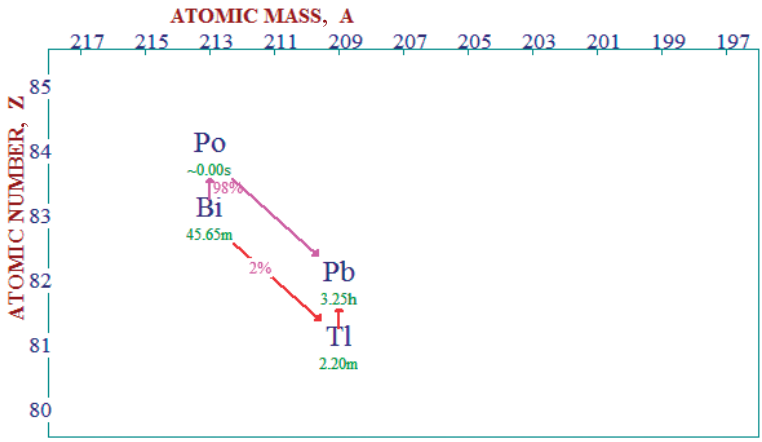

FIG. 2.6.1. Decay scheme of ^{213}Bi.

Electron emission products of ^{213}Bi

Fraction	Energy (MeV)	Fraction	Energy (MeV)
0.001327	0.059700	0.007187	0.423480
0.002263	0.436270	0.024264	0.008330
0.003395	0.199760	0.040831	0.347310

Photon emission products of ^{213}Bi

Fraction	Energy (MeV)	Fraction	Energy (MeV)
0.001327	0.323810	0.009410	0.089800
0.001479	0.659810	0.012519	0.076862
0.004438	0.807360	0.018304	0.011100
0.004790	1.100100	0.020970	0.079290
0.007397	0.292860	0.279670	0.440420

BIBLIOGRAPHY TO SECTION 2.6

ALLEN, B.J., Targeted alpha therapy: Evidence for potential efficacy of alpha-immunoconjugates in the management of micrometastatic cancer, Australas. Radiol. **43** (1999) 480–486.

BOLL, R., MALKEMUSA, D., MIRZADEH, S., Production of actinium-225 for alpha particle mediated radioimmunotherapy, Appl. Radiat. Isot. **62** (2005) 667–679.

IMAM, S.K., Advancements in cancer therapy with alpha-emitters: A review, Int. J. Radiat. Oncol. Biol. Phys. Rev. **51** (2001) 271–278.

KAIREMO, K.J., Radioimmunotherapy of solid cancers: A review, Acta Oncol. **35** (1996) 343–355.

McDEVITT, M.R., et al., Preparation of alpha-emitting ^{213}Bi-labeled antibody constructs for clinical use, J. Nucl. Med. **40** (1999) 1722–1727.

McDEVITT, M.R., et al., Radioimmunotherapy with alpha-emitting nuclides, Eur. J. Nucl. Med. **25** (1998) 1341–1351.

YUANFANG, L., CHUANCHU, W., Radiolabeling of monoclonal antibodies with metal chelates, Pure Appl. Chem. **63** (1991) 427–463.

2.7. BROMINE-75

Half-life: 97 min.

Decay mode

Bromine-75 decays with 71% positron emission and 29% electron capture. The positron end point energy is 1.7 MeV, and there are several gamma rays, with the most prominent being at 286.5 keV. Bromine-75 decays to ^{75}Se, which has a 120 day half-life and several gamma rays in the 100–300 keV range. This contributes to the overall dosimetry of the ^{75}Br-containing radiotracers.

Parent nucleus	Parent energy level	Parent half-life (min)	Decay mode	Daughter nucleus
Br-75	0.0	96.7	EC: 100%	Se-75

Positron emission products of ^{75}Br

This table is also continued on the next page.

Fraction	Average energy (keV)	End point energy (keV)
0.00031	196	447
0.00015	273	628
0.00046	275	633
0.0064	331	763
0.0043	351	809
0.0026	357	824
0.00057	374	863
0.0042	405	934
0.0065	429	988
0.0011	436	1005
0.00062	454	1045
0.0098	484	1113
0.034	500	1149
0.0047	536	1231

Fraction	Average energy (keV)	End point energy (keV)
0.0004	549	1260
0.033	587	1344
0.0121	622	1422
0.049	694	1580
0.52	758	1721
0.04	889	2008

Electron emission products of ^{75}Br

Type	Fraction	Energy (keV)
Auger	0.318	1.32
Auger	0.098	9.67
CE	0.00181	99.44
CE	0.00021	110.45
CE	0.000034	112.1
CE	0.0031	128.53
CE	0.00035	139.54
CE	0.000055	141.19
CE	0.00284	273.84
CE	0.00029	284.85

Photon emission products of ^{75}Br

This table is also continued on the next page.

Fraction	Energy (keV)	Fraction	Energy (keV)	Fraction	Energy (keV)	Fraction	Energy (keV)
0.0057	1.38	0.0061	315.61	0.00114	534.8	0.0033	788.7
0.0008	6.53	0.00097	319.7	0.003	551.65	0.0024	859.3
0.0432	11.182	0.0011	325.4	0.0045	566.43	0.0025	890.7
0.084	11.222	0.0013	325.4	0.0199	572.93	0.005	897.6
0.0057	12.49	0.0018	349.2	0.0018	586.1	0.0101	912.05

Fraction	Energy (keV)	Fraction	Energy (keV)	Fraction	Energy (keV)	Fraction	Energy (keV)
0.0111	12.496	0.0393	377.39	0.0033	598.2	0.0166	952.1
0.00079	12.652	0.044	427.79	0.0168	608.9	0.0026	959
0.0167	112.1	0.039	431.75	0.0015	646.1	0.0044	961.4
0.066	141.19	0.0011	460.9	0.0035	659.1	0.00088	974.9
0.0009	195.5	0.0012	467.3	0.00114	663.8	0.00106	1074.2
0.0079	236.1	0.0028	484.4	0.00114	676.6	0.0018	1144.5
0.88	286.5	0.0018	488.1	0.0018	701.6	0.0048	1245.5
0.0267	292.85	0.0033	490.7	0.0154	733.94	0.00114	1380.5
0.0024	299.4	1.46	511	0.0047	770.8	0.0033	1448.9
0.00088	309.4	0.00018	534.8	0.00106	781	0.00123	1561

Nuclear reactions

The nuclear reactions that produce ^{75}Br are shown in the following table.

Nuclear reaction	Useful energy range (MeV)	Natural abundance (%)	References
^{76}Se(p, 2n)^{75}Br	28–18	9.1	[2.7.1, 2.7.2]
^{77}Se(p, 3n)^{75}Br	38–28	7.7	[2.7.2]
^{78}Se(p, 4n)^{75}Br	55–40	23.5	[2.7.2]
^{74}Se(d, n)^{75}Br	10–0	0.9	[2.7.2]
^{76}Se(d, 3n)^{75}Br	35–20	9.1	[2.7.2]
^{77}Se(d, 4n)^{75}Br	45–30	7.7	[2.7.2]
^{76}Se(^{3}He, p3n)^{75}Br	36–30	9.1	[2.7.3]
^{76}Se(^{4}He, p4n)^{75}Br	85–70	9.1	[2.7.2]
^{75}As(^{3}He, 3n)^{75}Br	35–25	100	[2.7.2, 2.7.4, 2.7.5]
^{75}As(^{4}He, 4n)^{75}Br	56–48	100	[2.7.2, 2.7.4]
^{78}Kr(p, ^{4}He)^{75}Br	30–22	0.35	[2.7.6, 2.7.7]

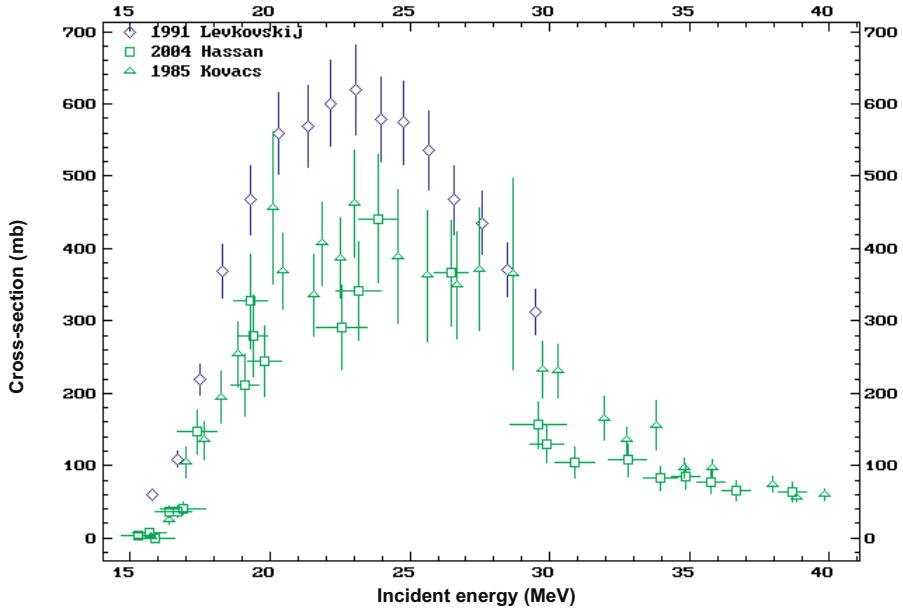

FIG. 2.7.1. Excitation function for the $^{76}Se(p, 2n)^{75}Br$ reaction.

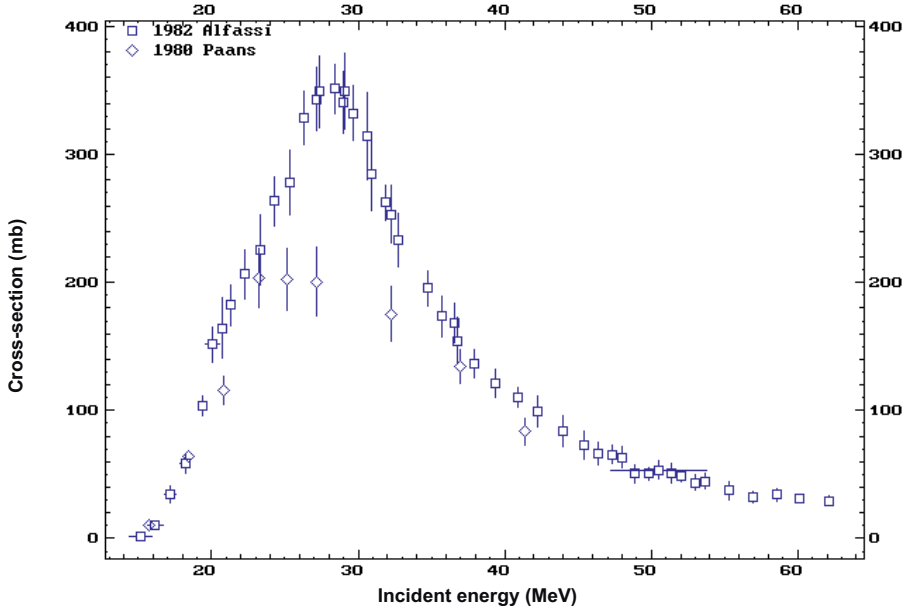

FIG. 2.7.2. Excitation function for the $^{75}As(^{3}He, 3n)^{75}Br$ reaction.

Excitation functions

The excitation functions for ^{76}Se(p, 2n)^{75}Br and ^{75}As(^{3}He, 3n)^{75}Br are shown in Figs 2.7.1 and 2.7.2, respectively.

REFERENCES TO SECTION 2.7

[2.7.1] KOVÁCS, Z., BLESSING, G., QAIM, S.M., STÖCKLIN, G., Production of ^{75}Br via the ^{76}Se(p, 2n)^{75}Br reaction at a compact cyclotron, Int. J. Appl. Radiat. Isot. **36** (1985) 635–642.

[2.7.2] PAANS, A.M.J., WELLEWEERD, J., VAALBURG, W., REIFFERS, S., WOLDRING, M.G., Excitation functions for the production of bromine-75: A potential nuclide for the labelling of radiopharmaceuticals, Int. J. Appl. Radiat. Isot. **31** (1980) 267–272.

[2.7.3] YOUFENG, H., QAIM, S.M., STÖCKLIN, G., Excitation functions for the ^{3}He-particle induced nuclear reactions on ^{76}Se, ^{77}Se and ^{nat}Se: Possibilities of production of ^{77}Kr, Int. J. Appl. Radiat. Isot. **33** (1982) 13–19.

[2.7.4] BLESSING, G., WEINREICH, R., QAIM, S.M., STÖCKLIN, G., Production of ^{75}Br and ^{77}Br via the ^{75}As(^{3}He, 3n)^{75}Br and the ^{75}As(^{4}He, 2n)^{77}Br reactions using Cu_3As-alloy as a high-current target material, Int. J. Appl. Radiat. Isot. **33** (1982) 333–339.

[2.7.5] SCHLYER, D.J., TISCHER, S., FIROUZBAKHT, M.L., Production and processing of bromine-75 from the ^{75}As(^{3}He, 3n)^{75}Br reaction, J. Labelled Compd. Radiopharm. **35** (1994) 260–262.

[2.7.6] FRIEDMAN, A.M., DEJESUS, O.J., HARPER, P., ARMSTRONG, C., Preparation of ^{75}Br by the ^{78}Kr(p, α)^{75}Br reaction, J. Labelled Compd. Radiopharm. **19** (1982) 1427–1428.

[2.7.7] TÁRKÁNYI, F., KOVÁCS, Z., QAIM, S.M., Excitation functions of proton induced nuclear reactions on highly enriched ^{78}Kr: Relevance to the production of ^{75}Br and ^{77}Br at a small cyclotron, Appl. Radiat. Isot. **44** (1993) 1105–1111.

BIBLIOGRAPHY TO SECTION 2.7

ALFASSI, Z.B., WEINREICH, R., The production of positron emitters ^{75}Br and ^{76}Br — Excitation functions and yields for ^{3}He and alpha-particle induced nuclear reactions on arsenic, Radiochim. Acta **30** (1982) 67.

BLUE, J.W., BENJAMIN, P.P., Production of ^{77}Br by the reaction ^{76}Se(α, 3n)^{77}Kr, J. Nucl. Med. **12** (1971) 416–417.

DE JONG, D., KOOIMAN, H., VEENBOER, J.T., ^{76}Br and ^{77}Br from decay of cyclotron produced ^{76}Kr and ^{77}Kr, Int. J. Appl. Radiat. Isot. **30** (1979) 786–788.

HASSAN, H.E., et al., Experimental studies and nuclear model calculations on proton-induced reactions on ^{nat}Se, ^{76}Se and ^{77}Se with particular reference to the production of the medically interesting radionuclides ^{76}Br and ^{77}Br, Appl. Radiat. Isot. **60** (2004) 899.

JANSSEN, A.G.M., VAN DEN BOSCH, R.L.P., DE GOEIJ, J.J.M., THEELEN, H.M.J., The reactions ^{77}Se(p, n)^{77}Br and ^{78}Se(p, 2n)^{77}Br as production routes for ^{77}Br, Int. J. Appl. Radiat. Isot. **31** (1980) 405–409.

LOCH, C., MAZIÈRE, B., ^{75}Br production: Electrochemical preparation of an As–Cu target, J. Labelled Compd. Radiopharm. **26** (1988) 169.

McCARTHY, T.J., et al., "Investigation of I-124, Br-76, and Br-77 production using a small biomedical cyclotron", Proc. 8th Workshop on Targetry and Target Chemistry, St. Louis, MO, 1999 (abstract).

NOZAKI, T., IWAMOTO, M., ITOH, Y., Production of ^{77}Br by various nuclear reactions, Int. J. Appl. Radiat. Isot. **30** (1979) 79–83.

NUNN, A.D., Techniques for the preparation of thick and thin arsenic targets suitable for cyclotron irradiation, Nucl. Instrum. Methods **99** (1972) 251–254.

NUNN, A.D., WATERS, S.L., Target materials for the cyclotron production of carrier-free ^{77}Br, Int. J. Appl. Radiat. Isot. **26** (1975) 731–735.

QAIM, S.M., Recent developments in the production of ^{18}F, ^{75,76,77}Br and ^{123}I, Appl. Radiat. Isot. **37** (1986) 803–810.

QAIM, S.M., STÖCKLIN, G., WEINREICH, R., Excitation functions for the formation of neutron deficient isotopes of bromine and krypton via high energy deuteron induced reactions on bromine: Production of ^{77}Br, ^{76}Br and ^{79}Kr, Int. J. Appl. Radiat. Isot. **28** (1977) 947–953.

SAKAMOTO, K., DOHNIWA, M., OKADA, K., Excitation functions for (p, xn) and (p, pxn) reactions on natural $^{79+81}$Br, $^{85+87}$Rb, ^{127}I and ^{133}Cs up to E_p = 52 MeV, Int. J. Appl. Radiat. Isot. **36** (1985) 481–488.

TOLMACHEV, V., LOVQVIST, A., EINARSSON, L., SCHULTZ, J., LUNDQVIST, H., Production of ^{76}Br by a low-energy cyclotron, Appl. Radiat. Isot. **49** (1998) 1537–1540.

VAALBURG, W., et al., Fast recovery by dry distillation of ^{75}Br induced in reusable metal selenide targets via the ^{76}Se(p, 2n)^{75}Br reaction, Int. J. Appl. Radiat. Isot. **36** (1985) 961–964.

WEINREICH, R., QAIM, S.M., STÖCKLIN, G., ALFASSI, Z.B., Comparative studies on the production of the positron emitters bromine-75 and phosphorus-30, J. Labelled Compd. Radiopharm. **18** (1981) 201.

ZEISLER, S.K., GASPER, H., "Routine production of [^{75}Br]bromide in a gas target", Proc. 8th Workshop on Targetry and Target Chemistry, St. Louis, MO, 1999 (abstract).

2.8. BROMINE-76

Half-life: 16.2 h.

Decay mode

Bromine-76 decays with both positron emission (54%) and electron capture. The half-life allows radiotracers to be used that have accumulation times of one or two days. The high end point energies of the positrons emitted may affect the positron emission image to some extent.

Parent nucleus	Parent energy level	Parent half-life (s)	Decay mode	Daughter nucleus
Br-76	102.59 (3)	1.31	IT[a]	Br-76

[a] IT: isomeric transition.

Electron emission products of ^{76}Br

Fraction	Energy (keV)	Fraction	Energy (keV)
1.54	1.41	0.0508	43.698
0.444	10.2	0.00822	45.223
0.455	32.006	0.115	55.328
0.74	43.636	0.019	56.854

Photon emission products of ^{76}Br

Fraction	Energy (keV)	Fraction	Energy (keV)
0.0305	1.48	0.0058	13.469
0.22	11.878	0.484	45.48
0.425	11.924	0.091	57.11
0.0299	13.284	0.0005	102.600

Parent nucleus	Parent energy level	Parent half-life (s)	Decay mode	Daughter nucleus
Br-76	102.0	1.31	β^+	Se-76

Photon emission products of ^{76}Br

Fraction	Energy (keV)	Fraction	Energy (keV)
0.005	511.0	0.0055	772
0.0055	559		

Parent nucleus	Parent energy level	Parent half-life (h)	Decay mode	Daughter nucleus
Br-76	0.0	16.2	EC: 100%	Se-76

Positron emission products of ^{76}Br

This table is also continued on the next page.

Fraction	Maximum energy (MeV)	Average energy (MeV)
0.0003	0.337	0.146
0.0004	0.385	0.166
0.0013	0.482	0.207
0.0092	0.589	0.253

Fraction	Maximum energy (MeV)	Average energy (MeV)
0.0144	0.781	0.336
0.063	0.871	0.375
0.052	0.990	0.427
0.0124	1.271	0.551
0.002	1.285	0.558
0.003	1.310	0.569
0.0035	1.426	0.621
0.005	1.512	0.659
0.0005	1.814	0.797
0.01	2.153	0.953
0.004	2.252	1.022
0.028	2.725	1.221
0.021	2.819	1.265
0.258	3.382	1.532
0.06	3.941	1.800

Electron emission products of ^{76}Br

Energy (keV)	Intensity (%)	Dose (MeV/(Bq·s))
Auger L: 1.32	51.9	6.85E–4
Auger K: 9.67	15.9	0.00154

Photon emission products of ^{76}Br

This table is also continued on the next page.

Energy (keV)	Fraction
511	1.09
559.09	0.74
563.2	0.036
657.02	0.159
1129.85	0.046

Energy (keV)	Fraction
1216.1	0.088
1853.67	0.147
2391.25	0.047
2792.69	0.056
2950.53	0.074

Nuclear reactions

The nuclear reactions that produce ^{76}Br are shown in the following table.

Nuclear reaction	Useful energy range (MeV)	Natural abundance (%)	References
^{76}Se(p, n)^{76}Br	16–10	9.1	[2.8.1]
^{77}Se(p, 2n)^{76}Br	25–16	7.7	[2.8.2]
^{75}As(^{4}He, 3n)^{76}Br	18–10	100	[2.8.2]
^{nat}Br(p, xn)^{76}Kr: ^{76}Br	65–50	100	[2.8.3, 2.8.4]
^{nat}Br(d, xn)^{76}Kr: ^{76}Br	80–55	100	[2.8.3]
^{76}Se(^{3}He, 3n)^{76}Kr: ^{76}Br	36–30	9.1	[2.8.5, 2.8.6]
^{76}Se(d, 2n)^{76}Br	10–25	9.1	[2.8.7]
^{78}Kr(d, α)^{76}Br			[2.8.8]

Excitation function

The excitation function for ^{76}Se(p, n)^{76}Br is shown in Fig. 2.8.1.

REFERENCES TO SECTION 2.8

[2.8.1] TOLMACHEV, V., LOVQVIST, A., EINARSSON, L., SCHULTZ, J., LUNDQVIST, H., Production of ^{76}Br by a low-energy cyclotron, Appl. Radiat. Isot. **49** (1998) 1537–1540.

[2.8.2] NOZAKI, T., IWAMOTO, M., ITOH, Y., Production of ^{77}Br by various nuclear reactions, Int. J. Appl. Radiat. Isot. **30** (1979) 79–83.

[2.8.3] QAIM, S.M., STÖCKLIN, G., WEINREICH, R., Excitation functions for the formation of neutron deficient isotopes of bromine and krypton via high energy deuteron induced reactions on bromine: Production of ^{77}Br, ^{76}Br and ^{79}Kr, Int. J. Appl. Radiat. Isot. **28** (1977) 947–953.

[2.8.4] DE VILLIERS, D., NORTIER, M., RICHTER, W., Experimental and theoretical functions for Br-nat(p, x) reactions, Appl. Radiat. Isot. **57** (2002) 907.

[2.8.5] BLUE, J.W., BENJAMIN, P.P., Production of ^{77}Br by the reaction ^{76}Se(α, 3n)^{77}Kr, J. Nucl. Med. **12** (1971) 416–417.

[2.8.6] DE JONG, D., KOOIMAN, H., VEENBOER, J.T., ^{76}Br and ^{77}Br from decay of cyclotron produced ^{76}Kr and ^{77}Kr, Int. J. Appl. Radiat. Isot. **30** (1979) 786–788.

[2.8.7] PAANS, A.M.J., WELLEWEERD, J., VAALBURG, W., REIFFERS, S., WOLDRING, M.G., Excitation functions for the production of bromine-75: A potential nuclide for the labelling of radiopharmaceuticals, Int. J. Appl. Radiat. Isot. **31** (1980) 267–272.

[2.8.8] SCHOLTEN, B., TAKÁCS, S., TÁRKÁNYI, F., COENEN, H.H., QAIM, S.M., Excitation functions of deuteron induced nuclear reactions on enriched ^{78}Kr with particular relevance to the production of ^{76}Br, Radiochim. Acta **92** (2004) 203–207.

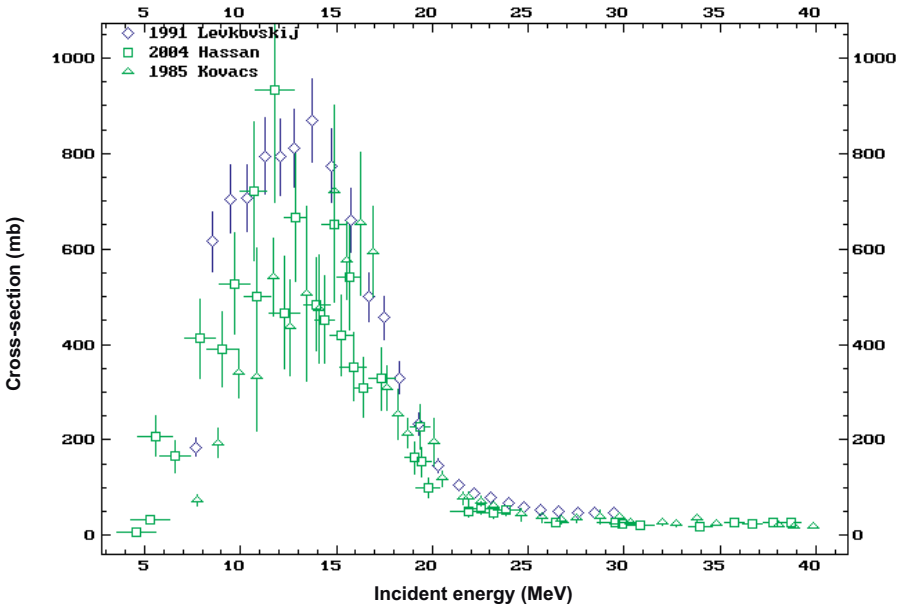

FIG. 2.8.1. Excitation function for the ^{76}Se(p, n)^{76}Br reaction.

BIBLIOGRAPHY TO SECTION 2.8

HASSAN, H.E., et al., Experimental studies and nuclear model calculations on proton-induced reactions on ^{nat}Se, ^{76}Se and ^{77}Se with particular reference to the production of the medically interesting radionuclides ^{76}Br and ^{77}Br, Appl. Radiat. Isot. **60** (2004) 899.

McCARTHY, T.J., et al., "Investigation of I-124, Br-76, and Br-77 production using a small biomedical cyclotron", Proc. 8th Workshop on Targetry and Target Chemistry, St. Louis, MO, 1999 (abstract).

QAIM, S.M., Recent developments in the production of ^{18}F, ^{75,76,77}Br and ^{123}I, Appl. Radiat. Isot. **37** (1986) 803–810.

SCHLYER, D.J., TISCHER, S., FIROUZBAKHT, M.L., Production and processing of bromine-75 from the ^{75}As(^{3}He, 3n)^{75}Br reaction, J. Labelled Compd. Radiopharm. **35** (1994) 260–262.

VAALBURG, W., et al., Fast recovery by dry distillation of ^{75}Br induced in resuable metal selenide targets via the ^{76}Se(p, 2n)^{75}Br reaction, Int. J. Appl. Radiat. Isot. **36** (1985) 961–964.

WEINREICH, R., KNIEPER, J., Production of ^{77}Kr and ^{79}Kr for medical applications via proton irradiation of bromine: Excitation functions, yields and separation procedures, Int. J. Appl. Radiat. Isot. **34** (1983) 1335–1338.

WEINREICH, R., QAIM, S.M., STÖCKLIN, G., ALFASSI, Z.B., Comparative studies on the production of the positron emitters bromine-75 and phosphorus-30, J. Labelled Compd. Radiopharm. **18** (1981) 201.

YOUFENG, H., QAIM, S.M., STÖCKLIN, G., Excitation functions for the ^{3}He particle induced nuclear reactions on ^{76}Se, ^{77}Se and ^{nat}Se: Possibilities of production of ^{77}Kr, Int. J. Appl. Radiat. Isot. **33** (1982) 13–19.

2.9. BROMINE-77

Half-life

Bromine-77 has a half-life of 56 h and decays nearly exclusively (99.3%) by electron capture, with prominent gamma rays at 239.0 and 520.7 keV. There are several other gamma rays, varying in energy from 238 to 820 keV.

Positron emission products of ^{77}Br

Fraction	Maximum energy (MeV)	Average energy (MeV)
0.007300	0.342700	0.151700

Electron emission products of ^{77}Br

Fraction	Energy (MeV)
0.001344	0.160280
0.001610	0.075218
0.002195	0.226340
0.007889	0.149280
0.356840	0.009670
1.151800	0.001320

Photon emission products of ^{77}Br

Fraction	Energy (MeV)
0.020790	0.817790
0.022869	0.281680
0.029568	0.578910
0.029799	0.249790
0.041580	0.297230
0.071826	0.012500
0.154330	0.011181
0.224070	0.520650
0.231000	0.239000
0.300260	0.011222

Nuclear reactions

The nuclear reactions that produce ^{77}Br are shown in the following table.

Nuclear reaction	Useful energy range (MeV)	Natural abundance (%)	References
^{77}Se(p, n)^{77}Br	10–20	7.7	[2.9.1]
^{78}Se(p, 2n)^{77}Br	20–30	23.6	[2.9.1]
^{75}As(^{4}He, 2n)^{77}Br	20–30	100	[2.92]
^{80}Se(p, 4n)^{77}Br		49.9	
^{82}Se(p, 6n)^{77}Br		8.9	
^{79}Br(p, 3n)^{77}Kr: ^{77}Br	35–50	50.7	[2.9.3, 2.9.4]
^{79}Br(d, 4n)^{77}Kr: ^{77}Br	25–40	50.7	[2.9.4]
^{78}Kr(d, 2pn)^{77}Br			[2.9.5]

Excitation function

The excitation function for ^{77}Se(p, n)^{77}Br is shown in Fig. 2.9.1.

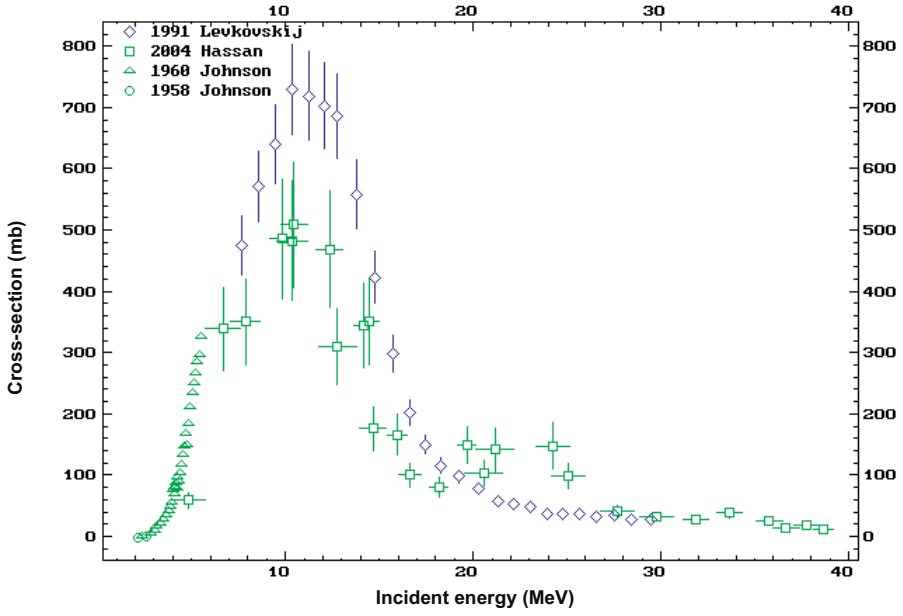

FIG. 2.9.1. Excitation function for the ^{77}Se(p, n)^{77}Br reaction.

REFERENCES TO SECTION 2.9

[2.9.1] DE JONG, D., KOOIMAN, H., VEENBOER, J.T., ^{76}Br and ^{77}Br from decay of cyclotron produced ^{76}Kr and ^{77}Kr, Int. J. Appl. Radiat. Isot. **30** (1979) 786–788.
[2.9.2] NOZAKI, T., IWAMOTO, M., ITOH, Y., Production of ^{77}Br by various nuclear reactions, Int. J. Appl. Radiat. Isot. **30** (1979) 79–83.
[2.9.3] DE JONG, D., BRINKMAN, G.A., LINDER, L., Excitation functions for the production of ^{76}Kr and ^{77}Kr, Int. J. Appl. Radiat. Isot. **30** (1979) 188–190.
[2.9.4] QAIM, S.M., Recent developments in the production of ^{18}F, ^{75,76,77}Br and ^{123}I, Appl. Radiat. Isot. **37** (1986) 803–810.
[2.9.5] TÁRKÁNYI, F., KOVÁCS, Z., QAIM, S.M., Excitation functions of proton induced nuclear reactions on highly enriched ^{78}Kr: Relevance to the production of ^{75}Br and ^{77}Br at a small cyclotron, Appl. Radiat. Isot. **44** (1993) 1105.

BIBLIOGRAPHY TO SECTION 2.9

BLUE, J.W., BENJAMIN, P.P., Production of ^{77}Br by the reaction ^{76}Se(α, 3n)^{77}Kr, J. Nucl. Med. **12** (1971) 416–417.

HASSAN, H.E., et al., Experimental studies and nuclear model calculations on proton-induced reactions on ^{nat}Se, ^{76}Se and ^{77}Se with particular reference to the production of the medically interesting radionuclides ^{76}Br and ^{77}Br, Appl. Radiat. Isot. **60** (2004) 899.

JOHNSON, C.H., GALONSKY, A., INSKEEP, C.N., Cross Sections for (p, n) Reactions in Intermediate-weight Nuclei, Rep. ORNL-2910, Oak Ridge Natl Lab., TN (1960) 25.

JOHNSON, C.H., GALONSKY, A., ULRICH, J.P., Proton strength functions from (p, n) cross sections, Phys. Rev. **109** (1958) 1243.

McCARTHY, T.J., et al., "Investigation of I-124, Br-76, and Br-77 production using a small biomedical cyclotron", Proc. 8th Workshop on Targetry and Target Chemistry, St. Louis, MO, 1999 (abstract).

QAIM, S.M., STÖCKLIN, G., WEINREICH, R., Excitation functions for the formation of neutron deficient isotopes of bromine and krypton via high energy deuteron induced reaction on bromine: Production of ^{77}Br, ^{76}Br and ^{79}Kr, Int. J. Appl. Radiat. Isot. **28** (1977) 947–953.

TOLMACHEV, V., LOVQVIST, A., EINARSSON, L., SCHULTZ, J., LUNDQVIST, H., Production of ^{76}Br by a low-energy cyclotron, Appl. Radiat. Isot. **49** (1998) 1537–1540.

YOUFENG, H., QAIM, S.M., STÖCKLIN, G., Excitation functions for the ^{3}He-particle induced nuclear reactions on ^{76}Se, ^{77}Se and ^{nat}Se: Possibilities of production of ^{77}Kr, Int. J. Appl. Radiat. Isot. **33** (1982) 13–19.

2.10. CADMIUM-109

Half-life: 461.4 d.

Uses

The radioisotope ^{109}Cd ($T_{1/2}$ = 461.4 d) is widely used as an excitation source for energy dispersive X ray fluorescence spectrometry, a non-destructive qualitative and quantitative analytical technique used to determine the metallic composition of samples. It has been used to determine the amount of lead in bone in vivo. It is also used to analyse metallic alloys and for checking stock and sorting scrap. Other applications range from its use as an electron source for the measurement of densities of air pollution samples to tracer studies in mushrooms as well as in mice and rats [2.10.1]. In the nuclear medicine field there is growing interest in employing ^{109}Cd in a ^{109}Cd/^{109m}Ag generator, as an alternative to other biomedical generators of ultra-short lived gamma emitters [2.10.2, 2.10.3].

Decay mode

Cadmium-109 decays by electron capture to ^{109m}Ag.

Electron emission products of ^{109}Cd

Fraction	Energy (MeV)
0.133620	0.018500
0.865380	0.002610

Photon emission products of ^{109}Cd

Fraction	Energy (MeV)
0.058184	0.002980
0.113670	0.024900
0.186150	0.021990
0.352560	0.022163

Nuclear reactions

The main production reactions are the ^{109}Ag(p, n)^{109}Cd reaction and the ^{107}Ag(α, x)^{109}Cd reaction on natural silver.

Excitation function

The excitation function for the ^{109}Ag(p, n)^{109}Cd reaction is shown in Fig. 2.10.1.

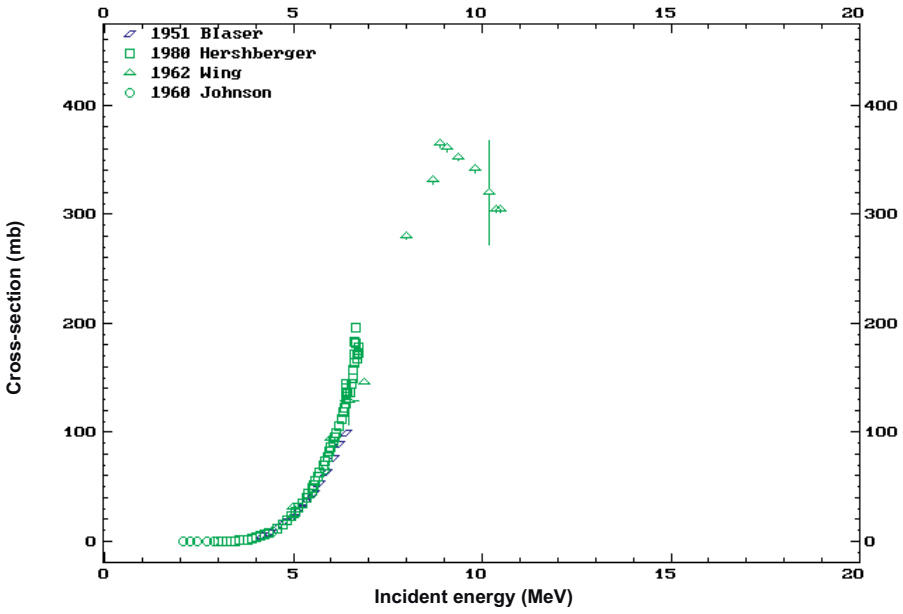

FIG. 2.10.1. Excitation function for the ^{109}Ag(p, n)^{109}Cd reaction.

Thick target yields

The $^{109}Ag(p, n)^{109}Cd$ reaction produces 22 MeV protons with a yield of 5.1 μCi/(μA·h).

Target materials

The target material for both these reactions is natural silver. The form can be either metallic silver or silver oxide. In the case of the oxide, the target is usually a pressed powder target. When metallic silver is used, the target is a silver foil.

Target preparation

The target for this process is a solid silver metal target. A silver foil alone is usually used, but the silver could be plated on to a solid support.

Target processing

The currently used wet chemical methods to recover and purify ^{109}Cd give rise to relatively large volumes of liquid radioactive waste. A new high temperature gas chemical procedure for ^{109}Cd recovery is being developed that would provide advantages over the wet chemical approach. In this process, cadmium is evaporated from metallic indium at a high temperature in a helium and hydrogen flow, and is then deposited on to a quartz surface or on to metallic catcher foils. Complete cadmium evaporation occurs at 700 ± 50°C under the given conditions, with no evaporation of other radionuclides observed in the targets (e.g., ^{114m}In, ^{113}In, ^{105}Ag, ^{110m}Ag and ^{102}Rh). During evaluation of this technique, it is important to understand the behaviour of ^{65}Zn, which is a volatile impurity in the spallation production on indium targets at higher proton energies. At 750°C, more than 98% of the cadmium is evaporated from the molten indium. At this same temperature, less than 0.2% of the zinc evaporates from molten gallium. At 900°C, more than 90% of the zinc is volatilized. On the basis of these experiments it appears probable that a clean separation of zinc and cadmium can be achieved from irradiated indium metal targets.

Specifications

The main radiocontaminant in the final product is ^{107}Cd, which, however, does not constitute a serious problem due to its very short half-life (6.50 h) compared with that of ^{109}Cd [2.10.1].

REFERENCES TO SECTION 2.10

[2.10.1] NORTIER, F.M., MILLS, S.J., STEYN, G.F., Excitation functions for the production of ^{109}Cd, ^{109}In and ^{109}Sn in proton bombardment of indium up to 200 MeV, Int. J. Radiat. Appl. Instrum. **42** (1991) 1105–1107.

[2.10.2] ERHARDT, G.J., LI, M., GOECKELER, W.F., BENNER, M.S., BENNER, S., "A new ^{109}Cd–^{109m}Ag generator system", Single-photon Ultrashort-lived Radionuclides (Proc. Symp. Oak Ridge, 1985), (PARAS, P., THIESSEN, J.W., Eds), United States Department of Energy, Oak Ridge, TN (1985) 182.

[2.10.3] STEINKRUEER, F.J., et al., "Production and recovery of large quantities of radionuclides for nuclear medicine generator systems", Radionuclide Generators (KNAPP, F.F., Jr., BUTLER, T.A., Eds), ACS Symp. Ser. **241** (1984) 179–184.

BIBLIOGRAPHY TO SECTION 2.10

BLASER, J.-P., BOEHM, F., MARMIER, P., PEASLEE, D.C., Fonctions d'éxcitation de la réaction (p, n), Helv. Phys. Acta **24** (1951) 3.

HERSHBERGER, R.L., FLYNN, D.S., GABBARD, F., JOHNSON, C.H., Systematics of proton absorption deduced from (p, p) and (p, n) cross sections for 2.0- to 6.7-MeV protons on ^{107,109}Ag and ^{115}In, Phys. Rev. C **21** (1980) 896–901.

JOHNSON, C.H., GALONSKY, A., INSKEEP, C.N., Cross Sections for (p, n) Reactions in Intermediate Weight Nuclei, ORNL Rep. No. 2910, Oak Ridge Natl Lab., TN (1960) 25.

READ, B.J., MILLER, J.M., Nuclear-structure effects in high-energy (p, n) reactions, Phys. Rev. B **140** (1965) 623–630.

WING, J., HUIZENGA, J.R., (p, n) Cross sections of V-51, Cr-52, Cu-63, Cu-65, Ag-107, Ag-109, Cd-111, Cd-114, and La-139 from 5 to 10.5 MeV, Phys. Rev. **128** (1962) 280–290.

ZHUIKOV, B.L., et al., "Production and recovery of ^{109}Cd from metallic indium targets", Proc. 7th Workshop on Targetry and Target Chemistry, Heidelberg, 1997 (abstract).

2.11. CARBON-11

Half life: 20.4 min.

Uses

Because carbon is the building block of all organic matter, ^{11}C can be substituted into these molecules without apparent disruption of the functional nature of the molecule [2.11.1]. However, in most cases, the ^{11}C is inserted in such a way as to produce an analogue of the target molecule; thus, this new molecule must be fully characterized with respect to its functional capacity.

Decay mode

Carbon-11 decays 100% by positron decay with a maximum β^+ energy of 968 keV.

Positron emission products of ^{11}C

Fraction	Maximum energy (MeV)	Average energy (MeV)
0.998	0.980	0.3856

Photon emission products of ^{11}C

Fraction	Energy (MeV)
2.00	0.5110

Nuclear reactions

While there are a number of routes to producing ^{11}C, only one is of importance in the context of routine production and use in biomedical research. The ^{14}N(p, α)^{11}C reaction using natural nitrogen gas is the

recommended mode. The production of ^{11}C from nitrogen has been studied extensively since the mid-1960s [2.11.2, 2.11.3]. The early papers dealt with the hot atom chemistry associated with radiogenic ^{11}C. The results of these early studies laid the groundwork for in situ production of the two most widely used ^{11}C species, $^{11}CO_2$ and $^{11}CH_4$ [2.11.4, 2.11.5]. These two precursor molecules can in turn be converted into a wide array of species for versatile labelling of biologically important molecules.

Excitation function

The excitation function for the $^{14}N(p, \alpha)^{11}C$ reaction is shown in Fig. 2.11.1.

Thick target yields of $^{14}N(p, \alpha)^{11}C$

Energy (MeV)	C-11 yield (GBq/(μA·h))	C-11 yield (mCi/(μA·h))
25→4	11.4	310
17→4	8.1	219
12.5→4	4.3	115
10→4	2.7	73

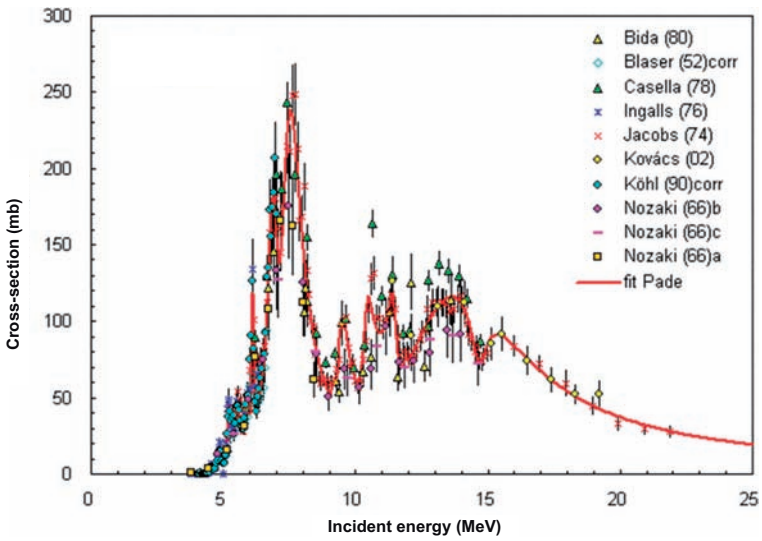

FIG. 2.11.1. Excitation function for the $^{14}N(p, \alpha)^{11}C$ reaction.

Target materials

The target material for producing $^{11}CO_2$ is nitrogen with a small percentage of O_2 (0.1–0.5%) [2.11.3, 2.11.4]. The minimum amount necessary to recover quantitatively the $^{11}CO_2$ generated is in dispute and apparently not reproducible, but a value in the above range has been shown to work. Early reports indicated that no added carrier oxygen was necessary, probably owing to the oxide layer in the target chamber. These reports all used aluminium target chambers. Aluminium readily oxidizes to form Al_2O_3. Anecdotal reports have shown that the production rate for such targets diminishes with time. There is speculation that the oxide layer is consumed over time. (See the Proceedings of the Workshops on Targetry and Target Chemistry (http://trshare.triumf.ca/~buckley/wttc/proceedings.html).)

The target material for $^{11}CH_4$ is nitrogen, with the carrier being hydrogen. The quantity of hydrogen appears to depend upon the size of the target chamber and the energy of the proton beam [2.11.6]. In addition, for small target chambers the material of choice appears to be niobium [2.11.6].

Target preparation

Ultra-high purity target gas is an absolute requirement if high SA ^{11}C is required. Specific activities as high as 100 Ci/μmol (EOB) (1 Ci = 37 GBq) have been reported (the theoretical SA is 9200 Ci/μmol and the typical SA is 1–20 Ci/μmol). All sources of carrier carbon need to be assessed and eliminated if possible [2.11.7–2.11.9].

Target processing

Extraction of $^{11}CO_2$ from the target gas by cryogenic trapping in a small metal loop is easy. Liquid nitrogen is typically used, although liquid argon is considered superior because the temperature is above that of liquid nitrogen and thus eliminates nitrogen trapping, thus keeping the total gas volume to a minimum. Transfer of the $^{11}CO_2$ to a synthesis unit is achieved by simply warming the loop and passing clean dry helium through the loop pushing the $^{11}CO_2$.

Starting with $^{11}CO_2$, it is possible to prepare simple small molecules such as CO, $COCl_2$, CHO, $MgBrCO_2$, CH_3OH and CH_4.

The production of $^{11}CH_4$ is usually associated with the on-line production of $^{11}CH_3I$ by reacting CH_4 with I_2 at high temperature (650ºC) [2.11.10, 2.11.11]. The choice is to produce $^{11}CO_2$ in the target and catalytically convert this into $^{11}CH_4$ on-line and finally into $^{11}CH_3I$. The idea of using $^{11}CH_4$ generated in situ

is to have a higher SA labelling agent. Nevertheless, a high SA can be generated while starting with CO_2 [2.11.7, 2.11.8, 2.11.10].

Enriched materials recovery

Natural isotopic nitrogen (99.6%) is used, and there is no need to recover the target material.

Specifications

Specific activity is the most important quantity associated with ^{11}C production. Most receptor based studies require a minimum of 500 mCi/μmol (end of synthesis, (EOS)) in order to maintain the tracer principle. In many cases, more than 1 Ci/μmol is required. Specific activity is determined by measuring the radioactivity as a function of molar mass. The means for determining mass may require the use of gas or liquid chromatography.

Radio-gas chromatography can be used for the initial set-up in order to verify the chemical nature of the gases emanating from the target.

REFERENCES TO SECTION 2.11

[2.11.1] FERRIERI, R.A., WOLF, A.P., The chemistry of positron emitting nucleogenic (hot) atoms with regard to preparation of labeled compounds of practical utility, Radiochim. Acta **34** (1983) 69–83.

[2.11.2] ACHE, H.J., WOLF, A.P., The effect of radiation on the reactions of recoil carbon-11 in the nitrogen–oxygen system, J. Phys. Chem. **72** (1968) 1988–1993.

[2.11.3] CHRISTMAN, D.R., FINN, R.D., KARLSTROM, K.I., WOLF, A.P., The production of ultra high activity ^{11}C-labelled hydrogen cyanide, carbon dioxide, carbon monoxide, and methane via the $^{14}N(p, \alpha)^{11}C$ reaction, Int. J. Appl. Radiat. Isot. **26** (1975) 435–442.

[2.11.4] VANDEWALLE, T., VANDECASTEELE, C., Optimisation of the production of $^{11}CO_2$ by proton irradiation of nitrogen gas, Int. J. Appl. Radiat. Isot. **34** (1983) 1459–1464.

[2.11.5] HELUS, F., HANISCH, M., LAYER, K., MAIER-BORST, W., Yield ratio of ^{11}C-CO_2, ^{11}C-CO, and ^{11}C-CH_4 from the irradiation of N_2/H_2 mixtures in the gas target, J. Labelled Compd. Radiopharm. **23** (1986) 1202–1205.

[2.11.6] BUCKLEY, K.R., HUSER, J., JIVAN, S., CHUN, K.S., RUTH, T.J., ^{11}C-methane production in small volume, high pressure gas targets, Radiochim. Acta **88** (2000) 201–205.

[2.11.7] SUZUKI, K., YAMAZAKI, I., SASAKI, M., KUBODERA, A., Specific activity of [^{11}C]CO_2 generated in a N_2 gas target: Effect of irradiation dose, irradiation history, oxygen content and beam energy, Radiochim. Acta **88** (2000) 211–216.

[2.11.8] NOGUCHI, J., SUZUKI, K., Automated synthesis of the ultra high specific activity of [^{11}C]Ro15-4513 and its application in an extremely low concentration region to an ARG study, Nucl. Med. Biol. **30** (2003) 335–343.

[2.11.9] ZHANG, M.-R., SUZUKI, K., Sources of carbon which decrease the specific activity of [^{11}C]CH_3I synthesized by the single pass I_2 method, Appl. Radiat. Isot. **62** (2005) 447–450.

[2.11.10] LINK, J.M., KROHN, K.A., CLARK, J.C., Production of [^{11}C]CH_3I by single pass reaction of [^{11}C]CH_4 with I_2, Nucl. Med. Biol. **24** (1997) 93–97.

[2.11.11] LARSEN, P., ULIN, J., DAHLSTRØM, K., JENSEN, M., Synthesis of [^{11}C]iodomethane by iodination of [^{11}C]methane, Appl. Radiat. Isot. **48** (1997) 153–157.

BIBLIOGRAPHY TO SECTION 2.11

BUCKLEY, K.R., JIVAN, S., RUTH, T.J., Improved yields for the in situ production of [^{11}C]CH_4 using a niobium target chamber, Nucl. Med. Biol. **31** (2004) 825–827.

INTERNATIONAL ATOMIC ENERGY AGENCY, Charged Particle Cross-section Database for Medical Radioisotope Production: Diagnostic Radioisotopes and Monitor Reactions, IAEA-TECDOC-1211, IAEA, Vienna (2001).

PROCEEDINGS OF THE WORKSHOP ON TARGETRY AND TARGET CHEMISTRY, http://www.triumf.ca/wttc/proceedings.html

TAKÁCS, S., TÁRKÁNYI, F., HERMANNE, A., PAVIOTTI DE CORCUERA, R., Validation and upgrading of the recommended cross section data of charged particle reactions used for production of PET radioisotopes, Nucl. Instrum. Methods Phys. Res. B **211** (2003) 169–189.

UNITED STATES NATIONAL NUCLEAR DATA CENTER, http://www.nndc.bnl.gov/index.jsp

2.12. CHLORINE-34m

Half-life

Chlorine-34m has a half-life of 32.0 min and decays via positron emission and electron capture. The ground state of ^{34}Cl decays with a 1.5 s half-life to stable ^{34}S. The positron energy is 2.5 MeV, and the gamma rays are fairly high in energy (2.1 and 1.2 MeV).

Parent nucleus	Parent energy level (keV)	Parent half-life (min)	Decay mode (%)	Daughter nucleus
Cl-34	146.36	32.00	IT[a]: 44.6	Cl-34

[a] IT: isomeric transition.

Electron emission products: Isomeric transitions

Fraction	Energy (keV)
0.0563	2.38
0.0624	143.5376
0.00551	146.0898

Photon emission products: Isomeric transitions

Fraction	Energy (keV)
0.00187	2.621
0.0038	2.622
0.00012	2.816
0.00024	2.816
0.405	146.36

Parent nucleus	Parent energy level	Parent half-life (min)	Decay mode	Daughter nucleus
Cl-34	146.36	32.00	EC: 55.4%	S-34

Positron emission products of ^{34m}Cl

Fraction	Energy (keV)	End point (keV)
0.00264	203.4	500.83
0.256	554.81	1311.43
0.284	1099.01	2488.08

Photon emission products of ^{34m}Cl

Fraction	Energy (keV)
0.00027	2.307
0.00055	2.308
1.28E–05	2.464
0.000025	2.464
1.085	511
0.1409	1176.626
0.00016	1572.59
0.00185	1987.18
0.428	2127.492
0.00033	2561.31
0.00022	2749.16
0.1229	3304.039
0.00273	4114.54

Nuclear reactions

The nuclear reactions that produce ^{34m}Cl are shown in the following table.

Nuclear reaction	Useful energy range (MeV)	Natural abundance (%)	References
^{35}Cl(p, pn)^{34m}Cl	20–30	75.8	[2.12.1, 2.12.2]
^{34}S(p, n)^{34m}Cl	15–25	4.21	[2.12.3, 2.12.4]
^{34}S(d, 2n)^{34m}Cl	15–25	4.21	[2.12.3, 2.12.4]
^{32}S(^{4}He, pn)^{34m}Cl	22–40	95.0	[2.12.4]
^{31}P(^{4}He, n)^{34m}Cl	12–30	100	[2.12.4]
^{35}Cl(^{4}He, ^{4}He n)^{34m}Cl	28–40	75.8	[2.12.4]
^{32}S(^{3}He, p)^{34m}Cl	10–25	95.0	[2.12.4]
^{35}Cl(^{3}He, ^{4}He)^{34m}Cl	15–30	75.8	[2.12.4]

Excitation function

The excitation function for the ^{34}S(p, n)^{34m}Cl reaction is shown in Fig. 2.12.1.

Thick target yields of ^{nat}S(p, x)^{34m}Cl

(from Ref. [2.12.5])

Energy (MeV)	Yield (μCi/(μA·h))
8.2	118.9189
9.67	189.1892
11.39	481.0811
12.79	956.7568
14.01	1297.297
15.61	1694.595
17.15	1943.243
18.99	2127.027
21.65	2405.405

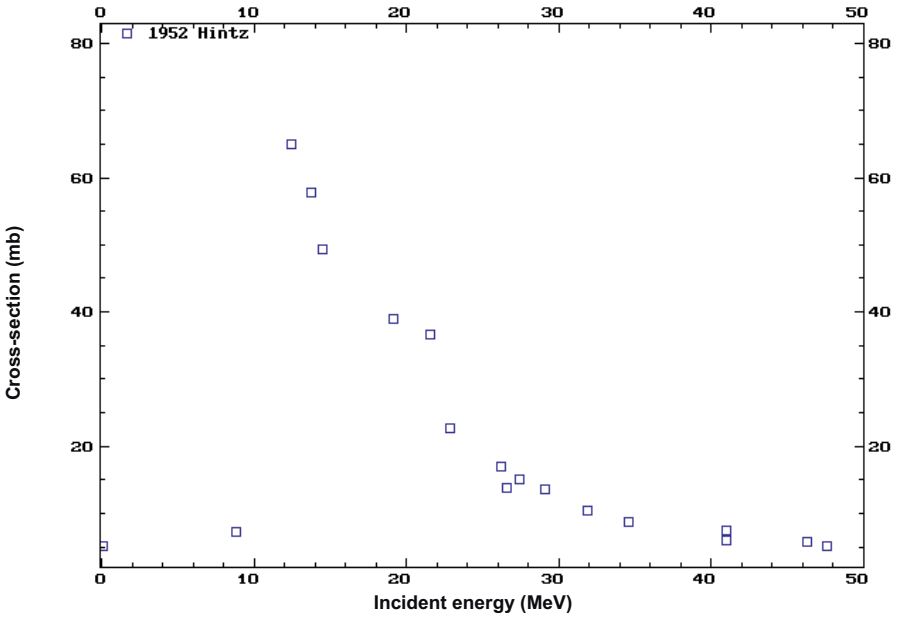

FIG. 2.12.1. Excitation function for the $^{34}S(p, n)^{34m}Cl$ reaction.

Excitation function

The excitation function for the $^{nat}Cl(p, x)^{34m}Cl$ reaction is shown in Fig. 2.12.2.

Thick target yields of $^{nat}S(\alpha, x)^{34m}Cl$

(from Ref. [2.12.1]).

This table is also continued on the next page.

Energy (MeV)	Yield (μCi/(μA·h))[a]
19.97	54.05405
23.7	2081.081
26.65	7351.351
29.71	13297.3
32.36	21054.05

Energy (MeV)	Yield (μCi/(μA·h))[a]
34.73	26135.14
37.21	30351.35
40.89	35297.3
44.23	38378.38

[a] 1 Ci = 37 GBq.

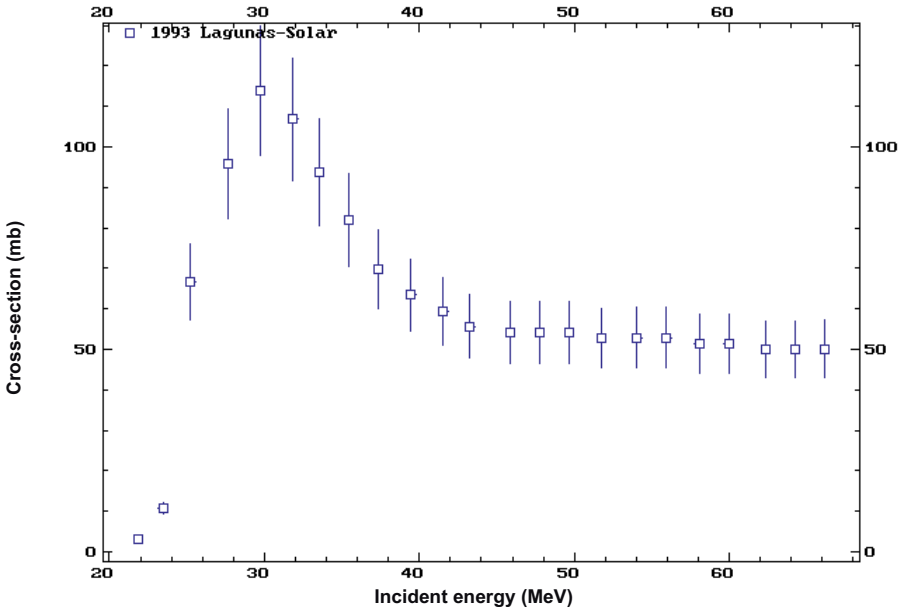

FIG. 2.12.2. Excitation function for the $^{nat}Cl(p, x)^{34m}Cl$ reaction.

REFERENCES TO SECTION 2.12

[2.12.1] LAGUNAS-SOLAR, M.C., CARVACHO, O.F., CIMA, R.R., Cyclotron production of PET radionuclides: ^{34m}Cl (33.99 min β^+53%; IT 47%) with protons on natural isotopic chlorine-containing targets, Appl. Radiat. Isot. **43** (1992) 1375–1381.

[2.12.2] WEINREICH, R., QAIM, S.M., STÖCKLIN, G., New excitation functions for the production of medically useful halogen radioisotopes, J. Labelled Compd. Radiopharm. **13** (1977) 233.
[2.12.3] ABRAMS, D.N., KNAUS, E.E., WIEBE, L.I., HELUS, F., MAIER-BORST, W., Production of ^{34m}Cl from a gaseous hydrogen sulfide target, Int. J. Appl. Radiat. Isot. **35** (1984) 1045–1048.
[2.12.4] ZATOLOKIN, B.V., KONSTANTINOV, I.O., KRASNOV, N.N., Thick target yields of ^{34m}Cl and ^{38}Cl produced by various charged particles on phosphorus, sulphur and chlorine targets, Int. J. Appl. Radiat. Isot. **27** (1976) 159–161.
[2.12.5] HINTZ, N.M., RAMSEY, N.E., Excitation functions to 100 MeV, Phys. Rev. **88** (1952) 19–27.

BIBLIOGRAPHY TO SECTION 2.12

LAGUNAS-SOLAR, M.C., HAFF, R.P., Theoretical and experimental excitation functions for proton induced nuclear reactions on Z = 10 to Z = 82 target nuclides, Radiochim. Acta **60** (1993) 57–67.

2.13. COBALT-55

Half-life

Cobalt-55 has a half-life of 17.6 h. It decays 23% by electron capture and 77% by positron emission. The end point energy of the positron is 1.5 MeV [2.13.1]. It has some higher energy gamma rays associated with the decay, and, in particular, a 931 keV gamma ray and a 1.4 MeV gamma ray with relatively high abundance. Cobalt-55 decays to ^{55}Fe, which has a 2.7 year half-life and decays exclusively by electron capture.

Parent nucleus	Parent energy level	Parent half-life (h)	Decay mode	Daughter nucleus
Co-55	0.0	17.53	EC: 100%	Fe-55

Positron emission products of ^{55}Co

Fraction	Energy (keV)	End point energy (keV)
0.000039	57.65	128
0.000178	94.53	217.1
0.000149	122.61	285.3
0.256	435.68	1020.8
0.0426	476.22	1112.7
0.46	648.98	1498

Electron emission products of ^{55}Co

Fraction	Energy (keV)
0.333	0.67
0.139	5.62
4.6E–06	378.3
1.39E–05	404.4
0.000169	470.09
1.11E–05	512.9
4.1E–06	796.59
0.000123	924
6.4E–06	1309.5

Photon emission products of ^{55}Co

This table is also continued on the next page.

Fraction	Energy (keV)
0.00201	0.7
0.022	6.391
0.0435	6.404

Fraction	Energy (keV)
0.0116	91.9
0.0107	411.5
0.202	477.2
1.52	511
0.0187	803.7
0.75	931.1
0.071	1316.6
0.029	1370
0.169	1408.5

Note: Gamma rays with less than 1% abundance are omitted from this table.

Nuclear reactions

The nuclear reactions that produce ^{55}Co are shown in the following table.

Nuclear reaction	Useful energy range (MeV)	Natural abundance (%)	References
^{58}Ni(p, α)^{55}Co	10–25	68.3	[2.13.2, 2.13.3]
^{56}Fe(p, 2n)^{55}Co	20–30	91.7	[2.13.4, 2.13.5]
^{54}Fe(d, n)^{55}Co	15–5	5.8	[2.13.6, 2.13.7]
^{55}Mn(^{3}He, 3n)^{52}Fe	15–25	100	[2.13.8]

Excitation function

The excitation functions for ^{55}Co are shown in Figs 2.13.1–2.13.3.

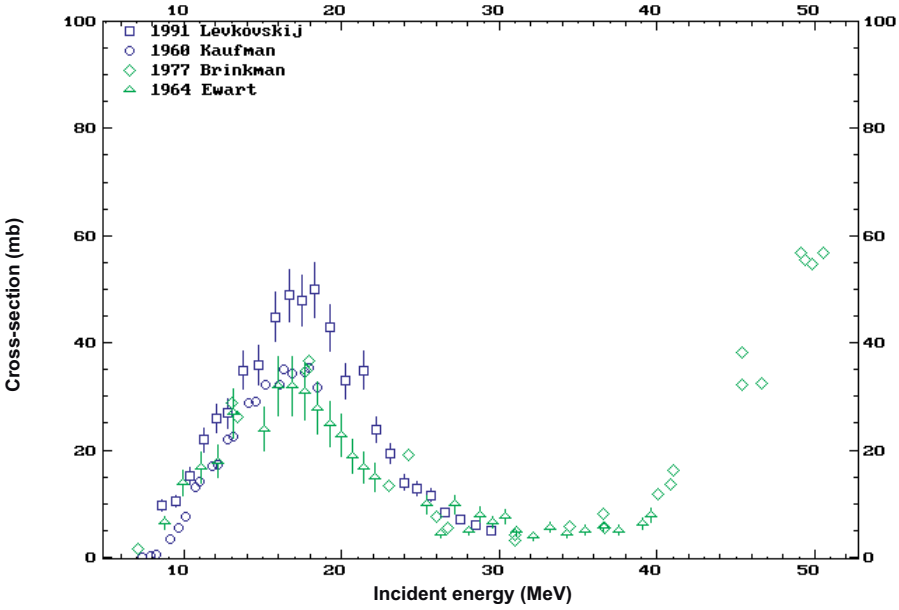

FIG. 2.13.1. Excitation function for the $^{58}Ni(p, \alpha)^{55}Co$ reaction.

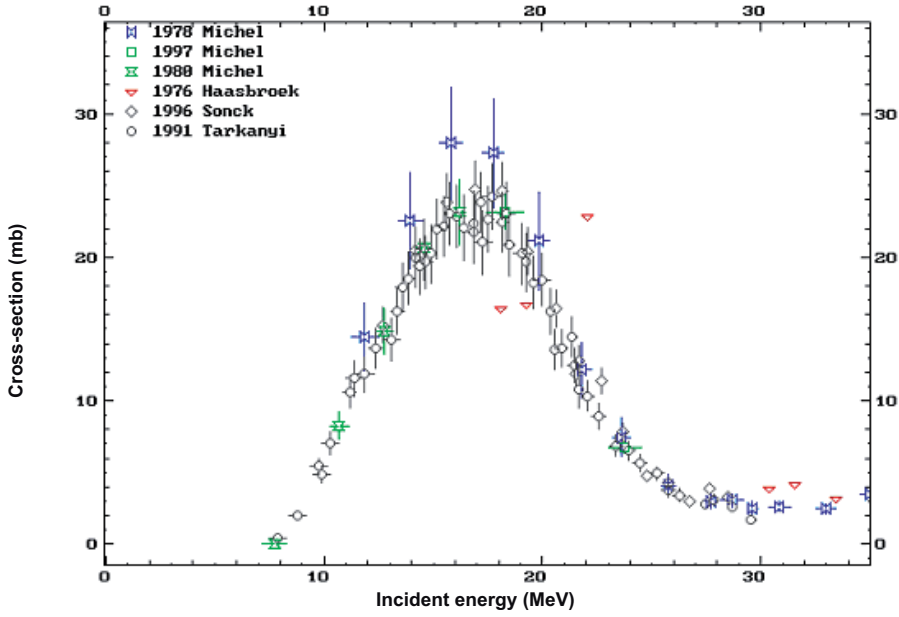

FIG. 2.13.2. Excitation function for the $^{nat}Ni(p, x)^{55}Co$ reaction.

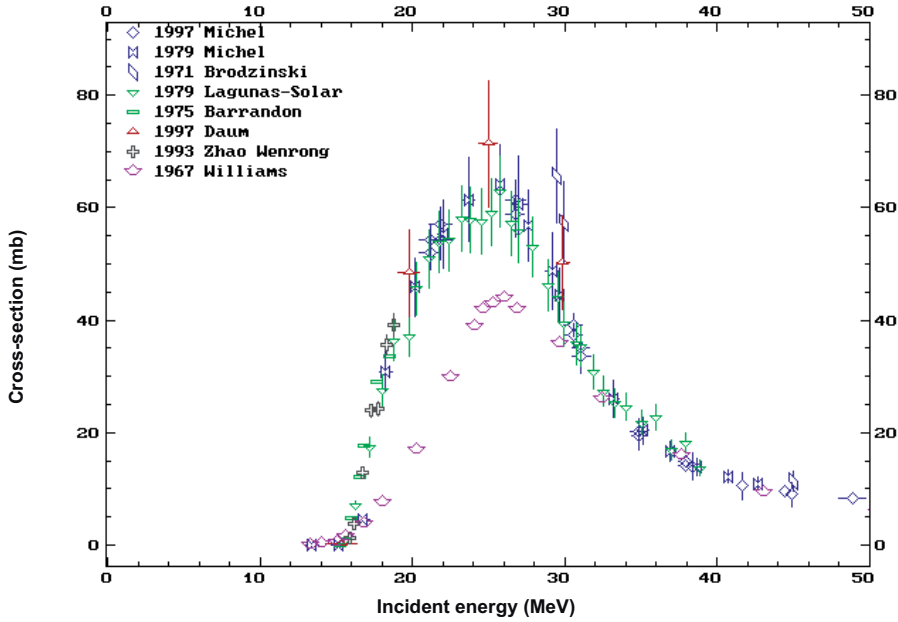

FIG. 2.13.3. Excitation function for the $^{nat}Fe(p, x)^{55}Co$ reaction.

REFERENCES TO SECTION 2.13

[2.13.1] GRÜTTER, A., Decay data of $^{55–58}Co$, ^{57}Ni, $^{60,61}Cu$ and $^{62,63}Zn$, Int. J. Appl. Radiat. Isot. **33** (1982) 533–535.

[2.13.2] REIMER, P., QAIM, S.M., Excitation functions of proton-induced reactions on highly enriched ^{58}Ni with special relevance to the production of ^{55}Co and ^{57}Co, Radiochim. Acta **80** (1998) 113–120.

[2.13.3] SPELLERBERG, S., REIMER, P., BLESSING, G., COENEN, H.H., QAIM, S.M., Production of ^{55}Co and ^{57}Co via proton induced reactions on highly enriched ^{58}Ni, Appl. Radiat. Isot. **49** (1998) 1519–1522.

[2.13.4] GOETHALS, P., SAMBRE, J., VOLKAERT, A., DAMS, R., "Production and applications of ^{55}Co in PET", Proc. 7th Workshop on Targetry and Target Chemistry, Heidelberg, 1997 (abstract) 217.

[2.13.5] LAGUNAS-SOLAR, M.C., JUNGERMAN, J.A., Cyclotron production of carrier-free cobalt-55, a new positron-emitting label for bleomycin, Int. J. Appl. Radiat. Isot. **30** (1979) 25–32.

[2.13.6] SHARMA, H., ZWEIT, J., SMITH, A.M., DOWNEY, S., Production of cobalt-55, a short-lived positron emitting radiolabel for bleomycin, Appl. Radiat. Isot. **37** (1986) 105–109.
[2.13.7] ZAMAN, M.R., QAIM, S.M., Excitation functions of (d, n) and (d, α) reactions on ^{54}Fe: Relevance to the production of high purity ^{55}Co at a small cyclotron, Radiochim. Acta **75** (1996) 59–63.
[2.13.8] WANTANABE, M., NAKAHARA, H., MURAKAMI, Y., ^{3}He bombardment of manganese for the production of ^{55}Co, Int. J. Radiat. Isot. **30** (1979) 625–630.

BIBLIOGRAPHY TO SECTION 2.13

BRINKMAN, G.A., HELMER, J., LINDNER, L., Nickel and copper foils as monitors for cyclotron beam intensities, Radiochem. Radioanal. Lett. **28** (1977) 9–19.

BRODZINSKI, R.L., RANCITELLI, L.A., COOPER, J.A., WOGMAN, N.A., High-energy proton spallation of iron, Phys. Rev. C **4** (1971) 1257–1265.

HAASBROEK, F.J., et al., Excitation Functions and Thick Target Yields for Radioisotopes Induced in Natural Mg, Co, Ni and Ta by Medium Energy Protons, Rep. CSIR-FIS-89, Laboratoire de chimie nucléaire analytique, Gradignan (1976).

KAUFMAN, S., Reactions of protons with Ni-58 and Ni-60, Phys. Rev. **117** (1960) 1532–1538.

KUBIK, P.-W., SYNAL, H.-A., FILGES, D., Cross sections for the production of residual nuclides by low- and medium-energy protons from the target elements C, N, O, Mg, Al, Si, Ca, Ti, V, Mn, Fe, Co, Ni, Cu, Sr, Y, Zr, Nb, Ba and Au, Nucl. Instrum. Methods Phys. Res. B **129** (1997) 153–193.

LEVKOVSKIJ, V.N., in Activation Cross Sections for the Nuclides of Medium Mass Region (A = 40–100) with Medium Energy (E = 10–50 MeV) Protons and Alpha-particles: Experiment and Systematics, Inter-Vesi, Moscow (1991).

MICHEL, R., BRINKMANN, G., On the depth-dependent production of radionuclides (A between 44 and 59) by solar protons in extraterrestial matter, J. Radioanal. Chem. **59** (1980) 467–510.

MICHEL, R., BRINKMANN, G., WEIGEL, H., HERR, W., Measurement and hybrid-model analysis of proton-induced reactions with V, Fe, and Co, Nucl. Phys., A **322** (1979) 40–60.

MICHEL, R., et al., Cross sections for the production of residual nuclides by low- and medium-energy protons from the target elements C, N, O, Mg, Al, Si, Ca, Ti, V, Mn, Fe, Co, Ni, Cu, Sr, Y, Zr, Nb, Ba and Au, Nucl. Instrum. Methods Phys. Res. B **129** (1997) 153–193.

MICHEL, R., WEIGEL, H., HERR, W., Proton-induced reactions on nickel with energies between 12 and 45 MeV, Z. Phys., A At. Nucl. **286** (1978) 393–400.

SONCK, M., VAN HOYWEGHEN, J., HERMANNE, A., Determination of the external beam energy of a variable energy multiparticle cyclotron, Appl. Radiat. Isot. **47** (1996) 445–449.

TAKÁCS, S., VASVÁRY, L., TÁRKÁNYI, F., Remeasurement and compilation of excitation function of proton induced reactions on iron for activation techniques, Nucl. Instrum. Methods Phys. Res. B **89** (1994) 88–94.

TÁRKÁNYI, F., SZELECSÉNYI, F., KOPECKY, P., Excitation functions of proton induced nuclear reactions on natural nickel for monitoring beam energy and intensity, Appl. Radiat. Isot. **42** (1991) 513–517.

WILLIAMS, I.R., FULMER, C.B., Excitation functions for radioactive isotopes produced by protons below 60 MeV on Al, Fe, and Cu, Phys. Rev. **162** (1967) 1055–1061.

ZHAO, W., LU, H., YU, W., Measurement of cross sections by bombarding Fe with protons up to 19 MeV, Chin. J. Nucl. Phys. **15** (1993) 337.

2.14. COBALT-57

Half-life: 271.8 d.

Uses

Cobalt-57 is used as a radiolabel for vitamin B_{12} in Schilling's test. The determination of gastrointestinal absorption of vitamin B_{12} was among the initial tests offered by nuclear medicine laboratories, and continues to be a useful procedure in the work-up and management of patients with megaloblastic anaemia, suspected vitamin B_{12} deficiency and gastrointestinal malabsorption. It has been used as a label for bleomycin and has been shown to be more sensitive than ^{67}Ga in the detection of certain tumours. Although the absorbed dose of patients with good renal function is low, the contamination hazards posed by this radionuclide with a half-life of 272 days have prevented

its widespread use. Unlike ^{67}Ga, ^{57}Co bleomycin is filtered by the kidneys, with no localization in normal tissue [2.14.1].

Sisson and Beierwaltes first suggested ^{57}Co labelled vitamin B_{12} to identify the parathyroid gland by an unclear mechanism. Unfortunately, vitamin B_{12} labelled with ^{57}Co cannot be used for external detection of the abnormal parathyroid gland, since excessive radiation is required to obtain a sufficient radioisotope concentration to identify the gland.

Electron emission products of ^{57}Co

Fraction	Energy (MeV)
0.001474	0.135630
0.001830	0.121220
0.011496	0.014320
0.014208	0.129360
0.018385	0.114950
0.077842	0.013567
0.695050	0.007301
1.054800	0.005620
2.493400	0.000670

Photon emission products of ^{57}Co

Fraction	Energy (MeV)
0.001599	0.692000
0.007754	0.000700
0.066234	0.007060
0.095429	0.014413
0.106030	0.136480
0.166290	0.006391
0.327990	0.006404
0.855100	0.122060

Nuclear reactions

There are several reactions for the production of ^{57}Co. The first is the alpha reaction on ^{55}Mn, ^{55}Mn(α, 2n)^{57}Co. The second reaction is the proton reaction on natural iron, ^{nat}Fe(p, x)^{57}Co, and the third is the proton reaction on natural nickel, ^{nat}Ni(p, x) ^{57}Co.

Excitation functions

The excitation functions for ^{57}Co are shown in Figs 2.14.1–2.14.3.

Target materials

A target insert with a 0.04 mm layer of enriched ^{58}Ni was electroplated onto a water cooled copper backing plate. The nickel layer should be thick enough to avoid copious production of unwanted ^{65}Zn in the copper backing plate. The high energy gamma rays emitted by ^{65}Zn and its long half-life complicate target handling and transport. The overall dimension of the insert is 8.1 cm × 3.1 cm × 1.5 cm, with thin cooling channels cut into the underside. The insert is compressed against a gasket in the copper target assembly to form a

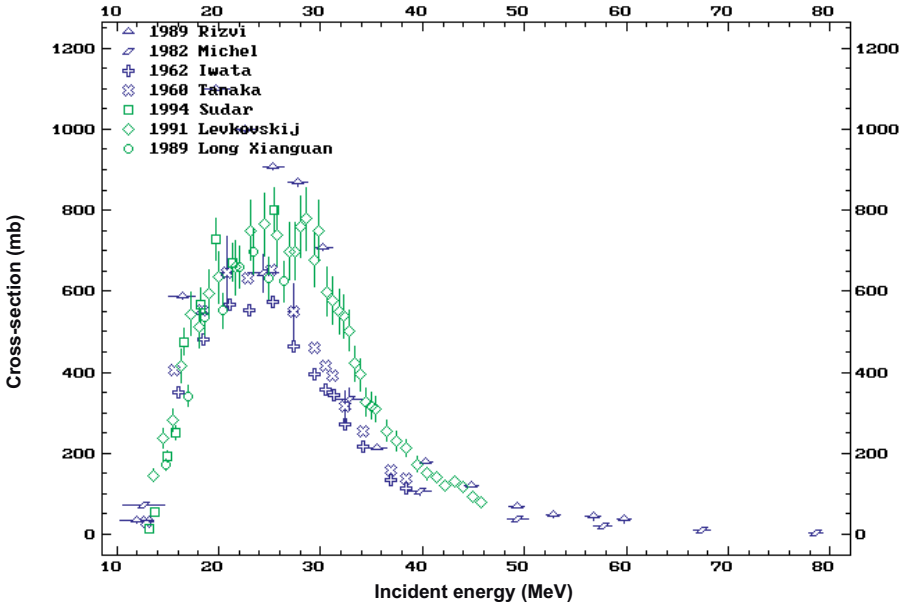

FIG. 2.14.1. Excitation function for the ^{55}Mn(α, 2n)^{57}Co reaction.

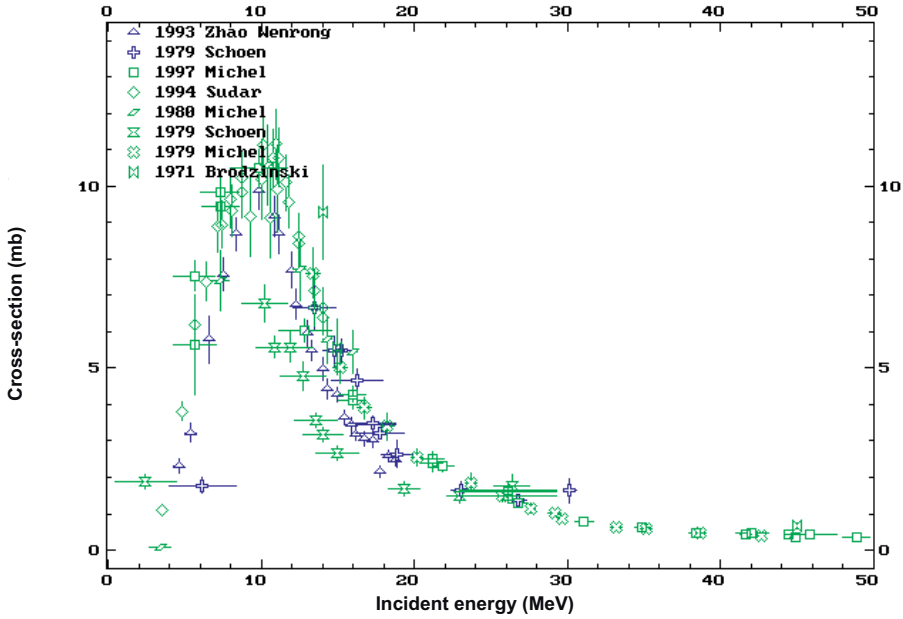

FIG. 2.14.2. Excitation function for the $^{nat}Fe(p, x)^{57}Co$ reaction.

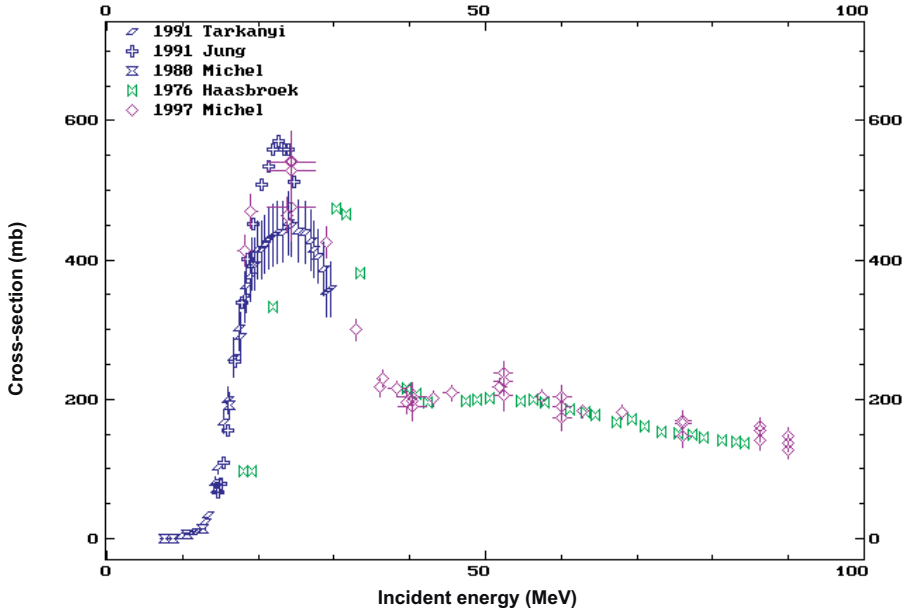

FIG. 2.14.3. Excitation function for the $^{nat}Ni(p, x)^{57}Co$ reaction.

water–vacuum seal. The entire target assembly is tilted at 7° with respect to the beam axis in order to reduce the power density.

The best combination of ^{57}Co yield and radiopurity was achieved with an energy window of 20–15 MeV. A target with natural nickel was irradiated at 20 MeV up to a beam current of 100 μA. There was no evidence of melting, flaking, mechanical distortion or sputtering.

Target preparation

The electrolytic solution is prepared by dissolving 500 mg ^{58}Ni in 5 mL concentrated HCl and a few drops of concentrated H_2O_2, evaporation to dryness and redissolution in about 5 mL water. Thereafter, 500 mg boric acid is added and, after dissolution, a few drops of dilute HCl are added to adjust the pH to about 3. The cell is filled with about 5 mL of the electrolytic solution, and the electrolysis is carried out at 2 ± 2.5 V, resulting in a current of 50 mA. The cell is maintained at 50ºC by electric heating. After an electroplating time of 2.5 h, the nickel deposit is washed with water and acetone, dried and weighed. Electrodeposited layers of ^{58}Ni of about 108 mm thickness (about 100 mg ^{58}Ni deposited on the area of 0.7 cm × 1.9 cm) are obtained. Thicker layers than this are difficult to produce.

Target processing

Chemical processing of the irradiated target has two goals:

(1) To obtain ^{55}Co and ^{57}Co in a pure form;
(2) To recover the highly enriched target material for reuse. The adopted procedure is described in the the following paragraph.

The irradiated target is removed from the target holder and transferred to the same electrolytic cell as used for electroplating. About 5 mL of 8M HCl are then filled into the cell and the electrolytic circuit is closed. On reversing the polarity, ^{58}Ni and radiocobalt go into solution and are thus separated from the copper backing. The current used was about 500 mA. By heating, the solution is then evaporated almost to dryness, the residue taken up in 12M HCl and subjected to anion exchange chromatography. As an alternative, the target surface layers may be dissolved in 8M HNO_3. After dissolution, the purification can be performed according to the following procedure:

(1) Convert solution to 12N HCl, and pass through a BioRad AG1X8 column and 100–200 mesh.

(2) Elute with 30mL of 8N HCl, 30mL of 6N HCl, 40 mL of 4.5N HCl and 40 mL of 0.1N HCl.
(3) Combine all 6–4.5N HCl fractions containing cobalt and some copper, and convert solution to 0.5M ammonium acetate.
(4) Load a Chelex column and wash with 35 mL of water.
(5) Elute the cobalt fraction with 50 mL of 0.1N HCl.

Specifications

The specifications of the ^{57}Co are:

(a) The chemical process recovers about 70% of the cobalt.
(b) Copper, silver, nickel, zinc and cadmium are analysed by gamma spectroscopy and ICP-AES.
(c) All of these metals are undetectable in the final product.

REFERENCE TO SECTION 2.14

[2.14.1] REIMER, P., QAIM, S.M., Excitation functions of proton induced reactions on highly enriched ^{58}Ni with special relevance to the production of ^{55}Co and ^{57}Co, Radiochim. Acta **80** (1998) 113–120.

BIBLIOGRAPHY TO SECTION 2.14

ALEKSANDROV, V.N., SEMENOVA, M.P., SEMENOV, V.G., Production cross section of radionuclides in (p, x) reactions at copper and nickel nuclei, At. Energ. **62** (1987) 411–413.

HAASBROEK, F.J., et al., Excitation functions and thick target yields for radioisotopes induced in natural Mg, Co, Ni and Ta by medium energy protons, Int. J. Appl. Radiat. Isot. **28** (1977) 533–534.

IWATA, S.J., Isomeric cross section ratios in alpha-particle reactions, J. Phys. Soc. Jpn. **17** (1962) 1323.

JONKERS, G., VONKEMAN, K., VAN DER WAL, S., VAN SANTEN, R., Surface catalysis studied by in situ positron emission, Nature **355** (1992) 63–66.

MICHEL, R., BRINKMANN, G., On the depth-dependent production of radionuclides (*A* between 44 and 59) by solar protons in extraterrestial matter, J. Radioanal. Chem. **59** (1980) 467–510.

MICHEL, R., et al., Cross sections for the production of residual nuclides by low- and medium-energy protons from the target elements C, N, O, Mg, Al, Si, Ca, Ti, V, Mn, Fe, Co, Ni, Cu, Sr, Y, Zr, Nb, Ba and Au, Nucl. Instrum. Methods Phys. Res. B **129** (1997) 153–193.

MICHEL, R., WEIGEL, H., HERR, W., Proton-induced reactions on nickel with energies between 12 and 45 MeV, Z. Phys., A At. Nucl. **286** (1978) 393.

SCHOEN, N.C., ORLOV, G., McDONALD, R.J., Excitation functions for radioactive isotopes produced by proton bombardment of Fe, Co, and W in the energy range from 10 to 60 MeV, Phys. Rev. C **20** (1979) 88–92.

SPELLERBERG, S., REIMER, P., BLESSING, G., COENEN, H., QAIM, S.M., Production of ^{55}Co and ^{57}Co via proton induced reactions on highly enriched ^{58}Ni, Appl. Radiat. Isot. **49** (1998) 1519–1522.

SUDÁR, S., QAIM, S.M., Excitation functions of proton and deuteron induced reactions on iron and alpha-particle induced reactions on manganese in the energy region up to 25 MeV, Phys. Rev. C **50** (1994) 2408–2419.

TANAKA, S., et al., Excitation functions for alpha-induced reactions on manganese-55, J. Phys. Soc. Jpn. **15** (1960) 545.

TÁRKÁNYI, F., SZELECSÉNYI, F., KOPECKY, P., Excitation functions of proton induced nuclear reactions on natural nickel for monitoring beam energy and intensity, Appl. Radiat. Isot. **42** (1991) 513–517.

ZAMAN, M.R., SPELLERBERG, S., QAIM, S.M., Production of ^{55}Co via the ^{54}Fe(d, n)-process and excitation functions of ^{54}Fe(d, t)^{53}Fe and ^{54}Fe(d, α)^{52m}Mn reactions from threshold up to 13.8 MeV, Radiochim. Acta **91** (2003) 105–108.

2.15. COPPER-61

Half-life

Copper-61 has a 3.4 h half-life and decays with a positron emission having a 1.2 MeV end point energy in 61% of the decays. The other decay mode is electron capture, which results in gamma rays predominately at 283 and 656 keV.

Positron emission products of ^{61}Cu

Fraction	Maximum energy (MeV)	Average energy (MeV)
0.000368	0.307800	0.133100
0.019800	1.149000	0.494200
0.025400	0.560390	0.238800
0.056000	0.933440	0.399300
0.513000	1.216400	0.524200

Electron emission products of ^{61}Cu

Fraction	Energy (MeV)
0.004766	0.059079
0.203670	0.006540
0.514960	0.000840

Photon emission products of ^{61}Cu

Fraction	Energy (MeV)
0.011808	0.588600
0.011931	0.908630
0.017115	0.008260
0.021156	0.373050
0.036285	1.185200
0.038745	0.067412
0.042708	0.007461
0.084070	0.007478
0.104920	0.656010
0.123000	0.282960
1.229100	0.511000

Nuclear reactions

The nuclear reactions that produce ^{61}Cu are shown in the following table.

Nuclear reaction	Useful energy range (MeV)	Natural abundance (%)	References
^{nat}Ni(α, p)^{61}Cu	15–25	100	[2.15.1]
^{61}Ni(p, n)^{61}Cu	9–12	1.13	[2.15.2]
^{59}Co(α, 2n)^{61}Cu	35–45	100	[2.15.3]
^{59}Co(^{3}He, n)^{61}Cu	30–40	100	[2.15.3]
^{60}Ni(d, n)^{61}Cu	10	26.1	[2.15.4]

Excitation functions

The excitation functions for ^{61}Cu are shown in Figs 2.15.1–2.15.3.

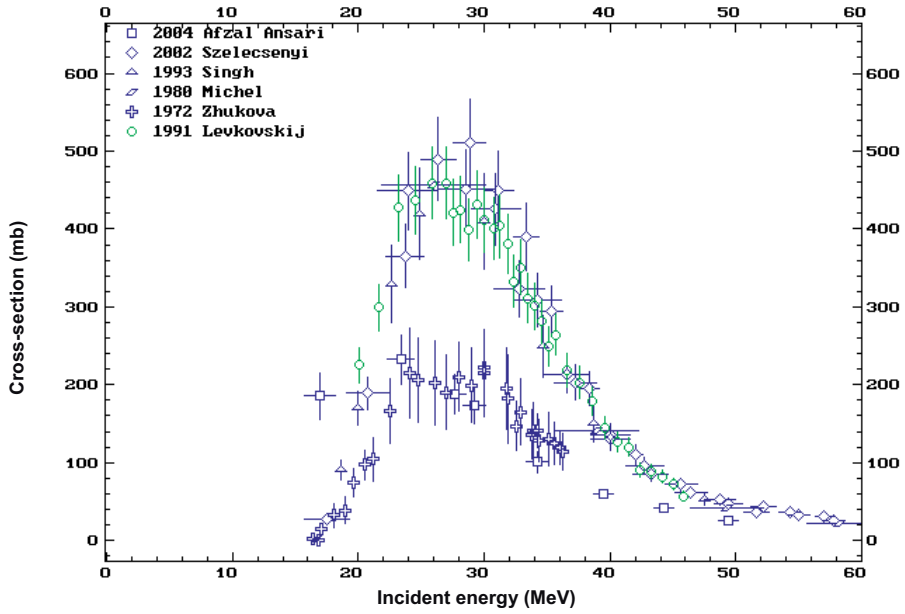

FIG. 2.15.1. Excitation function for the ^{59}Co(α, 2n)^{61}Cu reaction.

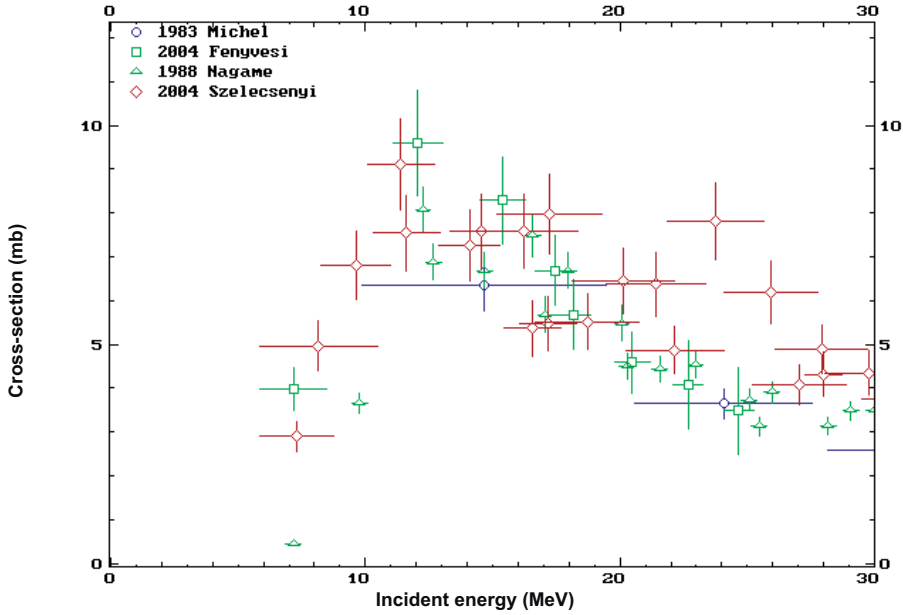

FIG. 2.15.2. Excitation function for the $^{59}Co(^{3}He, n)^{61}Cu$ reaction.

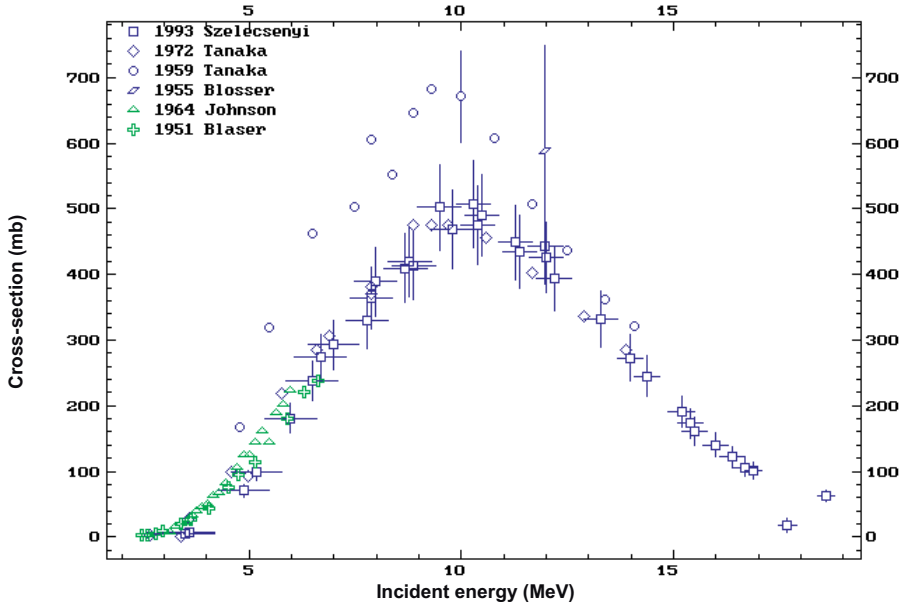

FIG. 2.15.3. Excitation function for the $^{61}Ni(p, n)^{61}Cu$ reaction.

REFERENCES TO SECTION 2.15

[2.15.1] MURAMATSU, H., SHIRAI, E., NAKAHARA, H., MURAKAMI, Y., Alpha particle bombardment of natural nickel target for the production of ^{61}Cu, Int. J. Radiat. Appl. Instrum. A **29** (1978) 611–615.

[2.15.2] SZELECSÉNYI, F., et al., Formation of ^{60}Cu and ^{61}Cu via Co + ^{3}He reactions up to 70 MeV: Production possibility of ^{60}Cu for PET studies, Nucl. Instrum. Methods Phys. Res. B **222** (2004) 364–370.

[2.15.3] HOMMA, Y., MURAKAMI, Y., Production of ^{61}Cu by α and ^{3}He bombardments on cobalt target, Chem. Lett. (Tokyo) **49** (1976) 397–400.

[2.15.4] McCARTHY, D.W., et al., "The efficient production of various positron copper radionuclides using a biomedical cyclotron", Proc. 7th Workshop on Targetry and Target Chemistry, Heidelberg, 1997 (abstract) 203–204.

BIBLIOGRAPHY TO SECTION 2.15

FENYVESI, A., TÁRKÁNYI, F., HESELIUS, S.J., Excitation functions of nuclear reactions induced by He-3 particles in cobalt, Nucl. Instrum. Methods Phys. Res. B **222** (2004) 355–363.

MICHEL, R., GALAS, M., He3-induced reactions on cobalt, Nucl. Phys., A **404** (1983) 77–92.

NAGAME, Y., NAKAMURA, Y., TAKAHASHI, M., SUEKI, K., NAKAHARA, H., Pre-equilibrium process in He3-induced reactions on Co-58, Ag-109, Ta-181 and Bi-209, Nucl. Phys., A **486** (1988) 77–90.

SZELECSÉNYI, F., STEYN, G.F., KOVÁCS, Z., VAN DER WALT, T.N., SUZUKI, K., Comments on the feasibility of ^{61}Cu production by proton irradiation of ^{nat}Zn on a medical cyclotron, Appl. Radiat. Isot. **64** (2006) 789–791.

2.16. COPPER-64

Half-life: 12.7 h.

Uses

There is an extensive literature discussing the use of copper in nuclear medicine [2.16.1]. Copper-64 has become of great interest in the last few years as a potential PET tracer because of its half-life, the fact that it is a positron emitter, and

its ability to be incorporated into complex molecules through chelating chemistry previously developed for ^{67}Cu. The chemistry continues to be developed because the original cages were not capable of holding the copper in place, in vivo. In addition, there is interest in using ^{64}Cu as a potential radiotherapeutic isotope because of its beta decay (both β^- and β^+). Smith provides an extensive review of the production and use of ^{64}Cu, with an excellent bibliography [2.16.2].

Decay mode

Copper-64 is a unique radionuclide as it decays by electron capture (44%), positron emission (17%) and β^- emission (39%). Thus, ^{64}Cu can be imaged by positron emission tomography, in addition to having the therapeutic potential associated with its beta particles (β^+ or β^-).

Positron emission products of ^{64}Cu

Fraction	Maximum energy (MeV)	Average energy (MeV)
0.174	0.653	0.2782

Electron emission products of ^{64}Cu

Fraction	Maximum energy (MeV)	Average energy (MeV)
0.390	0.578	0.1902

Photon emission products of ^{64}Cu

Fraction	Energy (MeV)
0.348	0.5110
0.00473	1.346
0.0947	0.007478
0.0485	0.007461
0.0197	0.008260
0.00486	0.000850
0.224	0.00654
0.574	0.000840

Nuclear reactions

Copper-64 can be produced in several ways: ^{64}Ni(p, n)^{64}Cu, ^{68}Zn(p, αn)^{64}Cu or ^{66}Zn(d, α)^{64}Cu, with the first reaction being more commonly used.

Copper-64 production via the ^{64}Ni(p, n)^{64}Cu reaction

The direct (p, n) reaction on highly enriched ^{64}Ni leads to large amounts of no carrier added (NCA) ^{64}Cu [2.16.3–2.16.5]. A relatively high current target has been produced by electroplating enriched target material on to a water cooled gold backing plate [2.16.6].

Production of ^{64}Cu via the ^{68}Zn(p, αn)^{64}Cu or ^{66}Zn(d, α)^{64}Cu reaction has also been reported, as well as via charged particle irradiation of natural zinc and enriched zinc targets [2.16.7, 2.16.8].

Excitation functions

The excitation functions for ^{64}Cu are shown in Figs 2.16.1–2.16.4.

Production by the deuteron reaction on enriched nickel has been described [2.16.9, 2.16.10] (Fig. 2.16.3).

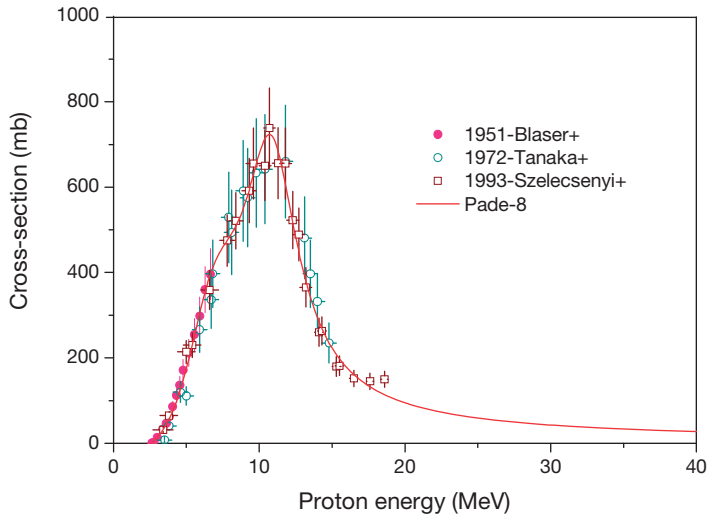

FIG. 2.16.1. Excitation function for the ^{64}Ni(p, n)^{64}Cu reaction.

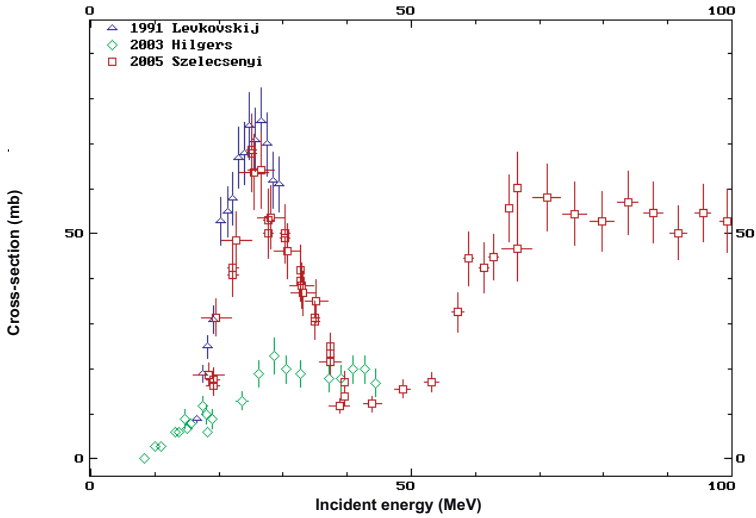

FIG. 2.16.2. Excitation function for the $^{68}Zn(p,\alpha n)^{64}Cu$ reaction.

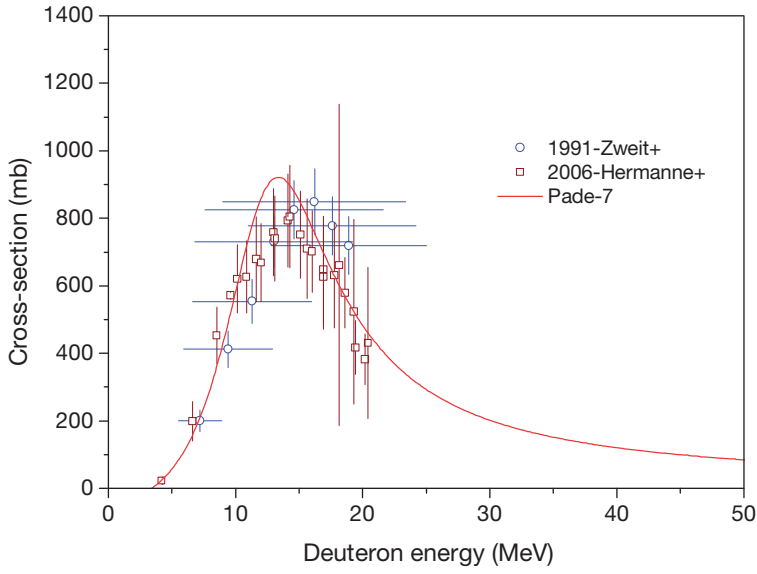

FIG. 2.16.3. Excitation function for the $^{64}Ni(d, 2n)^{64}Cu$ reaction.

Production using deuterons with enriched ^{66}Zn has also been proposed [2.16.7, 2.16.11] (Fig. 2.16.4).

Thick target yields of ^{66}Zn(d, α)^{64}Cu [2.16.7]

Energy range (MeV)	Yield (MBq/(μA·h))(μCi/(μA·h))
19–7	30.7 (830)

Target materials

Enriched ^{64}Ni (0.93% natural abundance) and enriched ^{68}Zn (18.8% natural abundance) are the required starting materials.

Target preparation

For nickel targets, enriched ^{64}Ni was plated on to a gold disc by electrodeposition. Details are contained in Ref. [2.16.4].

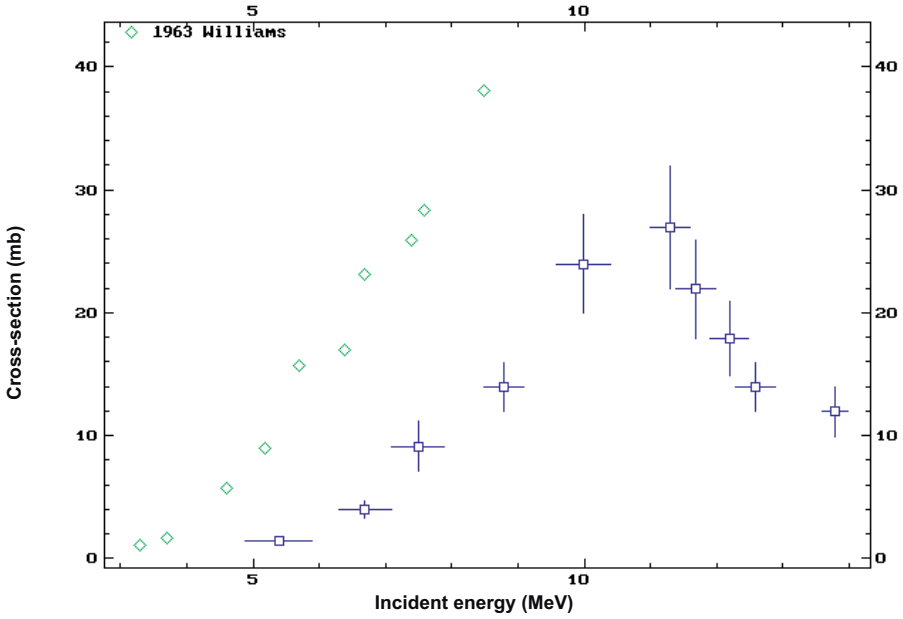

FIG. 2.16.4. Excitation function for the ^{66}Zn(d,α)^{64}Cu reaction.

Zinc targets were prepared by electrolytic deposition via a method described earlier [2.16.7]. About 50 mg of zinc was dissolved in 10 mL of 1M HCl, and 1 mL of this solution was transferred to an electrolytic cell. The electrolytic deposition was carried out on a gold foil (10 or 25 mm thick) at 5 V and a current of about 0.3 A for approximately 1 h. A rotating platinum foil was used as anode to avoid contact of the originating gas bubbles with the cathode foil (gold). Within 30 min, the current had decreased to 0.05 A. After 1 h, it had fallen to 0.01 A. The thin samples were rinsed with water and ethanol.

Target processing

$^{64}Ni(p, n)^{64}Cu$

After irradiation, the target material is dissolved off the target holder in HCl and then placed in an anion exchange column. The nickel fraction is eluted with 6.0N HCl, and the copper radioisotopes are eluted with water [2.16.4]. Alternatively, mixtures of ethanol and HCl may be used to separate ^{64}Cu from an enriched nickel target [2.16.5]. The use of this target system leads to the co-production of ^{61}Co contaminant, which can also be removed via anion exchange chromatography with ethanol/HCl mixtures [2.16.5]. Enriched ^{64}Ni is very expensive due to its naturally occurring low abundance (0.926%), and thus recycling of the target material is necessary, which is relatively simple with these methods.

$^{68}Zn(p, \alpha n)^{64}Cu$ or $^{66}Zn(d, \alpha)^{64}Cu$

Usually, a separation scheme involves isopropyl ether [2.16.7, 2.16.11] extraction (to extract the radiogallium contaminants) followed by anion exchange chromatography to separate the copper isotopes from the zinc target [2.16.7, 2.16.11]. The zinc is retained on a strong anion exchange column, while the copper is eluted with 2.0N HCl [2.16.11]. Alternatively, the copper and gallium isotopes can be co-extracted from the zinc target with carbon tetrachloride [2.16.12], followed by anion exchange chromatography for the separation of copper and gallium. Other extraction methods for the separation of copper and gallium isotopes involving organic liquid anion exchangers have been reported [2.16.7], as well as solvent extraction approaches.

Recovery of enriched materials

Recovery of enriched nickel

The following method is described in Ref. [2.16.6]. A 6.0N HCl fraction (containing enriched material) was heated to 150°C and evaporated to dryness in a silica glass flask. High purity water was added, and complete evaporation was again achieved. The residue was heated to 900°C in an oven. After heating for over 24 h, the ^{64}Ni was converted to ^{64}NiO, after which it was ready for target preparation.

Recovery of enriched zinc

Recovery of zinc target material was carried out by a method described in the literature [2.16.7]. The method consisted of precipitation of zinc as ZnS with Na_2S from a 5M NaOH solution. The precipitate was washed with water and centrifuged, then dissolved in concentrated HCl and re-precipitated at a pH of 8. The precipitate was washed and heated at 400 K to obtain ZnO.

Specifications

The enriched ^{64}Ni used for bombardment contains certain amounts of other nickel nuclides, for example, according to Ref. [2.16.6], 2.67% of ^{58}Ni, 1.75% of ^{60}Ni, 0.11% of ^{61}Ni and 0.67% of ^{62}Ni, in addition to 94.8 ± 0.4% of ^{64}Ni.

Care must be exercised in determining the quantify of ^{64}Cu, because of the low abundance of the 1346 keV photon. Depending upon the enrichment of nickel, there is the possibility of co-producing several radioisotopes: ^{60}Cu, ^{61}Cu, ^{55}Co, ^{61}Co and ^{57}Ni. However, with enrichments of around 95%, only trace amounts of ^{55}Co are detected and ^{64}Cu is produced with a purity of more than 99%. When using zinc targets, there will be the potential for large amounts of gallium isotopes to be co-produced. However, these can be effectively removed via solvent extraction [2.16.12]. There are no reported isotopic impurities associated with the ^{66}Zn(d, α)^{64}Cu reaction [2.16.11].

REFERENCES TO SECTION 2.16

[2.16.1] BLOWER, P.J., LEWIS, J.S., ZWEIT, J., Copper radionuclides and radiopharmaceuticals in nuclear medicine, Nucl. Med. Biol. **23** (1996) 957–980.

[2.16.2] SMITH, S.V., Molecular imaging with copper-64, J. Inorg. Biochem. **98** (2004) 1874–1901.
[2.16.3] SZELECSÉNYI, F., BLESSING, G., QAIM, S.M., Excitation functions of proton induced nuclear reaction on enriched Ni-61 and Ni-64: Possibility of production of no-carrier-added Cu-61 and Cu-64 at a small cyclotron, Appl. Radiat. Isot. **44** (1993) 575–580.
[2.16.4] McCARTHY, D.W., et al., Efficient production of high specific activity ^{64}Cu using a biomedical cyclotron, Nucl. Med. Biol. **24** (1997) 35–43.
[2.16.5] HOU, X., JACOBSON, U., JORGENSEN, J.C., Separation of no-carrier-added ^{64}Cu from a proton irradiated ^{64}Ni enriched target, Appl. Radiat. Isot. **57** (2002) 773–777.
[2.16.6] OBATA, A., et al., Production of therapeutic quantities of ^{64}Cu using a 12 MeV cyclotron, Nucl. Med. Biol. **30** (2003) 535–539.
[2.16.7] HILGERS, K., STOLL, T., SKAKUN, Y., COENEN, H.H., QAIM, S.M., Cross-section measurements of the nuclear reactions ^{nat}Zn(d, x)^{64}Cu, ^{66}Zn(d, α)^{64}Cu and ^{68}Zn(p, αn)^{64}Cu for production of ^{64}Cu and technical developments for small-scale production of ^{67}Cu via the ^{70}Zn(p, α)^{67}Cu process, Appl. Radiat. Isot. **59** (2003) 343–351.
[2.16.8] SZELECSÉNYI, F., et al., Investigation of the ^{66}Zn(p, 2pn)^{64}Cu and ^{68}Zn(p, x)^{64}Cu nuclear processes up to 100 MeV: Production of ^{64}Cu, Nucl. Instrum. Methods **240** (2005) 625–637.
[2.16.9] ZWEIT, J., SMITH, A.M., DOWNEY, S., SHARMA, H.L., Excitation functions for deuteron induced reactions in natural nickel: Production of no-carrier added Cu-64 from enriched Ni-64 targets for positron emission tomography, Appl. Radiat. Isot. **42** (1991) 193.
[2.16.10] HERMANNE, A., TÁRKÁNYI, F., TAKÁCS, S., KOVALEV, S.F., IGNATYUK, A., Activation cross sections of the ^{64}Ni(d, 2n)^{64}Cu reaction for the production of the medical radionuclide ^{64}Cu, Nucl. Instrum. Methods Phys. Res. B **258** (2007) 308–312.
[2.16.11] BONARDI, M.L., et al., Cross section studies on ^{64}Cu with zinc target in the proton energy range from 141 down to 31 MeV, J. Radioanal. Nucl. Chem. **264** (2005) 101–105.
[2.16.12] KASTLEINER, S., COENEN, H.H., QAIM, S.M., Possibility of production of ^{67}Cu at a small-sized cyclotron via the (p, α)-reaction on enriched ^{70}Zn, Radiochim. Acta **84** (1999) 107–110.

BIBLIOGRAPHY TO SECTION 2.16

INTERNATIONAL ATOMIC ENERGY AGENCY, Charged Particle Cross-section Database for Medical Radioisotope Production: Diagnostic Radioisotopes and Monitor Reactions, IAEA-TECDOC-1211, IAEA, Vienna (2001).

LAMBRECHT, R.M., SAJJAD, M., SYED, R.H., MEYER, W., Target preparation and recovery of enriched isotopes for medical radionuclide production, Nucl. Instrum. Methods Phys. Res. A **282** (1989) 296.

MUSHTAQ, A., QAIM, S.M., Excitation functions of α- and ^{3}He-particle induced nuclear reactions on natural germanium: Evaluation of production routes for ^{73}Se, Radiochim. Acta **50** (1990) 27–31.

TAKÁCS, S., TÁRKÁNYI, F., KIRALY, B., HERMANNE, A., SONCK, M., Evaluated activation cross sections of longer-lived radionuclides produced by deuteron-induced reactions on natural copper, Nucl. Instrum. Methods Phys. Res. B **251** (2006) 56–65.

TANAKA, S., FURUKAWA, M., CHIBA, M., Nuclear reactions of nickel with protons up to 56 MeV, J. Inorg. Nucl. Chem. **34** (1972) 2419–2426.

2.17. COPPER-67

Half-life: 62 h.

Uses

Copper-67 is an attractive radioisotope for radiotherapy. It has a long enough half-life for accumulation in a tumour tissue using monoclonal antibodies. Copper-67 decays to a stable daughter, ^{67}Zn.

Decay mode

Copper-67 is the longest lived radionuclide of copper, with a half-life of 62 h. It decays entirely by β^- emission: 50% to the 185 keV excited state of ^{67}Zn, resulting in the emission of a 0.395 MeV (E_{max}) particle; 20% to the ground state of ^{67}Zn, emitting a 0.577 MeV particle; 22% to the 93 keV state of ^{67}Zn, emitting a 0.484 MeV particle; and 1.2% to the 393 keV excited state of ^{67}Zn. These transitions give rise to three gamma rays, suitable for single photon imaging, with energies of 91 (7%), 93 (16%) and 185 (48%) keV, permitting imaging of the radionuclide distribution during therapy.

Beta emission products of ^{67}Cu

Fraction	Maximum energy (MeV)	Average energy (MeV)
0.011000	0.181470	0.050700
0.200000	0.575000	0.189000
0.220000	0.481690	0.154000
0.570000	0.390420	0.121000

Electron emission products of ^{67}Cu

Fraction	Energy (MeV)
0.004894	0.093175
0.005110	0.081607
0.008230	0.174920
0.014812	0.092117
0.069945	0.007530
0.120910	0.083652
0.191060	0.000990

Photon emission products of ^{67}Cu

Fraction	Energy (MeV)
0.000960	0.001010
0.001150	0.208950
0.002200	0.393530
0.007649	0.009570
0.007970	0.300220
0.019136	0.008616
0.037522	0.008639
0.070000	0.091266
0.161000	0.093311
0.487000	0.184580

Nuclear reactions

There are several reactions that may be used to produce ^{67}Cu. Most of these reactions require the use of high energy proton beams or an alpha particle beam. The only low energy reaction is the proton reaction on enriched ^{70}Zn, but this reaction has a small cross-section. The nuclear reactions that have been suggested for the production of ^{67}Cu, in quantities relevant to nuclear medicine applications, include ^{68}Zn(p, 2p), ^{68}Zn(d, 2pn), ^{67}Zn(d, 2p), ^{64}Ni(α, p), RbBr(p, spall), As(p, spall) and ^{67}Zn(n, p).

Excitation functions

The excitation functions for ^{67}Cu are shown in Figs 2.17.1–2.17.3.

Target materials

All of the common nuclear reactions used to produce ^{67}Cu rely on enriched isotopes as target materials. These isotopes have fairly low natural abundances with ^{70}Zn at 0.6%, ^{68}Zn at 18.8% and ^{64}Ni at 0.96%, thus making

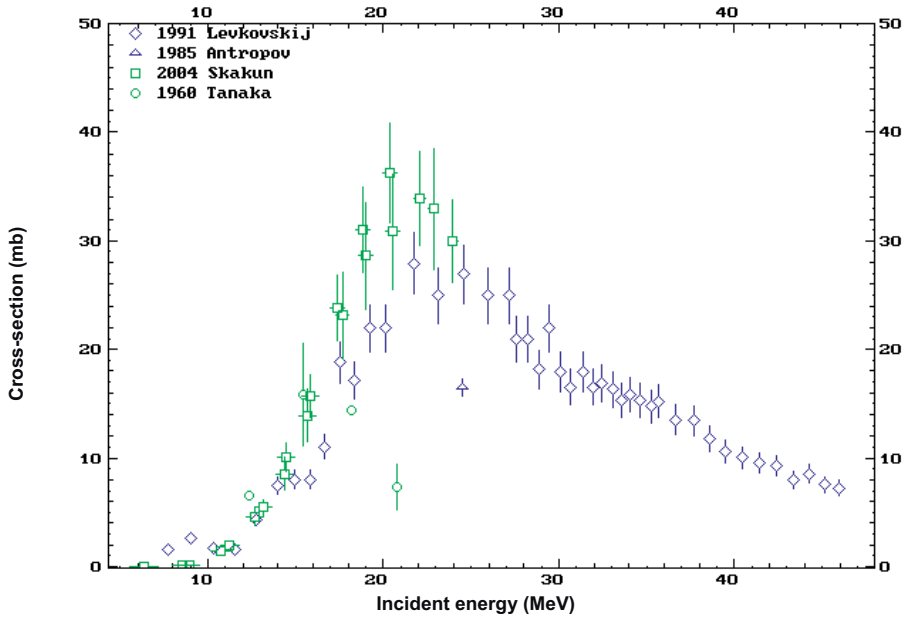

FIG. 2.17.1. Excitation function for the ^{64}Ni(α, p)^{67}Cu reaction.

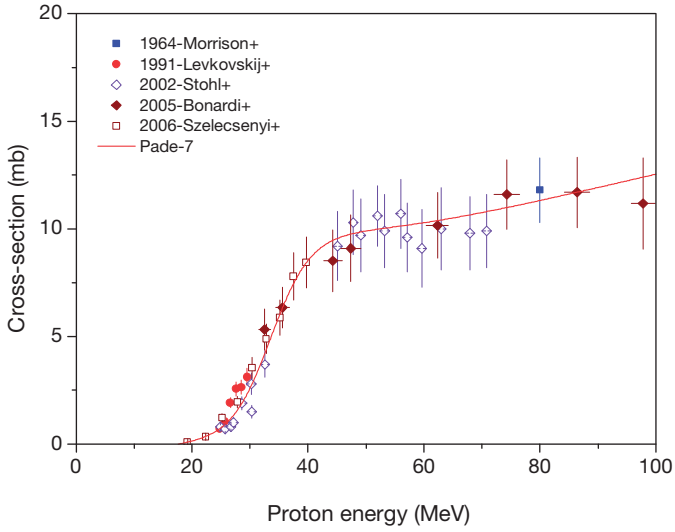

FIG. 2.17.2. Excitation function for the $^{68}Zn(p, 2p)^{67}Cu$ reaction.

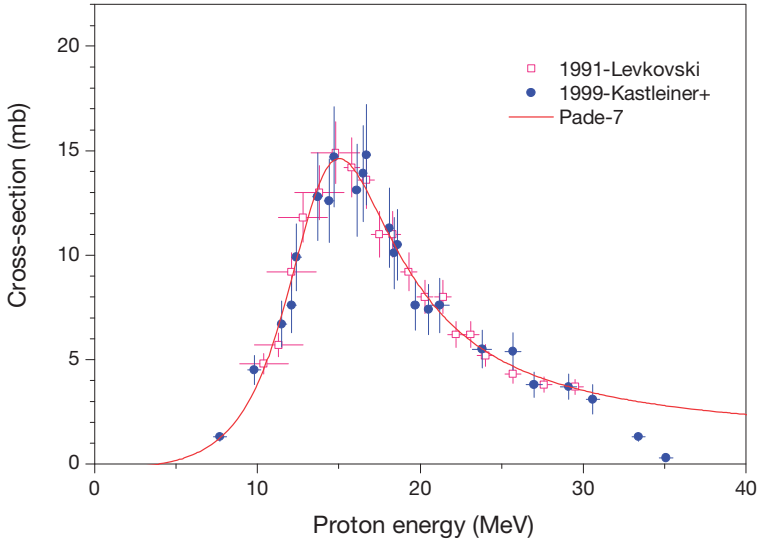

FIG. 2.17.3. Excitation function for the $^{70}Zn(p, \alpha)^{67}Cu$ reaction.

these targets relatively expensive. The $^{68}Zn(p, 2p)^{67}Cu$ reaction has a threshold at about 25 MeV, and is therefore not suitable for low energy cyclotrons.

Target preparation

Zinc or nickel may be plated on to a copper plate for irradiation in an internal beam of the cyclotron. Zinc oxide targets have been used for cross-section measurements but not for production.

Target processing

Proton and deuteron irradiation of nickel targets leads predominantly to the production of copper radionuclides, with trace quantities of cobalt isotopes. Radiochemical separation from nickel and cobalt are best achieved using anion exchange chromatography, which is simple and highly selective. The columns used are easily shielded, and the method is amenable to automated processing, reducing radiation exposure to personnel. The method is also well suited to the recovery of the expensive enriched ^{64}Ni, which, unlike copper and cobalt, is not adsorbed on the column. The separation of high purity ^{67}Cu from irradiated zinc targets has recently been critically examined [2.17.1]. A comparison of three separation methods, including solvent extraction, electrolysis and ion exchange chromatography, showed that, by using three ion exchange columns (with cation, Chelex and anion exchange), ^{67}Cu can be separated with a high quality and yield in a short time. The method was reproducible and hot cell compatible, yielding a product with an SA of 37 MBq/μg Cu.

Enriched materials recovery

The acidic aqueous layer containing enriched zinc from target processing is allowed to decay for some time, and pooled together from multiple targets. Zinc is precipitated as zinc sulphide with Na_2S solution, followed by dissolution in concentrated HCl. Zinc is precipitated from acid solutions as zinc hydroxide, by adding sufficient NaOH to attain basic pH values (8–10). Controlled drying produces the enriched zinc as the oxide, which can then be recycled to prepare additional targets.

Specifications

The typical batch production yield of ^{67}Cu at the Brookhaven Linac Isotope Producer (BLIP) (200 MeV protons) was 10 GBq at EOB with an average beam current of 43 μA for periods of five to six days. The only

radionuclidic impurities detected were ^{61}Cu and ^{64}Cu. At EOB, the ratio of ^{61}Cu to ^{67}Cu was 10.6, declining to 4.5×10^{-4} at the time of user receipt (51 h post-EOB). For ^{64}Cu, the ratio was 6.7 at EOB and 0.67 at receipt. The ^{67}Cu SA averaged 0.21 GBq/μg at EOB. The presence of chemical impurities, especially metals, can interfere with radionuclide attachment to monoclonal antibodies by competing for binding with the chelates used to link to monoclonal antibodies. The trace level metal contents (Zn, 2 ppm; Fe, 8 ppm; Pb, <0.1 ppm; Cd, <2 ppm; Mn, <0.04 ppm; Co, <0.1 ppm; Ni, <2.5 ppm) do not seem to compromise radiolabelling with ^{67}Cu. Activity after separation over three ion exchange columns (for two ^{nat}Zn plates, energy ranges from 67.7 to 52.8 MeV and 2000 $\mu A^{-1} \cdot h^{-1}$ at EOB) [2.17.1] is shown in the following table.

Nuclide	Starting solution (MBq/(μA·h))	After anion exchange (MBq/(μA·h))
Co-55	0.62	n.d.[a]
Co-56	0.037	0.00053
Co-57	0.052	0.00079
Co-58	0.56	n.d.
Co-60	0.0092	n.d.
Ga-67	4.8	n.d.
Zn-62	80	n.d.
Zn-65	1.1	0.00001
Zn-69m	0.73	n.d.
Cu-64	51	42
Cu-67	1.4	1.2
Ni-57	0.25	0.17

[a] n.d.: not detected.

REFERENCE TO SECTION 2.17

[2.17.1] SCHWARZBACH, R., ZIMMERMAN, K., BLÄUENSTEIN, P., SMITH, A., SCHUBIGER, P.A., Development of a simple and selective separation of ^{67}Cu from irradiated zinc for use in antibody labelling: A comparison of methods, Appl. Radiat. Isot. **46** (1995) 324–336.

BIBLIOGRAPHY TO SECTION 2.17

BLOWER, P.J., LEWIS, J.S., ZWEIT, J., Copper radionuclides and radiopharmaceuticals in nuclear medicine, Nucl. Med. Biol. **23** (1996) 957–980.

HILGERS, K., STOLL, T., SKAKUN, Y., COENEN, H.H., QAIM, S.M., Cross-section measurements of the nuclear reactions ^{nat}Zn(d, x)^{64}Cu, ^{66}Zn(d, α)^{64}Cu and ^{68}Zn(p, αn)^{64}Cu for production of ^{64}Cu and technical developments for small-scale production of ^{67}Cu via the ^{70}Zn(p, α)^{67}Cu process, Appl. Radiat. Isot. **59** (2003) 343–351.

INTERNATIONAL ATOMIC ENERGY AGENCY, Charged Particle Cross-section Database for Medical Radioisotope Production: Diagnostic Radioisotopes and Monitor Reactions, IAEA-TECDOC-1211, IAEA, Vienna (2001).

KOLSKY, K.L., et al., Improved production and evaluation of Cu-67 for tumor radioimmunotherapy, J. Nucl. Med. **35** (1994) 259.

MIRZADEH, S., KNAPP, F.F., Spontaneous electrochemical separation of carrier-free copper-64 and copper-67 from zinc targets, Radiochim. Acta **57** (1992) 193–199.

MIRZADEH, S., MAUSNER, L.F., SRIVASTAVA, S.C., Production of no-carrier added ^{67}Cu, Appl. Radiat. Isot. **37** (1986) 29–36.

NEIRINCKX, R.D., Simultaneous production of ^{67}Cu, ^{64}Cu and ^{67}Ga and labelling of Bleomycin with ^{67}Cu or ^{64}Cu, Int. J. Appl. Radiat. Isot. **28** (1977) 802–804.

STOLL, T., KASTLEINER, S., YU, N.S., COENEN, H.H., QAIM, S.M., Excitation functions of proton induced reactions on ^{68}Zn from threshold up to 71 MeV, with specific reference to the production of ^{67}Cu, Radiochim. Acta **90** (2002) 309.

TÁRKÁNYI, F., et al., Excitation functions of deuteron induced nuclear reactions on natural zinc up to 50 MeV, Nucl. Instrum. Methods Phys. Res. B **217** (2004) 531–550.

2.18. FLUORINE-18

Half-life: 109.8 min.

Uses

Because the atomic radius of fluorine is similar to that of hydrogen in most molecules, fluorine can be used as pseudohydrogen. Fluorine can be introduced into molecules using its electronegative and nucleophilic

properties. The electrophilic properties have relied upon the use of F_2 or other molecules generated from F_2, such as acetylhypofluorite. The nucleophilic nature has been exploited through the design of precursor molecules with specialized leaving groups. Since the ^{18}F in water targets is generated as the anion, the SA of the nucleophilic ^{18}F has the potential to be extremely high. However, stable fluorine can be found in many substances; thus, to achieve high SA final products, due consideration must be given to the chemical approach, the choice of materials and careful handling. Its half-life of nearly 2 h has made ^{18}F the most widely used PET radioisotope in research and diagnostic medicine.

Decay mode

Fluorine-18 decays by positron emission (97%) and by electron capture (3%), with a positron end point energy of 653 keV.

Positron emission products of ^{18}F

Fraction	Maximum energy (MeV)	Average energy (MeV)
0.967	0.633	0.2498

Photon emission products of ^{18}F

Fraction	Energy (MeV)
1.93	0.5110
0.0307	0.000520

Nuclear reactions

There are several nuclear reactions that are used to produce ^{18}F. Some of these reactions are given in the table below.

Nuclear reaction	Useful energy range (MeV)	Natural abundance (%)	References
$^{18}O(p, n)^{18}F$	14–4	0.2	[2.18.1]
$^{16}O(^{3}He, p)^{18}F$	15–1	99.7	[2.18.2]
$^{16}O(^{3}He, n)^{18}Ne$: ^{18}F	40–15	99.7	[2.18.3]
$^{16}O(\alpha, np)^{18}F$	40–20	99.7	[2.18.4]
$^{16}O(\alpha, 2n)^{18}Ne$: ^{18}F	52–10	99.7	[2.18.5]
$^{20}Ne(d, \alpha)^{18}F$	15–0	90.5	[2.18.6]
$^{20}Ne(p, 2pn)^{18}F$	40–30	90.5	[2.18.7, 2.18.8]
$^{20}Ne(^{3}He, \alpha p)^{18}F$	40–10	90.5	[2.18.9]

The present method consists of irradiating a small volume of enriched $H_2{}^{18}O$ in a metal target with protons of energies from near threshold (approximately 3 MeV) up to about 20 MeV [2.18.10–2.18.12]. The beam current that the water target is able to cope with is limited by vaporization/cavitation in the target water volume. At present, the maximum reported beam current is 60 μA. However, more typical beam currents are of the order of 20–40 μA. Various approaches have been tried to increase the ability to use higher beam currents, including building in a reflux chamber in the target body and increasing the overpressure on the water. The materials accepted for constructing the target include, but are not limited to, titanium, silver, gold plated metals (such as nickel), niobium and tantalum [2.18.13, 2.18.14].

Other systems that have been used include gas targets, where several other production schemes are possible:

(a) $H^{18}F$ is produced directly in a target consisting of Ne and H_2, with the target chamber heated to 700ºC [2.18.12]. The nuclear reaction utilized in this system is the $^{20}Ne(d, \alpha)^{18}F$ reaction [2.18.6].
(b) Using the same reaction, $^{20}Ne(d, \alpha)^{18}F$, after irradiation the gas is vented and the target washed with water to extract ^{18}F as aqueous fluoride [2.18.15]. The authors concerned felt that this approach did not have any advantages compared with the approach using an enriched water target.
(c) The $^{18}O(p, n)^{18}F$ reaction on a gas target provides higher yields of ^{18}F (more than a factor of 2 higher than that for a neon gas target) [2.18.1]. The $^{18}O_2$ gas target has the advantage of being able to be irradiated at higher beam currents than the enriched water target, as well as the advantage that the target gas can be quantitatively recovered and reused without any purification steps being required and without loss of enrichment.

For the production of F_2, the simplest method is to use the $^{20}Ne(d, \alpha)^{18}F$ reaction, where the target charge consists of natural abundance neon with a nominal charge of 0.1% F_2 (approximately 100 μmol; see Refs [2.18.6, 2.18.16] for discussions of yield versus carrier). In this system, the carrier fluorine exchanges with the nucleogenic ^{18}F to yield ^{18}F–^{19}F molecules in a 'sea' of ^{19}F–^{19}F molecules. Recovery from this target system ranges from about 50 to 70%, depending on conditions such as beam current, quantity of carrier and length of irradiation.

The $^{18}O(p, n)^{18}F$ reaction for production of elemental fluorine offers the opportunity to produce larger quantities, at the expense, however, of being rather more complicated. Attempts to use a direct mixture of $^{18}O_2$ and F_2 have resulted in a mixture of products, some of which contain enriched oxygen target gas [2.18.17]. However, a slightly different approach can be used that involves two sequential irradiations, one to produce ^{18}F and the second to generate $[^{18}F]F_2$ radiolytically [2.18.16, 2.18.18]. The so-called 'double shoot' method can produce several hundred millicuries' worth of $[^{18}F]F_2$.

A third method for production of elemental fluorine based on $[^{18}F]$fluoride has been proposed for use by a limited number of centres. This method first involves the production of $[^{18}F]$fluoride, which is then converted into $[^{18}F]CH_3F$, followed by conversion to $[^{18}F]F_2$ by reaction of the fluoromethane with F_2 [2.18.19]. Because the ^{18}F has been produced with high SAs, the resulting $[^{18}F]F_2$ can, in principle, also have a higher SA than that produced by either of the other two methods where fluorine carriers are added directly.

Excitation functions

The excitation functions for $^{18}O(p, n)^{18}F$ and $^{nat}Ne(d, x)^{18}F$ are shown in Figs 2.18.1 and 2.18.2, respectively.

Thick target yields of $^{18}O(p, n)^{18}F$

Energy range (MeV)	F-18 yield at saturation (mCi/μA)	F-18 yield at saturation (GBq/μA)
20–2.5	395	14.6
18–2.5	373	13.8
15–2.5	327	12.1
11–2.5	230	8.5
8–2.5	132	4.9

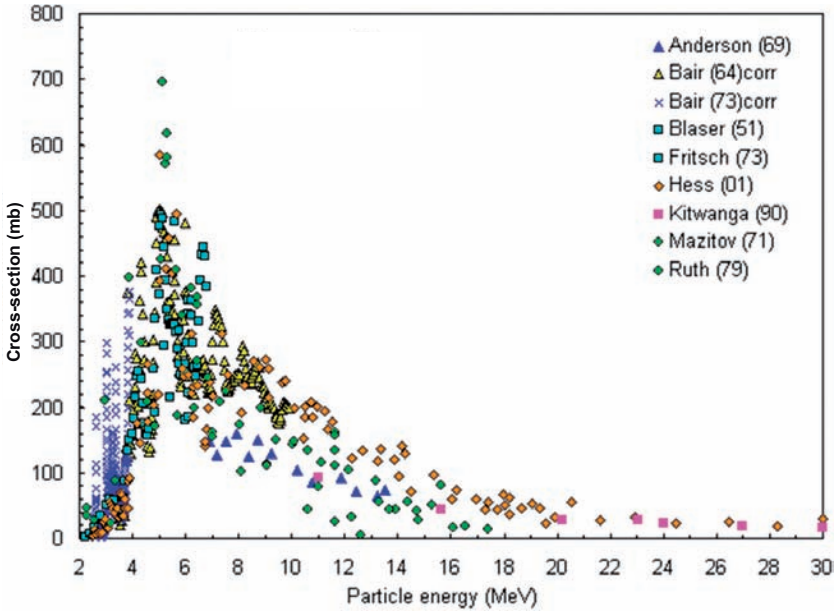

FIG. 2.18.1. Excitation function for the $^{18}O(p, n)^{18}F$ reaction.

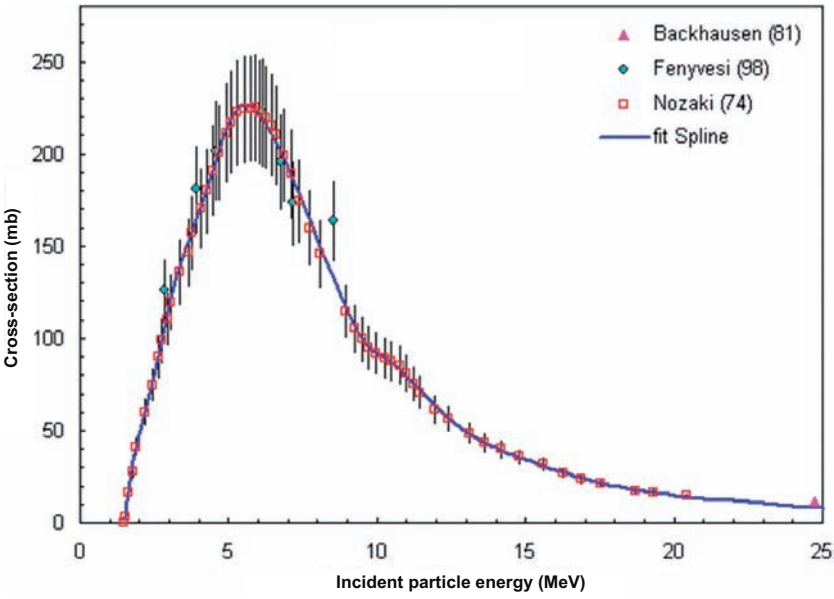

FIG. 2.18.2. Excitation function for the $^{nat}Ne(d, x)^{18}F$ reaction.

Thick target yields of $^{nat}Ne(d, x)^{18}F$

Energy range (MeV)	F-18 yield at saturation (mCi/μA)	F-18 yield at saturation (GBq/μA)
20–1.5	114	4.2
15–1.5	98	3.61
10–1.5	70	2.60
8–1.5	53	1.96
5.0–1.5	18	0.66

Target materials

There are two target materials that are used for the production of ^{18}F. The most widely used target for the production of [^{18}F]fluoride is water enriched in ^{18}O target (see above). However, more recently, a proposal to use oxygen gas in a two step procedure has been suggested [2.18.1]. The co-production of ^{13}N via the $^{16}O(p, \alpha)^{13}N$ reaction should be taken into account when using ^{18}O of lower enrichment (<90%).

For the production of [^{18}F]F_2 there are also two distinct approaches. Historically, irradiation of a mixture of F_2 in a high purity (>99.99%) neon gas of natural isotopic purity resulted in the production of [^{18}F]F_2 [2.18.7]. With the higher yields from the [^{18}O]O_2 target, the method of choice is the two shot method [2.18.16, 2.18.18].

Target preparation

A number of target chamber materials have been used for [^{18}F]fluoride production. The most widely used for many years was a silver chamber. However, more recently, the use of niobium and tantalum has been shown to provide highly reactive fluoride. The gas phase method also uses niobium as the chamber.

For electrophilic ^{18}F production, the old standard was to use nickel. However, it has been shown that aluminium works very well and is easier to machine while having low activation, whereas nickel is poor in both respects. Niobium has also been used with success.

Target processing

The [^{18}F]fluoride can be used directly in its aqueous matrix or extracted on to an ion retardation column and back-extracted with an appropriate solvent mixture for the reaction under consideration. If removed from an enriched water target, water can be recycled.

After the irradiation step in which the desired [^{18}F]fluoride is produced, the target water is transferred through a plastic tube to a collection point where the water either is collected directly or is passed through an ion retardation column to extract the radioactive fluoride [2.18.20]. The enriched water can be reused in the latter case. However, the water must be re-distilled to remove chemical impurities, and in this process the enrichment is compromised (being reduced from the typical 95% ^{18}O to a value of less than 90%, depending upon the set-up and the care taken with the process).

F_2 can be used directly, although typically it is produced in dilute solutions (approximately 100 μmol). Various electrophilic labelling agents have been prepared over the years, with acetylhypofluorite being the most widely used [2.18.21–2.18.23]. Acetylhypofluorite is a gentler agent than fluorine. The electrophilic agents are used to react with unsaturated bonds or in displacing metals. It should be pointed out that, by the nature of its production, F_2 will be of lower SA than fluoride.

Recovery of enriched materials

Enriched water can be recycled. However, the water must be re-distilled to remove chemical impurities. It should be noted that there will be a lowering of enrichment due to the inevitable contamination with natural abundance water (reduced from the typical 95% ^{18}O to a value of less than 90%, depending upon the set-up and the care taken with the process). Some suppliers will buy back used water. If water is recycled, its purity and suitability is the responsibility of the user.

The use of a gas target for either fluoride or F_2 production offers the advantage of quantitative recovery of the enriched $^{18}O_2$ gas. The degree of recovery will depend upon the type of cold trap used, which dictates the vapour pressure of the residual gas. Use of a substrate such as molecular sieves will lower this vapour pressure (and the losses) but will slow the turnaround time between trapping and release.

Specifications

Fluorine (F_2)

The quantity of carrier added to produce F_2 is a trade-off between recovery of F_2 from the target and the effect on SA. Most centres use approximately 100 μmol of carrier. The amount of carrier used can be determined as indicated below.

Fluoride (F^-)

The primary issue for [^{18}F]fluoride production is the carrier. While no carrier is added, the SAs of radiotracers containing ^{18}F are 100–1000 times lower than the theoretical value (1700 Ci/μmol). In order to maintain the tracer principle, the SA should be of the order of 1 Ci/μmol, although some tracers require much higher values.

The source of the carrier varies from the tubing used in the system, to possible releases in the target chamber, to contamination in the precursor. Nevertheless, care must be taken to minimize this contamination. The best available method for measuring fluoride is that using ion chromatography.

Co-production of ^{13}N via the ^{16}O(p, α)^{13}N reaction should be taken into account when using ^{18}O of lower enrichment (<90%).

The only gamma rays associated with ^{18}F decay are the annihilation photons. A simple gamma spectrum from either a NaI or high purity germanium detector system should be adequate for identification purposes. The level of ^{13}N contamination can be determined by following the half-life for at least two counting cycles, separated by 5–10 min.

For F_2 production, there is a simple procedure to determine the oxidation capacity of the generated [^{18}F]F_2. The amount of carrier F_2 can be obtained by passing the gas through an approximately 15 mL solution of 1 molar KI and titrating the resultant solution with standard thiosulphate ($F_2 + 2KI \rightarrow I_2 + 2KF$; $I_2 + 2S_2O_3^{2-} \leftrightarrow 2I^- + S_4O_6^{2-}$) using a starch indicator [2.18.6].

In addition for F_2 production, a simple test can be used to assess whether there is loss due to contamination with the presence of air, N_2 and/or CO_2, which would result in the production of NF_3 or CF_4 at the expense of F_2. Radio-gas chromatography is required in order to separate and detect these inert gases.

A method for checking to see if there is an unreactive ^{18}F label species in the target mix involves passing the F_2 target gas through a soda lime trap and then into a charcoal trap cooled by dry ice. The gas trapped in the charcoal can

be analysed by radio-gas chromatography to separate CF_4 from NF_3 [2.18.6, 2.18.24].

REFERENCES TO SECTION 2.18

[2.18.1] RUTH, T.J., WOLF, A.P., Absolute cross-section for the production of ^{18}F via the $^{18}O(p, n)^{18}F$ reaction, Radiochim. Acta **26** (1979) 21–24.

[2.18.2] FITSCHEN, J., BECKMANN, R., HOLM, U., NEUERT, H., Yield and production of ^{18}F by ^{3}He irradiation of water, Int. J. Appl. Radiat. Isot. **28** (1977) 781–784.

[2.18.3] KNUST, E.J., MACHULLA, H.-J., High yield production of ^{18}F in a water target via the $^{16}O(^{3}He, p)^{18}F$ reaction, Int. J. Appl. Radiat. Isot. **34** (1983) 1627–1628.

[2.18.4] CLARK, J.C., SILVESTER, D.J., A cyclotron method for the production of fluorine-18, Int. J. Appl. Radiat. Isot. **17** (1966) 151–154.

[2.18.5] NOZAKI, T., IWAMOTO, M., IDO, T., Yield of ^{18}F for various reactions from oxygen and neon, Int. J. Appl. Radiat. Isot. **25** (1974) 393–399.

[2.18.6] CASELLA, V., et al., Anhydrous F-18 labelled elemental fluorine for radiopharmaceutical preparation, J. Nucl. Med. **21** (1980) 750–757.

[2.18.7] RUTH, T.J., The production of ^{18}F-F_2 and ^{15}O-O_2 sequentially from the same target chamber, Appl. Radiat. Isot. **36** (1985) 107–110.

[2.18.8] REEDY, G.N., BEER, H.-F., SCHUBIGER, P.A., "Determination of excitation functions for $^{20}Ne(p, 2pn)^{18}Ne \rightarrow {}^{18}F$ and $^{20}Ne(p, 2pn)^{18}F$ and a re-examination of production of $[^{18}F]F_2$ with protons on neon", Targetry and Target Chemistry (Proc. 5th Workshop, Upton, 1993), Brookhaven Natl Lab., Upton, NY (1993) 226.

[2.18.9] CROUZEL, C., COMAR, D., Production of carrier-free ^{18}F-hydrofluoric acid, Int. J. Appl. Radiat. Isot. **29** (1978) 407–408.

[2.18.10] KILBOURN, M.R., HOOD, J.T., WELCH, M.J., A simple ^{18}O water target for ^{18}F production, Int. J. Appl. Radiat. Isot. **35** (1984) 599–602.

[2.18.11] KILBOURN, M.R., JERABEK, P.A., WELCH, M.J., An improved [^{18}O]water target for [^{18}F]fluoride production, Int. J. Appl. Radiat. Isot. **36** (1985) 327–328.

[2.18.12] TEWSON, T.J., BERRIDGE, M.S., BOLOMEY, L., GOULD, K.L., Routine production of reactive fluorine-18 salts from an oxygen-18 water target, Nucl. Med. Biol. **15** (1988) 499–504.

[2.18.13] ZEISLER, S.K., BECKER, D.W., PAVAN, R.A., MOSCHEL, R., RÜHLE, H., A water-cooled spherical niobium target for the production of [^{18}F]fluoride, Appl. Radiat. Isot. **53** (2000) 449–453.

[2.18.14] SATYAMURTHY, N., AMARASEKERA, B., ALVORD, C.W., BARRIO, J.R., PHELPS, M.E., Tantalum [^{18}O]water target for the production of [^{18}F]fluoride with high reactivity for the preparation of 2-deoxy-2-[^{18}F]fluoro-D-glucose, Mol. Imaging Biol. **4** (2002) 65–70.

[2.18.15] BLESSING, G., COENEN, H.H., FRANKEN, K., QAIM, S.M., Production of [^{18}F]F_2, H^{18}F and $^{18}F^-_{aq}$ using the ^{20}Ne(d, α)^{18}F process, Appl. Radiat. Isot. **37** (1986) 1135–1139.

[2.18.16] ROBERTS, A.D., OAKES, T.R., NICKLES, R.J., Development of an improved target for [^{18}F]F_2 production, Appl. Radiat. Isot. **46** (1995) 87–91.

[2.18.17] BISHOP, A., et al., Proton irradiation of [^{18}O]O_2: Production of [^{18}F]F_2 and [^{18}F]F_2 + [^{18}F]OF_2, Nucl. Med. Biol. **23** (1996) 189–199.

[2.18.18] DAUBE, M.E., NICKLES, R.J., RUTH, T.J., An $^{18}O_2$ target for the production of [^{18}F]F_2, Int. J. Appl. Radiat. Isot. **35** (1984) 117–122.

[2.18.19] BERGMAN, J., SOLIN, O., F-18 labeled fluorine gas for synthesis of tracer molecules, Nucl. Med. Biol. **24** (1997) 677–683.

[2.18.20] SCHLYER, D.J., BASTOS, M.A., ALEXOFF, D., WOLF, A.P., Separation of [^{18}F]fluoride from [^{18}O]water using anion exchange resin, Int. J. Radiat. Appl. Instrum. A **41** (1990) 531–533.

[2.18.21] ROZEN, S., LERMAN, O., KOL, M., Acetyl hypofluorite, the first member of a new family of organic compounds, J. Chem. Soc., Chem. Commun. (1981) 443–444.

[2.18.22] ADAM, M.J., RUTH, T.J., JIVAN, S., PATE, B.D., Fluorination of aromatic compounds with F_2 and acetyl hypofluorite: Synthesis of ^{18}F-aryl fluorides by cleavage of aryl–tin bonds, J. Fluor. Chem. **25** (1984) 329–337.

[2.18.23] EHRENKAUFER, R.E., et al., Production of H^{18}F by deuteron irradiation of a neon–hydrogen gas target, Radiochim. Acta **33** (1983) 49–56.

[2.18.24] BIDA, G.T., et al., The effect of target gas purity on the chemical form of ^{18}F during ^{18}F-F_2 production using the neon/fluorine (Ne/F_2) target, J. Nucl. Med. **21** (1980) 758–762.

BIBLIOGRAPHY TO SECTION 2.18

BACKHAUSEN, H., STÖCKLIN, G., WEINREICH, R., Formation of ^{18}F via its ^{18}Ne precursor: Excitation functions of reactions ^{20}Ne(d, x)^{18}Ne and ^{20}Ne(^{3}He, αn)^{18}Ne, Radiochim. Acta **29** (1981) 1–4.

EHRENKAUFER, R.E., POTOCKI, J.F., JEWETT, D.M., Simple synthesis of F-18-labeled 2-fluoro-2-deoxy-D-glucose: Concise communication, J. Nucl. Med. **25** (1984) 333–337.

HESS, E., et al., Excitation function of the $^{18}O(p, n)^{18}F$ nuclear reaction from threshold up to 30 MeV, Radiochim. Acta **89** (2001) 357.

INTERNATIONAL ATOMIC ENERGY AGENCY, Charged Particle Cross-section Database for Medical Radioisotope Production: Diagnostic Radioisotopes and Monitor Reactions, IAEA-TECDOC-1211, IAEA, Vienna (2001).

IWATA, R., IDO, T., BRAD, Y.F., TAKAHASHI, T., UJIIE, A., [^{18}F]fluoride production with a circulating [^{18}O]water target, Appl. Radiat. Isot. **38** (1987) 979–984.

KEINONEN, J., FONTELL, A., KAIRENTO, A.-L., Effective small-volume [^{18}O]water target for the production of [^{18}F]fluoride, Appl. Radiat. Isot. **37** (1986) 631–632.

NOZAKI, T., IWAMOTO, M., IDO, T., Yield of ^{18}F for various reactions from oxygen and neon, Int. J. Appl. Radiat. Isot. **25** (1974) 393–399.

RUTH, T.J., et al., A proof of principle for the targetry to produce ultra high quantities of ^{18}F-fluoride, Appl. Radiat. Isot. **55** (2001) 457–461.

STEINBACH, J., et al., Temperature course in small volume [^{18}O]water targets for [^{18}F]F-production, Int. J. Radiat. Appl. Instrum. A **41** (1990) 753–736.

UNITED STATES NATIONAL NUCLEAR DATA CENTER,
http://www.nndc.bnl.gov/index.jsp

VOGT, M., HUSAR, I., OEHNINGER, H., WEINREICH, R., Improved production of [^{18}F]fluoride via the [^{18}O]$H_2O(p, n)^{18}F$ reaction for no-carrier added nucleophilic syntheses, Appl. Radiat. Isot. **37** (1986) 448–449.

2.19. GALLIUM-67

Half-life: 3.26 d.

Uses

Gallium behaves in the body in a similar way to ferric iron. It is commonly used as a trivalent citrate compound for nuclear medicine imaging, and is a valuable agent in the detection and localization of certain neoplasms and inflammatory lesions.

Decay mode

Gallium-67 decays to stable ^{67}Zn by electron capture. Its decay emissions include gamma rays of 93.3 keV (37.0%), 184.6 keV (20.4%) and 300.2 keV (16.6%).

Electron emission products of ^{67}Ga

Fraction	Energy (MeV)
0.010853	0.093175
0.032844	0.092117
0.268110	0.083652
0.602060	0.007530
1.648900	0.000990

Photon emission products of ^{67}Ga

Fraction	Energy (MeV)
0.022420	0.208950
0.028560	0.091266
0.044768	0.393530
0.065838	0.009570
0.159940	0.300220
0.164720	0.008616
0.197060	0.184580
0.322970	0.008639
0.357000	0.093311

Nuclear reactions

Gallium-67 is commonly produced by using enriched ^{68}Zn targets through the ^{68}Zn(p, 2n)^{67}Ga nuclear reaction [2.19.1].

Excitation functions

The excitation functions for $^{67}Zn(p, n)^{67}Ga$ and $^{68}Zn(p, 2n)^{67}Ga$ are shown in Figs 2.19.1 and 2.19.2, respectively.

Target material

The target material is enriched ^{68}Zn.

Target preparation

The enriched ^{68}Zn may be pressed or electroplated onto a copper plate. Electroplating may be accomplished using a constant current; the electrolyte is $ZnCl_2$ solution (with pH5–6), and a small amount of hydrazine hydrate (NH_2NH_2) is added as a depolarizer [2.19.2]. The electroplated material should have a shiny metallic coloration, evenly distributed with no obvious dendrite formation and well adhered to the surface.

In a typical use of a powder target, a zinc target can be prepared by pressing metal powder uniaxially at 523 MPa under vacuum by means of a

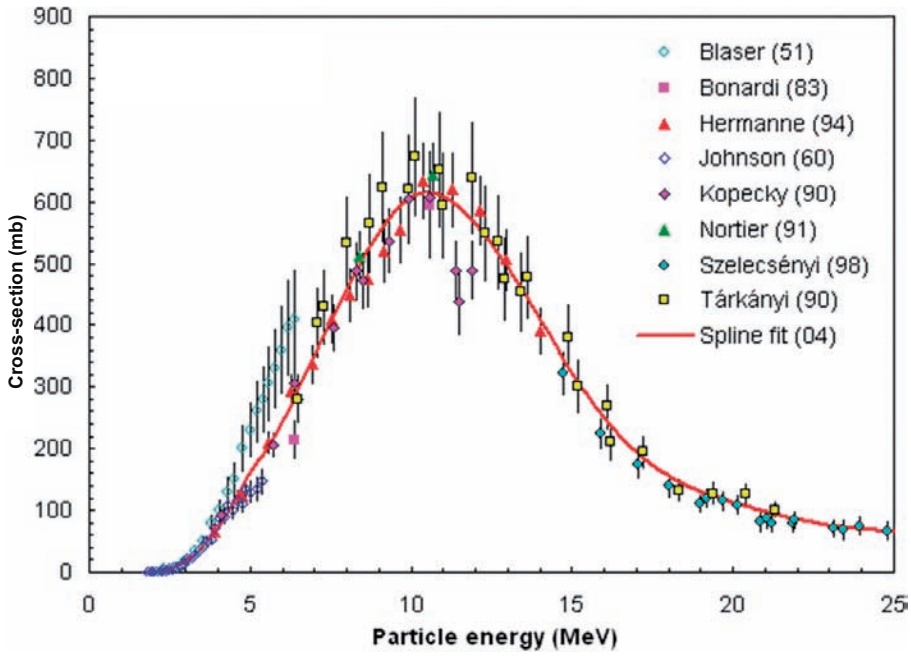

FIG. 2.19.1. Excitation function for the $^{67}Zn(p, n)^{67}Ga$ reaction.

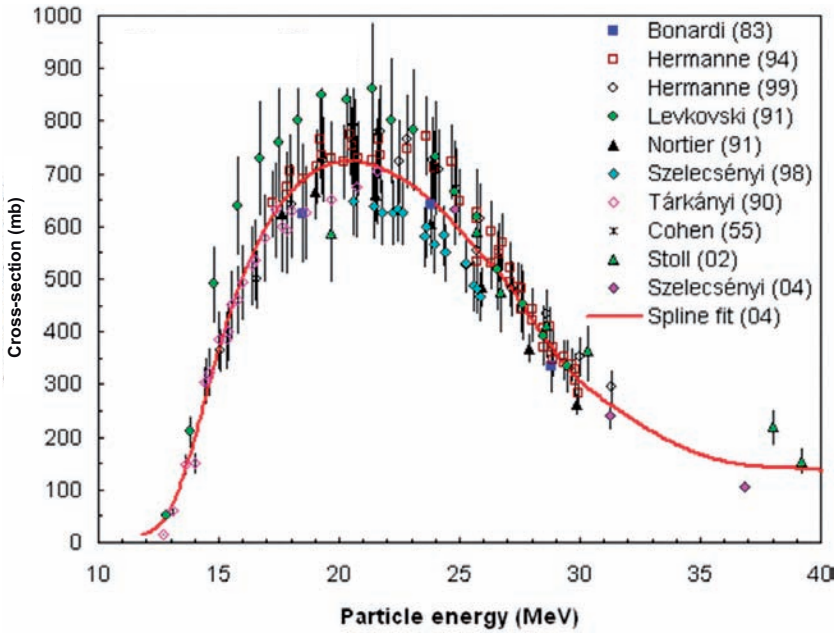

FIG. 2.19.2. Excitation function for the ^{68}Zn(p, 2n)^{67}Ga reaction.

suitable punch and die set, machined from a high carbon and high chromium steel used for tools. The metal disc, of 95% theoretical maximum density, is annealed/sintered in an oven for 0.5 h at 400°C.

Processing

There are several methods for separation of ^{67}Ga from a zinc target. Two commonly used methods entail ion exchange separation and solvent/solvent extraction.

Ion exchange method

After irradiation, the ^{68}Zn target is dissolved in concentrated HCl, followed by separation of ^{67}Ga from ^{68}Zn using a Dowex 50W-X8 resin. Target solution is loaded on the Dowex column, which has been previously conditioned with 10M HCl. Continued elution with 10M HCl removes the enriched ^{68}Zn (saved for later processing for recovery of enriched material). Gallium-67 is eluted with 3.5M HCl, and the solution is evaporated to near dryness. A few drops of 30% hydrogen peroxide are added, and the solution is

then evaporated very carefully to dryness. Gallium-67 is recovered as gallium citrate by dissolving the residue in a solution of 2–4% sodium citrate solution.

Solvent/solvent extraction method

Irradiated ^{68}Zn target is dissolved in 7.5M HCl, followed by extraction of ^{67}Ga in di-isopropyl ether (DIPE). Zinc-68 remains in the acidic aqueous layer. After three repeated extractions of ^{67}Ga with DIPE, and scrubbing of the organic layer with 7.5M HCl to remove residual ^{68}Zn, ^{67}Ga is back-extracted from DIPE with a small volume of sterile water. Extraction is repeated twice to recover all the ^{67}Ga. To the solution containing ^{67}Ga is added 0.5 mL of 2.5% sodium citrate, which is then carefully evaporated to dryness. The residue is dissolved in saline containing a sufficient amount of sodium citrate for manufacture of radiopharmaceuticals.

Enriched material recovery

The recommended method for recovery of the enriched material is electrochemical separation [2.19.3].

In the wet chemical method, the acidic aqueous layer containing ^{68}Zn from target processing is allowed to decay for some time and is pooled together from multiple targets. Zinc-68 is precipitated as zinc sulphide with Na_2S solution, followed by dissolution in concentrated HCl. Zinc-68 is also precipitated from acid solution as zinc hydroxide by adding sufficient NaOH to attain a basic pH (8–10). Controlled drying realizes ^{68}Zn as an oxide recycled to prepare additional targets.

Specifications

The radionuclidic impurity levels in the separated gallium citrate depend upon the radioisotopic enrichment of the target material and the efficiency of the separation method. Co-production of high energy ^{66}Ga (through the (p, 2n) reaction) should also be taken into account while processing the irradiated target. Sufficient time must be allowed post-irradiation for the short lived gallium isotopes to decay to an acceptable level (pharmacopoeia standard). The final ^{67}Ga products must have low levels of contaminants that are within acceptable human toxicity and pharmacopoeial limits.

It is essential to ensure through the chromatographic method a lower than acceptable level of free ^{67}Ga (<5%), and to assure more than 95% as gallium citrate.

REFERENCES TO SECTION 2.19

[2.19.1] INTERNATIONAL ATOMIC ENERGY AGENCY, Charged Particle Cross-section Database for Medical Radioisotope Production: Diagnostic Radioisotopes and Monitor Reactions, IAEA-TECDOC-1211, IAEA, Vienna (2001).

[2.19.2] VAN DEN WINKEL, P., et al., Vrije Universiteit Brussel, Brussels, personal communication, 1995.

[2.19.3] INTERNATIONAL ATOMIC ENERGY AGENCY, Standardized High Current Solid Targets for Cyclotron Production of Diagnostic and Therapeutic Radionuclides, Technical Reports Series No. 432, IAEA, Vienna (2005) CD-ROM.

BIBLIOGRAPHY TO SECTION 2.19

EL-AZONY, K.M., FERIEG, K.H., SALEH, Z.A., Direct separation of ^{67}Ga citrate from zinc and copper target materials by anion exchange, Appl. Radiat. Isot. **59** (2003) 329–331.

GUL, K., Calculations for the excitation functions of 3–26 MeV proton reactions on ^{66}Zn, ^{67}Zn and ^{68}Zn, Appl. Radiat. Isot. **54** (2001) 311–318.

HERMANNE, A., et al., New cross section data on ^{68}Zn(p, 2n)^{67}Ga and ^{nat}Zn(p, xn)^{67}Ga nuclear reactions for the development of a reference data base, J. Radioanal. Nucl. Chem. **240** (1999) 623–630.

INTERNATIONAL ATOMIC ENERGY AGENCY, Charged Particle Cross-section Database for Medical Radioisotope Production: Diagnostic Radioisotopes and Monitor Reactions, IAEA-TECDOC-1211, IAEA, Vienna (2001).

LITTLE, E., LAGUNAS-SOLAR, M.C., Cyclotron production of ^{67}Ga: Cross sections and thick-target yields for the ^{67}Zn(p, n) and ^{68}Zn(p, 2n) reactions, Int. J. Appl. Radiat. Isot. **34** (1983) 631–637.

NAIDOO, C., VAN DER WALT, T.N., Cyclotron production of ^{67}Ga(III) with a tandem ^{nat}Ge/^{nat}Zn target, Appl. Radiat. Isot. **54** (2001) 915–919.

STOLL, T., KASTLEINER, S., YU, N.S., COENEN, H.H., QAIM, S.M., Excitation functions of proton induced reactions on ^{68}Zn from threshold up to 71 MeV, with specific reference to the production of ^{67}Cu, Radiochim. Acta **90** (2002) 309.

SZELECSÉNYI, F., BOOTHE, T.E., TAKÁCS, S., TÁRKÁNYI, F., TAVANO, E., Evaluated cross section and thick target yield data bases of Zn + p processes for practical applications, Appl. Radiat. Isot. **49** (1998) 1005–1032.

SZELECSÉNYI, F., BOOTHE, T.E., TAVANO, E., PLITNIKAS, M.E., TÁRKÁNYI, F., Compilation of cross sections/thick target yields for ^{66}Ga, ^{67}Ga and ^{68}Ga production using Zn targets up to 30 MeV proton energy, Appl. Radiat. Isot. **45** (1994) 473–500.

TAKÁCS, F., TÁRKÁNYI, F., HERMANNE, A., Institute of Nuclear Research of the Hungarian Academy of Sciences, personal communication, 2005.

WEINER, R.E., The mechanism of ^{67}Ga localization in malignant disease, Nucl. Med. Biol. **23** (1996) 745–751.

2.20. GERMANIUM-68

Germanium-68 is mainly used as a calibration source for PET. The decay of ^{68}Ge to ^{68}Ga gives a long lived, pure positron, source for use in PET instruments. It can also be used to generate ^{68}Ga on a column, which can then be used in biomedical experiments.

Half-life: 270.8 d.

Uses

The ^{68}Ge/^{68}Ga generator is ideally suited to on-demand availability of ^{68}Ga for biomedical experiments and clinical applications. Gallium-68 finds significant applications in assessments of blood–brain barrier integrity as well as for tumour localization. It is also widely used as a source for the attenuation

correction of most positron emission tomographs. It is an ideal PET radiotracer, owing to its non-halogenated and non-volatile chemical properties and its 68 min half-life, which permits chemical manipulation for the production of many PET radiopharmaceuticals. However, little progress towards using ^{68}Ga in clinical applications has been made, due to the long synthesis times required by manual production of ^{68}Ga labelled PET imaging agents.

Electron emission products of ^{68}Ge

Fraction	Energy (MeV)
0.424340	0.008040
1.215000	0.001100

Photon emission products of ^{68}Ge

Fraction	Energy (MeV)
0.006719	0.001100
0.054578	0.010300
0.130910	0.009225
0.256180	0.009252

Nuclear reactions

The nuclear reactions for the production of ^{68}Ge are the alpha reaction on natural zinc and the proton reaction on either natural gallium or more often on enriched ^{69}Ga.

Excitation functions

The excitation functions for ^{68}Ge are shown in Figs 2.20.1–2.20.3.

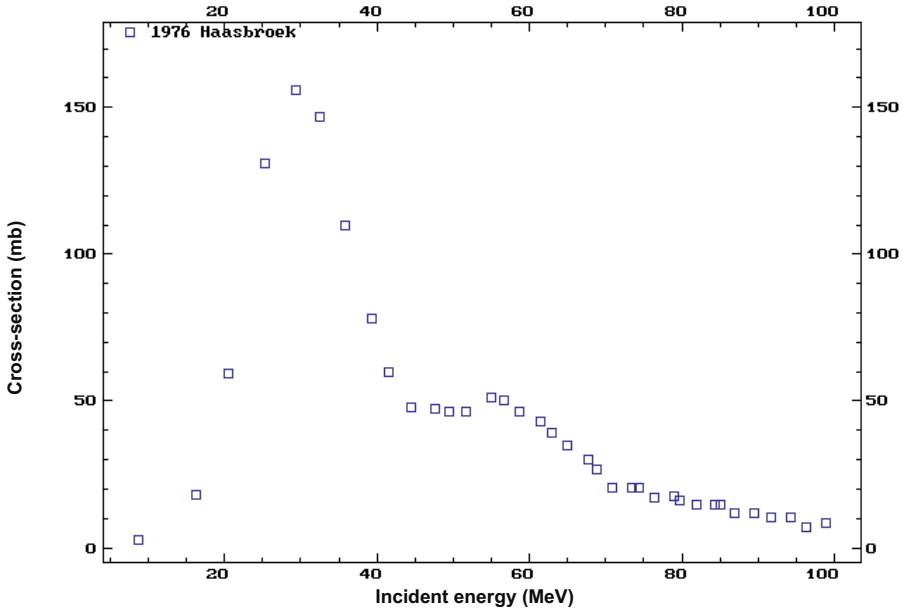

FIG. 2.20.1. Excitation function for the $^{nat}Zn(\alpha, x)^{68}Ge$ reaction.

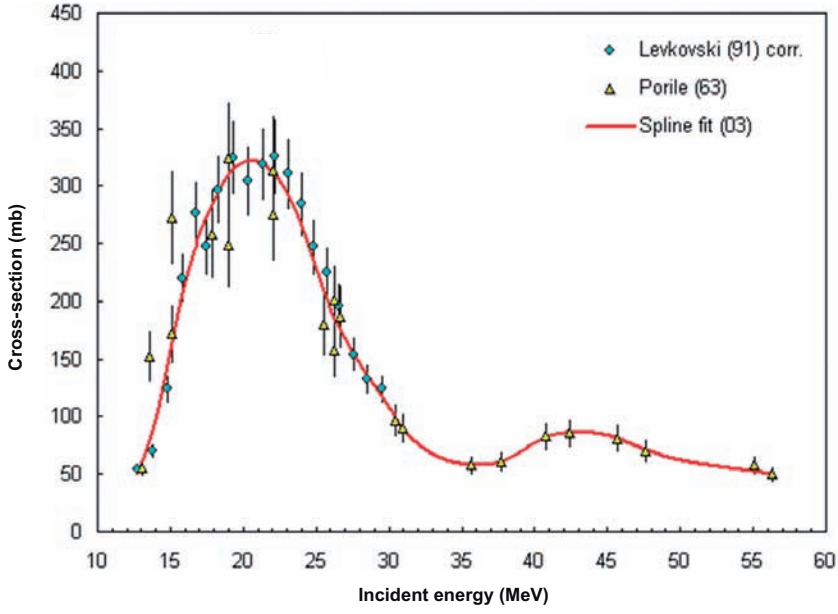

FIG. 2.20.2. Excitation function for the $^{nat}Ga(p, x)^{68}Ge$ reaction.

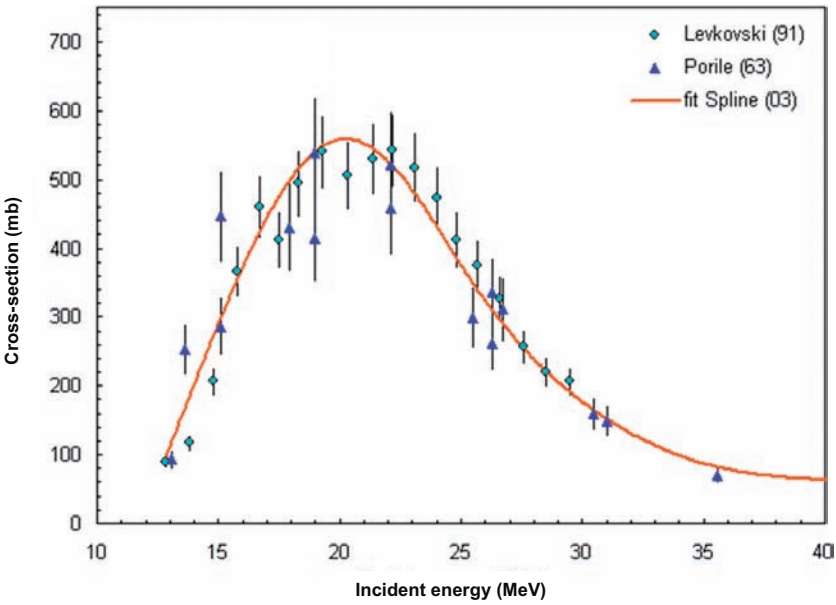

FIG. 2.20.3. Excitation function for the $^{69}Ga(p, 2n)^{68}Ge$ reaction.

Thick target yields

The thick target yields for ^{68}Ge are shown in the table below.
This table is also continued on the next page.

Energy (MeV)	TT yield (μCi/(μA·h))[a]	Energy (MeV)	TT yield (μCi/(μA·h))	Energy (MeV)	TT yields (μCi/(μA·h))
13	0.214008	25.5	52.52918	38	78.79377
13.5	0.680934	26	54.47471	38.5	78.79377
14	1.361868	26.5	56.42023	39	79.76654
14.5	2.237354	27	58.36576	39.5	80.7393
15	3.307393	27.5	59.33852	40	80.7393
15.5	4.571984	28	61.28405	40.5	81.71206
16	6.031128	28.5	62.25681	41	81.71206
16.5	7.684825	29	64.20233	41.5	82.68482
17	9.533074	29.5	65.1751	42	82.68482

Energy (MeV)	TT yield (μCi/(μA·h))[a]	Energy (MeV)	TT yield (μCi/(μA·h))	Energy (MeV)	TT yields (μCi/(μA·h))
17.5	11.67315	30	66.14786	42.5	83.65759
18	13.61868	30.5	67.12062	43	83.65759
18.5	16.53696	31	69.06615	43.5	84.63035
19	18.48249	31.5	70.03891	44	84.63035
19.5	21.40078	32	71.01167	44.5	85.60311
20	24.31907	32.5	71.01167	45	85.60311
20.5	27.23735	33	71.98444	45.5	86.57588
21	29.18288	33.5	72.9572	46	86.57588
21.5	32.10117	34	73.92996	46.5	87.54864
22	35.01946	34.5	74.90272	47	87.54864
22.5	37.93774	35	74.90272	47.5	88.5214
23	40.85603	35.5	75.87549	48	88.5214
23.5	42.80156	36	76.84825	48.5	89.49416
24	45.71984	36.5	76.84825	49	90.46693
24.5	47.66537	37	77.82101	49.5	90.46693
25	50.58366	37.5	77.82101	50	91.43969

[a] 1 Ci = 37 GBq.

Target material

Germanium-68 is long lived ($T_{1/2}$ = 271 d), and attempts to produce it on medium energy accelerators are not generally made due to the low production yields. The primary source for the parent radionuclide is from the spallation processes available at large energy accelerators, where parasitic position and operation are available. Recovery of ^{68}Ge involves several multistep chemical processes that are not appropriate at classical PET facilities.

Target preparation

Targets consist of gallium metal encapsulated in niobium with a 0.051 cm window welded to the target body using an electron beam. Niobium is used, since gallium is very corrosive and attacks other metals and alloys such as

stainless steel. Targets typically accumulate 33 000–45 000 μA·h of beams during an irradiation period of four weeks, to produce 14.8–18.5 GBq (400–500 mCi) of ^{68}Ge at EOB. The primary long lived contaminant is ^{65}Zn ($T_{1/2}$ = 244 d), whose excitation function peaks at $E_p \approx 25$ MeV. The ^{68}Ge/^{65}Zn impurity ratio is ≈1.1 at EOB [2.20.1].

Target processing

After irradiation, the target is not processed for approximately two weeks to allow decay of short lived isotopes such as ^{69}Ge and ^{67}Ga. The niobium can is then opened by cutting off one of the windows. Opening the target probably releases some fraction of the total ^{68}Ge activity, presumably in the form of germane, GeH_4, produced during the irradiation. A typical irradiation would deposit more than 33 000 μA·h, or 1.3 mmol of hydrogen ions in the target. Therefore, the hydrogen source is most likely to be the proton beam itself, since the target acts as a beam stop.

The target can is heated gently to liquefy gallium (with a melting point of 29.76°C), after which the gallium is poured into a beaker. A solution of 6 mL of 4N HCl and 2 mL of 30% H_2O_2 is added to the beaker, gently stirred, and ^{68}Ge is extracted from the gallium in the form of the tetrachloride, $GeCl_4$. Gallium does not appreciably dissolve. Several extractions are required to achieve quantitative recovery. Zinc-65 is co-extracted, as is a trace amount of the gallium target (milligram quantities). The separation of ^{68}Ge from ^{65}Zn and gallium is based on the extraction of the germanium tetrachloride from 9–12N HCl into organic solvents such as toluene, carbon tetrachloride and benzene. The final product is prepared as follows. Germanium-68 is back-extracted twice from the organic phase into small volumes of 0.1N HCl. Recovery of ^{68}Ge varies with the volume of aqueous phase used in the back-extraction, reaching a high of 99% when the aqueous phase is 30% of the organic phase.

Germanium-68/gallium-68 generators

Germanium-68/gallium-68 generators are ideally suited to the on-demand availability of ^{68}Ga for biomedical experiments and clinical applications. The earlier generator systems provided the gallium product in a complex form as a result of using either solvent/solvent extraction techniques or chromatographic supports of alumina or antimony oxide. Refinements made to elute the ^{68}Ga in an ionic form were compromised by solubility problems of the oxide in the eluent and therefore slowed the potential for direct clinical use. Many of the limitations of previous chromatographic systems were overcome

with the first report of a tin oxide/HCl generator [2.20.2]. Negative pressure generators consisted of tin oxide (of diameter 0.16–0.25 mm) contained in a glass column (of diameter 10 mm) between glass wool plugs on top of a sintered glass base. The eluent is 1N HCl, with its flow rate controlled by a valve at the base of the column. Results indicate a radiochemical yield approaching 80% after roughly 2 min using 5 mL of eluent, with the generator performance remaining high in spite of the accumulated dose delivered to the solid support.

Researchers from the M.D. Anderson Cancer Center have developed an automated ^{68}Ga based radiopharmaceutical synthesis system. An infrared based system has also been developed [2.20.3]. This device is capable of synthesizing ^{68}Ga tagged agents within 20 min, compared with manual operation, which can take 60 min or more. In essence, ^{68}Ge would be purchased and kept in the ^{68}Ga module for a shelf life of approximately one year. The ^{68}Ga isotope would be eluted twice a day as needed from an internal ^{68}Ge generator, and then used to tag various biological targeting agents to produce the radiopharmaceutical desired within this device on the basis of a choice of kits. The entire process from elution to radiopharmaceutical synthesis would be automated, monitored and controlled by a PC based computer program.

Such a generator is shown in Fig. 2.20.4. The device allows availability of ^{68}Ga at any time. As an eluent, 0.1M HCl was used. In all cases, the ^{68}Ga yield in 5 mL of eluate was not less than 60% at the time of first operation. The breakthrough for ^{68}Ge was not more than 5×10^{-3}%. During operation the ^{68}Ga yield is gradually decreased.

Specifications

The SA of this product is typically about 58 MBq (1.57 mCi) per μg of stable germanium, with a gallium separation factor of 3.4×10^5. Other stable metal impurities were typically 37 ppm Zn, <1 ppm Cu, Pb, Co, Cr, Cd, Ni, Fe, Mn and Al, and <7 ppm Nb. The radiopurity was higher than 99% [2.20.3], and activity concentrations were higher than 3.15 GBq/mL (85 mCi/mL). The final pH of the product solution, which is 0.03M diethylene-triamine-penta-acetate (DTPA), is adjusted to user specifications.

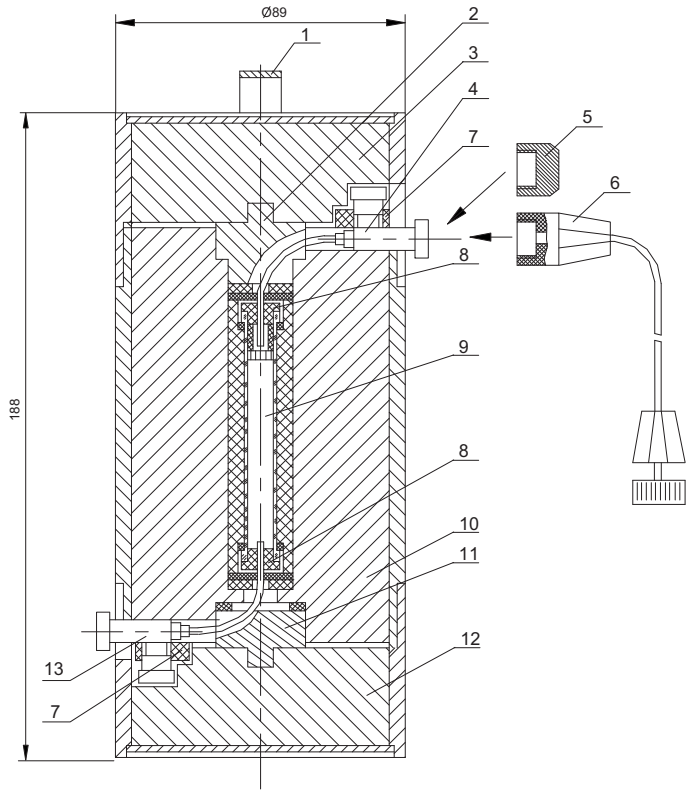

1 – handle
2 – upper shielding insert
3 – upper cover of shielding container
4 – cannula of catheter of eluent line (inlet line)
5 – plug of catheter
6 – extension line
7 – buckle (holder) of catheter's cannula
8 – perforated stopper
9 – generator column
10 – shielding container body
11 – lower shielding insert
12 – lower cover of shielding container
13 – cannula of catheter of eluate line (outlet line).

FIG. 2.20.4. Schematic diagram of a $^{68}Ge/^{68}Ga$ generator (courtesy: CYCLOTRON Ltd, Obninsk, Russian Federation).

REFERENCES TO SECTION 2.20

[2.20.1] MEINKEN, G.E., KURCZAK, S., MAUSNER, L.F., KOLSKY, K.L., SRIVASTAVA, S.C., Production of high specific activity ^{68}Ge at Brookhaven National Laboratory, J. Radioanal. Nucl. Chem. **263** (2005) 553–557.

[2.20.2] LOC'H, C., MAZIÈRE, B., COMAR, D., KNEPPER, R.A., A new preparation of germanium 68, Int. J. Appl. Radiat. Isot. **33** (1982) 267–270.

[2.20.3] AZHDARINIA, A., YANG, D.J., CHAO, C., MOURTADA, F., Infrared based module for the synthesis of ^{68}Ga-labeled radiotracers, Nucl. Med. Biol. **34** (2007) 121–127.

BIBLIOGRAPHY TO SECTION 2.20

EHRHARDT, G.J., WELCH, M.J., A new germanium 68/gallium-68 generator, J. Nucl. Med. **19** (1978) 925–929.

HAASBROEK, F.J., BURDZIK, G.F., COGNEAU, M., WANET, P., Excitation functions and thick-target yields for Ga-67, Ge-68/Ga-68, Cd-109 and In-111 induced in natural zinc and silver by 100 MeV alpha particles, Rep. 91, Council of Scientific and Industrial Research, Pretoria (1976).

INTERNATIONAL ATOMIC ENERGY AGENCY, Charged Particle Cross-section Database for Medical Radioisotope Production: Diagnostic Radioisotopes and Monitor Reactions, IAEA-TECDOC-1211, IAEA, Vienna (2001).

KARPELES, A., Herstellung eines ^{68}Ga-Generators, Radiochim. Acta **12** (1969) 22–25.

KOPECKÝ, P., MUDROVA, B., SVOBODA, K., The study of conditions for the preparation and utilization of a ^{68}Ge–^{68}Ga generator, Int. J. Appl. Radiat. Isot. **24** (1973) 73–80.

MAECKE, H.R., ANDRE, J.P., ^{68}Ga-PET radiopharmacy: A generator-based alternative to ^{18}F-radiopharmacy, Ernst Schering Res. Found. Workshop **62** (2007) 215–242.

NAGAME, Y., NAKAHARA, H., FURUKAWA, M., Excitation functions for alpha and He-3 particle induced reactions on zinc, Radiochim. Acta **46** (1989) 5–12.

NAKAYAMA, M.L., et al., A new ^{68}Ge/^{68}Ga generator system using an organic polymer containing N-methylglucamine groups as adsorbent for ^{68}Ge, Appl. Radiat. Isot. **58** (2003) 9–14.

PAGANI, M., STONE-ELANDER, S., LARSSON, S.A., Alternative positron emission tomography with non-conventional positron emitters: Effects of their physical properties on image quality and potential clinical applications, Eur. J. Nucl. Med. Mol. Imaging **24** (1997) 1301–1327.

RAZBASH, A.A., SEVASTIANOV, Y.G., "Production of Ge-68 in Russia", Targetry and Target Chemistry (Proc. 6th Workshop Vancouver, 1995), TRIUMF, Vancouver (1995) 99–100.

TAKÁCS, S., TÁRKÁNYI, F., HERMANNE, A., PAVIOTTI DE CORCUERA, R., Validation and upgrade of the recommended cross section data of charged particle reactions used for production PET radioisotopes, Nucl. Instrum. Methods Phys. Res. B **211** (2003) 169–189.

2.21. INDIUM-110

Half-life

The half-life of the metastable state is 69 min, and the half-life of the ground state is 4.9 h. Indium-110m is an isotope that decays by positron emission 62% of the time and by electron capture the remainder of the time. Indium-110 has some interesting production problems since it has a metastable state with a 69.1 min half-life, which decays by electron capture to the ^{110}In ground state. There is one route that does not proceed through the metastable state and this is through the ^{110}Sn parent. Thus, one way to produce pure ^{110}In is to produce pure ^{110}Sn and use it as a generator for the ^{110}In [2.21.1, 2.21.2].

There are two modes of decay.

Data set No. 1

Parent nucleus	Parent energy level (keV)	Parent half-life (min)	Decay mode	Daughter nucleus
In-110	62.1	69.1	EC: 100%	Cd-110

Beta$^+$ emission

This table is also continued on the next page.

Fraction	Energy (keV)	End point energy (keV)
0.000005	162	285
0.000014	229	441
0.000008	249	485
0.000057	282	562
0.000029	312	631
0.000127	366	755
0.000230	403	839
0.002660	533	1135
0.000110	556	1187
0.000400	641	1376

Fraction	Energy (keV)	End point energy (keV)
0.002800	671	1442
0.000500	672	1445
0.620000	1043	2260

Note: Mean β^+ energy is 1.04×10^3 keV.

Electron emission products

Energy (keV)	Intensity (%)
Auger L: 2.72	32.4
Auger K: 19.3	5.0

Photon emission products

Gamma rays with less than 1% abundance are not shown in the following table.

Fraction	Energy (keV)
0.0218	3.13
0.078	22.984
0.147	23.174
0.0128	26.06
0.0246	26.095
1.25	511
0.98	657.75
0.022	2129.4
0.0175	2211.33
0.0129	2317.410

Data set No. 2

Parent nucleus	Parent energy level	Parent half-life (h)	Decay mode	Daughter nucleus
In-110	0.0	4.9	EC: 100%	Cd-110

Positron emission products

Fraction	Energy (keV)	End point energy (keV)
0.00019	201	376
0.00014	285	569

Note: Mean β^+ energy is 2.4×10^2 keV; total β^+ intensity is 0.033%.

Electron emission products

This table is also continued on the next page.

Fraction	Energy (keV)	Fraction	Energy (keV)	Fraction	Energy (keV)
0.853	2.72	0.000121	650.9	0.000149	880.649
0.132	19.3	0.000334	653.732	0.000787	910.767
0.000014	382.9	1.45E–05	673.6	9.58E–05	933.46
1.66E–06	405.6	0.000737	680.689	4.52E–05	970.45
9.56E–06	440.2988	0.000088	703.382	7.9E–06	1018.53
1.2E–06	462.992	3.91E–05	717.55	9.7E–07	1041.22
2.34E–07	466.2398	6.83E–05	733.16	1.13E–05	1058.81
0.000078	533.61	4.91E–06	740.24	1.35E–06	1081.5
1.01E–05	556.3	8.2E–06	755.85	1.44E–05	1090.649
0.000046	599.53	8.4E–06	768.71	1.6E–06	1098.96

Fraction	Energy (keV)	Fraction	Energy (keV)	Fraction	Energy (keV)
0.000833	614.97	3.87E–05	791.305	1.9E–07	1121.65
0.000012	621.87	4.52E–06	813.998	1.93E–06	1278.4
5.7E–06	622.22	4.74E–05	817.956	4.9E–06	1307.43
0.00267	631.039	5.84E–06	840.649	2.4E–06	1394.33
9.86E–05	637.66	0.001217	857.956	5.5E–06	1449.05
1.4E–06	644.56				

Photon emission products

Gamma rays with less than 1% abundance are not shown in the following table.

Fraction	Energy (keV)	Fraction	Energy (keV)
0.0575	3.13	0.045	677.6
0.205	22.984	0.295	707.4
0.387	23.174	0.016414	708.12
0.0335	26.06	0.0197	744.26
0.0645	26.095	0.0315	759.87
0.0166	26.644	0.0226	818.016
0.02261	461.1	0.0324	844.667
0.04718	461.8	0.929	884.667
0.0187	560.32	0.0197	901.53
0.086	581.93	0.684	937.478
0.0649	584.21	0.1052	997.16
0.0147	626.24	0.0137	1085.52
0.259	641.68	0.0423	1117.36
0.983	657.75	0.0125	1475.76

Nuclear reactions

Nuclear reaction	Useful energy range (MeV)	Natural abundance (%)	References
$^{110}Cd(p, n)^{110}In$	10–20	12.5	[2.21.1]
$^{110}Cd(^{3}He, 3n)^{110}Sn$: ^{110}In	18–36	12.5	[2.21.2, 2.21.3]
$^{109}Ag(^{3}He, 2n)^{110}In$		48.2	
$^{113}In(p, 4n)^{110}Sn$: ^{110}In	60–80	4.3	[2.21.1]
$^{110}Cd(d, 2n)^{110}In$		12.5	

Excitation function

The excitation function for $^{110}Cd(p, n)^{110}In$ is shown in Fig. 2.21.1.

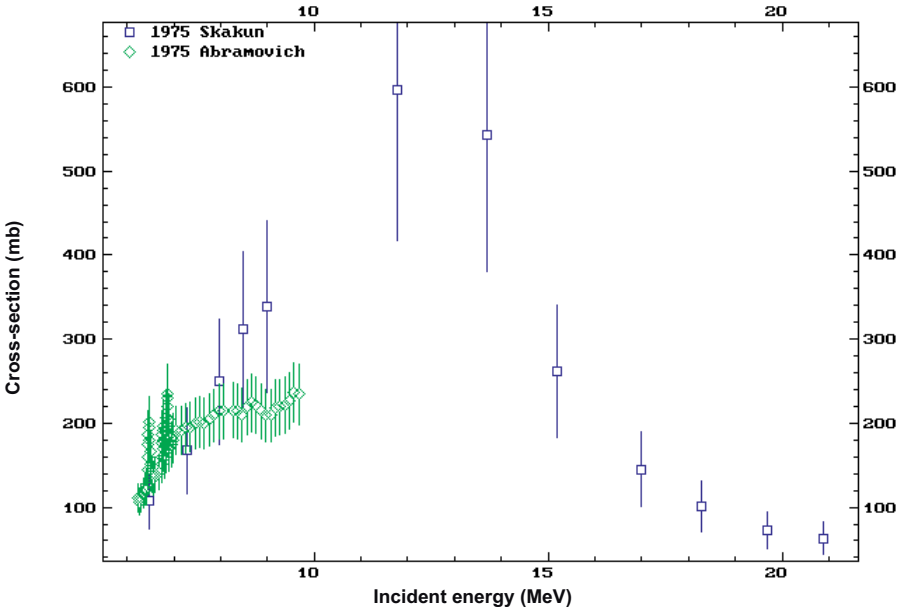

FIG. 2.21.1. Excitation function of $^{110}Cd(p, n)^{110}In$.

REFERENCES TO SECTION 2.21

[2.21.1] LUNDQVIST, H., SCOTT-ROBSON, S., EINARSSON, L., MALMBORG, P., ^{110}Sn/^{110}In: A new generator system for positron emission tomography, Appl. Radiat. Isot. **42** (1991) 447–450.

[2.21.2] SZELECSÉNYI, F., KOVÁCS, Z., TÁRKÁNYI, F., TÓTH, G.Y., "Production of ^{110}In for PET investigation via Cd(^{3}He, xn)^{110}Sn → ^{110}In reaction with low energy cyclotron", paper presented at 8th Int. Symp. on Radiopharmaceutical Chemistry, Princeton, NJ, 1990 (J. Labelled Compd. Radiopharm. **30** (1991) 98–99 (abstract)).

[2.21.3] RÖSCH, F., NOVGORODOV, A.F., TSAI, Y.-M., QAIM, M., "Production of the positron-emitting indium isotope ^{110g}In via the ^{110}Cd(^{3}He, 3n)^{110}Sn → ^{110g}In-process", Targetry and Target Chemistry (Proc. 6th Workshop Vancouver, 1995), TRIUMF, Vancouver (1995) 119–121.

BIBLIOGRAPHY TO SECTION 2.21

ABRAMOVICH, S.N., GUZHOVSKIJ, B.J.A., ZVENIGORODSKIJ, A.G., TRUSILLO, S.V., Isobar-analog resonances displayed by proton elastic and inelastic scattering and (p, n) reaction with Cd-110, Cd-112, Cd-114, Cd-116, Izv. Akad. Nauk. SSSR, Ser. Fiz. **39** (1975) 1688–1694.

INTERNATIONAL ATOMIC ENERGY AGENCY, Charged Particle Cross-section Database for Medical Radioisotope Production: Diagnostic Radioisotopes and Monitor Reactions, IAEA-TECDOC-1211, IAEA, Vienna (2001).

LUNDQVIST, H., TOLMACHEV, V., BRUSKIN, A., EINARSSON, L., MALMBORG, P., Rapid separation of ^{110}In from enriched Cd targets by thermal diffusion, Appl. Radiat. Isot. **46** (1995) 859–863.

OTOZAI, K., et al., Excitation functions for the reactions induced by protons on Cd up to 37 MeV, Nucl. Phys. **80** (1966) 335.

SKAKUN, E.A., KLJUCHAREV, A.P., RAKIVNENKO, Yu.N., ROMANIJ, I.A., Excitation functions of (p, n)- and (p, 2n)-reactions on cadmium isotopes, Izv. Akad. Nauk SSSR, Ser. Fiz. **39** (1975) 24–30.

TÁRKÁNYI, F., et al., Activation cross-sections on cadmium: Proton induced nuclear reactions up to 80 MeV, Nucl. Instrum. Methods Phys Res. B **245** (2006) 379–394.

2.22. INDIUM-111

Half-life: 2.83 d.

Decay mode

Indium-111 decays by electron capture. There are two prominent gamma rays, one at 171.3 keV and one at 245.4 keV.

Uses

Indium-111 as a lipophilic complex (e.g. ^{111}In oxine) is used for labelling blood cells. Indium-111 octreotide, a radiolabelled somatostatin analogue, binds to somatostatin receptors, which are very common in several cancers. Indium-111 may, therefore, be useful for the visualization of metastases in cancer patients.

Electron emission products of ^{111}In

Fraction	Energy (MeV)
0.001814	0.244620
0.002450	0.170510
0.007849	0.241370
0.010499	0.167260
0.050384	0.218680
0.084090	0.144570
0.157720	0.019300
1.002700	0.002720

Photon emission products of ^{111}In

This table is also continued on the next page.

Fraction	Energy (MeV)
0.000028	0.150810
0.070853	0.003130
0.145970	0.026100
0.236280	0.022984
0.445810	0.023174
0.902400	0.171280
0.940000	0.245390

Nuclear reactions

Nuclear reactions such as Cd(p, xn)^{111}In, Cd(d, xn)^{111}In and ^{109}Ag(α, 2n)^{111}In are used to produce ^{111}In for medical use. The yield of ^{111}In from the nuclear reaction on silver is much lower than that from the irradiation of cadmium targets with protons [2.22.1]. However, ^{111}In obtained from a silver target is free from long lived ^{114m}In ($T_{1/2}$ = 49.5 d), which emits high energy gamma radiation, whereas variable amounts of ^{114m}In are always present in ^{111}In derived from the cadmium route [2.22.1–2.22.3]. There is really only one reaction that is used commercially to produce ^{111}In: the proton reaction on natural cadmium. The two reactions possible are the ^{111}Cd(p, n)^{111}In and ^{112}Cd(p, 2n)^{111}In reactions [2.22.4].

Excitation functions

The excitation functions for ^{111}In are shown in Figs 2.22.1–2.22.3.

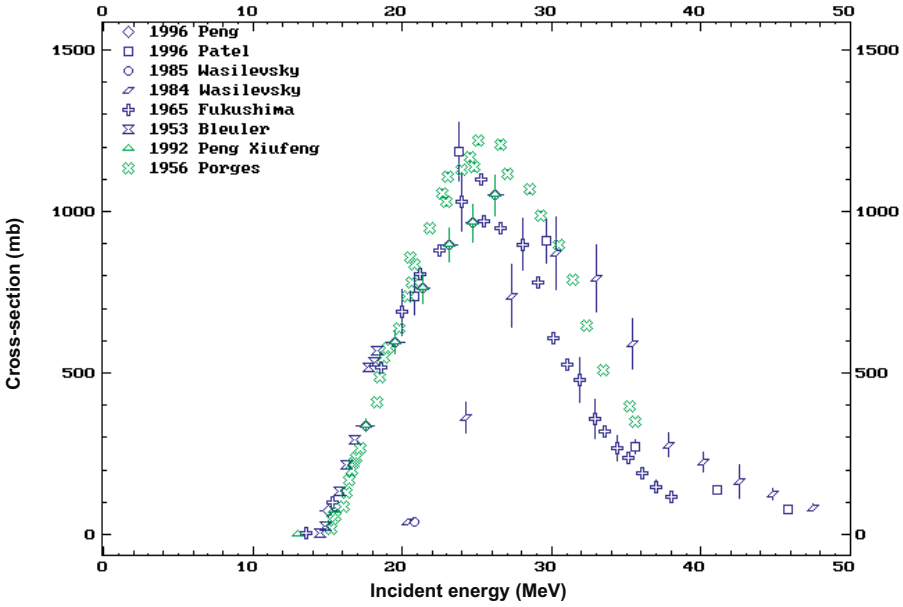

FIG. 2.22.1. Excitation function for the $^{109}Ag(\alpha, 2n)^{111}In$ reaction.

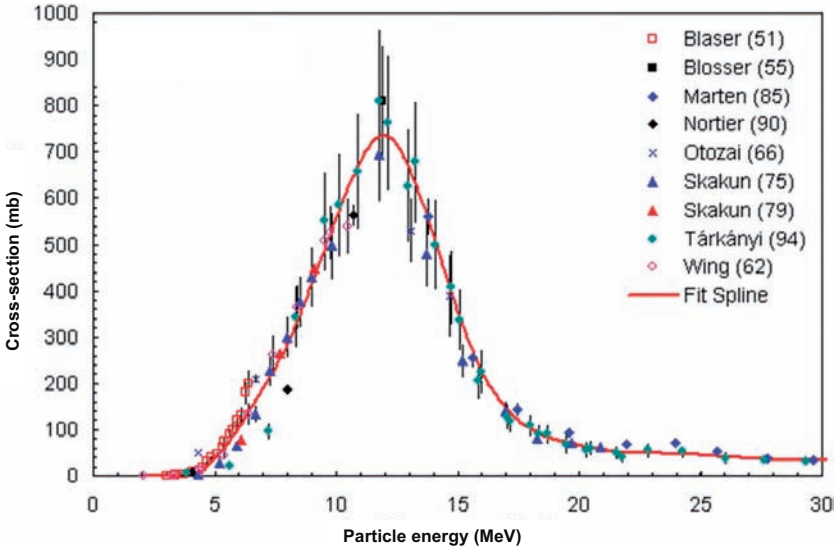

FIG. 2.22.2. Excitation function for the $^{111}Cd(p, n)^{111}In$ reaction.

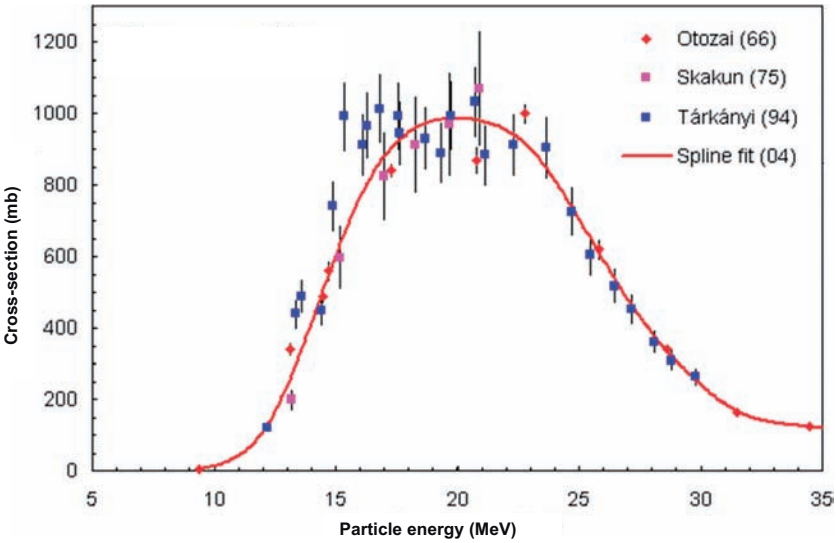

FIG. 2.22.3. Excitation function for the $^{112}Cd(p, 2n)^{111}In$ reaction.

Thick target yields

The following table is taken from IAEA-TECDOC-1211 [2.22.5]. This table is also continued on the next page.

Energy (MeV)	Activity (GBq) A2[a]	Energy (MeV)	Activity (GBq) A2	Energy (MeV)	Activity (GBq) A2	Energy (MeV)	Activity (GBq) A2
11.5	0.0014	17.5	6.35	23.5	20.3	29.5	29.3
12.0	0.033	18.0	7.45	24.0	21.4	30.0	29.7
12.5	0.12	18.5	8.60	24.5	22.3	30.5	30.1
13.0	0.29	19.0	9.79	25.0	23.3	31.0	30.5
13.5	0.54	19.5	11.0	25.5	24.2	31.5	30.8
14.0	0.90	20.0	12.2	26.0	25.0	32.0	31.1
14.5	1.37	20.5	13.4	26.5	25.8	32.5	31.4
15.0	1.96	21.0	14.6	27.0	26.5	33.0	31.7
15.5	2.65	21.5	15.8	27.5	27.1	33.5	31.9

Energy (MeV)	Activity (GBq) A2[a]	Energy (MeV)	Activity (GBq) A2	Energy (MeV)	Activity (GBq) A2	Energy (MeV)	Activity (GBq) A2
16.0	3.44	22.0	17.0	28.0	27.7	34.0	32.1
16.5	4.33	22.5	18.2	28.5	28.3	34.5	32.3
17.0	5.31	23.0	19.3	29.0	28.8	35.0	32.5

[a] A2 is the saturation activity of 1 μA irradiation.

Target materials

The target material is natural cadmium, enriched ^{112}Cd or natural silver. It can be either electroplated or pressed as a powder into a target holder (see target preparation below).

Target preparation

Internal irradiation can be carried out on a hemispherical copper target head [2.221.6]. The outer surface of the copper target is electroplated with 80 μm thick cadmium metal. The target head is irradiated tangentially with a 20 MeV, 10–40 μA proton beam.

An external target is constructed as follows: cadmium metal (≈2 g) is first melted into a groove (15 mm diameter by 1 mm deep) cut into an aluminium disc. The molten cadmium is then pressed with an aluminium plate, ensuring complete filling of the cavity. The surface of the cadmium is then carefully polished, finally cleaned with soap and water, and dried. The target is mounted on a target holder, which can be fixed in the beam line. The rear of the target is cooled with a jet of low conductivity water [2.22.7]. The beam current is much lower for the external target than for the internal target.

Target processing

The separation of the ^{111}In from the cadmium target plates has been accomplished by two different methods. Both ion exchange chromatography and solvent extraction have been used. These methods give similar recoveries of ^{111}In [2.22.8]. The solvent extraction method is described here.

Irradiated ^{112}Cd target is dissolved in concentrated HBr, and ^{111}In is extracted in DIPE. The enriched ^{112}Cd remains in the acid aqueous layer. Indium-111 is then back-extracted into a small volume of 8M HCl, followed by evaporation to dryness. Indium-111 is redissolved in 0.05M HCl.

Recovery of enriched materials

Cadmium-112 solution pooled from several irradiated targets with a manageable radiation level is boiled to remove residual DIPE, and a sufficient volume of 5N NaOH is added to precipitate ^{112}Cd (pH > 12). The resulting precipitate is dissolved by gradual addition of NaCN (≈2.0 g/g of ^{112}Cd). Cadmium-112 is precipitated in sulphide form with sodium sulphide solution (2M), followed by dissolution in concentrated HCl. Cadmium is then reprecipitated as $Cd(OH)_2$ with 5M NaOH. If desired, hydroxide can be converted to oxide by heating at 90–130°C.

Specifications

The main impurity resulting from preparation from a natural cadmium target is ^{114m}In. The gamma spectrum of the final product will allow identification of the impurity. The chemical impurities of the target material (either cadmium or silver) must be separated along with the other target holder materials such as copper, aluminium and iron. Other radionuclidic impurities must also be separated using either solvent extraction or ion exchange chromatography.

Quality assurance tests for [^{111}In]$InCl_3$

Physicochemical tests can be carried out to check the quality of the final product. The radionuclidic purity of the final product is checked by gamma ray spectroscopy. Radiochemical purity is assessed by paper chromatography using Whatman No. 1 paper and a solvent system composed of 10% ammonium formate: methanol: 0.2M citric acid in the ratio 2:2:1 [2.22.9]. The chemical purity of the final product is tested by checking for the presence of Cu, Fe and Al by the ferric-iron–thiosulphate reaction, $\alpha\alpha'$-dipyridyl reagent and Alizarin-S reagent tests, respectively.

REFERENCES TO SECTION 2.22

[2.22.1] MacDONALD, N.S., et al., Methods for compact cyclotron production of indium-111 for medical use, Int. J. Appl. Radiat. Isot. **26** (1975) 631–633.

[2.22.2] DAHL, J.R., TILBURY, R.S., The use of a compact, multi-particle cyclotron for the production of ^{52}Fe, ^{67}Ga, ^{111}In and ^{123}I for medical purposes, Int. J. Appl. Radiat. Isot. **23** (1972) 431–437.

[2.22.3] ZAITSEVA, N.G., et al., Excitation functions and yields for ^{111}In production using $^{113,114,nat.}$Cd(p, xn)^{111}In reactions with 65 MeV protons, Appl. Radiat. Isot. **41** (1990) 177–183.

[2.22.4] NORTIER, F.M., MILLS, S.J., STEYN, G.F., Excitation functions and production rates of relevance to the production of ^{111}In by proton bombardment of ^{nat}Cd and ^{nat}In up to 100 MeV, Int. J. Radiat. Isot. **41** (1990) 1201–1208.

[2.22.5] INTERNATIONAL ATOMIC ENERGY AGENCY, Charged Particle Cross-section Database for Medical Radioisotope Production: Diagnostic Radioisotopes and Monitor Reactions, IAEA-TECDOC-1211, IAEA, Vienna (2001).

[2.22.6] DAS, M.K., RAMAMOORTHY, N., ^{67}Ga-gallium citrate I: Production experience at Variable Energy Cyclotron Centre, Calcutta, Ind. J. Nucl. Med. **10** (1995) 63–66.

[2.22.7] DAS, M.K., RAMAMOORTHY, N., SARKAR, B.R., MANI, R.S., Yield of ^{52}Fe by α-particle reaction on natural chromium at 70 MeV, Radiochim. Acta **47** (1989) 173–175.

[2.22.8] SZELECSÉNYI, F., et al., "Excitation functions of proton induced nuclear reactions on ^{111}Cd and ^{112}Cd: Production of ^{111}In", Nuclear Data for Science and Technology (QAIM, S.M., Ed.), Springer-Verlag, Berlin (1992) 603–605.

[2.22.9] PAIK, C.H., et al., Radiolabeled products in rat liver and serum after administration of antibody-amide-DTPA-indium-111, Int. J. Radiat. Appl. Instrum. B **19** (1992) 517–522.

BIBLIOGRAPHY TO SECTION 2.22

CHATTOPADHYAY, S., DAS, M.K., SARKAR, B.R., RAMAMOORTHY, N., Radiochemical separation of high purity ^{111}In from cadmium, copper, aluminium and traces of iron: Use of a cation exchange resin with hydrobromic acid and hydrochloric acid, Appl. Radiat. Isot. **48** (1997) 1063–1067.

DAS, M.K., CHATTOPADHYAY, S., SARKAR, B.R., RAMAMOORTHY, N., A cation exchange method for separation of ^{111}In from inactive silver, copper, traces of iron and radioactive gallium and zinc isotopes, Appl. Radiat. Isot. **48** (1997) 11–14.

TAKÁCS, S., TÁRKÁNYI, F., HERMANNE, A., PAVIOTTI DE CORCUERA, R., Validation and upgrading of the recommended cross section data of charged particle reactions used for production of PET radioisotopes, Nucl. Instrum. Methods Phys. Res. B **211** (2003) 169–189.

2.23. INDIUM-114m

Half-life: 49.5 d.

Electron emission products of ^{114m}In

Fraction	Energy (MeV)
0.006104	0.019300
0.013370	0.190150
0.038953	0.002720
0.059878	0.020100
0.066468	0.189440
0.317060	0.186030
0.399190	0.162330
0.641760	0.002840

Photon emission products of ^{114m}In

Fraction	Energy (MeV)
0.002753	0.003130
0.005649	0.026100
0.009144	0.022984
0.017253	0.023174
0.044779	0.558430
0.044887	0.725240
0.050538	0.003290
0.060502	0.027300
0.096700	0.024002
0.159490	0.190270
0.182110	0.024210

Nuclear reactions

The nuclear reactions that produce ^{114m}In are:

(a) ^{114}Cd(p, n)^{114m}In;
(b) ^{114}Cd(d, 2n)^{114m}In;
(c) ^{116}Cd(p, 3n)^{114m}In.

Excitation functions

The excitation functions for ^{114m}In are shown in Figs 2.23.1–2.23.3.

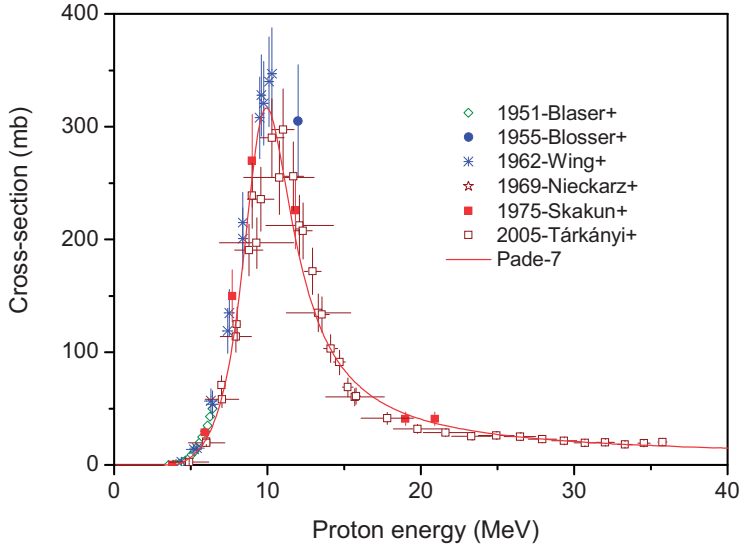

FIG. 2.23.1. Excitation function for the ^{114}Cd(p, n)^{114m}In reaction.

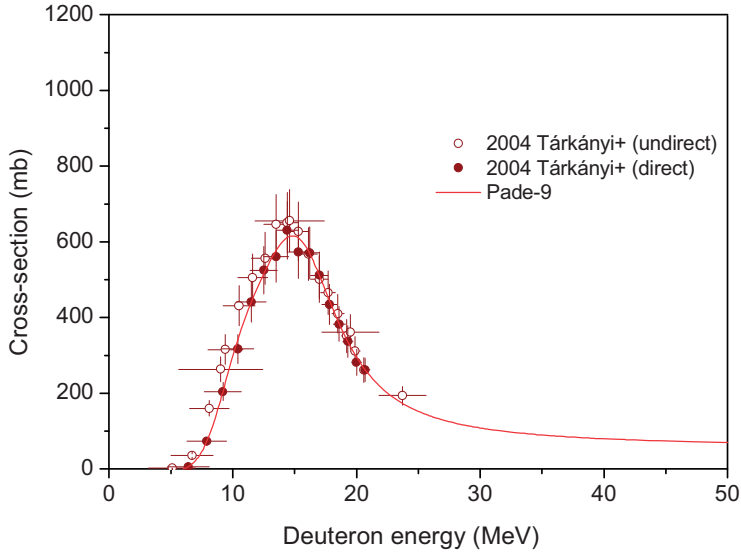

FIG. 2.23.2. Excitation function for the $^{114}Cd(d, 2n)^{114m}In$ reaction.

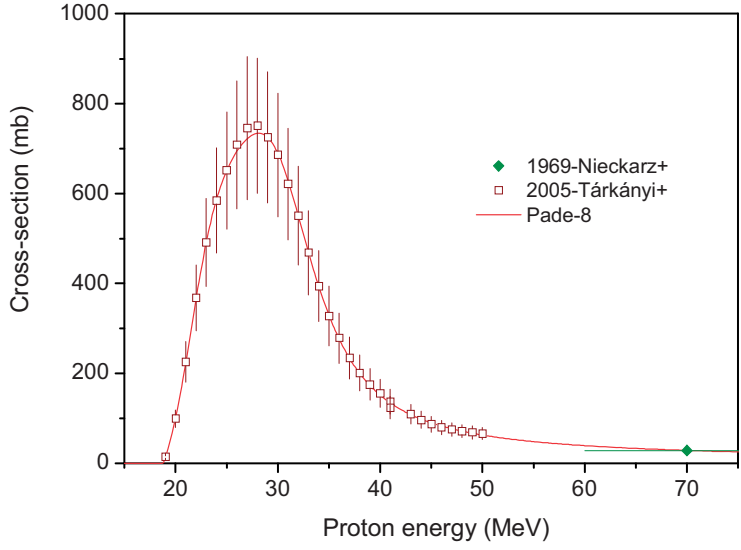

FIG. 2.23.3. Excitation function for the $^{116}Cd(p, 3n)^{114m}In$ reaction.

BIBLIOGRAPHY TO SECTION 2.23

BLOSSER, H.G., HANDLEY, T.H., Survey of (p, n) reactions at 12 MeV, Phys. Rev. **100** (1955) 1340–1344.

INTERNATIONAL ATOMIC ENERGY AGENCY, Charged Particle Cross-section Database for Medical Radioisotope Production: Diagnostic Radioisotopes and Monitor Reactions, IAEA-TECDOC-1211, IAEA, Vienna (2001).

TÁRKÁNYI, F., et al., Investigation of the production of the therapeutic radioisotope ^{114m}In through proton and deuteron induced nuclear reactions on cadmium, Radiochim. Acta **93** (2005) 561–571.

WING, J., HUIZENGA, J.R., (p, n) Cross sections of V-51, Cr-52, Cu-63, Cu-65, Ag-107, Ag-109, Cd-111, Cd-114, and La-139 from 5 to 10.5 MeV, Phys. Rev. **128** (1962) 280–290.

ZAITSEVA, N.G., et al., Excitation functions and yields for ^{111}In production using $^{113,114,nat.}$Cd(p, xn)^{111}In reactions with 65 MeV protons, Appl. Radiat. Isot. **41** (1990) 177–183.

2.24. IODINE-120g

Half-life

Iodine-120g decays with a half-life of 1.35 h and about 39% positron emission. The beta energy is quite high (4.0 MeV).

Parent nucleus	Parent energy level	Parent half-life (min)	Decay mode	Daughter nucleus
I-120	0.0	81.6	EC: 100%	Te-120

Positron emission products

Fraction	Energy (keV)	End point (keV)	Fraction	Energy (keV)	End point (keV)
2.6E–06	145.7	305	0.00155	652.1	1457
7.3E–06	147.8	310	0.0043	689.7	1541
0.000027	189.4	405	0.00068	716.4	1557
1.58E–05	207	445	0.0053	729.2	1629
0.000056	214.8	463	0.0094	741.5	1656
0.000046	220.1	475	0.0065	826.9	1845
0.000029	258.3	563	0.00264	853.5	1903
0.000082	270.6	591	0.00422	888.5	1980
0.00044	316.3	696	0.0213	960.1	2137
0.000037	320.6	706	0.062	1131.4	2510
0.0014	373.5	827	0.00235	1199.2	2656
0.000024	414.4	921	0.00664	1204.7	2668
0.00069	417.1	927	0.0007	1233.2	2730
0.0025	492.9	1099	0.0019	1354.8	2980
0.0015	547.1	1222	0.0193	1386	3058
0.0012	549.4	1226	0.027	1542.4	3392
0.000657	560.4	1251	0.0093	1561.3	3431
0.00162	585.1	1307	0.002	1588.4	3490
0.00069	598.7	1337	0.293	1845	4033
0.00131	640.1	1430	0.19	2099.3	4593

Electron emission products

This table is also continued on the next page.

Fraction	Energy (keV)	Fraction	Energy (keV)
0.265	3.19	1.04E–06	648.0608
0.0346	22.7	4.94E–06	657.2
1.9E–05	302.1862	1.04E–05	669.6
2.67E–06	329.0608	1.36E–06	696.5

Fraction	Energy (keV)	Fraction	Energy (keV)
5.35E–07	332.994	1.95E–05	943.3
1.25E–07	333.8317	2.5E–06	970.2
3.51E–05	401.2	4.72E–06	1069.2
5.04E–06	428.1	5.75E–07	1096.1
0.000001	432	0.000017	1169.8
0.000054	510.9	3.6E–06	1379.1
0.00354	528.6	5.04E–06	1391.1
7.5E–06	537.8	2.71E–05	1491.2
0.000487	555.5	6.3E–07	2346.6
0.000256	569.3	1.27E–06	2372.2
0.000312	609.3	3.1E–06	2423
8.28E–06	621.1862	9.3E–07	2460
3.89E–05	630.3	2.3E–06	2532.6
4.13E–05	636.2		

Photon emission products

This table is also continued on the next page.

Fraction	Energy (keV)	Fraction	Energy (keV)	Fraction	Energy (keV)	Fraction	Energy (keV)
0.025	3.77	0.00031	735.3	0.0125	1410.9	0.0106	2404
0.0691	27.202	0.00327	735.3	0.00752	1422.9	0.0195	2454.8
0.128	27.472	0.000974	749	0.00466	1451.7	0.0068	2462.8
0.0118	30.944	0.00432	763	0.109	1523	0.0116	2491.8
0.0227	30.995	0.00188	853.3	0.0181	1534.9	0.025	2564.4
0.00655	31.704	0.003	881.8	0.0055	1601	0.00487	2602.5
0.000835	334	0.0023	921.3	4.2E–06	1614	0.002506	2613
0.0008	412	0.00362	921.3	0.0086	1775.8	0.002784	2800
0.00334	433	0.001183	950	0.0025	1851.4	0.0081	2811.2
0.000035	511	0.0018	969.1	0.0054	1874.7	0.002088	2829
1.365	511	0.015	975.1	0.0065	1895	0.0061	2932.9
0.000139	529	0.003202	1053	0.00348	2034	0.00418	2987

Fraction	Energy (keV)	Fraction	Energy (keV)	Fraction	Energy (keV)	Fraction	Energy (keV)
0.00174	529	0.0058	1074	0.00348	2034	0.00348	3029
0.0098	542.7	0.00411	1101	0.002088	2045	0.002784	3082
0.696	560.4	0.000028	1103	0.00905	2082	0.002088	3334
0.0551	601.1	0.025	1201.6	0.003	2094	0.002088	3442
0.0047	614	0.00675	1255	0.0055	2129.4	0.002784	4120
0.0842	641.1	0.000696	1255.4	0.00404	2165	0.002784	4134
0.00212	653	0.0024	1283.4	0.00696	2172	0.002784	4148
0.0105	662.1	0.00828	1302.7	0.00341	2180	0.002784	4188
0.0035	701.4	0.00661	1363.5	0.0144	2188	0.002784	4283
0.0019	729.2	0.00529	1402	0.007	2378.4	0.002088	4288

Nuclear reactions

Nuclear reaction	Useful energy range (MeV)	Natural abundance (%)	Reference
^{127}I(p, 8n)^{120}Xe: ^{120g}I	>65	100	[2.24.1]
^{122}Te(p, 3n)^{120g}I	32–38	0.095	[2.24.2]
^{120}Te(p, n)^{120g}I	15–25	4.8	[2.24.3]

Excitation function

The excitation function for ^{122}Te(p, 3n)^{120g}I is shown in Fig. 2.24.1.

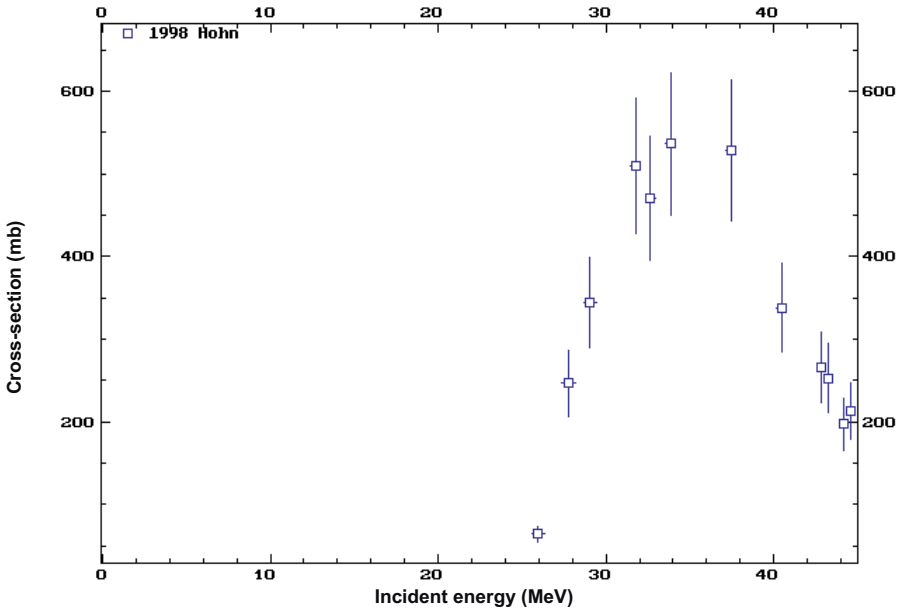

FIG. 2.24.1. Excitation function for the $^{122}Te(p, 3n)^{120g}I$ reaction.

REFERENCES TO SECTION 2.24

[2.24.1] BUTEMENT, F.D.S., QAIM, S.M., Radioisotopes of iodine and xenon of masses 120 and 121, J. Inorg. Nucl. Chem. **27** (1965) 907–917.

[2.24.2] ZWEIT, J., et al., "Iodine-120, a new positron emitting radionuclide for PET radiopharmaceuticals", Targetry and Target Chemistry (Proc. 6th Workshop Vancouver, 1995), TRIUMF, Vancouver (1995) 76–78.

[2.24.3] HOHN, A., COENEN, H.H., QAIM, S.M., Positron emission intensity in the decay of ^{120g}I, Radiochim. Acta **88** (2000) 139–141.

BIBLIOGRAPHY TO SECTION 2.24

HERZOG, H.R., HOHN, A., QAIM, S.M., TELLMANN, L., COENEN, H.H., Phantom study to test positron-emitting iodine-120, J. Nucl. Med. **40** (1999) 124.

2.25. IODINE-121

Half-life

Iodine-121 has a half-life of 2.12 h and decays with 94% electron capture and 6% positron emission. There is a prominent gamma ray at 212.2 keV, which can be used in gamma camera images. It decays to ^{121}Te, which has a long half-life and decays with the same 212.2 keV gamma ray.

Parent nucleus	Parent energy level	Parent half-life (h)	Decay mode	Daughter nucleus
I-121	0.0	2.12	EC: 100%	Te-121

Positron emission products

Fraction	Energy (keV)	End point energy (keV)
0.000007	163	330.00
3.1E–06	174	360.00
5.3E–07	199	420.00
0.0001	207	440.00
0.000012	209	440.00
0.000108	263	560.00
0.000115	264	570.00
0.000134	302	650.00
0.000029	326	710.00
0.0025	329	710.00
0.1	469	1030.00

Note: Mean β^+ energy, 4.6×10^2 keV; total β^+ intensity, 10.3%; mean β^+ dose, 0.048 MeV/(Bq·s).

Electron emission products

Fraction	Energy (keV)
0.812	3.19
0.106	22.7
0.00277	24.99
0.00177	51.86
0.06331	180.39
0.00835	207.26

Photon emission products

Gamma rays with less than 1% abundance are not shown in the following table.

Fraction	Energy (keV)
0.077	3.77
0.211	27.202
0.391	27.472
0.036	30.944
0.0694	30.995
0.02	31.704
0.843	212.2
0.0102	475.28
0.206	511
0.061	532.08
0.0147	598.74

Nuclear reactions

The only practical method of production is from the ^{122}Te(p, 2n)^{121}I nuclear reaction on highly enriched ^{122}Te [2.25.1].

Excitation function

The excitation function for ^{122}Te(p, 2n)^{121}I is shown in Fig. 2.25.1.

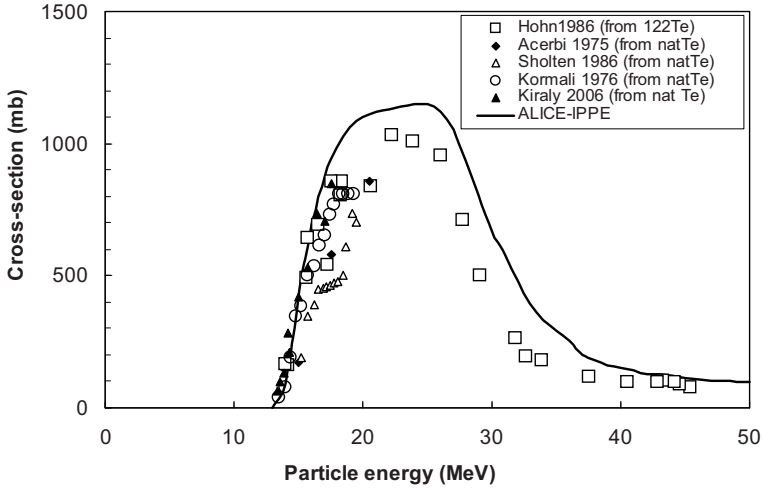

FIG. 2.25.1. Excitation function for the ^{122}Te(p, 2n)^{121}I reaction.

REFERENCE TO SECTION 2.25

[2.25.1] BUTEMENT, F.D.S., QAIM, S.M., Radioisotopes of iodine and xenon of masses 120 and 121, J. Inorg. Nucl. Chem. **27** (1965) 907–917.

BIBLIOGRAPHY TO SECTION 2.25

HOHN, A., SCHOLTEN, B., COENEN, H.H., QAIM, S.M., Excitation functions of (p, xn) reactions on highly enriched ^{122}Te: Relevance to the production of ^{120g}I, Appl. Radiat. Isot. **49** (1998) 93–98.

KIRÁLY, B., TÁRKÁNYI, F., TAKÁCS, S., KOVÁCS, Z., Excitation functions of proton induced nuclear reactions on natural tellurium up to 18 MeV for validation of isotopic cross sections, J. Radioanal. Nucl. Chem. **270** (2006) 369.

2.26. IODINE-123

Half-life: 13.2 h.

Uses

The most widely used cyclotron produced radiohalogen is probably ^{123}I. It has gradually replaced ^{131}I as the isotope of choice for diagnostic radiopharmaceuticals containing radio-iodine. It gives a much lower radiation dose to the patient, and the gamma ray energy of 159 keV is ideally suited for use in a gamma camera. The gamma ray will penetrate tissue very effectively without an excessive radiation dose. For this reason, it has in many instances replaced reactor produced ^{131}I. A large number of radiopharmaceuticals have been labelled using ^{123}I, and the number is increasing.

Decay mode

Iodine-123 decays 100% by electron capture, with two main gamma rays at 0.028 and 0.160 MeV.

Electron emission products of ^{123}I

Fraction	Energy (MeV)
0.017597	0.154060
0.123630	0.022700
0.135940	0.127190
0.940730	0.003190

Photon emission products of ^{123}I

Fraction	Energy (MeV)
0.013928	0.528960
0.093039	0.003770
0.159520	0.031000
0.246310	0.027202
0.459540	0.027472
0.834000	0.159000

Nuclear reactions

The major reactions for the production of ^{123}I are given in the following table. As can be seen from this table, there are two major routes to ^{123}I. The first is the direct route and the second is through the ^{123}Xe precursor. The advantage of going through ^{123}Xe is that the xenon can be separated from the original target material and allowed to decay in isolation, which gives an ^{123}I with very little contamination from other radioisotopes of iodine. The most common reaction for the production of ^{123}I in the recent past has been the ^{124}Te(p, 2n)^{123}I reaction on highly enriched ^{124}Te. The high enrichment is necessary since, in addition to the (p, n) reaction on ^{124}Te, there is a second source of ^{124}I contamination and this comes from the ^{125}Te(p, 2n)^{124}I nuclear reaction on any ^{125}Te, which may be present in the target material [2.26.1, 2.26.2].

Nuclear reaction	Useful energy range (MeV)	Natural abundance (%)	References
^{127}I(p, 5n)^{123}Xe: ^{123}I	55+	100	[2.26.3–2.26.7]
^{127}I(d, 6n)^{123}Xe: ^{123}I	83	100	[2.26.8]
^{122}Te(d, n)^{123}I	14–8	2.4	[2.26.9]
^{123}Te(p, n)^{123}I	15–8	0.87	[2.26.10]
^{124}Te(p, 2n)^{123}I	26–20	4.6	[2.26.11–2.26.13]
^{122}Te(^{4}He, 3n)^{123}Xe: ^{123}I			[2.26.14, 2.26.15]
^{124}Xe(p, pn)^{123}Xe: ^{123}I	15–30	0.10	[2.26.16–2.26.20]
^{121}Sb(^{4}He, 2n)^{123}I	15–25	57.4	[2.26.21, 2.26.22]
^{123}Sb(^{3}He, 3n)^{123}I	20–30	42.6	[2.26.21, 2.26.22]

Excitation functions

The excitation functions for ^{123}I are shown in Figs 2.26.1–2.26.5.

Target materials

The targets used for production of ^{123}I can be grouped into three types: solid targets, liquid or molten targets, and gaseous targets. Iodine-123 is commonly produced in all three types of target, depending on the energy of the cyclotron being used and on the availability of enriched ^{124}Xe as a target material. Each type of target has its own advantages and disadvantages. There is a set of criteria first proposed by Van den Bosch et al. [2.26.23] and Tertoolen et al. [2.26.24] that serve as guidelines for ^{123}I target construction. These criteria are:

(a) Thermal and radiation stability of the target and target support under irradiation, combined with adequate thermal conductivity and heat dissipation;
(b) Simple and almost complete separation of iodine from tellurium within a short period of time, preferably less than 30 min;
(c) Simple and almost complete reprocessing of the target; the loss of expensive enriched tellurium should be kept below 1% per irradiation and separation;
(d) The chemical state of the iodine produced should not handicap any in vivo application or labelling procedure.

These criteria, although applied to solid tellurium targets, serve as good guidelines for all iodine targets. Similar guidelines were reiterated by Qaim [2.26.25], who emphasized the power dissipation of the targets and the fact that efficient heat transfer is one of the prime requirements in target construction. He also emphasized the need for accurate nuclear data in order to design targets efficiently.

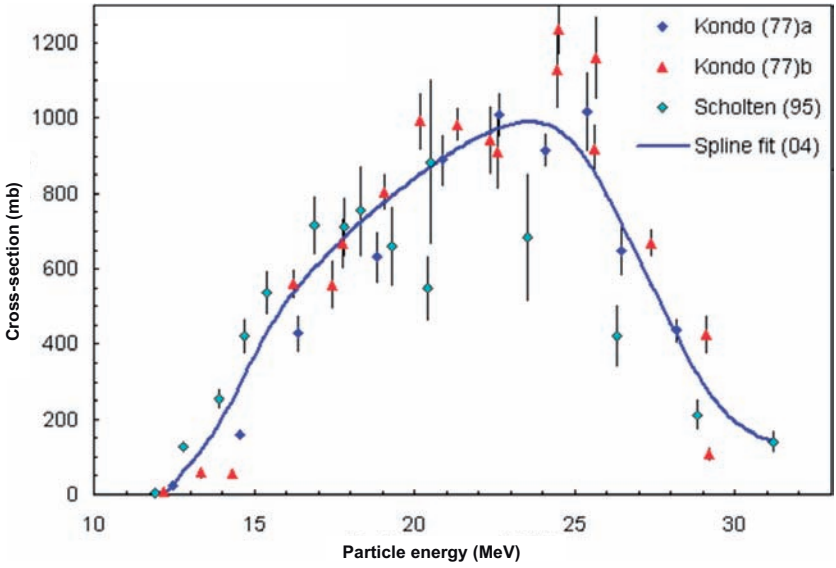

FIG. 2.26.1. Excitation function for the $^{124}Te(p, 2n)^{123}I$ reaction.

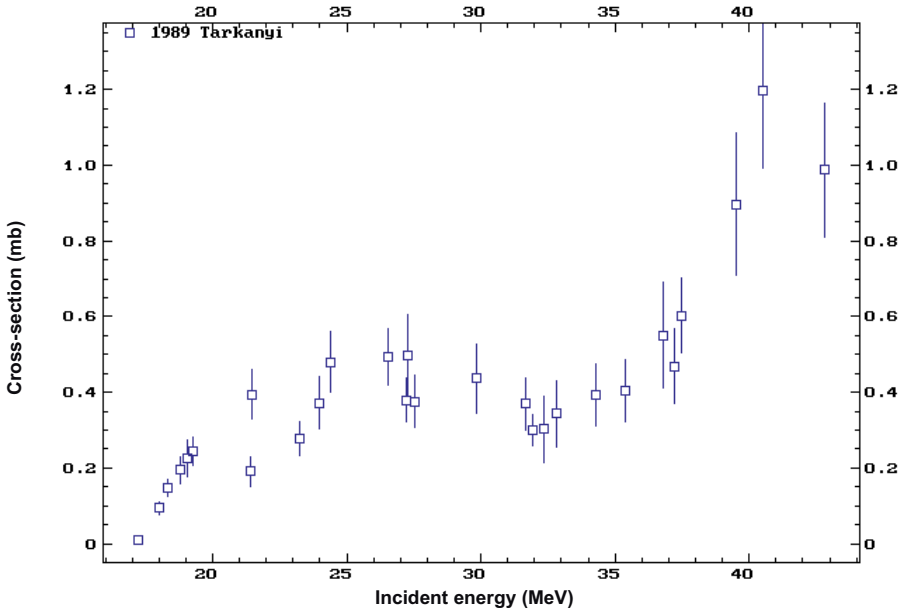

FIG. 2.26.2. Excitation function for the $^{nat}Xe(p, x)^{123}I$ reaction.

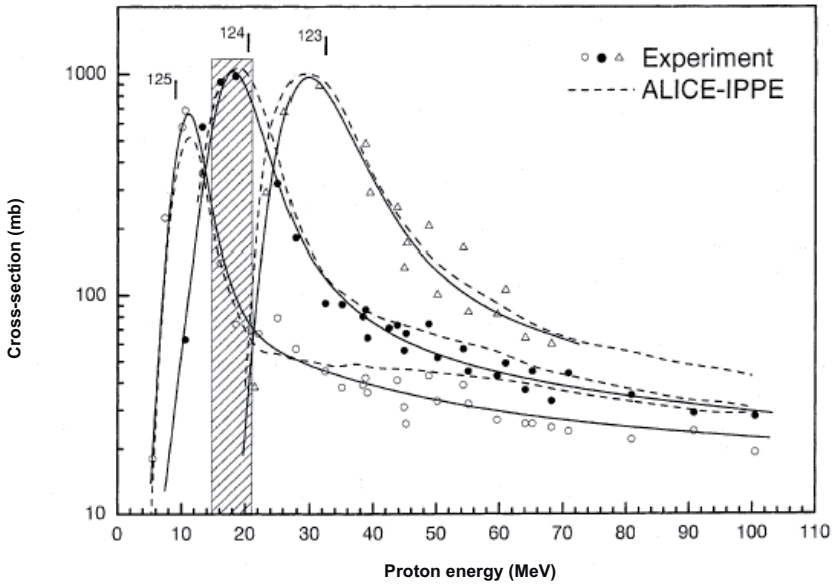

FIG. 2.26.3. Competing reactions of protons on natural xenon (normalized).

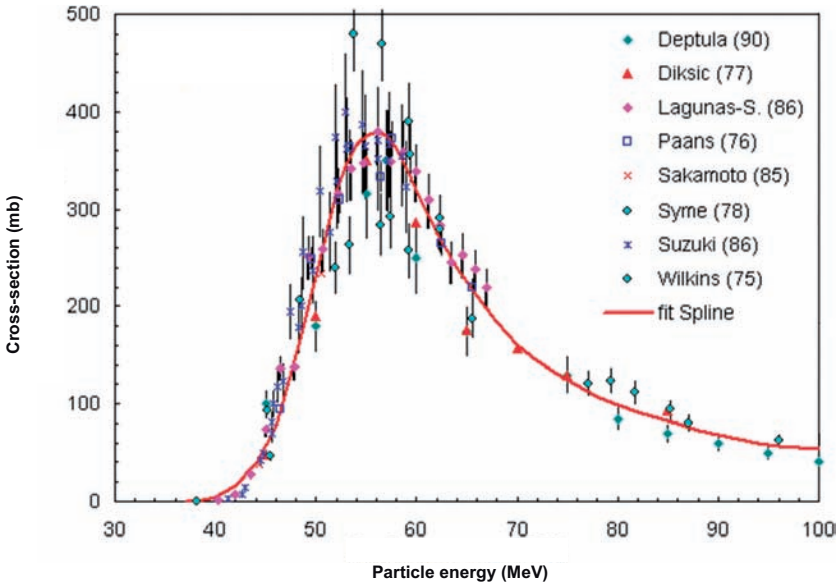

FIG. 2.26.4. Excitation function for the $^{127}I(p, 5n)^{123}Xe \rightarrow {}^{123}I$ reaction.

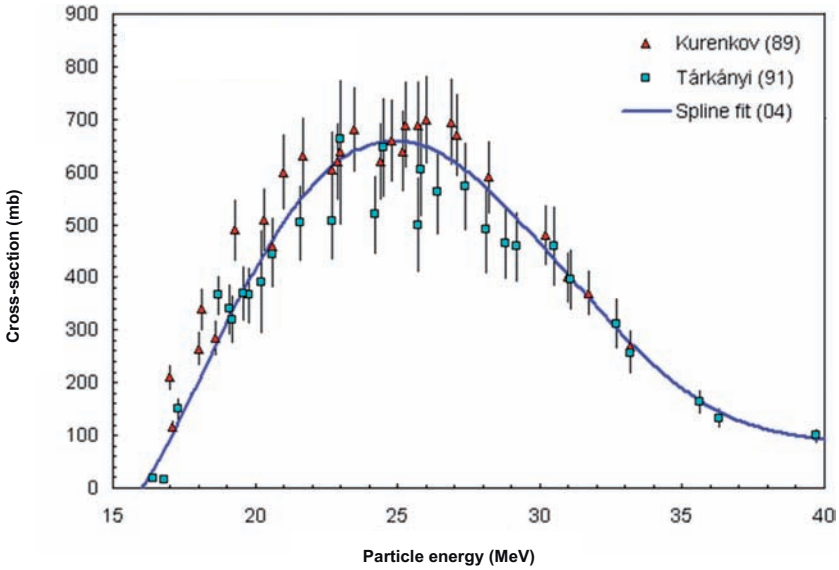

FIG. 2.26.5. Excitation function for the $^{124}Xe(p, 2n)^{123}Cs \rightarrow {}^{123}Xe \rightarrow {}^{123}I$ reaction.

Solid targets

One of the most common targets for production of ^{123}I is the reaction involving tellurium. The typical targets are of two different materials: the first is elemental tellurium and the second is tellurium oxide [2.26.2, 2.26.25]. A typical target would be tellurium electrodeposited onto a copper plate, which was then irradiated internally in the cyclotron.

Solid targets made from powdered tellurium have also been widely used for the production of ^{123}I [2.26.1, 2.26.8, 2.26.10–2.26.13, 2.26.26–2.26.30]. Tellurium powder has often been mixed with aluminium powder to increase the heat transfer characteristics of targets. A common problem with these targets is melting of the elemental tellurium and consequent loss of radio-iodine from the matrix.

An internal powder target has been developed and used with the ^{122}Te(d, n)^{123}I reaction [2.26.9]. This target has a flow-through design to extract the ^{123}I during the irradiation.

Other types of alloy target, such as a tellurium–gold alloy, have been used for production of ^{123}I [2.26.31]. This technique has been used extensively when the thermal conductivity of the primary material is low and/or the melting point is low. Tellurium oxide has been used for production of ^{123}I. The oxide has the advantage of a high melting point and, therefore, of a low loss of iodine from the matrix during irradiation.

A final type of solid target is the cryogenic target for production of ^{123}I from enriched ^{124}Xe [2.26.32]. This type of target has the advantage of being fail-safe in the sense that the xenon is frozen and therefore will not be lost in the case of a foil rupture. The disadvantage is that the target must be kept supplied with liquid nitrogen during irradiation.

Liquid targets

There were three types of liquid targets used for the production of ^{123}I:

(1) The molten salt targets used for production of ^{123}I from the ^{127}I(p, 5n)^{123}Xe reaction in a sodium iodide salt with a high energy beam [2.26.5, 2.26.33]. These have been used on their own or as the first target of several for isotope production [2.26.34].
(2) Liquid iodine targets have been used for routine production at low beam intensities with a sweep gas to remove the ^{123}Xe as it is made [2.26.35].

(3) The final type of target involved the use of a liquid such as methylene iodide in a recirculating flowing target [2.26.4]. This target had some problems with polymerization of the target material and was not a popular target.

Gaseous targets

Increasingly, ^{123}I is being made from the reaction of protons on enriched ^{124}Xe gas. This target has the advantage of producing very high purity ^{123}I with easy recovery of the target material. These targets typically contain 1–2 L of gas at elevated pressure. The real danger here is the possibility of losing a foil, which may result in the loss of the target gas into the cyclotron and then into the atmosphere. Several designs have been published to reduce or eliminate the possibility of such a loss [2.26.36]. In most cases, the xenon gas is trapped in a loop contained at liquid nitrogen temperatures. These loops, if properly constructed, can trap more than 99% of the xenon gas in the targets. This type of target has been tested extensively and has proved to be reliable in routine operation.

Target preparation

The targets may be prepared by electrodeposition of metallic tellurium or by use of tellurium oxide on a pressed target. Details of the preparation of these targets can be found in Ref. [2.26.37].

Target processing

The separation of radio-iodine from the target matrix is accomplished in two ways, depending on whether the ^{123}I is made by the indirect method or by the direct method. In the indirect method, the ^{123}Xe is isolated from the matrix and is then allowed to decay to ^{123}I in a separate vessel. This separation is usually not a difficult one since xenon is very unreactive and can usually be readily extracted from the target. In the case of direct production from tellurium, the problem is slightly more difficult.

In the direct production method, ^{123}I may be isolated through dry or wet distillation, or through a chemical process. The use of dry distillation is a common method of extraction. In this method, the tellurium powder or tellurium oxide powder is heated to near its melting point with a flow of gas over the plate. The ^{123}I is distilled out of the matrix and carried by the sweep gas to a receiver vessel where it is trapped. This vessel usually contains a base solution, and the iodine is in the chemical form of iodide. A wet chemical

method can also be used, dissolving the tellurium, then oxidizing the iodide to iodine, and finally distilling it out of the solution [2.26.26].

Alternatively, ^{123}I can be collected as iodide by dissolving the irradiated target in an oxidizing alkaline solution, followed by reduction of the enriched tellurium to the elemental state and iodine to iodide with aluminium powder. Precipitated tellurium metal is removed through filtration, and iodide is purified by passing it through a cation exchange resin. The drawback of this procedure is that the aqueous solution is of a relatively low concentration. Hence, if a high concentration is desired, the excess water must be removed through an additional step of concentration.

Recovery of enriched materials

Tellurium-124 can be recovered through a fairly simple chemical process. Tellurium-124 from a number of targets is dissolved, after a certain cooling period, in a HCl–hydrogen peroxide mixture, followed by reduction of Te^{6+} to Te^{4+} with HBr, and then precipitated as free tellurium metal by addition of hydrazine hydrate and sodium sulphite.

Specifications

Iodine-123 obtained through the indirect method is of very high radionuclidic purity in relation to the contamination of other iodine species in direct production. Iodine-123 produced through the (p, 2n) reaction on enriched ^{124}Te is contaminated with co-produced ^{124}I, which limits the shelf life of products prepared using the direct production method.

It is essential to monitor and control the presence of several different iodine species such as iodates and periodates. These species may also be generated during storage of high SA products [2.26.38]. Stabilization of radioiodine, predominantly as iodide, can be achieved by the addition of a small amount of a reductant such as sodium sulphite. It must be noted, however, that the presence of reductants is known to interfere with the radiolabelling of proteins.

Iodine batches produced through irradiation of solid tellurium and TeO_2 targets are tested for their chemical purity on aluminium and tellurium. Use is made of emission spectrometry or of colorimetry. The iodine batches produced through both targets meet all the pharmacopoeial criteria. The chemical impurities determined by colorimetric spot tests are typically: Te < 0.5 μg/mCi; Al < 0.25 μg/mCi.

REFERENCES TO SECTION 2.26

[2.26.1] GUILLAUME, M., LAMBRECHT, R.M., WOLF, A.P., Cyclotron production of ^{123}Xe and high purity ^{123}I: A comparison of tellurium targets, Int. J. Appl. Radiat. Isot. **26** (1975) 703–707.

[2.26.2] KONDO, K., LAMBRECHT, R.M., WOLF, A.P., Iodine-123 production for radiopharmaceuticals, XX: Excitation functions for the ^{124}Te(p, 2n)^{123}I and ^{124}Te(p, n)^{124}I reactions and the effect of target enrichment on radionuclidic purity, Int. J. Appl. Radiat. Isot. **28** (1977) 395–401.

[2.26.3] ADILBISH, M., et al., ^{123}I production from radioxenon formed in spallation reactions by 660 MeV protons for medical research, Int. J. Appl. Radiat. Isot. **31** (1980) 163–167.

[2.26.4] CUNINGHAME, J.G., MORRIS, B., NICHOLS, A.L., TAYLOR, N.K., Large scale production of ^{123}I from a flowing liquid target using the (p, 5n) reaction, Int. J. Appl. Radiat. Isot. **27** (1976) 597–603.

[2.26.5] JUNGERMAN, J.A., LAGUNAS-SOLAR, M.C., Cyclotron production of high purity iodine-123 for medical applications, J. Radioanal. Chem. **65** (1981) 31–45.

[2.26.6] ZAITSEVA, N.G., et al., Cross sections for the 100 MeV proton-induced nuclear reactions and yields of some radionuclides used in nuclear medicine, Radiochim. Acta **54** (1991) 57–72.

[2.26.7] LAGUNAS-SOLAR, M.C., CARVACHO, O.F., LIU, B.-L., JIN, Y., SUN, Z.X., Cyclotron production of high purity ^{123}I, I: A revision of excitation functions, thin-target and cumulative yields for ^{127}I(p, xn) reactions, Appl. Radiat. Isot. **37** (1986) 823–833.

[2.26.8] WEINREICH, R., QAIM, S.M., MICHAEL, H., STÖCKLIN, G., Production of ^{123}I and ^{28}Mg by high energy nuclear reactions for applications in life sciences, J. Radioanal. Chem. **30** (1976) 53–66.

[2.26.9] ZAIDI, J.H., QAIM, S.M., STÖCKLIN, G., Excitation functions of deuteron induced nuclear reactions on natural tellurium and enriched ^{122}Te: Production of ^{123}I via the ^{122}Te(d, n)^{123}I-process, Int. J. Appl. Radiat. Isot. **34** (1983) 1425–1430.

[2.26.10] BARRALL, R.C., BEAVER, J.E., HUPF, H.B., RUBIO, F.F., Production of Curie quantities of high purity I-123 with 15 MeV protons, Eur. J. Nucl. Med. **6** (1981) 411–415.

[2.26.11] FIROUZBAKHT, M.L., SCHLYER, D.J., FINN, R.D., LAGUZZI, G., WOLF, A.P., Iodine-124 production: Excitation function for the ^{124}Te(d, 2n)^{124}I and the ^{124}Te(d, 3n)^{123}I reactions from 7 to 24 MeV, Nucl. Instrum. Methods Phys. Res. B **79** (1993) 909–910.

[2.26.12] CLEM, R.G., LAMBRECHT, R.M., Enriched ^{124}Te targets for production of ^{123}I and ^{124}I, Nucl. Instrum. Methods Phys. Res. A **303** (1991) 115–118.

[2.26.13] HUPF, H.B., ELDRIDGE, J.S., BEAVER, J.E., Production of iodine-123 for medical applications, Int. J. Appl. Radiat. Isot. **19** (1968) 345–351.

[2.26.14] LAMBRECHT, R.M., WOLF, A.P., "Cyclotron and short-lived halogen isotopes for radiopharmaceutical applications", Radiopharmaceuticals and Labelled Compounds, Vol. 1, IAEA, Vienna (1973) 275–290.
[2.26.15] SILVESTER, D.J., SUGDEN, J., WATSON, I.A., Preparation of iodine-123 by alpha particle bombardment of natural antimony, Radiochem. Radioanal. Lett. **2** (1969) 17–20.
[2.26.16] GRAHAM, D., TREVENA, I.C., WEBSTER, B., WILLIAMS, D., Production of high purity iodine-123 using xenon-124, J. Nucl. Med. **26** (1985) 105.
[2.26.17] WITSENBOER, A.J., DE GOEIJ, J.J.M., REIFFERS, S., "Production of iodine-123 via proton irradiation of 99.8% enriched xenon-124", Proc. 6th Int. Symp. on Radiopharmaceutical Chemistry, Boston, MA, 1986 (abstract) 259.
[2.26.18] FIROUZBAKHT, M.L., TENG, R.R., SCHLYER, D.J., WOLF, A.P., Production of high purity iodine-123 from xenon-124 at energies between 15 and 34 MeV, Radiochim. Acta **41** (1987) 1–4.
[2.26.19] TÁRKÁNYI, F., et al., Excitation functions of (p, 2n) and (p, pn) reactions and differential and integral yields of ^{123}I in proton induced nuclear reactions on highly enriched ^{124}Xe, Appl. Radiat. Isot. **42** (1991) 221–228.
[2.26.20] KURENKOV, N.V., MALININ, A.B., SEBYAKIN, A.A., VENIKOV, N.I., Excitation functions of proton-induced nuclear reactions on ^{124}Xe: Production of ^{123}I, J. Radioanal. Nucl. Chem. Lett. **135** (1989) 39–50.
[2.26.21] WATSON, I.A., WATERS, S.L., SILVESTER, D.J., Excitation functions for the reactions producing ^{121}I, ^{123}I and ^{124}I from irradiation of natural antimony with ^{3}He and ^{4}He particles with energies up to 30 MeV, J. Inorg. Nucl. Chem. **35** (1973) 3047–3053.
[2.26.22] HASSAN, K.F., QAIM, S.M., SALEH, Z.A., COENEN, H.H., Alpha-particle induced reactions on ^{nat}Sb and ^{121}Sb with particular reference to the production of the medically interesting radionuclide ^{124}I, Appl. Radiat. Isot. **64** (2006) 101–109.
[2.26.23] VAN DEN BOSCH, R., et al., A new approach to target chemistry for the iodine-123 production via the ^{124}Te(p, 2n)^{123}I reaction, Int. J. Appl. Radiat. Isot. **28** (1977) 255–261.
[2.26.24] TERTOOLEN, J.F.W., et al., A new approach to target chemistry for the iodine-123 production via the ^{124}Te(p, 2n)^{123}I reaction, J. Labelled Compd. Radiopharm. **13** (1977) 232.
[2.26.25] QAIM, S.M., Target development for medical radioisotope production at a cyclotron, Nucl. Instrum. Methods Phys. Res. A **282** (1989) 289–295.
[2.26.26] ACERBI, E., BIRATTARI, C., CASTIGLIONI, M., RESMINI, F., Production of ^{123}I for medical purposes at the Milan AVF cyclotron, Int. J. Appl. Radiat. Isot. **26** (1975) 741–747.
[2.26.27] KONDO, K., LAMBRECHT, R.M., NORTON, E.F., WOLF, A.P., Improved target and chemistry for the production of ^{123}I and ^{124}I, Int. J. Appl. Radiat. Isot. **28** (1977) 765–771.

[2.26.28] MAHUNKA, I., ANDO, L., MIKECZ, P., TCHELTSOV, A.N., SUVOROV, I.A., Iodine-123 production at a small cyclotron for medical use, J. Radioanal. Nucl. Chem. Lett. **213** (1996) 135–142.

[2.26.29] MICHAEL, H., et al., Some technical improvements in the production of ^{123}I via the ^{124}Te(p, 2n)^{123}I reaction at a compact cyclotron, Int. J. Appl. Radiat. Isot. **32** (1981) 581–587.

[2.26.30] SODD, V.J., BLUE, J.W., SCHOLZ, K.L., OSELKA, M.C., A gas-flow powder target for the cyclotron production of pure ^{123}I, Int. J. Appl. Radiat. Isot. **24** (1973) 171–177.

[2.26.31] LAMBRECHT, R.M., RITTER, E., BECKER, R., WOLF, A.P., Cyclotron isotopes and radiopharmaceuticals, XXI: Fabrication of ^{122}Te–Au targets for isotope production, Int. J. Appl. Radiat. Isot. **28** (1977) 567–571.

[2.26.32] FIROUZBAHKT, M.L., SCHLYER, D.J., WOLF, A.P., "A solid xenon ice target for the production of I-123", paper presented at 9th Int. Symp. on Radiopharmaceutical Chemistry, Paris, 1992.

[2.26.33] MAUSNER, L.F., SRIVASTAVA, S.C., MIRZADEH, S., MEINKEN, G.E., PRACH, T., ^{123}I research and production at Brookhaven National Laboratory, Appl. Radiat. Isot. **37** (1986) 843–851.

[2.26.34] SUZUKI, K., IWATA, R., A multi-target assembly in an irradiation with high energy particles: Simultaneous production of ^{123}I, ^{62}Zn and $^{13}NH_3$, Int. J. Appl. Radiat. Isot. **28** (1977) 663–665.

[2.26.35] GODART, J., BARAT, J.L., MENTHE, A., Beam collection of ^{123}Xe for carrier-free ^{123}I production, Int. J. Appl. Radiat. Isot. **28** (1978) 967–969.

[2.26.36] FIROUZBAKHT, M.L., SCHLYER, D.J., WOLF, A.P., "'Failsafe' gas target for the production of I-123 from Xe-124", Targetry and Target Chemistry (Proc. 6th Workshop Vancouver, 1995), TRIUMF, Vancouver (1995) 79–81.

[2.26.37] INTERNATIONAL ATOMIC ENERGY AGENCY, Standardized High Current Solid Targets for Cyclotron Production of Diagnostic and Therapeutic Radionuclides, Technical Reports Series No. 432, IAEA, Vienna (2004) CD-ROM.

[2.26.38] SAJJAD, M., LAMBRECHT, R.M., BAKR, S., Autoradiolytic decomposition of reductant-free sodium ^{124}I and ^{123}Iodide, Radiochim. Acta **50** (1990) 123–127.

BIBLIOGRAPHY TO SECTION 2.26

BEYER, G.-J., et al., Production of ^{123}I for medical use with small accelerators, Isotopenpraxis **24** (1988) 297.

BEYER, G.-J., PIMENTEL-GONZALES, G., Physicochemical and radiochemical aspects of separation of radioiodine from TeO_2-targets, Radiochim. Acta **88** (2000) 175.

ČOMOR, J.J., STEVANOVIĆ, Ž., RAJČEVIĆ, M., KOŠUTIĆ, Đ., Modeling of thermal properties of a TeO_2 target for radioiodine production, Nucl. Instrum. Methods Phys. Res. A **521** (2004) 161–170.

FIROUZBAKHT, M.L., SCHLYER, D.J., WOLF, A.P., Production of iodine-123 from xenon-124: Cross-sections and yields, Radiochim. Acta **56** (1992) 167–171.

FIROUZBAKHT, M.L., SCHLYER, D.J., WOLF, A.P., Effect of foil material on the apparent yield of the $^{124}Xe(p, x)^{123}I$ reaction, Appl. Radiat. Isot. **43** (1992) 741–745.

FREY, P.E., et al., Tomographic imaging of the human thyroid using ^{124}I, J. Clin. Endocrinol. Metab. **63** (1986) 918–927.

HASSAN, K.F., QAIM, S.M., SALEH, Z.A., COENEN, H.H., ^{3}He-particle-induced reactions on ^{nat}Sb for production of ^{124}I, Appl. Radiat. Isot. **64** (2006) 409–413.

INTERNATIONAL ATOMIC ENERGY AGENCY, Charged Particle Cross-section Database for Medical Radioisotope Production: Diagnostic Radioisotopes and Monitor Reactions, IAEA-TECDOC-1211, IAEA, Vienna (2001).

KNUST, E.J., DUTSCHKA, K., WEINREICH, R., Preparation of ^{124}I solutions after thermodistillation of irradiated $^{124}TeO_2$ targets, Appl. Radiat. Isot. **52** (2000) 181–184.

KUDELIN, B.K., GROMOVA, E.A., GAVRILINA, L.V., SOLIN, L.M., Purification of recovered tellurium dioxide for re-use in iodine radioisotope production, Appl. Radiat. Isot. **54** (2001) 383–386.

LAMBRECHT, R.M., MANTESCU, C., REDVANLY, C., WOLF, A.P., Preparation of high purity carrier-free ^{123}I-iodine monochloride as iodination reagent for synthesis of radiopharmaceuticals, IV, J. Nucl. Med. **13** (1972) 266–273.

LAMBRECHT, R.M., SAJJAD, M., QURESHI, M.A., AL-YANBAWI, S.J., Production of iodine-124, J. Radioanal. Nucl. Chem. Lett. **127** (1988) 143–151.

LAMBRECHT, R.M., WOLF, A.P., The $^{122}Te(^{4}He, 3n)^{123}Xe \rightarrow {}^{123}I$ generator, Radiat. Res. **52** (1972) 32–46.

LAMBRECHT, R.M., et al., Investigational study of iodine-124 with a positron camera, Am. J. Physiol. Imaging **3** (1988) 197–200.

QAIM, S.M., STÖCKLIN, G., Production of some medically important short-lived neutron deficient radioisotopes of halogens, Radiochim. Acta **34** (1983) 25–40.

SCHOLTEN, B., KOVÁCS, Z., TÁRKÁNYI, F., QAIM, S.M., Excitation functions of the ^{124}Te(p, xn)^{124,123}I reactions from 6 to 31 MeV with special reference to the production of ^{124}I at a small cyclotron, Appl. Radiat. Isot. **46** (1995) 255–259.

SHARMA, H.L., ZWEIT, J., DOWNEY, S., SMITH, A.M., SMITH, A.G., Production of ^{124}I for positron emission tomography, J. Labelled Compd. Radiopharm. **26** (1988) 165–167.

SHEH, Y., et al., Low energy cyclotron production and chemical separation of 'no carrier added' iodine-124 from a reusable, enriched tellurium-124 dioxide/aluminum oxide solid solution target, Radiochim. Acta **88** (2000) 169–173.

STEVENSON, N.R., et al., "On-line production of radioiodines with low energy accelerators", Targetry and Target Chemistry (Proc. 6th Workshop Vancouver, 1995), TRIUMF, Vancouver (1995) 82–83.

WEINREICH, R., et al., Production and quality assurance of 5-[^{124}I]iodo-2′-deoxyuridine for functional imaging of cell proliferation in vivo, J. Labelled Compd. Radiopharm. **40** (1977) 346–347.

2.27. IODINE-124

Half-life: 4.2 d.

Uses

Although ^{124}I has often been considered as an impurity in preparations of ^{123}I, it does have attractive attributes for use in some PET radiopharmaceuticals [2.27.1–2.27.3]. The half-life of 4.2 d is long enough for localization with monoclonal antibodies, and the 23% positron decay allows imaging with PET. The use of ^{124}I is becoming more widespread. Iodine-124 has potential as both a diagnostic and a therapeutic radionuclide [2.27.3, 2.27.4].

Decay mode

Iodine-124 has many gamma emissions and some low energy beta emissions, as well as the two high energy positron emissions.

Positron emission products of ^{124}I

Fraction	Maximum energy (MeV)	Average energy (MeV)
0.110000	1.532300	0.685900
0.120000	2.135000	0.973600

Electron emission products of ^{124}I

Fraction	Energy (MeV)
0.082801	0.022700
0.630130	0.003190

Photon emission products of ^{124}I

Fraction	Energy (MeV)
0.012061	1.175200
0.013983	1.325500
0.016225	1.376300
0.029146	1.509500
0.062320	0.003770
0.097350	0.722780
0.101480	1.691000
0.106840	0.031000
0.164980	0.027202
0.307790	0.027472
0.465450	0.511000
0.590000	0.602710

Nuclear reactions

The best nuclear reaction for the production of ^{124}I is the ^{124}Te(p, n)^{124}I reaction on enriched ^{124}Te.

Nuclear reaction	Useful energy range (MeV)	Natural abundance (%)	References
^{124}Te(p, n)^{124}I	10–20	4.8	[2.27.5–2.27.7]
^{124}Te(d, 2n)^{124}I		4.8	[2.27.8–2.27.10]
^{124}Te(d, 3n)^{124}I	15–30	4.8	[2.27.9]
^{121}Sb(^{4}He, n)^{124}I	15–25	57.4	[2.27.11]
^{123}Sb(^{3}He, 2n)^{124}I		42.6	[2.27.11]

Excitation functions

The excitation functions for ^{124}I are shown in Figs 2.27.1–2.27.4.

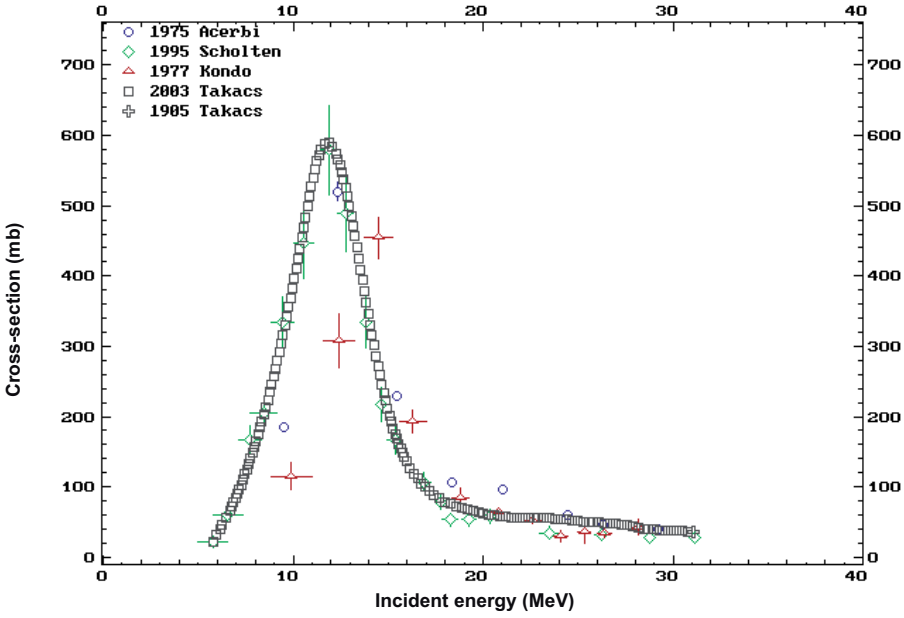

FIG. 2.27.1. Excitation function for the ^{124}Te(p, n)^{124}I reaction.

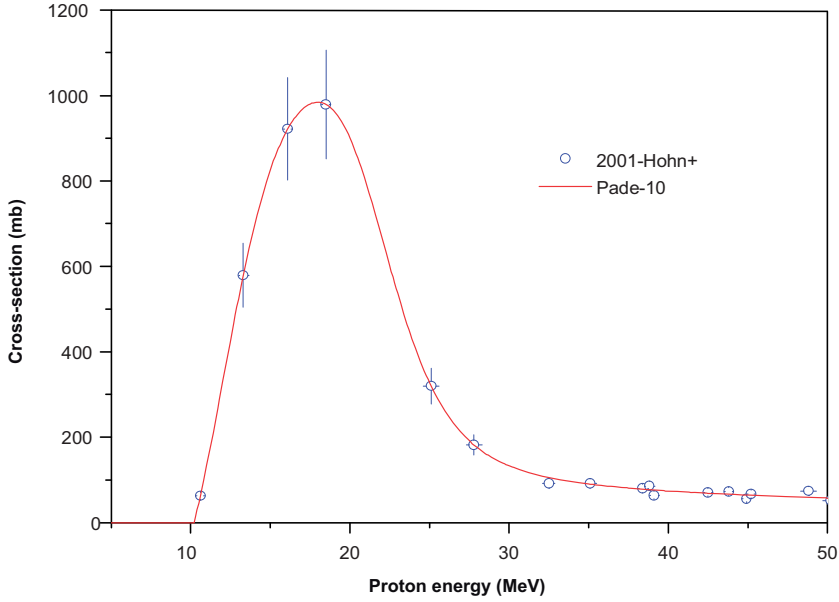

FIG. 2.27.2. Excitation function for the $^{125}Te(p, 2n)^{124}I$ reaction.

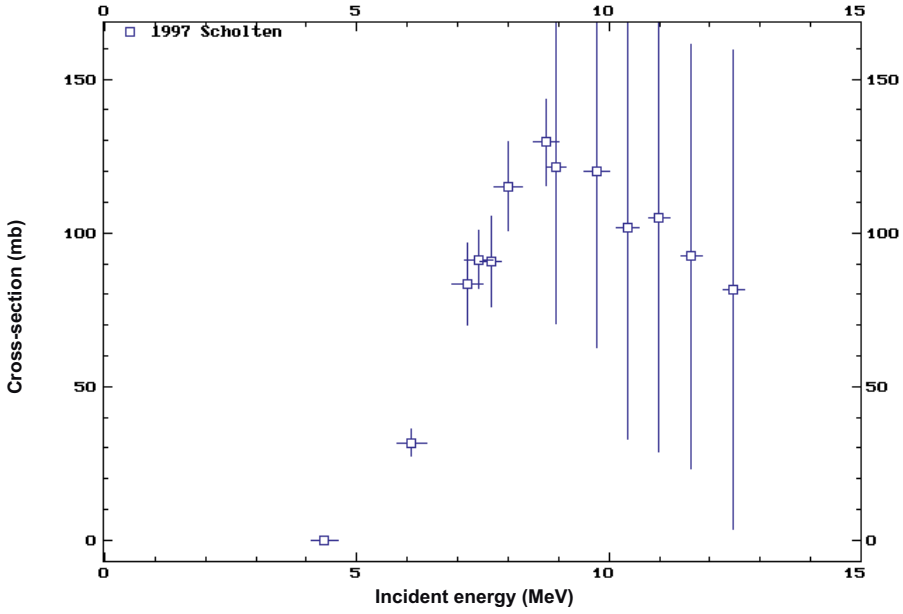

FIG. 2.27.3. Excitation function for the $^{123}Te(d, n)^{124}I$ reaction.

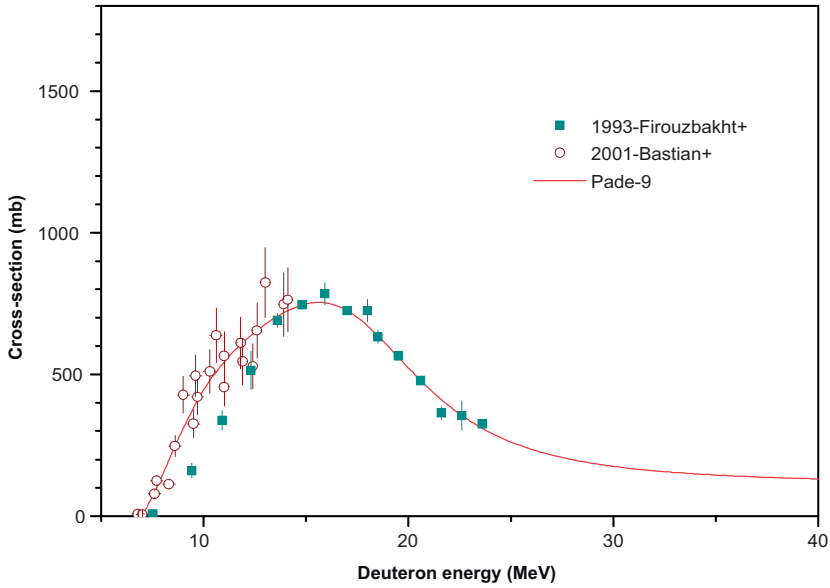

FIG. 2.27.4. Excitation function for the ^{124}Te(d, 2n)^{124}I reaction.

Target materials

The targetry for production of ^{124}I is limited to solid targets. The target is either elemental tellurium or tellurium oxide [2.27.12, 2.27.13]. The targets are identical to those used for the production of ^{123}I from tellurium. The target plates can be made from either platinum or tantalum. Elemental tellurium can be electrodeposited on to the target plate. Tellurium oxide is usually melted into a cavity on the target plate. In some cases, small amounts of aluminium oxide are added to the tellurium to aid in adhesion of the oxide to the surface of the plate [2.27.4].

Target preparation

The targets may be prepared by electrodeposition of metallic tellurium or by using tellurium oxide in a pressed target. The new electroplating technology developed allows the production of high quality enriched ^{124}Te targets. Microscopic inspection shows a smooth dendrite-free surface area with excellent granulometry. The targets withstand a 150°C thermal shock test. Details of the preparation of these targets can be found in Ref. [2.27.14].

Target processing

The separation of iodine from tellurium can be accomplished by distillation of ^{124}I from the tellurium oxide matrix. This is usually performed at temperatures of about 750°C. The iodine is carried away from the target with a sweep of either oxygen or helium. Oxygen tends to keep the tellurium in the oxide form and reduces the loss from distillation of elemental tellurium [2.27.4, 2.27.15, 2.27.16].

Alternatively, the irradiated target is dissolved in an oxidizing alkaline medium, followed by reduction of enriched tellurium to the metallic state and of iodine to the I^- state by aluminium powder. The iodine is purified by cation exchange chromatography. A drawback of this procedure is that the aqueous solution has a relatively low concentration. Hence, if a high concentration is desired, the excess water must be removed through an additional concentration step.

Recovery of enriched materials

The enriched material from a set of partially depleted plating solutions and/or from combined recovery/rinsing solutions obtained after solubilization of irradiated targets and separation of iodine (90 mg Te per run) is recovered as solid tellurium metal. Therefore, the enriched material is dissolved as a tellurate in a mixture of hydrochloric acid and hydrogen peroxide, followed by partial reduction to tellurite by hydrogen bromide. Quantitative precipitation as metallic tellurium is achieved by reduction with hydrazine and sodium sulphite.

The recovery of enriched material from irradiated TeO_2 targets is achieved through a multistage process. It involves vacuum distillation of Te and TeO_2, acid dissolution and ultimate precipitation as metallic tellurium.

Specifications

It is essential to monitor and control the presence of several different iodine species such as iodates and periodates. These species may also arise during storage of high SA products [2.27.17]. Stabilization of radio-iodine predominantly as iodide can be achieved by addition of a small amount of a reductant such as sodium sulphite. It must be noted, however, that the presence of a reductant is known to interfere with the radiolabelling of proteins.

Iodine batches produced through irradiation of solid tellurium and TeO_2 targets are submitted to chemical purity tests on aluminium and tellurium. Use is made of emission spectrometry or colorimetry. The chemical impurities determined by colorimetric spot tests are typically: Te < 0.5 μg/mCi; Al < 0.25 μg/mCi.

REFERENCES TO SECTION 2.27

[2.27.1] FREY, P.E., et al., Tomographic imaging of the human thyroid using ^{124}I, J. Clin. Endocrinol. Metab. **63** (1986) 918–927.

[2.27.2] LAMBRECHT, R.M., et al., Investigational study of iodine-124 with a positron camera, Am. J. Physiol. Imaging **3** (1988) 197–200.

[2.27.3] WEINREICH, R., et al., Production and quality assurance of 5-[^{124}I]iodo-2′-deoxyuridine for functional imaging of cell proliferation in vivo, J. Labelled Compd. Radiopharm. **40** (1997) 346–347.

[2.27.4] SHEH, Y., et al., Low energy cyclotron production and chemical separation of no carrier added iodine-124 from a reusable, enriched tellurium-124 dioxide/aluminum oxide solid solution target, Radiochim. Acta **88** (2000) 169–173.

[2.27.5] KONDO, K., LAMBRECHT, R.M., NORTON, E.F., WOLF, A.P., Improved target and chemistry for the production of ^{123}I and ^{124}I, Int. J. Appl. Radiat. Isot. **28** (1977) 765–771.

[2.27.6] KONDO, K., LAMBRECHT, R.M., WOLF, A.P., Iodine-123 production for radiopharmaceuticals, XX: Excitation functions for the ^{124}Te(p, 2n)^{123}I and ^{124}Te(p, n)^{124}I reactions and the effect of target enrichment on radionuclidic purity, Int. J. Appl. Radiat. Isot. **28** (1977) 395–401.

[2.27.7] SCHOLTEN, B., TAKÁCS, S., KOVÁCS, Z., TÁRKÁNYI, F., QAIM, S.M., Excitation function of deuteron induced reactions on ^{123}Te: Relevance to the production of ^{123}I and ^{124}I at low and medium sized cyclotrons, Appl. Radiat. Isot. **48** (1997) 267–271.

[2.27.8] LAMBRECHT, R.M., SAJJAD, M., QURESHI, M.A., AL-YANBAWI, S.J., Production of iodine-124, J. Radioanal. Nucl. Chem. Lett. **127** (1988) 143–145.

[2.27.9] FIROUZBAKHT, M.L., SCHLYER, D.J., FINN, R.D., LAGUZZI, G., WOLF, A.P., Iodine-124 production: Excitation function for the ^{124}Te(d, 2n)^{124}I and the ^{124}Te(d, 3n)^{123}I reactions from 7 to 24 MeV, Nucl. Instrum. Methods Phys. Res. B **79** (1993) 909–910.

[2.27.10] SHARMA, H.L., ZWEIT, J., DOWNEY, S., SMITH, A.M., SMITH, A.G., Production of ^{124}I for positron emission tomography, J. Labelled Compd. Radiopharm. **26** (1988) 165–167.

[2.27.11] SILVESTER, D.J., SUGDEN, J., WATSON, I.A., Preparation of iodine-123 by alpha particle bombardment of natural antimony, Radiochem. Radioanal. Lett. **2** (1969) 17–20.

[2.27.12] STEVENSON, N.R., et al., "On-line production of radioiodines with low energy accelerators", Targetry and Target Chemistry (Proc. 6th Workshop Vancouver, 1995), TRIUMF, Vancouver (1995) 82–83.
[2.27.13] QAIM, S.M., Target development for medical radioisotope production at a cyclotron, Nucl. Instrum. Methods Phys. Res. A **282** (1989) 289–295.
[2.27.14] INTERNATIONAL ATOMIC ENERGY AGENCY, Standardized High Current Solid Targets for Cyclotron Production of Diagnostic and Therapeutic Radionuclides, Technical Reports Series No. 432, IAEA, Vienna (2004) CD-ROM.
[2.27.15] KNUST, E.J., DUTSCHKA, K., WEINREICH, R., Preparation of ^{124}I solutions after thermodistillation of irradiated $^{124}TeO_2$ targets, Appl. Radiat. Isot. **52** (2000) 181–184.
[2.27.16] MICHAEL, H., et al., Some technical improvements in the production of ^{123}I via the ^{124}Te(p, 2n)^{123}I reaction at a compact cyclotron, Int. J. Appl. Radiat. Isot. **32** (1981) 581–587.
[2.27.17] SAJJAD, M., LAMBRECHT, R.M., BAKR, S., Autoradiolytic decomposition of reductant-free sodium ^{124}I and ^{123}Iodide, Radiochim. Acta **50** (1990) 123–127.

BIBLIOGRAPHY TO SECTION 2.27

BASTIAN, T., COENEN, H.H., QAIM, S.M., Excitation functions of Te-124(d, xn)I-124, I-125 reactions from threshold up to 14 MeV: Comparative evaluation of nuclear routes for the production of I-124, Appl. Radiat Isot. **55** (2001) 303–308.

BEYER, G.-J., PIMENTEL-GONZALES, G., Physicochemical and radiochemical aspects of separation of radioiodine from TeO_2-targets, Radiochim. Acta **88** (2000) 175.

CLEM, R.G., LAMBRECHT, R.M., Enriched ^{124}Te targets for production of ^{123}I and ^{124}I, Nucl. Instrum. Methods Phys. Res. A **303** (1991) 115.

ČOMOR, J.J., STEVANOVIĆ, Ž., RAJČEVIĆ, M., KOŠUTIĆ, Đ., Modeling of thermal properties of a TeO_2 target for radioiodine production, Nucl. Instrum. Methods Phys. Res. A **521** (2004) 161–170.

GLASER, M., et al., Improved targetry and production of iodine-124 for PET studies, Radiochim. Acta **92** (2004) 951.

INTERNATIONAL ATOMIC ENERGY AGENCY, Charged Particle Cross-section Database for Medical Radioisotope Production: Diagnostic Radioisotopes and Monitor Reactions, IAEA-TECDOC-1211, IAEA, Vienna (2001).

QAIM, S.M., et al., Some optimisation studies relevant to the production of high-purity ^{124}I and ^{120g}I at a small-sized cyclotron, Appl. Radiat. Isot. **58** (2003) 69.

SCHOLTEN, B., KOVÁCS, Z., TÁRKÁNYI, F., QAIM, S.M., Excitation functions of the ^{124}Te(p, xn)^{124,123}I reactions from 6 to 31 MeV with special reference to the production of ^{124}I at a small cyclotron, Appl. Radiat. Isot. **46** (1995) 255–259.

TAKÁCS, S., TÁRKÁNYI, F., HERMANNE, A., Institute of Nuclear Research of the Hungarian Academy of Sciences, Debrecen, personal communication, 2005.

TAKÁCS, S., TÁRKÁNYI, F., HERMANNE, A., PAVIOTTI DE CORCUERA, R., Validation and upgrading of the recommended cross section data of charged particle reactions used for production of PET radioisotopes, Nucl. Instrum. Methods Phys. Res. B **211** (2003) 169–189.

TERTOOLEN, J.F.W., et al., New approach to target chemistry for the iodine-123 production via the ^{124}Te(p, 2n)^{123}I reaction, J. Labelled Compd. Radiopharm. **13** (1977) 232.

VAN DEN BOSCH, R., et al., A new approach to target chemistry for the iodine-123 production via the ^{124}Te(p, 2n)^{123}I reaction, Int. J. Appl. Radiat. Isot. **28** (1977) 255–261.

2.28. IRON-52

Half-life

Iron-52 has an 8.3 h half-life and decays with 56% positron emission. The end point energy of the positron is 0.804 MeV. Both modes of decay result in a 169 keV gamma ray to be emitted and both lead to ^{52m}Mn, which is also a positron emitter with a 21 min half-life.

Positron emission products of ^{52}Fe

Fraction	Maximum energy (MeV)	Average energy (MeV)
0.560000	0.803580	0.340000

Electron emission products of ^{52}Fe

Fraction	Energy (MeV)
0.003000	0.167920
0.030000	0.162150
0.289490	0.005190
0.662650	0.000610

Photon emission products of ^{52}Fe

Fraction	Energy (MeV)
0.001994	0.000640
0.015658	0.006490
0.039260	0.005888
0.077590	0.005899
0.966000	0.168680
1.120000	0.511000

Nuclear reactions for production of ^{52}Fe

Nuclear reaction	Useful energy range (MeV)	Natural abundance (%)	References
^{nat}Ni(p, x)^{52}Fe	55–68	100	[2.28.1, 2.28.2]
^{55}Mn(p, 4n)^{52}Fe	40–60	100	[2.28.2, 2.28.3]
^{50}Cr(^{4}He, 2n)^{52}Fe	25–35	4.35	[2.28.4]
^{52}Cr(^{3}He, 3n)^{52}Fe	25–40	83.8	[2.28.4]

Excitation functions

The excitation functions for ^{52}Fe are shown in Figs 2.28.1–2.28.3.

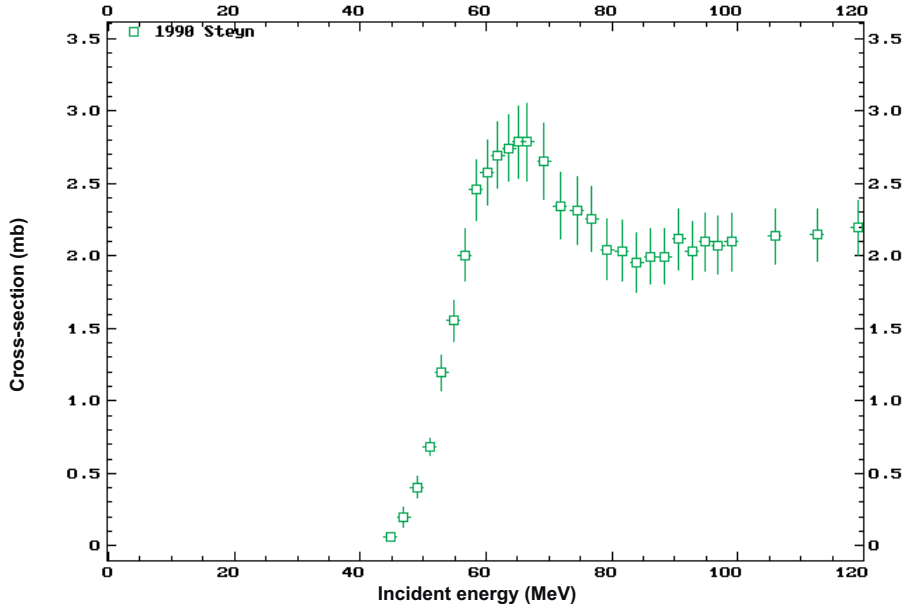

FIG. 2.28.1. Excitation function for the $^{58}Ni(p, x)^{52}Fe$ reaction.

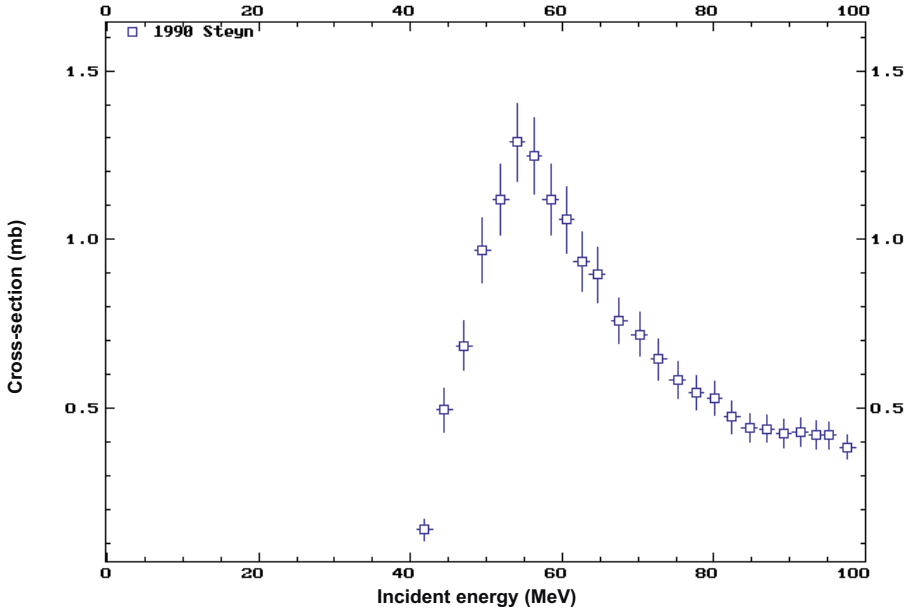

FIG. 2.28.2. Excitation function for the $^{55}Mn(p, 4n)^{52}Fe$ reaction.

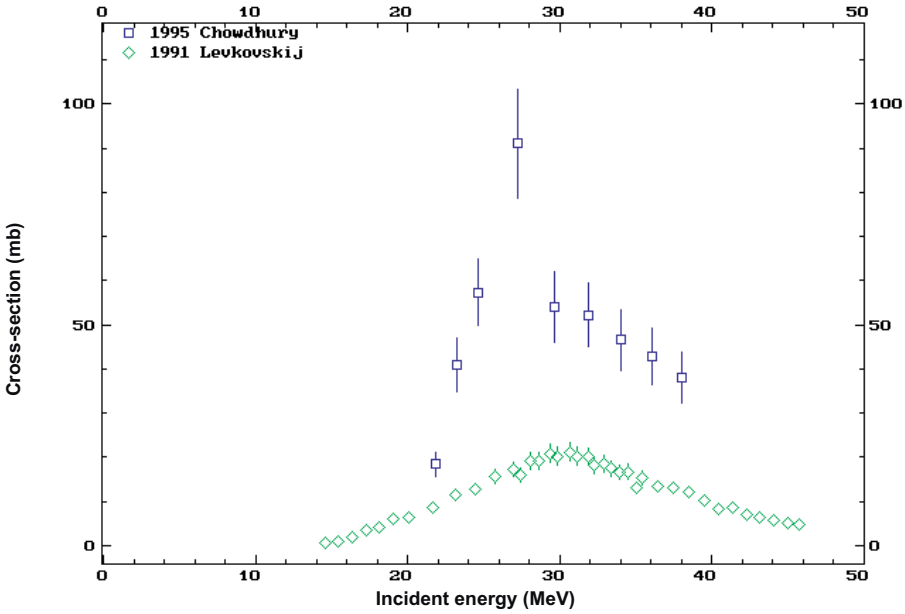

FIG. 2.28.3. Excitation function for the $^{50}Cr(\alpha, 2n)^{52g}Fe$ reaction.

REFERENCES TO SECTION 2.28

[2.28.1] SMITH-JONES, P., SCHWARTZBACH, R., WEINREICH, R., The production of ^{52}Fe by means of a medium energy proton accelerator, Radiochim. Acta **50** (1990) 33–39.

[2.28.2] STEYN, G.F., et al., Production of ^{52}Fe by proton-induced reactions on manganese and nickel, Appl. Radiat. Isot. **41** (1990) 315–325.

[2.28.3] SAHA, G.B., FARRER, P.A., Production of ^{52}Fe by the ^{55}Mn(p, 4n)^{52}Fe reaction for medical use, Int. J. Appl. Radiat. Isot. **22** (1971) 495–498.

[2.28.4] AKIHA, F., ABURAI, T., NOZAKI, T., MURAKAMI, Y., Yield of ^{52}Fe for the reactions of ^{3}He and α on chromium, Radiochim. Acta **18** (1972) 108–111.

BIBLIOGRAPHY TO SECTION 2.28

GRANT, M., et al., Spallation yields of Fe-52, Cu-67, and Tl-201 from reactions of 800 MeV protons with Ni, As, Pb and Bi targets, J. Labelled Compd. Radiopharm. **16** (1979) 212–213.

LEENDERS, K.L., et al., "Blood to brain iron transport in man using [Fe-52]-citrate and positron emission tomography (PET)", Quantification of Brain Function Tracer Kinetics and Image Analysis in Brain PET (UEMURA, K., et al., Eds), Elsevier, Amsterdam and New York (1993) 145–150.

LEENDERS, K.L., et al., Blood to brain iron uptake in one rhesus monkey using [Fe-52]-citrate and positron emission tomography (PET): Influence of haloperidol, J. Neural Transm. **43** (1994) 123–132.

THAKUR, M.L., NUNN, A., WATERS, S., Iron-52: Improving its recovery from cyclotron targets, Int. J. Appl. Radiat. Isot. **22** (1971) 481–483.

2.29. IRON-55

Half-life: 2.7 a.

Electron emission products of ^{55}Fe

Fraction	Energy (MeV)
0.607380	0.005190
1.394800	0.000610

Photon emission products of ^{55}Fe

Fraction	Energy (MeV)
0.004197	0.000640
0.032852	0.006490
0.082372	0.005888
0.162790	0.005899

Nuclear reactions

There are two nuclear reactions that have reasonable yields with an accelerator: the $^{55}Mn(p, n)^{55}Fe$ reaction and the $^{56}Fe(p, pn)^{55}Fe$ reaction on natural iron. The disadvantage of the second reaction is that there is a large amount of carriers, which makes this route undesirable for tracer studies.

Excitation functions

The excitation functions for $^{55}Mn(p, n)^{55}Fe$ and $^{58}Ni(p, x)^{55}Cu$ are shown in Figs 2.29.1 and 2.29.2, respectively.

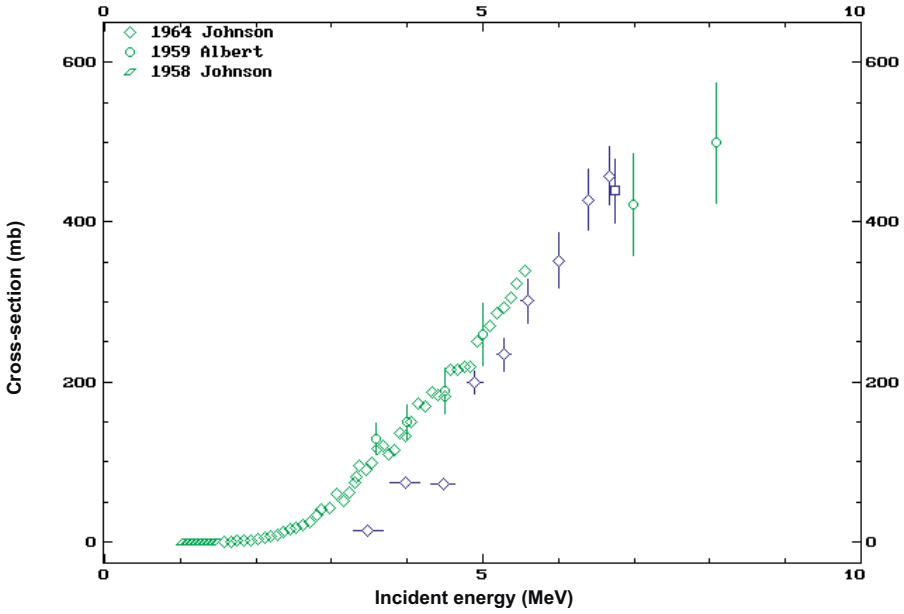

FIG. 2.29.1. Excitation function for the $^{55}Mn(p, n)^{55}Fe$ reaction.

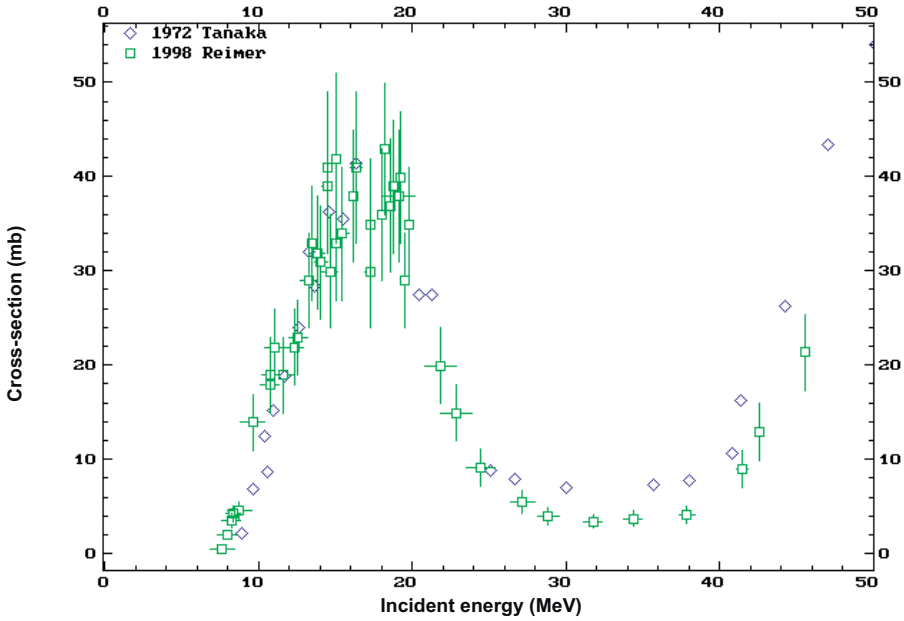

FIG. 2.29.2. Excitation function for the $^{58}Ni(p, x)^{55}Cu \rightarrow {}^{55}Ni \rightarrow {}^{55}Co \rightarrow {}^{55}Fe$ reaction.

BIBLIOGRAPHY TO SECTION 2.29

GECKEIS, H., HENTSCHEL, D., JENSEN, D., GORTZEN, A., KERNER, N., Determination of Fe-55 and Ni-63 using semipreparative ion chromatography: A feasibility study, Fresenius' J. Anal. Chem. **357** (1997) 864–869.

HUMES, R.M., DELL, G.F., Jr., PLOUGHE, W.D., HAUSMAN, H.J., (p, n) Cross sections at 6.75 MeV, Phys. Rev. **130** (1963) 1522–1524.

JOHNSON, C.H., GALONSKY, A., ULRICH, J.P., Proton strength functions from (p, n) cross sections, Phys. Rev. **109** (1958) 1243–1254.

JOHNSON, C.H., TRAIL, C.C., GALONSKY, A., Thresholds for (p, n) reactions on 26 intermediate-weight nuclei, Phys. Rev. B **136** (1964) 1719.

MELLADO, J., TARANCÓN, A., GARCÍA, J.F., RAURET, G., WARWICK, P., Combination of chemical separation and data treatment for ^{55}Fe, ^{63}Ni, ^{99}Tc, ^{137}Cs and ^{90}Sr/^{90}Y activity determination in radioactive waste by liquid scintillation, Appl. Radiat. Isot. **63** (2005) 207–215.

REIMER, P., QAIM, S.M., Excitation functions of proton induced reactions on highly enriched ^{58}Ni with special relevance to the production of ^{55}Co and ^{57}Co, Radiochim. Acta **80** (1998) 113.

STEYN, G., SIMPSON, B.R.S., MILLS, S.J., NORTIER, F.M., The production of Fe-55 with medium-energy protons, Appl. Radiat. Isot. **43** (1992) 1323–1327.

TANAKA, S., FURUKAWA, M., CHIBA, M., Nuclear reactions of nickel with protons up to 56 MeV, J. Inorg. Nucl. Chem. **34** (1972) 2419–2426.

2.30. RUBIDIUM-81/KRYPTON-81m GENERATOR SYSTEM

Half-lives: Rubidium-81, 4.6 h;
Kyrpton-81m (daughter), 13.1 s.

Uses

Rubidium-81/kyrpton-81m generators are used either in gaseous form for ventilation imaging or in solution for perfusion imaging.

Decay mode

Rubidium-81 decays by positron emission and electron capture.

Fraction	Maximum energy (MeV)	Average energy (MeV)
0.017000	0.603370	0.264000
0.314000	1.049500	0.458000

Electron emission products of ^{81}Rb

Fraction	Energy (MeV)
0.014388	0.190010
0.043690	0.188380
0.255570	0.175970
0.297030	0.010800
1.062600	0.001500

Photon emission products of ^{81}Rb

Fraction	Energy (MeV)
0.010256	0.626620
0.013996	0.001590
0.015505	0.537600
0.023126	0.456710
0.077963	0.014100
0.157950	0.012598
0.189540	0.446140
0.306110	0.012649
0.657000	0.190300
0.662000	0.511000

Decay modes of ^{81m}Kr

Parent nucleus	Parent energy level (eV)	Parent half-life (s)	Decay mode	Daughter nucleus
Kr-81m	190.38	13.10	EC	Br-81

Electron emission products of ^{81m}Kr

Fraction	Energy (keV)
0.000027	1.41
0.000008	10.2

Photon emission products of ^{81m}Kr

Fraction	Energy (keV)
5.4E–07	1.48
0.000004	11.878
7.7E–06	11.924
5.4E–07	13.284
1.05E–06	13.292
1.05E–07	13.469

Parent nucleus	Parent energy level	Parent half-life (a)	Decay mode	Daughter nucleus
Kr-81m	0	2.29E5	EC	Br-81

Fraction	Energy (keV)
0.676116	190.46

Nuclear reactions

The primary reaction for the production of ^{81}Rb for the ^{81}Rb/^{81m}Kr generator system is the proton reaction of natural krypton.

The recommended reaction cross-section values are shown as the green triangles in Fig. 2.30.1.

Excitation function

The excitation function for ^{81m}Kr(p, x)^{81}Rb is shown in Fig. 2.30.1.

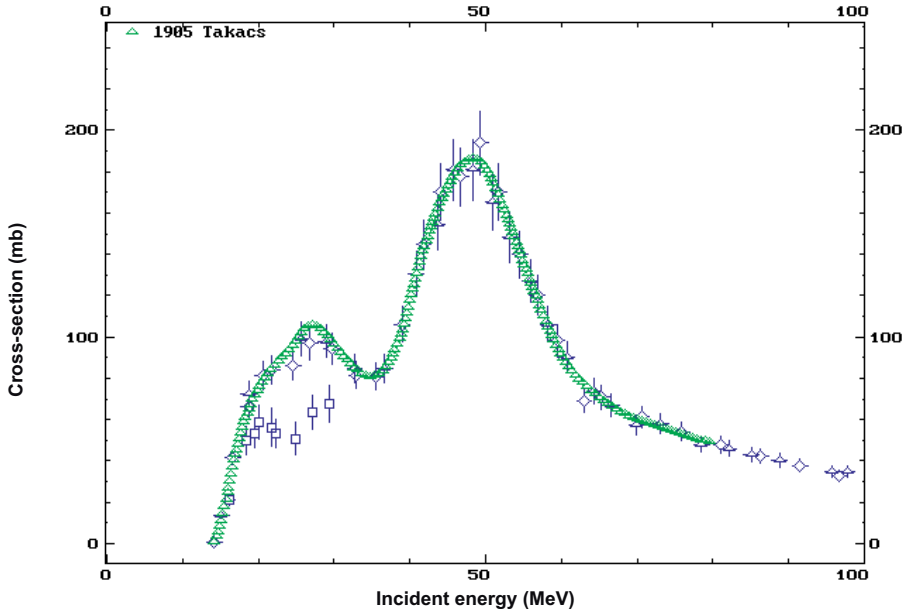

FIG. 2.30.1. Excitation function for the $^{81m}Kr(p, x)^{81}Rb$ reaction.

Target material

The target material is natural krypton gas (of high purity).

Target preparation

The gas target is loaded under pressure, and this pressure is then maintained throughout irradiation.

Target processing

At EOB, the natural krypton target gas is collected into a cold finger with vacuum, followed by filling of the target with 0.001M KCl solution to dissolve the rubidium isotopes. Dissolved activity is gathered in a collection vessel for filling the generators.

Preparation of the generator

The calculated amount of ^{81}Rb solution (based upon the concentration determined) is loaded on to a column (an AG50W-X8 cation exchange column)

well shielded inside a lead casing. The cation resin has a high affinity for rubidium; the daughter ^{81m}Kr is eluted by sterile air or sterile water. In the case of an aqueous solution, an adjustment must be made with a sodium chloride solution of appropriate concentration [2.30.1].

Radionuclidic specifications

For preparation of a ^{81}Rb(^{81m}Kr) generator column, the radionuclidic purity of ^{81}Rb is not very critical. The radiocontaminants ^{82m}Rb and ^{84}Rb decay to stable krypton isotopes, and ^{83}Rb decays 24% to stable ^{83}Kr and 76% to ^{83m}Kr with a half-life of 1.8 h. The latter isomer emits only soft X rays (E < 33 keV). None of these decay products disturbs investigations with ^{8lm}Kr, which has a half-life of 13.1 s. For direct application of ^{81}Rb and from generator shielding considerations, however, it is essential to have ^{81}Rb of good radionuclidic purity [2.30.2]. The eluent (air or water) must be passed through a 0.22 μm filter, to ensure a physiologically acceptable product.

REFERENCES TO SECTION 2.30

[2.30.1] ELLIOT, A.T., in Textbook of Radiopharmacy: Theory and Practice (SAMPSON, C.B., Ed.), Gordon and Breach, New York (1990).

[2.30.2] KOVÁCS, Z., TÁRKÁNYI, F., QAIM, S.M., STÖCKLIN, G., Excitation functions for the formation of some radioisotopes of rubidium in proton induced nuclear reactions on ^{nat}Kr, ^{82}Kr and ^{83}Kr with special reference to the production of ^{81}Rb(^{81m}Kr) generator radionuclide, Appl. Radiat. Isot. **42** (1991) 329–335.

BIBLIOGRAPHY TO SECTION 2.30

BLESSING, G., TÁRKÁNYI, F., QAIM, S.M., Production of ^{82m}Rb via the ^{82}Kr(p, n)-process on highly enriched ^{82}Kr: A remotely controlled compact system for irradiation, safe handling and recovery of the target gas and isolation of the radioactive product, Appl. Radiat. Isot. **48** (1997) 37–43.

FINN, R.D., in Single-photon Ultra-short Lived Radionuclides (PARAS, P., THIESSEN, J.W., Eds), Office of Scientific and Technical Information, US Department of Energy, Washington, DC (1985).

LAMBRECHT, R.M., GALLAGHER, B.M., WOLF, A.P., BENNETT, G.W., Cyclotron isotopes and radiopharmaceuticals, XXIX: ^{81,82m}Rb for positron emission tomography, Int. J. Appl. Radiat. Isot. **31** (1980) 343–349.

POMMET, R., THERAIN, F., The use of Kr-81m in ventilation imaging, Clin. Nucl. Med. **7** (1982) 122–130.

2.31. LEAD-201

Half-life: 9.33 h.

Decay modes

The decay modes for ^{201}Pb are electron capture and positron emission, as given in the following table.

Radiation	Fraction	Energy (MeV)
β^+	0.00054	0.268
γ	0.791	0.3312
ce-K, γ	0.0846	0.2456
γ	0.0356	0.5846
γ	0.0427	0.6924
γ	0.0570	0.9076
γ	0.0736	0.9460
Kα1 X ray	0.433	0.07287
Kβ X ray	0.191	0.0826
L X ray	0.343	0.0103
Auger L	0.591	0.00778

Excitation function

See Section 2.40 (^{201}Tl).

2.32. LEAD-203

Half-life: 51.9 h (electron capture decay).

Electron emission products of ^{203}Pb

Fraction	Energy (MeV)
0.003379	0.278340
0.005020	0.315780
0.010522	0.275480
0.031299	0.055200
0.043238	0.263840
0.168190	0.193660
0.588000	0.007780

Photon emission products of ^{203}Pb

Fraction	Energy (MeV)
0.006682	0.680500
0.033024	0.401320
0.199500	0.082600
0.266300	0.070832
0.392000	0.010300
0.451350	0.072871
0.768000	0.279190

Nuclear reactions

The nuclear reactions for production of ^{203}Pb are:

(a) ^{nat}Tl(p, x)^{203}Pb;
(b) ^{205}Tl(p, 3n)^{203}Pb.

Excitation functions

The excitation functions for ^{nat}Tl(p, x)^{203}Pb and ^{205}Tl(p, 3n)^{203}Pb are shown in Figs 2.32.1 and 2.32.2, respectively.

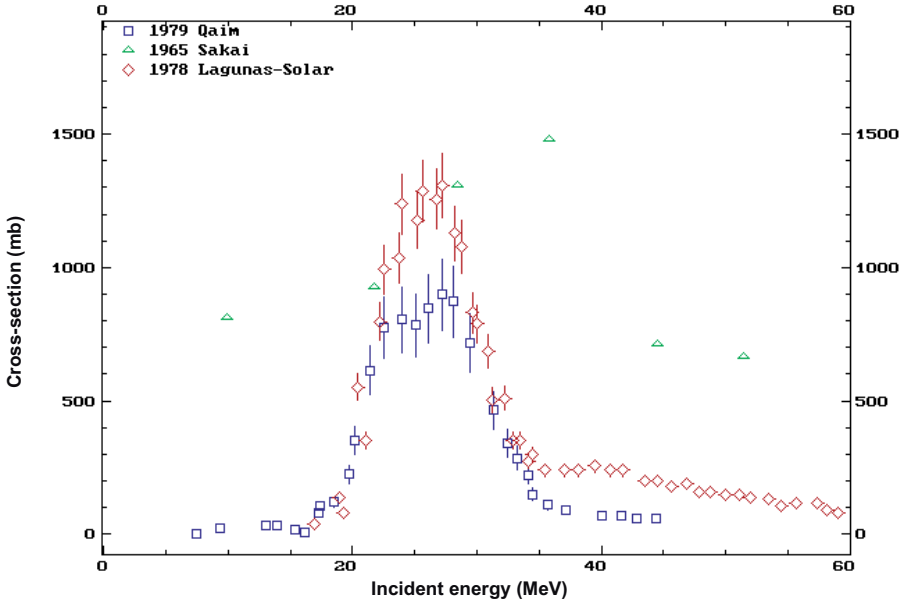

FIG. 2.32.1. Excitation function for the $^{nat}Tl(p, x)^{203}Pb$ reaction.

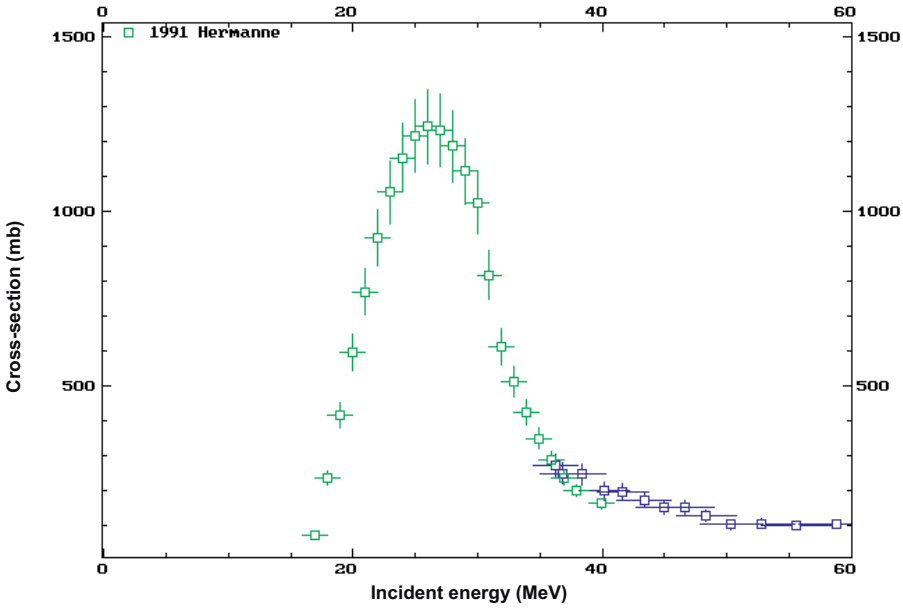

FIG. 2.32.2. Excitation function for the $^{205}Tl(p, 3n)^{203}Pb$ reaction.

BIBLIOGRAPHY TO SECTION 2.32

BIRATTARI, C., BONARDI, M., SALOMONE, A., Tl-201 production studies by Tl-203(p, 3n)Pb-201 and Hg-202(p, 2n)Tl-201 nuclear-reactions, J. Labelled Compd. Radiopharm. **19** (1982) 1330–1332.

BLUE, J.W., LIU, D.C., SMATHERS, J.B., Thallium-201 production with the idle beam from neutron therapy, Med. Phys. **5** (1978) 532–535.

DMITRIEV, P.P., Systematics of nuclear reaction yields for thick target at 22 MeV, Vopr. At. Nauki Tekh., Ser. Yad. Konst. **51** (1983) 57–61.

INTERNATIONAL ATOMIC ENERGY AGENCY, Charged Particle Cross-section Database for Medical Radioisotope Production: Diagnostic Radioisotopes and Monitor Reactions, IAEA-TECDOC-1211, IAEA, Vienna (2001).

JAMES, H.M., HILBURN, M.E., BLAIR, J.A., Lead uptake in humans by whole-body counting of ^{203}Pb: Assessment of errors, Clin. Phys. Physiol. Meas. **6** (1985) 247–250.

LAGUNAS-SOLAR, M.C., JUNGERMANN, J.A., PEEK, N.F., THEUS, R.M., Thallium-201 yields and excitation functions for the lead radioactivities produced by irradiation of natural thallium with 15–60 MeV protons, Int. J. Appl. Radiat. Isot. **29** (1978) 159–165.

QAIM, S.M., WEINREICH, R., OLLIG, H., Production of Tl-201 and Pb-203 via proton-induced nuclear-reactions on natural thallium, Appl. Radiat. Isot. **30** (1979) 85–95.

RMESTANI, K., MILENIC, D., BRADY, E., PLASCJAK, P., BRECHBIEL, M., Purification of cyclotron-produced ^{203}Pb for labeling Herceptin, Nucl. Med. Biol. **32** (2005) 301–305.

SAKAI, M., IKEGAMI, H., YAMAZAKI, T., SAITO, K., Nuclear structure of Hg-200, Nucl. Phys. **65** (1965) 177–202.

2.33. MERCURY-195m

Half-life: 41 h

Parent nucleus	Parent energy level	Parent half-life (h)	Decay mode	Daughter nucleus
Hg-195m	176.07	41.6	EC: 45.8%	Au-195

Positron emission products of ^{195m}Hg

Energy (keV)	End point energy (keV)	Intensity (%)
176	3.5E2	0.006

Note: Mean β^+ energy: 1.8×10^2 keV; total β^+ intensity: 0.006%.

Electron emission products of ^{195m}Hg

This table is also continued on the next page.

Fraction	Energy (keV)	Fraction	Energy (keV)	Fraction	Energy (keV)
0.526	7.42	0.00122	186.03	0.00073	304.25
2.7E–06	9.7	0.00049	192.75	0.00039	305.68
0.31	42.45	0.00031	196.96	0.00072	307.15
0.008	47.11	0.00048	198.53	0.0002	315.18
0.019	52.4	0.000097	199.62	0.000064	317.84
0.091	53.38	0.00013	203.68	0.000025	338.28
0.0292	56.04	0.000039	206.34	0.000089	354.2
0.002	58.04	0.000025	206.7	0.000037	360.78
0.00062	60.7	0.00113	237.88	2.04E–05	365.13
5.3E–07	76.07	0.02	247.4	6.4E–06	367.79
1.2E–07	87	0.0047	258.33	0.000192	371.32
3.7E–08	89.66	0.00147	260.99	0.000064	372.05
0.0007	91.59	0.00008	264.9	0.000262	373.52

Fraction	Energy (keV)	Fraction	Energy (keV)	Fraction	Energy (keV)
0.00135	119.66	4.1E–06	273	3.6E–07	381.4
0.00057	126.38	0.000018	275.83	1.48E–05	382.98
0.000117	157.96	5.8E–06	278.49	0.000065	384.45
0.000027	168.89	9E–07	284	4.6E–06	385.64
8.5E–06	171.55	2.9E–07	286.6		
0.106	181.03	0.00054	287.83		

Photon emission products of ^{195m}Hg

Fraction	Energy (keV)
0.275	9.71
0.131	66.991
0.221	68.806
0.0265	77.577
0.051	77.982
0.0183	80.13
0.31	261.75
0.0215	387.87
0.07	560.27

Parent nucleus	Parent energy level	Parent Jπ	Parent half-life (h)	Decay mode	Daughter nucleus
Hg-195	176.07	13/2+	41.6	IT: 54.2%	Hg-195

Electron emission products of ^{195m}Hg

Fraction	Energy (keV)
0.41	1.37
0.77	7.6
0.097	12.65
0.39	22.25
0.092	33.53
0.0069	38.45
0.047	39.68
0.0018	49.73
0.00056	52.49
0.00179	53.8
0.345	107.94
0.112	119.22
0.039	121.98

Photon emission products of ^{195m}Hg

Gamma rays with less than 1% abundance are not given in the following table.

Fraction	Energy (keV)
0.42	9.99
0.00159	16.207
0.0184	37.09
0.000092	53.29
0.013	68.894
0.0218	70.818
0.00263	79.824
0.005	80.225
0.00182	82.473
0.000283	122.780

Nuclear reactions

The nuclear reactions for production of ^{195m}Hg are:

(a) ^{197}Au(p, 3n)^{195m}Hg;
(b) ^{nat}Pt(α, x)^{195m}Hg.

Excitation functions

The excitation functions for ^{197}Au(p, 3n)^{195m}Hg and ^{nat}Pt(α, x)^{195m}Hg are shown in Figs 2.33.1 and 2.33.2, respectively.

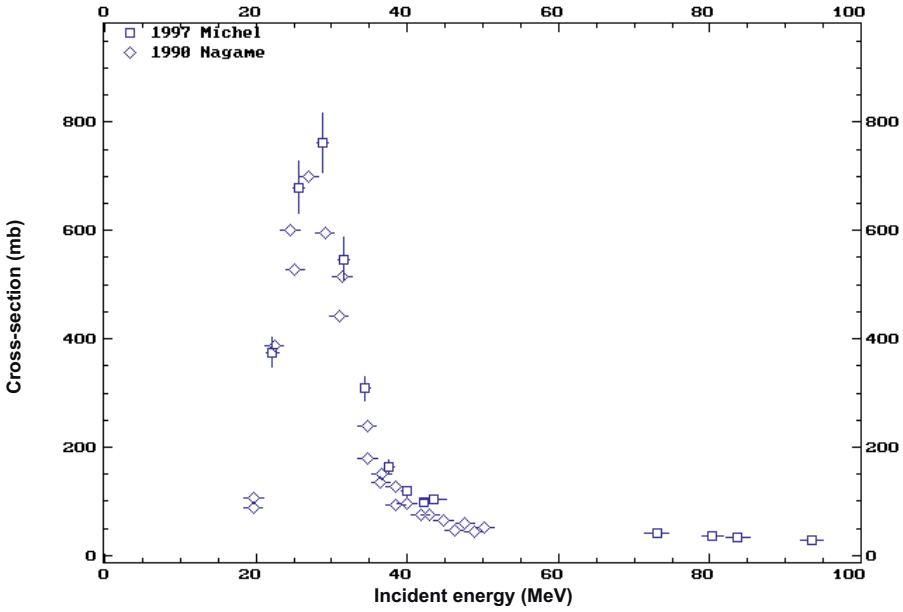

FIG. 2.33.1. Excitation function for the ^{197}Au(p, 3n)^{195m}Hg reaction.

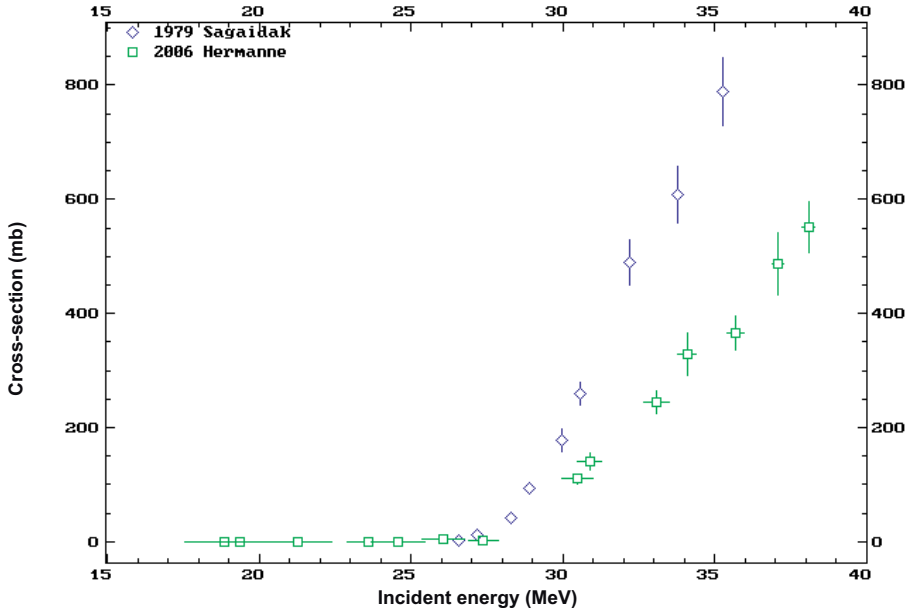

FIG. 2.33.2. Excitation function for the $^{nat}Pt(\alpha, x)^{195m}Hg$ reaction.

BIBLIOGRAPHY TO SECTION 2.33

ASANO, Y., et al., Spallation and fission yields in the interactions of tantalum, tungsten and gold with 500-MeV protons, J. Phys. Soc. Jpn. **54** (1985) 3734–3741.

GLORIS, M., et al., Proton-induced production of residual radionuclides in lead at intermediate energies, Nucl. Instrum. Methods Phys. Res. A **463** (2001) 593–633.

NAGAME, Y., SUEKI, K., BABA, S., NAKAHARA, H., Isomeric yield ratios in proton-, ^{3}He-, and alpha-particle-induced reactions on ^{197}Au, Phys. Rev. C **41** (1990) 889–897.

PORRAS, E., et al., Production rate of proton-induced isotopes in different materials, Nucl. Instrum. Methods Phys. Res. B **160** (2000) 73–125.

2.34. NITROGEN-13

Half-life: 10 min.

Uses

Several compounds incorporating ^{13}N have been made, but the time of accumulation in the body is short and so the physiological processes that can be studied must be rapid [2.34.1, 2.34.2]. By far the most widely used compound of ^{13}N for PET is the chemical form of ammonia. It is used as a blood flow tracer and has found utility in cardiac studies to determine areas of ischaemic or infarcted tissue. As with ^{11}C, the short half-life limits the potential utility of this radionuclide to some extent.

Decay characteristics

Nitrogen-13 decays by pure positron emission (100%) to stable ^{13}C. The end point energy of the positron is 1.19 MeV.

Nuclear reactions

There are several reactions leading to the production of ^{13}N. These are listed in the following table.

Nuclear reaction	Useful energy range (MeV)	Natural abundance (%)	References
$^{13}C(p, n)^{13}N$	4–9	1.1	[2.34.3, 2.34.4]
$^{12}C(d, n)^{13}N$	1–6	98.9	[2.34.3]
$^{16}O(p, \alpha)^{13}N$	8–15	99.8	[2.34.5, 2.34.6]
$^{10}B(\alpha, n)^{13}N$	4–6	19.9	[2.34.7]
$^{11}B(\alpha, 2n)^{13}N$	6–10	80.1	[2.34.8]
$^{14}N(p, pn)^{13}N$	14–30	99.6	[2.34.5]

The proton on ^{13}C reaction has an advantage in that it requires a lower incident proton energy, but suffers from the disadvantage of requiring isotopically enriched material.

Positron emission products of ^{13}N

Fraction	Maximum energy (MeV)	Average energy (MeV)
0.998040	1.198500	0.491800

Electron emission products of ^{13}N

Fraction	Energy (MeV)
0.1856	0.000260

Excitation functions

The excitation function for ^{13}C(p, n)^{13}N is shown in Fig. 2.34.1.

The most common reaction is the ^{16}O(p, α)^{13}N reaction on natural water [2.34.9–2.34.13], which is shown in Fig. 2.34.2.

The final common reaction is the ^{12}C(d, n)^{13}N reaction on natural carbon, which is shown in Fig. 2.34.3.

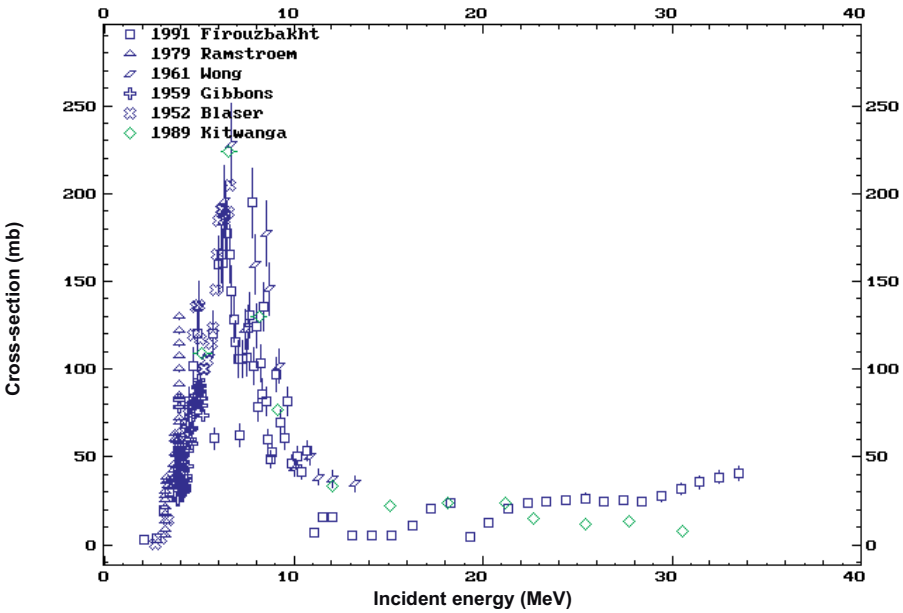

FIG. 2.34.1. Excitation function for the ^{13}C(p, n)^{13}N reaction.

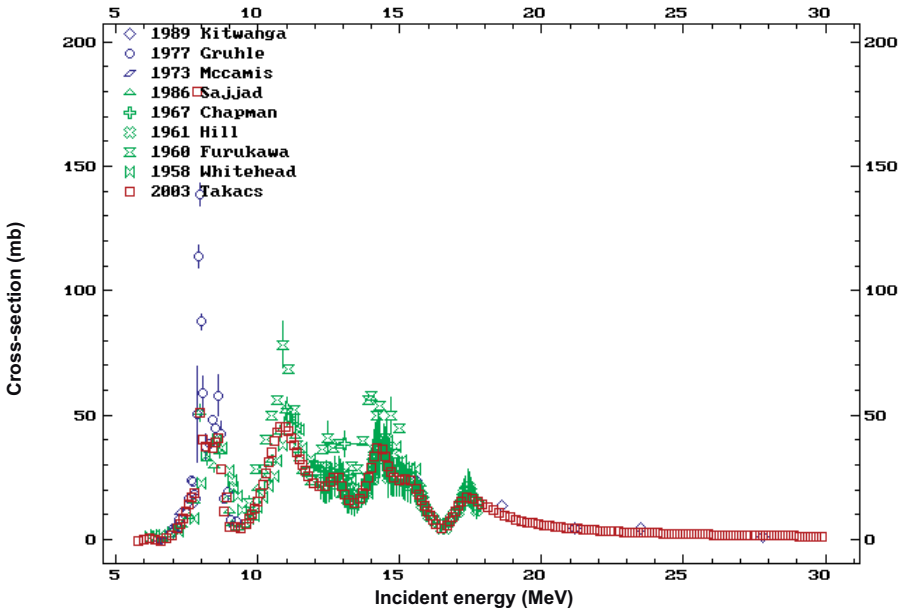

FIG. 2.34.2. Excitation function for the $^{16}O(p, \alpha)^{13}N$ reaction.

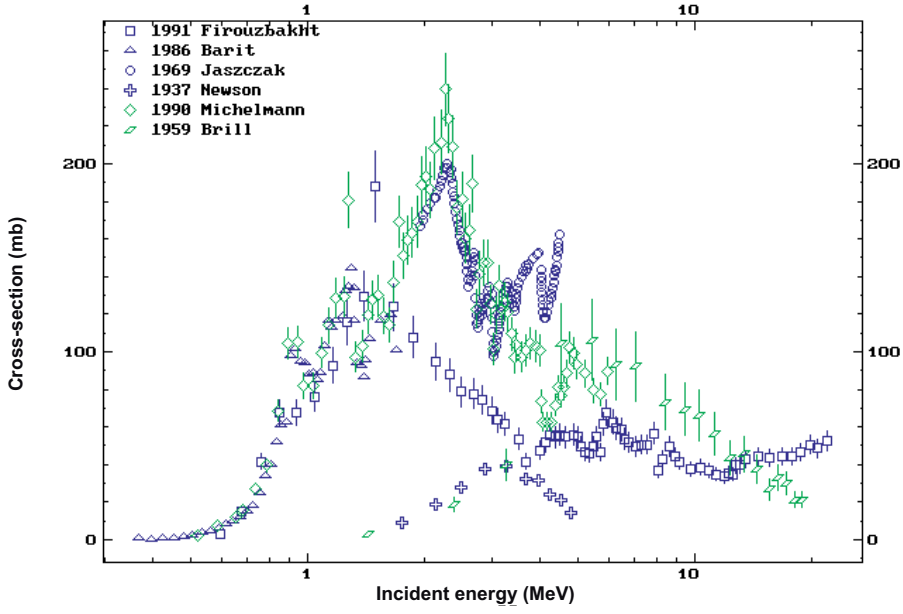

FIG. 2.34.3. Excitation function for the $^{12}C(d, n)^{13}N$ reaction.

Target materials

The targets for production of ^{13}N can be solids, liquids or gases, depending on the chemical form of the nitrogen that is desired. The chemical form can also be changed by a number of other factors, such as the dose and dose rate to the target, the pH of liquid targets and the physical state.

The first target for production of ^{13}N was a solid target of boron, which Joliot and Curie [2.34.8] bombarded with an alpha particle beam. Solid targets have been used extensively for production of ^{13}N, particularly in the form of either nitrogen gas or ammonia [2.34.14–2.34.17]. Solids mixed with liquids have also been used, particularly in production of ammonia [2.34.18–2.34.20]. Solid targets of frozen water have also been used to produce ammonia [2.34.21].

Liquid targets are by far the most popular and widely used. The reaction of protons on natural water produces nitrate and nitrite ions, which can be converted to ammonia by reduction [2.34.2, 2.34.9–2.34.11, 2.34.22]. Water targets can also be used to form ammonia directly with the addition of a reducing agent or with a radical inhibitor [2.34.23–2.34.28]. The chemistry involved in producing the final product distribution in a water target has been a topic of interest and debate [2.34.9, 2.34.21, 2.34.29, 2.34.30], and it has been found that high dose irradiation of the physical form of water results in the formation of oxidized species, while the same irradiation of ice maintains the initial distribution of reduced products [2.34.21].

Gas targets have also been used, particularly for production of nitrogen gas, but there have also been attempts to use gas targets for production of ammonia [2.34.31, 2.34.32, 2.34.33].

Target preparation

In most cases, there is no target preparation for production of ^{13}N. The most widely used targets are water targets and water targets with added ethanol. Solid targets of graphite are also used with additional treatment, except for baking the graphite under vacuum to remove oxygen. Slurry targets present a different problem, i.e. plugging of the flow by sintered material. Care must be taken to clean the frits.

Target processing

The separation of ^{13}N from a target is usually accomplished by burning or heating the solids involved [2.34.15, 2.34.16, 2.34.34]. When ammonia is produced via the $^{16}O(p, \alpha)^{13}N$ reaction on natural water without additives, conversion of nitrogen, nitrates or nitrites to other chemical forms is usually achieved by reduction with de Varda's alloy [2.34.17]. This gives a high yield of ammonia. The first use of additives to water to produce ammonia was carried out by Tilbury and Dahl [2.34.9]. This concept was focused in later years on ethanol, hydrogen and carbon powder as the reducing agents [2.34.18, 2.34.27]. Another approach was to use frozen water as the target material, which also eliminated the radiolysis reactions leading to nitrates and nitrites [2.34.21].

Recovery of enriched materials

The primary enriched material is the ^{13}C powder used in water slurry targets. This material is reused in 'as is' form and therefore requires no recovery chemistry.

Specifications

Validation of the method used for production of ^{13}N ammonia should include inspection of contamination from particulate matter. Radiochemical purity analysis should ensure the absence of nitrites and nitrates. Radionuclidic specifications should ensure the absence of ^{18}F from the aqueous solution. In the water targets that are commonly used in most PET facilities for production of ^{13}N ammonia, the incidence of pyrogen growth has been reported from several laboratories. Flushing of the target with sterile water prior to use helps to reduce the possibility of contamination of the pyrogen. The target should also receive regular maintenance, to reduce the incidence of particulate matter contaminating the product.

REFERENCES TO SECTION 2.34

[2.34.1] STRAATMANN, M.G., WELCH, M.J., Enzymatic synthesis of nitrogen-13 labeled amino acids, Radiat. Res. **56** (1973) 48–56.

[2.34.2] TILBURY, R.S., EMRAN, A.M., "[^{13}N] labeled tracers, synthesis and applications", New Trends in Radiopharmaceutical Synthesis, Quality Assurance, and Regulatory Control (EMRAN, A., Ed.), Plenum Press, New York and London (1991) 39–51.

[2.34.3] FIROUZBAKHT, M.L., SCHLYER, D.J., WOLF, A.P., Cross-section measurements for the ^{13}C(p, n)^{13}N and ^{12}C(d, n)^{13}N nuclear reactions, Radiochim. Acta **55** (1991) 1–5.

[2.34.4] AUSTIN, S.M., GALONSKY, A., BORTINS, J., WOLK, C.P., A batch process for the production of ^{13}N-labeled nitrogen gas, Nucl. Instrum. Methods **126** (1975) 373–379.

[2.34.5] SAJJAD, M., LAMBRECHT, R.M., WOLF, A.P., Cyclotron isotopes and radiopharmaceuticals, XXXVII: Excitation functions for the ^{16}O(p, α)^{13}N and ^{14}N(p, pn)^{13}N reactions, Radiochim. Acta **39** (1986) 165–168.

[2.34.6] PARKS, N.J., KROHN, K.A., The synthesis of ^{13}N labeled ammonia, dinitrogen, nitrite, nitrate using a single cyclotron target system, Int. J. Appl. Radiat. Isot. **29** (1978) 754–757.

[2.34.7] GIBBONS, J.H., MACKLIN, R.L., Total neutron yields from light elements under proton and alpha bombardment, Phys. Rev. **114** (1959) 571–580.

[2.34.8] JOLIOT, F., CURIE, I., Artificial production of a new kind of radio-element, Nature **133** (1934) 201–202.

[2.34.9] TILBURY, R.S., DAHL, J.R., ^{13}N species formed by the proton irradiation of water, Radiat. Res. **79** (1979) 22–33.

[2.34.10] TILBURY, R.S., DAHL, J.R., MARANO, S.J., N-13 species formed by proton irradiation of water, J. Labelled Compd. Radiopharm. **13** (1977) 208.

[2.34.11] HELMEKE, H.J., HARMS, T., KNAPP, W.H., "Home-made routinely used targets for the production of PET radionuclides", Targetry and Target Chemistry (Proc. 7th Workshop Heidelberg, 1997), TRIUMF, Vancouver (1997) 241.

[2.34.12] MULHOLLAND, G.K., SUTORIK, A., JEWETT, D.M., MANAGER, T.J., KILBOURN, M.R., Direct in-target synthesis of aqueous N-13 ammonia by proton irradiation of water under hydrogen pressure, J. Nucl. Med. **30** (1989) 926.

[2.34.13] INTERNATIONAL ATOMIC ENERGY AGENCY, Charged Particle Cross-section Database for Medical Radioisotope Production: Diagnostic Radioisotopes and Monitor Reactions, IAEA-TECDOC-1211, IAEA, Vienna (2001).

[2.34.14] SHEFER, R.E., HUGHEY, B.J., KLINKOWSTEIN, R.E., WELCH, M.J., DENCE, C.S., A windowless ^{13}N production target for use with low energy deuteron accelerators, Nucl. Med. Biol. **21** (1994) 977–986.

[2.34.15] FERRIERI, R.A., SCHLYER, D.J., WIELAND, B.W., WOLF, A.P., On-line production of ^{13}N-nitrogen gas from a solid enriched ^{13}C-target and its application to ^{13}N-ammonia synthesis using microwave radiation, Int. J. Appl. Radiat. Isot. **34** (1983) 897–900.

[2.34.16] DENCE, C.S., WELCH, M.J., HUGHEY, B.J., SHEFER, R.E., KLINKOWSTEIN, R.E., Production of [^{13}N] ammonia applicable to low energy accelerators, Nucl. Med. Biol. **21** (1994) 987–996.

[2.34.17] VAALBURG, W., et al., Production of ^{13}N-labelled molecular nitrogen for pulmonary function studies, J. Labelled Compd. Radiopharm. **18** (1981) 303–308.

[2.34.18] BIDA, G., et al., An economical target for ^{13}N production by proton bombardment of a slurry of ^{13}C powder on ^{16}O water, J. Labelled Compd. Radiopharm. **23** (1986) 1217–1218.

[2.34.19] ALVORD, C.W., BIDA, G.T., WIELAND, B.W., ZIPPI, E.M., "Multi-particle bombardment and in-target chemistry of porous carbon materials", Targetry and Target Chemistry (Proc. 7th Workshop Heidelberg, 1997), TRIUMF, Vancouver (1997) 104.

[2.34.20] ZIPPI, E.M., VALIULIS, M.B., GROVER, J., "Synthesis of carbon-13 sulfonated poly(styrene/divinylbenzene) for production of a nitrogen-13 target material", Targetry and Target Chemistry (Proc. 6th Workshop Vancouver, 1995), TRIUMF, Vancouver (1995) 185–188.

[2.34.21] FIROUZBAKHT, M.L., SCHLYER, D.J., FERRIERI, R.A., WOLF, A.P., FOWLER, J.S., Mechanisms involved in the production of nitrogen-13 labeled ammonia in a cryogenic target, Nucl. Med. Biol. **26** (1999) 437–441.

[2.34.22] WIELAND, B.W., McKINNEY, C.J., COLEMAN, R.E., "A tandem target system using $^{16}O(p, pn)^{15}O$ and $^{16}O(p, \alpha)^{13}N$ on natural water", Targetry and Target Chemistry (Proc. 6th Workshop Vancouver, 1995), TRIUMF, Vancouver (1995) 173–179.

[2.34.23] BERRIDGE, M.S., LANDMEIER, B.J., In-target production of [^{13}N]ammonia: Target design, products and operating parameters, Appl. Radiat. Isot. **44** (1993) 1433–1441.

[2.34.24] KORSAKOV, M.V., KRASIKOVA, R.N., FEDOROVA, O.S., Production of high yield [^{13}N]ammonia by proton irradiation from pressurized aqueous solutions, J. Radioanal. Nucl. Chem. **204** (1996) 231–239.

[2.34.25] MEDEMA, J., ELSINGA, P.H., KEIZER, H., FRANSSEN, E.J.F., VAALBURG, W., "Remote controlled in-target production of [^{13}N]ammonia using a circulating target", Targetry and Target Chemistry (Proc. 7th Workshop Heidelberg, 1997), TRIUMF, Vancouver (1997) 80–81.

[2.34.26] MULHOLLAND, G.K., KILBOURN, M.R., MOSKWA, J.J., Direct simultaneous production of [^{15}O]water and [^{13}N]ammonia or [^{18}F]fluoride ion by 26 MeV proton irradiation of a double chamber water target, Appl. Radiat. Isot. **41** (1990) 1193–1199.
[2.34.27] WIELAND, B.W., et al., In-target production of [^{13}N] ammonia via proton irradiation of dilute aqueous ethanol and acetic acid mixtures, Appl. Radiat. Isot. **42** (1991) 1095–1098.
[2.34.28] BIDA, G., SATYAMURTHY, N., "[^{13}N]ammonia production via proton irradiation of CO_2/H_2O: A work-in-progress", Targetry and Target Chemistry (Proc. 6th Workshop Vancouver, 1995), TRIUMF, Vancouver (1995) 189–191.
[2.34.29] PATT, J.T., NEBLING, B., STÖCKLIN, G., Water target chemistry of nitrogen-13 recoils revisited, J. Labelled Compd. Radiopharm. **30** (1991) 122–123.
[2.34.30] SASAKI, M., HARADAHIRA, T., SUZUKI, K., Effect of dissolved gas on the specific activity of N-13 labeled ions generated in water by the ^{16}O(p, α)^{13}N reaction, Radiochim. Acta **88** (2000) 217–220.
[2.34.31] MIKECZ, P., DOOD, M.G., CHALONER, F., SHARP, P.F., "Glass target for production of [^{13}N]NH_3 from methane", Targetry and Target Chemistry (Proc. 7th Workshop Heidelberg, 1997), TRIUMF, Vancouver (1997) 163–164.
[2.34.32] WELCH, M.J., Production of active molecular nitrogen by the reaction of recoil nitrogen-13, Chem. Comm. (1968) 1354–1355.
[2.34.33] STRAATMANN, M.G., A look at ^{13}N and ^{15}O in radiopharmaceuticals, Int. J. Appl. Radiat. Isot. **28** (1977) 13–20.
[2.34.34] McCARTHY, T.J., GAEHLE, G.G., MARGENAU, W.H., GURLEYIK, K., "An inductive heater for the rapid combustion of graphite disks", Targetry and Target Chemistry (Proc. 7th Workshop Heidelberg, 1997), TRIUMF, Vancouver (1997) 205.

2.35. OXYGEN-15

Half-life: 122 s.

Uses

Oxygen-15 is used to label gases, such as oxygen, carbon dioxide and carbon monoxide, for inhalation, and it is also used to label water for injection. The major purpose of these gases and liquids is to measure blood flow, blood volume and oxygen consumption in the body.

Decay characteristics

Oxygen-15 is the longest lived of the positron emitting isotopes (99.9% positron emission) of oxygen. The end point energy of the positron is 1.72 MeV. Oxygen-15 decays to stable ^{15}N and was one of the first artificial radioisotopes produced with low energy deuterons on a cyclotron [2.35.1].

Positron emission products of ^{15}O

Fraction	Maximum energy (MeV)	Average energy (MeV)
0.999000	1.731900	0.735200

Photon emission products of ^{15}O

Fraction	Energy (MeV)
1.998000	0.511000

Nuclear reactions for production of ^{15}O

Nuclear reaction	Useful energy range (MeV)	Natural abundance (%)	References
^{16}O(p, pn)^{15}O	26.5–20	99.8	[2.35.2]
^{15}N(p, n)^{15}O	4–10	0.4	[2.35.3]
^{14}N(d, n)^{15}O	2–10	99.6	[2.35.4–2.35.6]
^{12}C(α, n)^{15}O	12–18	98.9	[2.35.7]

Excitation functions

The excitation functions for ^{14}N(d, n)^{15}O and ^{15}N(p, n)^{15}O are shown in Figs 2.35.1 and 2.35.2, respectively.

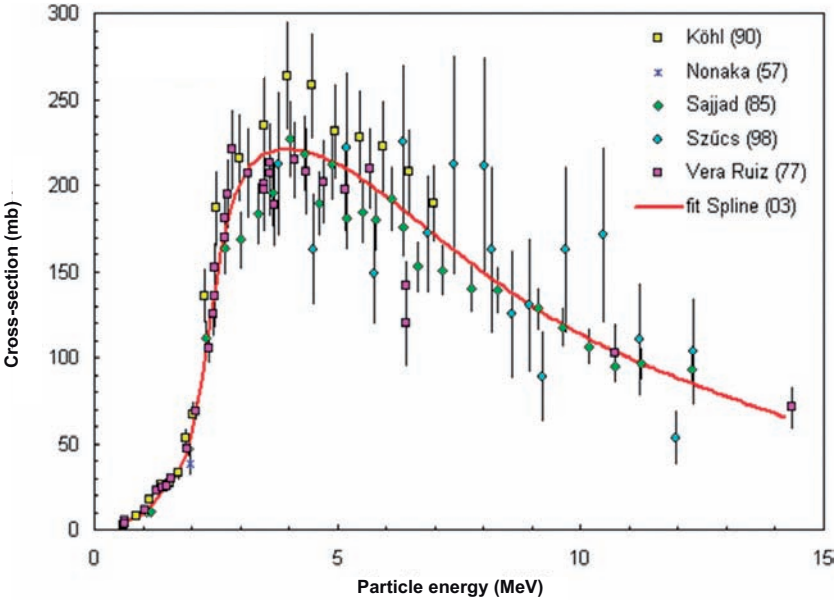

FIG. 2.35.1. Excitation function for the $^{14}N(d, n)^{15}O$ reaction.

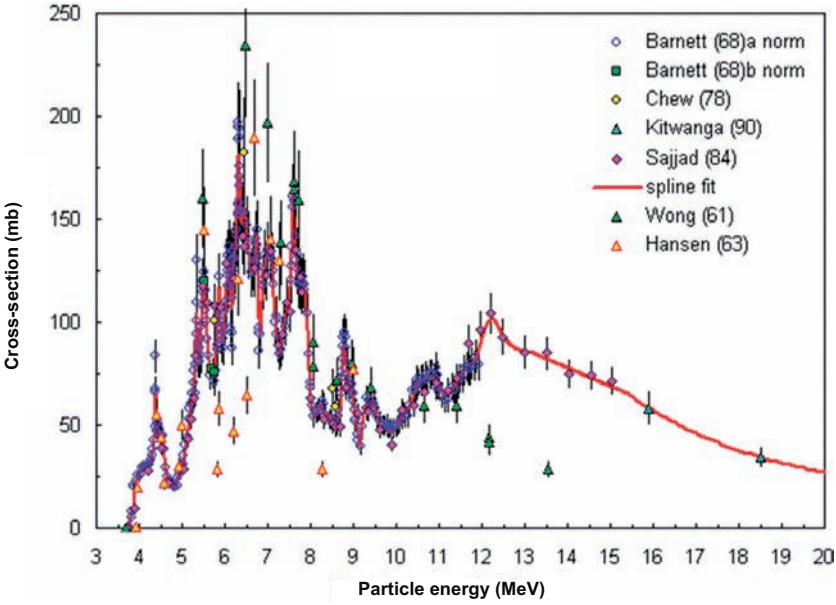

FIG. 2.35.2. Excitation function for the $^{15}N(p, n)^{15}O$ reaction.

Thick target yields (at saturation)

The following table is taken from Ref. [2.35.8].

Energy (MeV)	Yield (mCi/μA)[a]	Energy (MeV)	Yield (mCi/μA)	Energy (MeV)	Yield (mCi/μA)
4	0.459	12	92.61	20	209.25
4.5	2.268	12.5	102.87	20.5	213.57
5	3.51	13	112.32	21	217.35
5.5	7.83	13.5	122.04	21.5	221.13
6	13.23	14	131.22	22	224.64
6.5	22.41	14.5	140.13	22.5	228.15
7	30.51	15	149.04	23	231.39
7.5	37.8	15.5	157.41	23.5	234.63
8	46.17	16	164.97	24	237.6
8.5	50.49	16.5	172.26	24.5	240.57
9	55.89	17	178.74	25	243.54
9.5	60.48	17.5	184.68	25.5	246.24
10	64.8	18	190.35	26	248.94
10.5	70.47	18.5	195.48	26.5	251.64
11	77.22	19	200.34	27	254.34
11.5	83.97	19.5	204.93	27.5	256.77

[a] 1 Ci = 37 GBq.

The excitation function for the reaction $^{16}O(p, np)^{15}O$ is shown in Fig. 2.35.3.

Target materials

Gaseous targets are, for the most part, used for these compounds. Oxygen-15 containing compounds can be made either directly in the target [2.35.9–2.35.11] or outside the target in a separate recovery module. Gas targets are usually made of nitrogen and are bombarded with either protons or deuterons, depending on which particle is available.

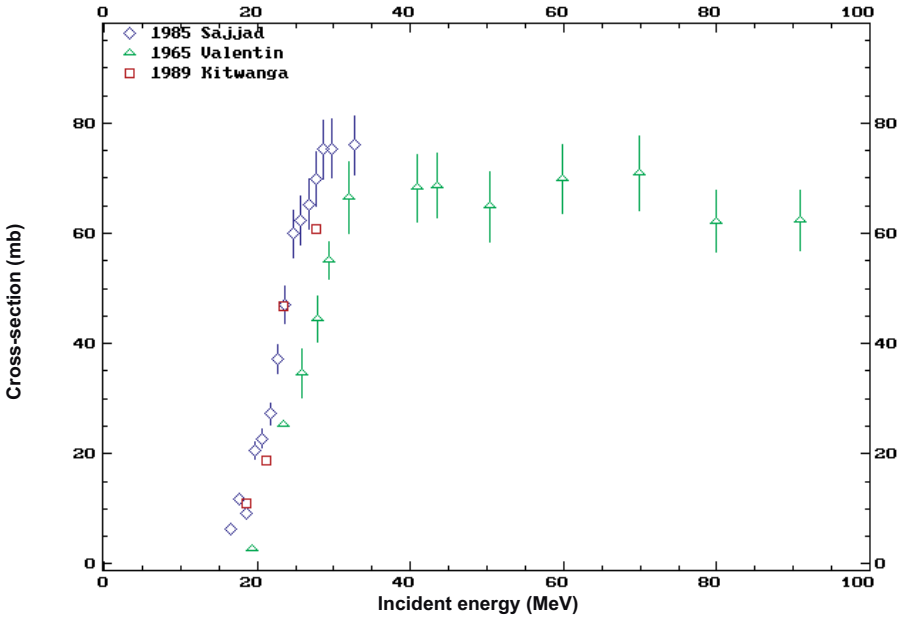

FIG. 2.35.3. Excitation function for the $^{16}O(p, np)^{15}O$ reaction.

Solid targets have been explored as a source for producing [^{15}O]ozone [2.35.12]. In this target, ^{15}O is produced by irradiating quartz microfibres and allowing the nucleogenic atoms that leave the fibres to react with the surrounding gas.

Target preparation

Oxygen-15 is usually produced using a deuteron reaction on nitrogen gas or a proton reaction on ^{15}N enriched nitrogen gas. In either case, the target is filled with nitrogen gas and irradiated.

Target processing

The radioisotopes produced can be separated or, in some circumstances, the target gas can be used with a minimum of processing [2.35.2, 2.35.13, 2.35.14]. An example of this is the production of [^{15}O]water. It can be made directly in the target by adding 5% hydrogen to the nitrogen gas in the target [2.35.9]. In this case, the water is produced directly. Ammonia is also produced in the targets by radiolysis of nitrogen, but it must be removed. The other option is to produce ^{15}O labelled oxygen gas in the target and then process it to water outside the target. Details of these procedures can be found elsewhere.

[^{15}O]water has also been produced by bombarding ordinary water using the ^{16}O(p, pn)^{15}O reaction, with a final cleanup on an ion exchange column [2.35.15].

Enriched materials recovery

Nitrogen-15 enriched nitrogen gas is not usually recovered. It can be trapped cryogenically after the ^{15}O has been removed by chemical reaction or trapping.

Specifications

Radiochemical purity should be higher than 98% and radionuclidic purity higher than 99%. Gas chromatography should be used for radiochemical purity measurements.

REFERENCES TO SECTION 2.35

[2.35.1] LIVINGSTON, M.S., McMILLAN, E., The production of radioactive oxygen, Phys. Rev. **46** (1934) 439–440.

[2.35.2] BEAVER, J.E., FINN, R.D., HUPF, H.B., A new method for the production of high concentration oxygen-15 labeled carbon dioxide with protons, Int. J. Appl. Radiat. Isot. **27** (1976) 195–197.

[2.35.3] SAJJAD, M., LAMBRECHT, R.M., WOLF, A.P., Cyclotron isotopes and radiopharmaceuticals, XXXIV: Excitation function for the ^{15}N(p, n)^{15}O reaction, Radiochim. Acta **36** (1984) 159–162.

[2.35.4] DEL FIORE, G., DEPRESSEUX, J.C., BARTSCH, P., QUAGLIA, L., PETERS, J.-M., Production of oxygen-15, nitrogen-13 and carbon-11 and of their low molecular weight derivatives for biomedical applications, Int. J. Appl. Radiat. Isot. **30** (1979) 543–549.

[2.35.5] RETZ-SCHMIDT, T., WEIL, J.L., Excitation curves and angular distributions for ^{14}N(d, n)^{15}O, Phys. Rev. **119** (1960) 1079–1084.

[2.35.6] VERA-RUIZ, H., WOLF, A.P., Direct synthesis of oxygen-15 labeled water of high specific activity, J. Labelled Compd. Radiopharm. **15** (1978) 186–189.

[2.35.7] BLACK, J.L., KUAN, H.M., GRUHLE, W., SUFFERT, M., LATSHAW, G.L., Reactions ^{12}C(α, n)^{15}O and ^{12}C(α, p)^{15}N, Nucl. Phys. A **115** (1968) 683–696.

[2.35.8] TAKÁCS, S., TÁRKÁNYI, F., HERMANNE, A., PAVIOTTI DE CORCUERA, R., Validation and upgrade of the recommended cross section data of charged particle reactions used for production PET radioisotopes, Nucl. Instrum. Methods Phys. Res. B **211** (2003) 169–189.

[2.35.9] VERA-RUIZ, H., WOLF, A.P., Excitation function of ^{15}O production via the $^{14}N(d, n)^{15}O$ reaction, Radiochim. Acta **24** (1977) 65–67.
[2.35.10] VOTAW, J.R., SATTER, M.R., SUNDERLAND, J.J., MARTIN, C.C., NICKLES, R.J., The Edison lamp: O-15 carbon monoxide production in the target, J. Labelled Compd. Radiopharm. **23** (1986) 1211–1213.
[2.35.11] HARPER, P.V., WICKLAND, T., Oxygen-15 labeled water for continuous intravenous administration, J. Labelled Compd. Radiopharm. **18** (1981) 186.
[2.35.12] WIELAND, B.W., RUSSEL, M.L., DUNN, W.L., BIDA, G.T., "Quartz microfiber target for the production of O-15 ozone for pulmonary applications", Targetry and Target Chemistry (Proc. 7th Workshop Heidelberg, 1997), TRIUMF, Vancouver (1997) 114–119.
[2.35.13] STRIJCKMANS, K., VANDECASTEELE, C., SAMBRE, J., Production and quality control of $^{15}O_2$ and $C^{15}O_2$ for medical use, Int. J. Appl. Radiat. Isot. **36** (1985) 279–283.
[2.35.14] WIELAND, B.W., SCHMIDT, D.G., BIDA, G., RUTH, T.J., HENDRY, G.O., Efficient, economical production of oxygen-15 labeled tracers with low energy protons, J. Labelled Compd. Radiopharm. **23** (1986) 1214–1216.
[2.35.15] VAN NAEMEN, J., MONCLUS, M., DAMHAUT, P., LUXEN, A., GOLDMAN, S., Production, automatic delivery and bolus injection of [^{15}O]water for positron emission tomography studies, Nucl. Med. Biol. **23** (1966) 413–416.

BIBLIOGRAPHY TO SECTION 2.35

INTERNATIONAL ATOMIC ENERGY AGENCY, Charged Particle Cross-section Database for Medical Radioisotope Production: Diagnostic Radioisotopes and Monitor Reactions, IAEA-TECDOC-1211, IAEA, Vienna (2001).

2.36. PALLADIUM-103

Half-life: 17 d.

Uses

Owing to its half-life and its electron capture decay resulting in abundant emission of Auger electrons and low energy X rays (20–22 keV), ^{103}Pd can be used for the preparation of seeds used as permanent interstitial implants for the treatment of rapidly proliferating tumours. Along with ^{125}I, the radionuclide has been used in treatment of various cancers, such as those of the eye, brain, neck, uterus and colon, but it is now primarily used for prostate tumours. Over

the last decade, it has proved to be very effective in treating this cancer with minimal side effects.

Electron emission products of ^{103}Pd

Fraction	Energy (MeV)
0.165760	0.017000
0.907710	0.002390

Photon emission products of ^{103}Pd

Fraction	Energy (MeV)
0.000308	0.359610
0.047774	0.002700
0.117440	0.022700
0.198430	0.020074
0.377240	0.020216

Nuclear reactions

Palladium-103 is mainly produced by proton bombardment of rhodium (^{103}Rh(p, n)^{103}Pd). The electroplating of the target can be carried out by applying either a DC constant voltage (or current) or an AC constant voltage (or current) at an elevated temperature (typically 40–60°C).

Excitation functions

The excitation functions for ^{103}Rh(p, n)^{103}Pd and ^{103}Rh(d, 2n)^{103}Pd are shown in Figs 2.36.1 and 2.36.2, respectively.

Target materials

Although soluble rhodium compounds have been tried, at present commercial productions involve the use of solid targetry, such as powder, wires, foils or electroplated layers. The latter may be prepared by electrodeposition of the precious metal on a (copper) target carrier from home-made rhodium

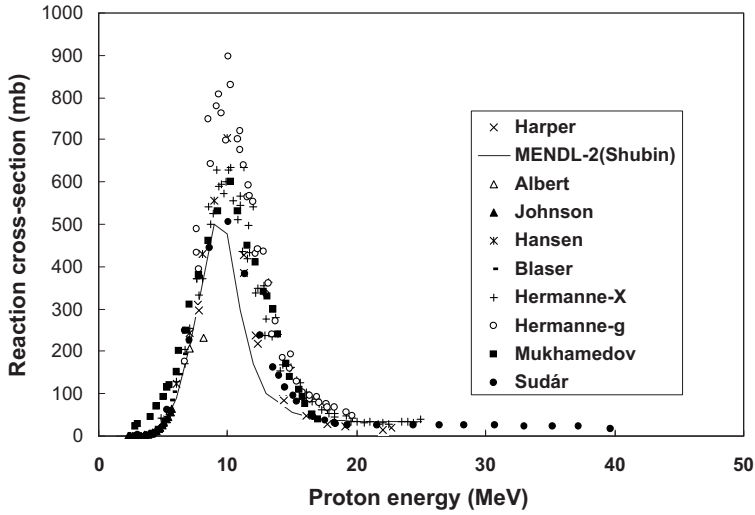

FIG. 2.36.1. Excitation function for the ^{103}Rh(p, n)^{103}Pd reaction.

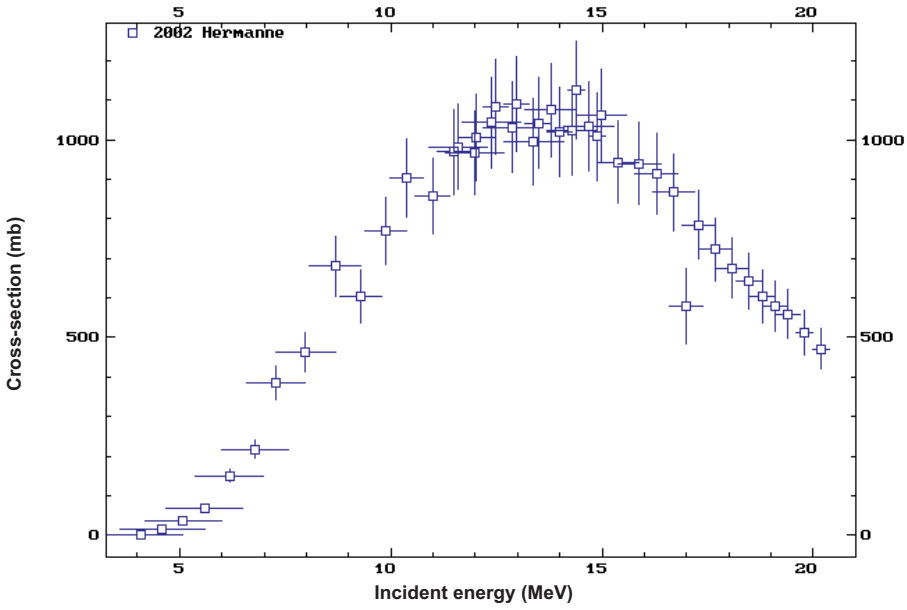

FIG. 2.36.2. Excitation function for the ^{103}Rh(d, 2n)^{103}Pd reaction.

sulphate or rhodium chloride plating solutions containing appropriate amounts of plating additives (tensides, and depolarising, stress reducing and/or complexing agents) or from commercially available rhodium plating baths.

Target preparation

An in-house plating–electrodissolution–recovery cycle starts with preparation of a sulphate plating solution from recovered hydrated rhodium oxide. Commercially available sulphate plating baths (Rhodex, Enthone, USA) can also be used to start up.

Rhodium is recovered as hydrated rhodium oxide from a freshly prepared aqueous $RhCl_3$ solution obtained by dissolution of analytical grade compound or from a mixture of hydrochloric acid recovery solutions obtained after centrifugal electrodissolution of the irradiated rhodium and subsequent extraction of ^{103}Pd. Details of target preparation can be found in Ref. [2.36.1].

Rhodium chloride plating solutions can be prepared by dissolution of analytical grade compound or from rhodium recovery solutions obtained after electrosolubilization of irradiated targets and extraction of palladium. Commercially available plating solutions (Degussa, Germany) containing some plating additives can also be used. Direct constant current or AC constant voltage plating up to a depletion level of more than 98% at about 40°C can be used.

Other solid rhodium targets

Rhodium foils (10–100 μm), rhodium wires (0.5 mm) or rhodium powder can be used as other solid target materials. In either case, centrifugal electrodissolution combined with wet chemistry can be applied for separation of ^{103}Pd. Foils, wires and fragmented rhodium allow partial recovery of ^{103}Pd when the thermal diffusion technique is applied.

Target processing

Irradiated rhodium metal targets (plated layers, foils and wires) have frequently been dissolved by sodium bisulphate fusion (a complex medium and a time-consuming process), by gold tetrachloroaurate oxidation (a very expensive and time-consuming process) and by static AC electrodissolution in hydrochloric acid. Until now, the latter method has been recommended for solubilization of foils (not applicable to rhodium powder, wires or fragments), but it suffers from a number of limitations, such as incomplete dissolution due to partial fragmentation, limited and non-time-controlled solubilization rate,

and large volume of hydrochloric acid required for gram sized amounts of target material. A new time controlled, centrifugal, high current density, electrodissolution technique resulting in quantitative (>99%) solubilization of up to 3 g of target material in a limited volume (40 mL) of acid has been developed. This technique is described in detail in Ref. [2.36.1].

Separation of carrier-free ^{103}Pd

Wet chemistry methods

Separation of ^{103}Pd from the solubilized rhodium matrix can be achieved by solvent/solvent extraction, by anion or cation exchange chromatography, or by electroseparation, i.e. separation by controlled cathode potential electrolysis.

For solvent extraction, the 3N HCl/furyldioxime–chloroform system should be applied, as it does not require evaporation of the solution obtained after centrifugal electrodissolution. Only a twofold dilution with water prior to extraction is necessary. Application of ion exchange chromatography first requires evaporation to dryness. For cation exchange chromatography, the residue is taken up in 0.1–0.4N HCl. Rhodium and palladium are then separated on an AG50WX8(H^+)/100–200 mesh column (1.5 g resin): rhodium is eluted first, after which palladium is collected in 10 mL HCl. Anion exchange involves dissolution in 0.03N HCl, and separation of copper, rhodium and palladium is achieved using a Dowex1X8(Cl^-)/100–200 mesh column (1.5 cm × 10 cm). Copper is eluted with 0.03M HCl, rhodium with 6M HCl and palladium with a 1:1 mixture of 0.5M NH_3/NH_4Cl. To apply electroseparation, the 7.3N HCl solution should be partially neutralized (1–2M HCl). The rhodium is then plated out on a cathode, the potential of which is set at –0.54 V with respect to a $Ag/AgCl_{sat}$ reference electrode. The disadvantage of this method is that the rhodium target material cannot be recycled in a simple way.

Thermal diffusion

Thermal diffusion involves migration of carrier-free ^{103}Pd to the surface area of foils, fragments or wires under the influence of heating up (in the air or in vacuum) to a temperature higher than 1000°C. Upon cooling, the palladium can be dissolved in a suitable acid, typically HCl. Although extremely simple, one main disadvantage of this method is the limited extraction yield. As the melting point of rhodium metal is 1966°C, higher temperature (up to 1900°C) diffusion should be tried.

Recovery of enriched materials

Minor quantities of longer lived rhodium isotopes (^{102m,102g}Rh) formed should be taken into account when this expensive target material is recycled.

Quality control

Target quality control

Three criteria are used to estimate the quality of the electroplated rhodium targets, namely, the homogeneity of the rhodium layer, the surface area granulometry and the behaviour during a thermal shock test. The thermal shock test involves heating of the target up to 500°C (the maximum allowable temperature of the rhodium layer during irradiation) for 1 hour, followed by submersion of the hot target in cold (15°C) water and by multiple bending of the target carrier. There should not be any cracks formed or any peeling off of the rhodium layer. A thermal shock test is a measure of the incorporation of plating bath compounds into the rhodium crystal lattice and/or of their presence in the carrier–rhodium layer interface.

Radiochemical quality control

The final radiochemical used for seed preparation should preferably be a carrier-free (SA >> 50 Ci/g) palladium chloride solution in dilute ammonium hydroxide (7 < pH < 10). Commercially available solutions show an activity concentration higher than 500 mCi/mL. The accepted radionuclidic purity is at least 99.95% ^{103}Pd.

REFERENCE TO SECTION 2.36

[2.36.1] INTERNATIONAL ATOMIC ENERGY AGENCY, Standardized High Current Solid Targets for Cyclotron Production of Diagnostic and Therapeutic Radionuclides, Technical Reports Series No. 432, IAEA, Vienna (2004) CD-ROM.

BIBLIOGRAPHY TO SECTION 2.36

CARDEN, J.L., Jr., TUCKER, G.A., X-ray Emitting Interstitial Implants, United States Patent 5 405 309, filed 11 Apr. 1995; copies available from United States Patent and Trademark Office, Alexandria, VA.

FUKS, Z., et al., The effect of local control on metastatic carcinoma of the prostate: Long term results in patients treated with I-125, Int. J. Radiat. Oncol. Biol. Phys. **21** (1991) 537–547.

HERMANNE, A., SONCK, M., FENYVESI, A., DARABAN, L., Study on production of Pd-103 and characterisation of possible contaminants in the proton irradiation of Rh-103 up to 28 MeV, Nucl. Instrum. Methods Phys. Res. B **170** (2000) 281–292.

HERMANNE, A., SONCK, M., TAKÁCS, S., TÁRKÁNYI, F., SHUBIN, Y., Study on alternative production of ^{103}Pd and characterisation of contaminants in the deuteron irradiation of ^{103}Rh up to 21 MeV, Nucl. Instrum. Methods Phys. Res. B **187** (2002) 3–14.

LAGUNAS-SOLAR, M.C., AVILA, M.J., JOHNSON, P.C., Cyclotron production of ^{101m}Rh via proton-induced reactions on ^{103}Rh targets, Int. J. Appl. Radiat. Isot. **35** (1984) 743.

LAGUNAS-SOLAR, M.C., AVILA, M.J., JOHNSON, P.C., Targetry and radiochemical methods for the simultaneous cyclotron production of no-carrier-added radiopharmaceutical-quality ^{100}Pd, ^{97}Ru and ^{101m}Rh, Int. J. Appl. Radiat. Isot. **38** (1987) 151–157.

LAGUNAS-SOLAR, M.C., AVILA, M.J., NAVANRO, N.J., JOHNSON, P.C., Cyclotron production of non-carrier-added ^{97}Ru by bombardment of ^{103}Rh targets, Int. J. Appl. Radiat. Isot. **34** (1983) 915–922.

LAGUNAS-SOLAR, M.C., THIBEAU, H.L., LITTLE, F.E., "A remote system for multicurie radiochemical separations", Remote Systems Technology (Proc. 27th Conf. San Francisco, 1979), CRSTBJ 27 1-432 (1979) 301–306.

LING, C.C., Permanent implants using Au-198, Pd-103 and I-125: Radiobiological considerations based on the linear quadratic model, Int. J. Radiat. Oncol. Biol. Phys. **23** (1972) 81–87.

MORTON, J.D., PESCHEL, R.E., Iodine-125 implants versus external beam therapy for stage-A2, -B and -C prostate cancer, Int. J. Radiat. Oncol. Biol. Phys. **14** (1988) 1152–1157.

NAG, S., et al., Palladium-103 vs. iodine-125 brachytherapy in the Danning-PAP rat prostate tumor, Endocuriether. Hypertherm. Oncol. **12** (1996) 119–124.

NAG, S., SWEENEY, P.J., WIENTJES, M.G., Dose-response study of iodine-125 and palladium-103 brachytherapy in a rat prostate tumor (Nb AI-1), Endocuriether. Hypertherm. Oncol. **9** (1993) 97–104.

PRESTIDGE, B.R., et al., A survey of current clinical practice of permanent prostate brachytherapy in the United States, Int. J. Radiat. Oncol. Biol. Phys. **40** (1998) 461–463.

RAGDE, H., ELGAMAL, A.A., SNOW, P.B., Ten-year disease free survival after transperineal sonography-guided iodine-125 brachytherapy with or without 45-Gray external beam irradiation in the treatment of patients with clinically localized, low to high Gleason grade prostate carcinoma, Cancer **83** (1998) 989–1001.

RAMLI, M., SHARMA, H.L., Radiochemical separation of ^{101m}Rh via ^{101}Pd from a rhodium target, Int. J. Appl. Radiat. Isot. **48** (1997) 327–331.

SCHOLZ, K.L., SODD, V.J., BLUE, J.W., Cyclotron production of rhodium-101m through its precursor palladium-101, Int. J. Appl. Radiat. Isot. **28** (1997) 207–211.

SUDAR, S., CSERPAK, F., QAIM, S.M., Measurements and nuclear model calculation on proton-induced reactions on ^{103}Rh up to 40 MeV: Evaluation of the excitation function of the ^{103}Rh(p, n)^{103}Pd reaction relevant to the production of the therapeutic radionuclide ^{103}Pd, Appl. Radiat. Isot. **56** (2002) 821–831.

TARAPCIK, P., MIKULAJ, V., Separation of ^{103}Pd from cyclotron irradiated rhodium targets, Radiochem. Radioanal. Lett. **48** (1981) 15–20.

ZHANG, C., WANG, Y., ZHANG, Y., ZHANG, X., Cyclotron production of no-carrier-added palladium-103 by bombardment of rhodium-103 target, Appl. Radiat. Isot. **55** (2001) 441–445.

2.37. SODIUM-22

Half-life: 2.6 a.

Uses

As a positron emitter with a long half-life, ^{22}Na is often used as a positron source in calibrating ion chambers and PET cameras. Sodium-22 has been proposed as a source of 511 keV gamma rays for attenuation in PET cameras [2.37.1].

Decay mode

The radioisotope ^{22}Na decays by positron emission (90.6%) and electron capture (9.4%).

Positron emission products of ^{22}Na

Fraction	Maximum energy (MeV)	Average energy (MeV)
0.905	0.540	0.2155
0.000560	2.842100	0.8350

Photon emission products of ^{22}Na

Fraction	Energy (MeV)
1.81	0.5110
0.999	1.275

Nuclear reactions for production of ^{22}Na

For large amounts, purchase of ^{22}Na is probably the best option. While ^{22}Na can be produced by a wide range of reactions, typically at high energy, the most accessible approach is via the ^{22}Ne(p, n)^{22}Na reaction [2.37.2]. An alternative reaction is the ^{24}Mg(p, α)^{22}Na reaction [2.37.3]. The disadvantage is the need to chemically separate ^{22}Na from the magnesium target.

Excitation functions

The excitation functions for ^{22}Na are shown in Figs 2.37.1–2.37.3.

Thick target yields of ^{22}Ne(p, n)^{22}Na

Energy (MeV)	^{22}Na yield (μCi/(μA·h))	^{22}Na yield (MBq/(μA·h))
17 → 0	10.9	405
11 → 0	5.97	221

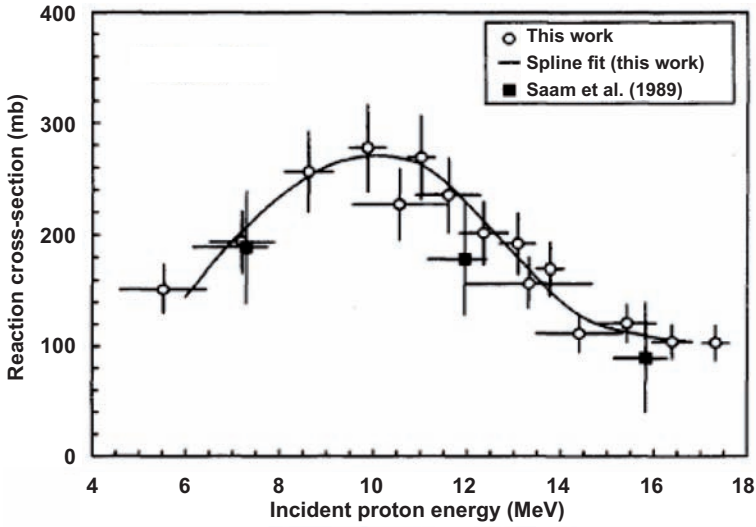

FIG. 2.37.1. Excitation function for the $^{22}Ne(p, n)^{22}Na$ reaction (from Ref. [2.37.2]; 'this work' in the inset refers to Ref. [2.37.2]).

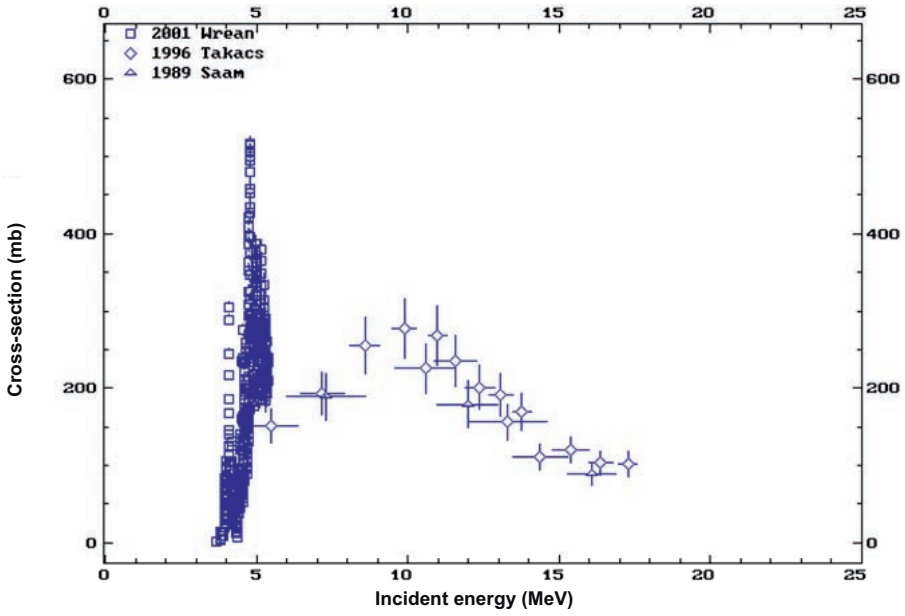

FIG. 2.37.2. Excitation function for the $^{22}Ne(p, n)^{22}Na$ reaction.

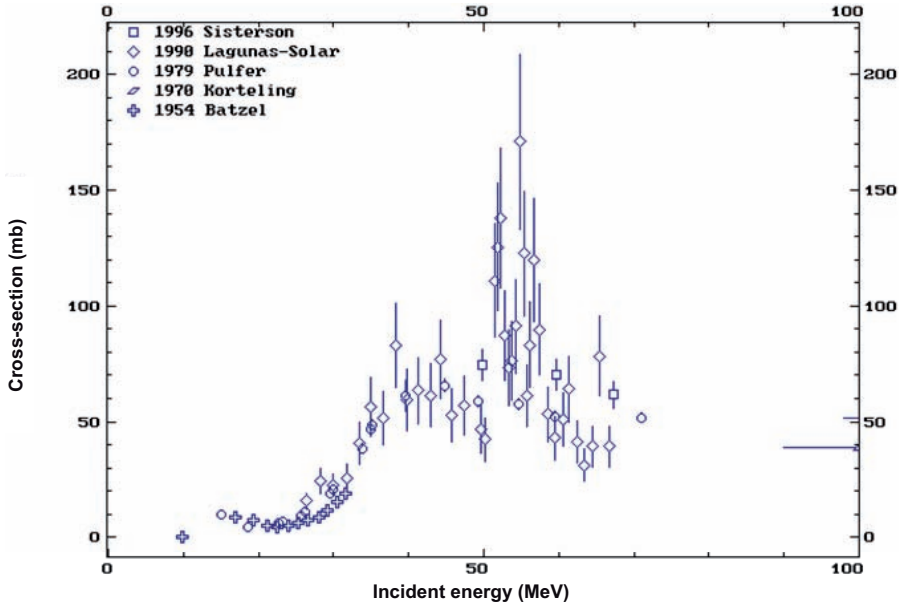

FIG. 2.37.3. Excitation function for the $^{nat}Mg(p, x)^{22}Na$ reaction.

Thick target yields of $^{nat}Mg(p, x)^{22}Na$

Energy (MeV)	^{22}Na yield (μCi/(μA·h))	^{22}Na yield (kBq/(μA·h))
22 → 5	0.45	16.5
67.5 → 40	8.3	307

Target materials

Depending upon the quantity of ^{22}Ne desired, natural enrichment neon can be used or neon enriched in the isotope 22 to whatever level is desired. If, however, enriched neon is used, then the target material should be recovered via cryogenic trapping. However, because of the low boiling point of neon (T_b = 27 K), liquid helium would probably be required.

Target preparation

If natural enrichment neon is used, then the target charge simply comes from the high pressure cylinder. In using enriched material, a recycling system should be used where the target chamber is charged with the desired quantity of neon and recovered after irradiation.

Target processing

At EOB, the neon is either released or trapped (see above), and the target walls can be washed with a very dilute solution of NaOH to recover the ^{22}Na. The target chamber can be made from aluminium, although materials such as niobium would probably be preferred.

Recovery of enriched materials

If enriched neon is used, then the target material should be recovered via cryogenic trapping. However, because of the low boiling point of neon (T_b = 27 K), liquid helium would probably be required.

Specifications

See target processing above. The ^{22}Na should be ready for use following a simple washing procedure from the target. Gamma ray spectroscopy will clearly identify ^{22}Na with its positron annihilation peak and the photon at 1275 keV.

REFERENCES TO SECTION 2.37

[2.37.1] GONZALES-LEPERA, C., "Production of long-lived radioisotopes and its application to calibration sources for PET cameras", Targetry and Target Chemistry (Proc. 5th Int. Workshop Brookhaven, 1993), Rep. BNL-61149, Brookhaven Natl Lab., Upton, NY (1994) 26.

[2.37.2] TAKÁCS, S., TÁRKÁNYI, F., QAIM, S.M., Excitation function of ^{22}Ne(p, n)^{22}Na reaction: Possibility of production of ^{22}Na at a small cyclotron, Appl. Radiat. Isot. **47** (1996) 303–307.

[2.37.3] BODEMANN, R., et al., Production of residual nuclei by proton-induced reactions on C, N, O, Mg, Al and Si, Nucl. Instrum. Methods Phys. Res. B **82** (1993) 9–31.

BIBLIOGRAPHY TO SECTION 2.37

BATZEL, R.E., COLEMAN, G.H., Cross sections for formation of ^{22}Na from aluminium and magnesium bombarded with protons, Phys. Rev. **93** (1954) 280–282.

BIMBOT, R., GAUVIN, H., Réactions de spallation de noyaux légers induites par des protons de 50, 100 et 153 MeV, Compt. Rend. **273** (1971) 1054–1057.

BRITS, R.J.N., TOERIEN, F., VON, S., The separation of ^{22}Na from Mg by cation exchange on a macroporous resin, Appl. Radiat. Isot. **39** (1988) 1045–1050.

FURUKAWA, M., KUME, S., OGAWA, M., Excitation functions for the formation of ^{7}Be and ^{22}Na in proton induced reactions on ^{27}Al, Nucl. Phys. **69** (1965) 362–368.

FURUKAWA, M., SHIZURI, K., KOMURA, K., SAKAMOTO, K., TANAKA, S., Production of ^{26}Al and ^{22}Na from proton bombardment of Si, Al and Mg, Nucl. Phys. A **174** (1971) 539–544.

GUSAKOW, M., Des réactions (p, pn) a moyenne énergie, Ann. Phys. (Les Ulis) **7** (1962) 67.

HINTZ, N.M., RAMSEY, N.F., Excitation functions to 100 MeV, Phys. Rev. **88** (1952) 19–27.

JACOBS, G., LISKIEN, H., Energy spectra of neutrons produced by alpha-particles in thick targets of light elements, Ann. Nucl. Energy **10** (1978) 541–552.

KORTELING, R.G., CARETTO, J.R., A systematics of ^{24}Na and ^{22}Na production with 400 MeV protons, J. Inorg. Nucl. Chem. **29** (1967) 2863–2878.

LAGUNAS-SOLAR, M.C., Radionuclide production on a >70 MeV proton accelerator: Current and future prospects, Nucl. Instrum. Methods Phys. Res. B **69** (1992) 452–462.

LAGUNAS-SOLAR, M.C., CARVACHO, O.F., Cyclotron production of PET radionuclides: ^{18}F (109.77 min; beta+ 96.9%; EC 3.1%) from high-energy protons on natural magnesium targets, Int. J. Appl. Radiat. Isot. **41** (1990) 349–353.

MEADOWS, J.W., HOLT, R.B., Excitation functions for proton reactions with sodium and magnesium, Phys. Rev. **83** (1951) 47–49.

MIYANO, K., The ^{7}Be, ^{22}Na and ^{24}Na production cross sections with 22 to 52 MeV protons on ^{27}Al, J. Phys. Soc. Jpn. **34** (1973) 853–856.

NORMAN, E.B., CHUPP, T.E., LESKO, K.T., GRANT, P.J., WOODRUFF, G.L., ^{22}Na production cross section from the ^{19}F(α, n) reaction, Phys Rev. C **30** (1984) 1339–1340.

Proceedings of the Workshops on Targetry and Target Chemistry, http://www.triumf.ca/wttc/proceedings.html

ROEHM, H.F., VERWEY, C.J., STEYN, J., RAUTENBACH, W.L., Excitation functions for the ^{24}Mg(d, α)^{22}Na, ^{26}Mg(d, α)^{24}Na and ^{27}Al(d, αp)^{24}Na reactions, J. Inorg. Nucl. Chem. **31** (1969) 3345–3356.

SAAM, B., SKALSEY, M., VAN HOUSE, J., Measurement of the cross section ^{22}Ne(p, n)^{22}Na, Phys. Rev. C **40** (1989) R1563–R1566.

TÁRKÁNYI, F., SZELECSÉNYI, F., TAKÁCS, S., Determination of effective bombarding energies and fluxes using improved stacked-foil technique, Acta Radiol. Suppl. **376** (1992) 72.

UNITED STATES NATIONAL NUCLEAR DATA CENTER, Decay Radiation Database, http://www.nndc.bnl.gov/nudat2/indx_dec.jsp

WALTON, J.R., HEYMANN, D., YANIV, A., Cross sections for He and Ne isotopes in natural Mg, Al, and Si, He isotopes in CaF_2, Ar isotopes in natural Ca, and radionuclides in natural AlI, Si, Ti, Cr and stainless steel induced by 12 to 45 MeV protons, J. Geophys. Res. **81** (1976) 5689–5699.

WALTON, J.R., YANIV, A., HEYMANN, D., He and Ne cross sections on natural Mg, Al and Si targets and radionuclide cross sections in natural Si, Ca, Ti and Fe targets bombarded with 14 to 45 MeV protons, J. Geophys. Res. **78** (1973) 6428–6442.

2.38. STRONTIUM-82/RUBIDIUM-82 GENERATOR SYSTEM

Half-lives

The half-life of ^{82}Sr is 25 d and that of ^{82}Rb is 1.25 min.

Uses

Cardiac PET with generator produced ^{82}Rb provides information for optimal diagnosis and management of cardiac diseases. This information includes: accurate non-invasive diagnosis of coronary artery disease in asymptomatic or symptomatic patients, non-invasive assessment of the severity of coronary stenosis, myocardial infarction imaging, myocardial viability, collateral function and cardiomyopathy.

Decay mode

Strontium-82 decays via electron capture, while the daughter, ^{82}Rb, decays through positron emission and electron capture.

Photon emission products of ^{82}Sr

Fraction	Energy (MeV)
1.92	0.511
0.09	0.777

Note: Maximum β^+ energy is 3.18 MeV.

Nuclear reactions

The only viable nuclear reaction for the production of ^{82}Sr using protons is the high energy reaction of metallic rubidium, ^{85}Rb(p, 4n)^{82}Sr. Some other reactions use ^{3}He and alpha particles.

Excitation functions

The excitation functions for ^{85}Rb(p, 4n)^{82}Sr and ^{82}Kr(^{3}He, 3n)^{82}Sr are shown in Figs 2.38.1 and 2.38.2, respectively.

Target materials

The target material is rubidium metal of natural abundance.

Target preparation

Target containers are prepared from stainless steel (SS-316) to enclose a hole measuring 2.22 cm in diameter and 1.3 cm in thickness, covered with 0.13 mm thick stainless steel windows and assembled by TIG welding. A male connector (Swagelok) is welded into the side of each target, providing a means to check for leaks and fill the target frame with molten rubidium. Protons with an incident energy of about 60 MeV and a current of 30–80 μA can be used to bombard the target until the desired integrated current is reached. The targets are set aside for one week to allow for decay of short lived species [2.38.1] prior to processing.

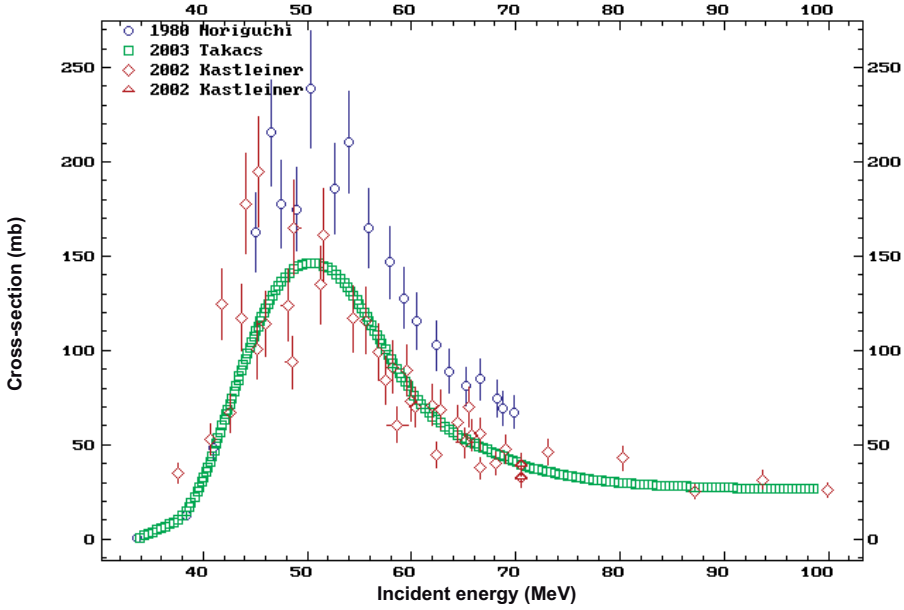

FIG. 2.38.1. Excitation function for the $^{85}Rb(p, 4n)^{82}Sr$ reaction.

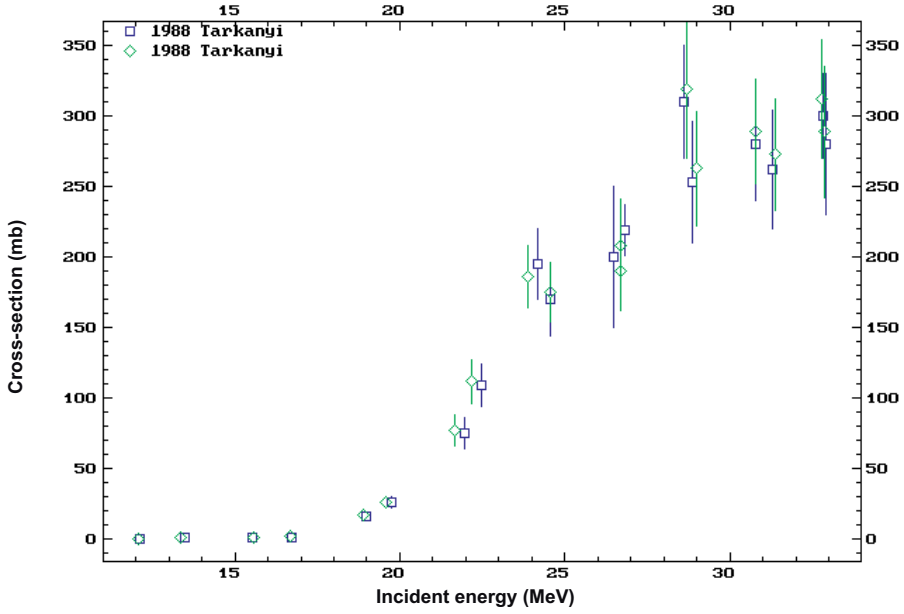

FIG. 2.38.2. Excitation function for the $^{82}Kr(^{3}He, 3n)^{82}Sr$ reaction.

Preparation of the generator

Strontium-82 in 0.1N HCL with a concentration of less than 50 mCi is mixed with 15 mL of 0.5M Tris buffer at pH7.5. Using a remote syringe, the ^{82}Sr is withdrawn into the shielded syringe of the isolator with a 19G sterile spinal needle. The ^{82}Sr solution is then pumped from the isolator through the generator column at a flow rate of 2 mL/h. After the generator column has been loaded with ^{82}Sr, the column is purged with 500 mL of 0.9% NaCl at a moderate flow rate of 0.5 mL/min. Washing the column with a large volume of saline is intended to remove any possible impurities contained in the ^{82}Sr stock solution.

Specifications

The most important contaminant is ^{85}Sr ($T_{1/2}$ = 64.8 d). The (p, xn) reaction on natural rubidium at 48–60 MeV produces about 0.4 times as much ^{85}Sr as ^{82}Sr at the EOB. The ratio increases with time due to the longer half-life of ^{85}Sr. The ratio ^{85}Sr/^{82}Sr must not exceed 5.0 if the generators are for human use. This ratio is exceeded about 150 days after EOB. Generators can thus be prepared from ^{82}Sr for several months after production using natural rubidium targets. The shelf life for a particular generator would, of course, depend upon the time after EOB at which the generator was prepared. Typically, the quantity of ^{82}Rb available from the generator would be the limiting factor, rather than the contamination [2.38.2].

The ^{82}Sr/^{82}Rb generators are eluted with sterile and pyrogen-free 0.9% NaCl. In addition to the customary quality assessment of a radiopharmaceutical preparation, it is essential to assess the radionuclidic purity (^{82}Sr and ^{85}Sr breakthrough). The ^{82}Sr/^{82}Rb ratio limit established should be 0.02 mCi/mCi. The limit of the ^{85}Sr/^{82}Rb ratio is 0.2 mCi/mCi.

REFERENCES TO SECTION 2.38

[2.38.1] CACKETTE, M.R., RUTH, T.J., VINCENT, J.S., ^{82}Sr production from metallic Rb targets and development of an ^{82}Rb generator system, Appl. Radiat. Isot. **44** (1993) 917–922.

[2.38.2] ALVAREZ-DIEZ, T.M., DEKEMP, R., BEANLANDS, R., VINCENT, R.J., Manufacture of strontium-82/rubidium-82 generators and quality control of rubidium-82 chloride for myocardial perfusion imaging in patients using positron emission tomography, Appl. Radiat. Isot. **50** (1999) 1015–1023.

BIBLIOGRAPHY TO SECTION 2.38

BUTHELEZI, E.Z., NORTIER, F.M., SCHROEDER, I.W., Excitation functions for the production of ^{82}Sr by proton bombardment of ^{nat}Rb at energies up to 100 MeV, Appl. Radiat. Isot. **64** (2006) 915–924.

DEPTULA, C., et al., Excitation function and yields for medically important generators Sr-82→Rb-82, Xe-123→I-123 and Bi-201→Pb-201→Tl-201 obtained with 100 MeV protons, Nucleonika **35** (1990) 3.

HORIGUCHI, T., et al., Excitation functions of proton induced nuclear reactions on ^{85}Rb, Int. J. Appl. Radiat. Isot. **31** (1980) 141.

IDO, T., et al., Excitation functions of proton induced nuclear reactions on ^{nat}Rb from 30 to 70 MeV — Implication for the production of ^{82}Sr and other medically important Rb and Sr radioisotopes, Nucl. Instrum. Methods Phys. Res. B **194** (2002) 369–389.

INTERNATIONAL ATOMIC ENERGY AGENCY, Charged Particle Cross-section Database for Medical Radioisotope Production: Diagnostic Radioisotopes and Monitor Reactions, IAEA-TECDOC-1211, IAEA, Vienna (2001).

KASTLEINER, S.M., et al., Excitation functions of ^{85}Rb(p, xn)^{85m,g,83,82,81}Sr reactions up to 100 MeV: Integral tests of cross section data, comparison of production routes of ^{83}Sr and thick target yield of ^{82}Sr, Appl. Radiat. Isot. **56** (2002) 685–695.

LAGUNAS-SOLAR, M.C., Radionuclide production with >70-MeV proton accelerators: Current and future prospects, Nucl. Instrum. Methods Phys. Res. B **69** (1992) 452.

QAIM, S.M., et al., Yield and purity of ^{82}Sr produced via the ^{nat}Rb(p, xn)^{82}Sr process, Appl. Radiat. Isot. **65** (2007) 247–252.

SYLVESTER, P., MÖLLER, T., ADAMS, T.W., CISAR, A., New ion exchange materials for use in a ^{82}Sr/^{82}Rb generator, Appl. Radiat. Isot. **61** (2004) 1139–1145.

TAKÁCS, S., TÁRKÁNYI, F., HERMANNE, A., PAVIOTTI DE CORCUERA, R., Validation and upgrade of the recommended cross section data of charged particle reactions used for production PET radioisotopes, Nucl. Instrum. Methods Phys. Res. B **211** (2003) 169.

TÁRKÁNYI, F., QAIM, S.M., STÖCKLIN, G., Excitation functions of high-energy He-3 and alpha-particle induced nuclear reactions on natural krypton with special reference to the production of Sr-82, Appl. Radiat. Isot. **41** (1990) 91–95.

2.39. TECHNETIUM-94m

Half-life

Technetium-94m has a half-life of 52 min and decays 72% by positron emission and 28% by electron capture. The end point energy of the positron is 2.47 MeV. Technetium-94m decays to the ^{94}Tc ground state, which has a half-life of 153 min and decays via both positron emission (11%) and electron capture (89%) to stable ^{94}Mo [2.39.1, 2.39.2]. The fact that it can be directly substituted for ^{99m}Tc gives this isotope great potential utility for PET. The drawback is the radiation dose associated with this isotope, which is 7 times greater than that for ^{99m}Tc [2.39.1].

Beta$^+$ rays

The total intensity of β^+ rays is 70.2%.

Parent nucleus	Parent half-life (min)	Decay mode	Daughter nucleus
Tc-94m	52.0	β^+: 100%	Mo-94

Positron emission products of ^{94m}Tc

Fraction	Energy (keV)	End point energy (keV)
0.0099	639.3	1445
0.676	1094.2	2438

Note: Mean β^+ energy: 1072 keV; total β^+ intensity: 70.2%.

Electron emission products of ^{94m}Tc

Fraction	Energy (keV)
0.288	2.27
0.0606	14.8

Photon emission products of ^{94m}Tc

Fraction	Energy (keV)
0.0114	2.29
0.0583	17.374
0.111	17.479
0.0172	19.607
1.404	511
0.942	871.05
0.0221	993.19
0.045	1522.1
0.057	1868.68
0.035	2740.1
0.0138	3129.1

Nuclear reactions for production of ^{94m}Tc

Nuclear reaction	Useful energy range (MeV)	Natural abundance (%)	References
^{94}Mo(p, n)^{94m}Tc	10–15	9.25	[2.39.3]
^{96}Mo(p, 3n)^{94m}Tc	25–40	16.68	[2.39.4]
^{92}Mo(α, pn)^{94m}Tc	20–30	14.82	[2.39.5, 2.39.6]
^{92}Mo(α, 2n)^{94}Ru: ^{94m}Tc	20–30	14.82	[2.39.5, 2.39.6]
^{93}Nb(α, 3n)^{94m}Tc	25–40	100	[2.39.1]
^{93}Nb(^{3}He, 2n)^{94m}Tc	35–45	100	[2.39.1, 2.39.7]

Excitation function

The excitation function for ^{94}Mo(p, n)^{94m}Tc is shown in Fig. 2.39.1.

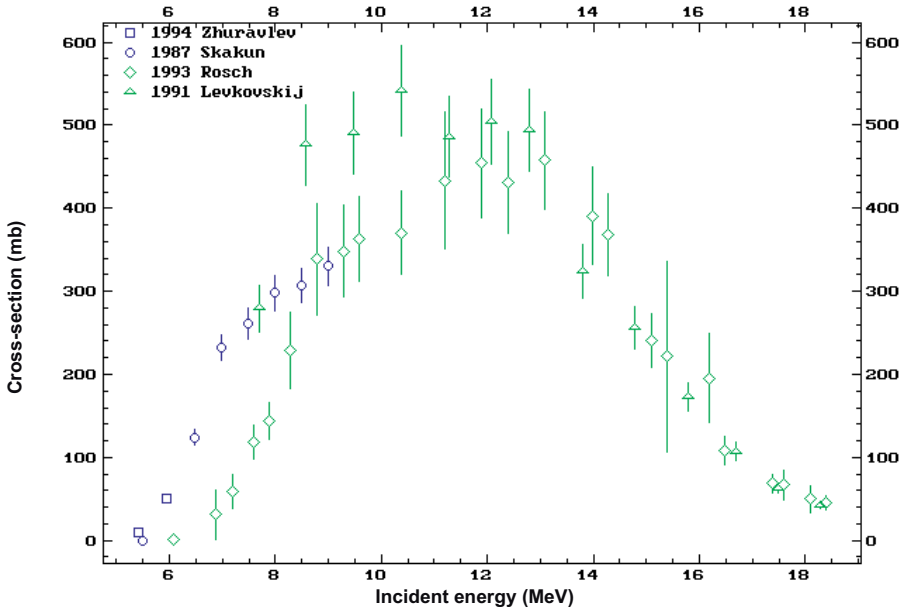

FIG. 2.39.1. Excitation function for the ^{94}Mo(p, n)^{94m}Tc reaction.

REFERENCES TO SECTION 2.39

[2.37.1] CHRISTIAN, B.T., NICKLES, R.J., STONE, C.K., MULNIX, T.L., CLARK, J., Improving the radionuclidic purity of ^{94m}Tc for PET imaging, Appl. Radiat. Isot. **46** (1995) 69–73.

[2.37.2] QAIM, S.M., Production of high purity ^{94m}Tc for positron emission tomography studies, Nucl. Med. Biol. **27** (2000) 323–328.

[2.37.3] RÖSCH, F., QAIM, S.M., Nuclear data relevant to the production of the positron emitting technetium isotope ^{94m}Tc via the ^{94}Mo(p, n)-reaction, Radiochim. Acta **62** (1993) 15–121.

[2.37.4] HOGAN, J.J., Comparison of the ^{94}Mo(p, n)^{94}Tc^{m,g} and ^{96}Mo(p, n)^{96}Tc^{m,g} reactions, J. Inorg. Nucl. Chem. **35** (1975) 2123–2125.

[2.37.5] GRAF, H.P., MUNZEL, H., Excitation functions for α-particle reactions with molybdenum isotopes, J. Inorg. Nucl. Chem. **36** (1974) 3647.

[2.37.6] DENZLER, F.-O., RÖSCH, F., QAIM, S.M., Excitation functions of α-particle induced nuclear reactions on highly enriched ^{92}Mo: Comparative evaluation of production routes for ^{94m}Tc, Radiochim. Acta **68** (1995) 13–20.

[2.37.7] FASSBENDER, M., NOVGORODOV, A.F., RÖSCH, F., QAIM, S.M., Excitation functions of ^{93}Nb(^{3}He, xn)^{93m,g,94m,g,95m,g}Tc-processes from threshold up to 35 MeV: Possibility of production of ^{94m}Tc in high radiochemical purity using a thermochromatographic separation technique, Radiochim. Acta **65** (1994) 215–221.

BIBLIOGRAPHY TO SECTION 2.39

BONARDI, M., BIRATTARI, C., GROPPI, F., SABBIONI, E., Thin-target excitation functions, cross-sections and optimised thick-target yields for ^{nat}Mo(p, xn)$^{(94g,95m,95g,96(m+g))}$Tc nuclear reactions induced by protons from threshold up to 44 MeV: No carrier added radiochemical separation and quality control, Appl. Radiat. Isot. **57** (2002) 617–635.

CHRISTIAN, B.T., NICKLES, R.J., STONE, C.K., Producing Tc-94m from isotopically enriched [^{94}Mo]MoO_3, J. Nucl. Med. **34** (1993) 248.

RÖSCH, F., NOVGORODOV, A.F., QAIM, S.M., Thermochromatographic separation of ^{94m}Tc from enriched molybdenum targets and its large scale production for nuclear medicine application, Radiochim. Acta **64** (1994) 113–120.

TAKÁCS, S., TÁRKÁNYI, F., HERMANNE, A., PAVIOTTI DE CORCUERA, R., Validation and upgrade of the recommended cross section data of charged particle reactions used for production PET radioisotopes, Nucl. Instrum. Methods Phys. Res. B **211** (2003) 169–189.

2.40. THALLIUM-201

Half-life: 73.06 h.

Uses

The thallium stress test has become one of the more widely used nuclear medicine diagnostic tests in recent years. Imaging with ^{201}Tl facilitates a functional assessment of the myocardium. This allows an assessment of the extent of damage after a heart attack or from chronic heart disease [2.40.1].

Decay mode

Thallium-201 decays by electron capture with the emission of gamma rays at 167 and 135 keV, which are ideal for use in gamma cameras [2.40.2–2.40.4].

Electron emission products of ^{201}Tl

Fraction	Energy (MeV)
0.001960	0.166630
0.002400	0.082778
0.003922	0.131780
0.006100	0.163870
0.012747	0.120500
0.021736	0.028628
0.025300	0.027038
0.026200	0.152590
0.033207	0.053800
0.070180	0.017351
0.074730	0.052238
0.081400	0.015761
0.113000	0.000770
0.154000	0.084328
0.725060	0.007600

Photon emission products of ^{201}Tl

Fraction	Energy (MeV)
0.001600	0.165880
0.002200	0.030600
0.002200	0.032190
0.026500	0.135340
0.100000	0.167430
0.204650	0.080300
0.273570	0.068895
0.444390	0.009990
0.465250	0.070819

Nuclear reactions for production of ^{201}Tl

There is only one reaction commonly used to produce ^{201}Tl, i.e. the ^{203}Tl(p, 3n)^{201}Pb $\rightarrow$ ^{201}Tl reaction on enriched ^{203}Tl.

Excitation function

The excitation function for ^{203}Tl(p, 3n)^{201}Pb is shown in Fig. 2.40.1.

Target material

The target material is enriched ^{203}Tl.

Target preparation

The preferred process for target preparation is electrochemical deposition. Details of this process are given in Ref. [2.40.5].

Target processing

Thallium-201 produced via the ^{203}Tl(p, n)^{201}Pb $\rightarrow$ ^{201}Tl reaction entails target processing in two stages. The first stage involves separation of ^{201}Pb from

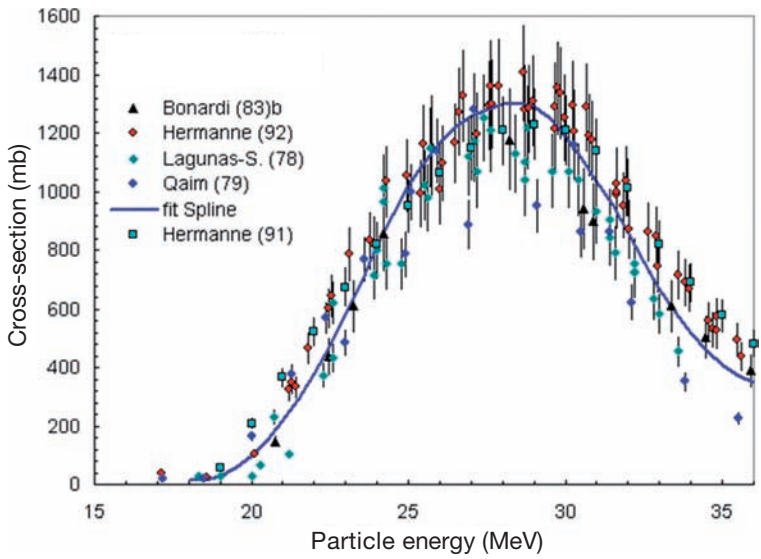

FIG. 2.40.1. Excitation function for the ^{203}Tl(p, 3n)^{201}Pb reaction.

^{203}Tl target material, and the second stage involves separation of ^{201}Tl from ^{201}Pb after a waiting period of about 32 hours for the growth of ^{201}Tl. These separations are generally achieved using ion exchange resins or solvent/solvent extraction. The detailed procedure for this extraction is described in Ref. [2.40.5].

Recovery of enriched materials

Recovery of ^{201}Tl can be achieved by either the chemical method or the electrodeposition method.

Specifications

The radionuclidic purity is measured by multichannel pulse–height analysis, using a gamma spectrometer. The gamma spectrum of the ^{201}TlCl solution was also followed for approximately one week, to confirm the half-lives of the product and of the main impurities. The main gamma peaks are the X rays (70.8 and 80.2 keV) and photons (135 and 167 keV) of ^{201}Tl, the photons (368 keV) of ^{200}Tl and the photons (439 keV) of ^{202}Tl.

Radiochemical purity

The radiochemical purity of ^{201}Tl is checked by ascending paper chromatography to differentiate Tl^{+} and Tl^{3+}. Whatman 3MM paper and a solvent, 10% ($Na_2HPO_4 \cdot 5H_2O$) and 90% (acetone), are used [2.40.6].

Chemical purity

The hydrazine level in the ^{201}Tl solution is determined by spectrophotometric adsorption analysis, using a calibration curve in accordance with the method of Novak and Hlatky [2.40.6, 2.40.7].

REFERENCES TO SECTION 2.40

[2.40.1] WEINER, R.E., THAKUR, M.L., Metallic radionuclides: Applications in diagnostic and therapeutic nuclear medicine, Radiochim. Acta **70/71** (1995) 273–287.
[2.40.2] BELGRAVE, E., LEBOWITZ, E., Development of ^{201}Tl for medical use, J. Nucl. Med. **13** (1972) 781.
[2.40.3] LEBOWITZ, E., et al., ^{201}Tl for medical use, J. Nucl. Med. **14** (1973) 421–422.

[2.40.4] LEBOWITZ, E., et al., Thallium-201 for medical use, J. Nucl. Med. **16** (1975) 151–155.
[2.40.5] INTERNATIONAL ATOMIC ENERGY AGENCY, Standardized High Current Solid Targets for Cyclotron Production of Diagnostic and Therapeutic Radionuclides, Technical Reports Series No. 432, IAEA, Vienna (2004) CD-ROM.
[2.40.6] FERNANDES, L., GONÇALVES DA SILVA, C.P., Quality control of ^{201}TlCl solution obtained at IPEN-CNEN/SP, J. Radioanal. Nucl. Chem. **172** (1993) 313–318.
[2.40.7] NOVAK, M., HLATKY, J., Determination of flow concentrations of hydraxzine in waters of both the primary and secondary circuits of NPPs with VVER, J. Radioanal. Nucl. Chem. **126** (1988) 337–344.

BIBLIOGRAPHY TO SECTION 2.40

ASHOK RAO, K., ACHARYA, B.V., MURALIDHAR, N., RANGAMANNAR, B., Separation of Tl/III/ from Tl/I/, J. Radioanal. Nucl. Chem. **94** (1985) 351–355.

BLUE, J.W., LIU, D.C., SMATHERS, J.B., Thallium-201 production with the idle beam from neutron therapy, Med. Phys. **5** (1978) 532–535.

DE BRITTO, J.L.Q., BRAGHIROLLI, A.M.S, DA SILVA, A.G., A new production method for carrier-free ^{201}Tl using IEN's cyclotron in Rio de Janeiro, J. Radioanal. Nucl. Chem. Lett. **96** (1985) 181–186.

INTERNATIONAL ATOMIC ENERGY AGENCY, Charged Particle Cross-section Database for Medical Radioisotope Production: Diagnostic Radioisotopes and Monitor Reactions, IAEA-TECDOC-1211, IAEA, Vienna (2001).

KOZLOVA, M.D., et al., New method of ^{201}Tl production from ^{203}Tl-targets, Int. J. Radiat. Appl. Instrum. A, Appl. Radiat. Isot. **38** (1987) 1090–1091.

MALININ, A.B., et al., Production of 'no-carrier-added' ^{201}Tl, Int. J. Appl. Radiat. Isot. **35** (1981) 685–687.

QAIM, S.M., WEINREICH, R., OLLIG, H., Production of ^{201}Tl and ^{203}Pb via proton induced nuclear reactions on natural thallium, Int. J. Appl. Radiat. Isot. **30** (1979) 85–95.

REDDY, A.S., REDDY, M.L.P., Solvent extraction separation of In/III/-Tl/III/ and Hg/II/-Cd/II/-Co/II/ with sulphoxides, J. Radioanal. Nucl. Chem. **87** (1984) 397–403.

TAKÁCS, S., TÁRKÁNYI, F., HERMANNE, A., Validation and upgrading of the recommended cross-section data of charged particle reactions: Gamma emitter radioisotopes, Nucl. Instrum. Methods Phys. Res. B **240** (2005) 790–802.

2.41. TUNGSTEN-178

Half-life: 21.6 d.

Parent nucleus	Parent energy level	Parent half-life (d)	Decay mode	Daughter nucleus
W-178	0.0	21.6	EC: 100%	Ta-178

Electron emission products of ^{178}W

Fraction	Energy (keV)
0.542	6.35
0.0125	46.2

Photon emission products of ^{178}W

Fraction	Energy (keV)
0.203	8.15
0.071	56.28
0.123	57.535
0.0138	64.948
0.0268	65.222

Excitation function

The excitation function for ^{181}Ta(p, 4n)^{178}W is shown in Fig. 2.41.1.

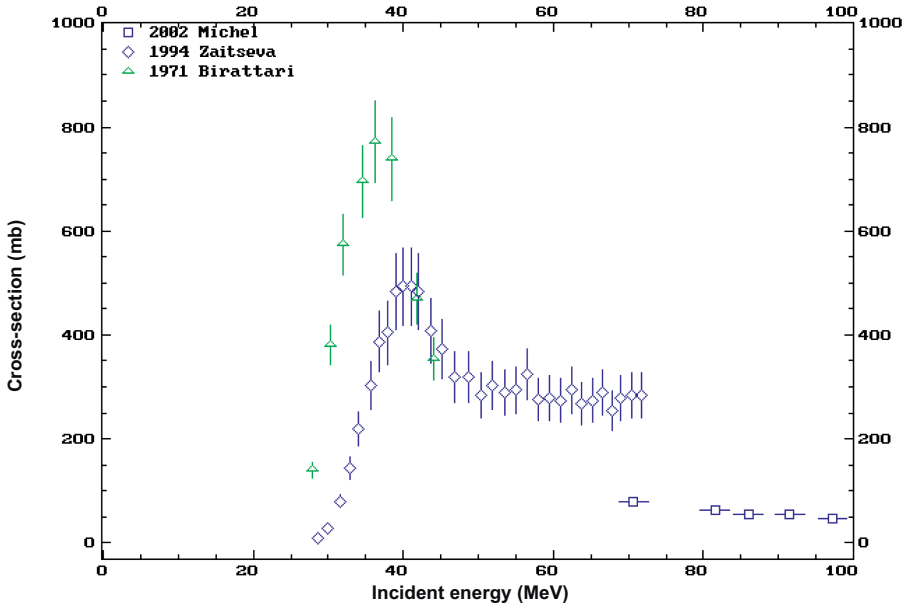

FIG. 2.41.1. Excitation function for the ^{181}Ta(p, 4n)^{178}W reaction.

BIBLIOGRAPHY TO SECTION 2.41

BIRATTARI, C., et al., (p, xn) Reactions induced in Tm-169, Ta-181 and Bi-209 with 20 to 45 MeV protons, Nucl. Phys. A **166** (1971) 605–623.

MICHEL, R., et al., Cross sections for the production of radionuclides by proton-induced reactions on W, Ta, Pb and Bi from thresholds up to 2.6 GeV, Nucl. Sci. Technol. Tokyo, Suppl. **2** (2002) 242.

ZAITSEVA, N.G., RURARZ, E., KHALKIN, V.A., STEGAILOV, V.I., POPINENKOVA, L.M., Excitation function for W-178 production in the Ta-181(p, 4n)W-178 reaction over proton energy range 28.8–71.8 MeV, Radiochim. Acta **64** (1994) 1–6.

2.42. VANADIUM-48

Half-life

Vanadium-48 has a half-life of 16 d and 50% of its decay is by positron emission. It has two high abundance gamma rays, one at 984 keV and the other at 1312 keV. It has non-medical uses and has been suggested as an alternative for the ^{68}Ge/^{68}Ga generator system for calibrating PET instruments [2.42.1].

Parent nucleus	Parent energy level	Parent half-life (d)	Decay mode	Daughter nucleus
V-48	0.0	15.9735	EC: 100%	Ti-48

Positron emission products of ^{48}V

Fraction	Energy (keV)	End point energy (keV)
0.499	290.3	694.7

Note: Mean β^+ energy: 295 keV; total β^+ intensity: 50.3%; mean β^+ dose: 0.148 MeV/(Bq·s).

Electron emission products of ^{48}V

Fraction	Energy (keV)
0.748	0.42
0.348	4

Photon emission products of ^{48}V

This table is also continued on the next page.

Fraction	Energy (keV)
0.0287	4.505
0.057	4.511
1.006	511

Fraction	Energy (keV)
0.0776	944.132
1	983.521
0.975	1312.096
0.0241	2240.395

Nuclear reactions for production of ^{48}V

The reaction for production of ^{48}V is the ^{48}Ti(p, n)^{48}V reaction on natural titanium [2.42.2]. Since ^{48}Ti has a natural abundance of 73.8%, this is a good choice. Another potential reaction would be the ^{45}Sc(α, n)^{48}V reaction on natural scandium.

Excitation function

The excitation function for ^{nat}Ti(p, x)^{48}V is shown in Fig. 2.42.1.

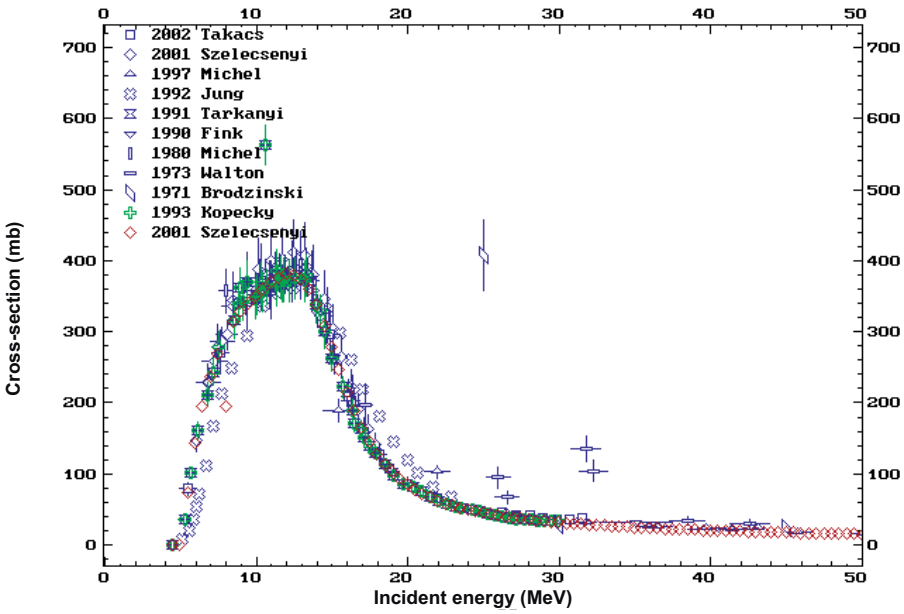

FIG. 2.42.1. Excitation function for the ^{nat}Ti(p, x)^{48}V reaction.

REFERENCES TO SECTION 2.42

[2.42.1] HICHWA, R.D., et al., Vanadium-48: A renewable source for transmission scanning with PET, Nucl. Instrum. Methods Phys. Res. B **99** (1995) 804–806.
[2.42.2] GOODMAN, C.D., ANDERSON, J.D., WONG, C., Quasi-elastic (p, n) scattering from scandium and titanium isotopes, Phys. Rev. **156** (1967) 1249–1254.

BIBLIOGRAPHY TO SECTION 2.42

KOPECKY, P., SZELECSÉNYI, F., MOLNAR, T., MIKECZ, P., TÁRKÁNYI, F., Excitation functions of (p, xn) reactions on nat-Ti: Monitoring of bombarding proton beams, Appl. Radiat. Isot. **44** (1993) 687–692.

MICHEL, R., et al., Cross sections for the production of residual nuclides by low- and medium-energy protons from the target elements C, N, O, Mg, Al, Si, Ca, Ti, V, Mn, Fe, Co, Ni, Cu, Sr, Y, Zr, Nb, Ba and Au, Nucl. Instrum. Methods Phys. Res. B **129** (1997) 153–193.

SZELECSÉNYI, F., et al., Excitation function for the ^{nat}Ti(p, x)^{48}V nuclear process: Evaluation and new measurements for practical applications, Nucl. Instrum. Methods Phys. Res. B **174** (2001) 47.

TAKÁCS, S., TÁRKÁNYI, F., SONCK, M., HERMANNE, A., New cross sections and intercomparison of proton monitor reactions on Ti, Ni and Cu, Nucl. Instrum. Methods Phys. Res. B **188** (2002) 106.

2.43. XENON-122

Half-life: 20.1 h.

Electron emission products of ^{122}Xe

Fraction	Energy (MeV)
0.011702	0.028631
0.104310	0.023600
0.838960	0.003310

Photon emission products of ^{122}Xe

Fraction	Energy (MeV)
0.020700	0.416900
0.036800	0.148800
0.088068	0.003940
0.092000	0.350200
0.144760	0.032300
0.221830	0.028317
0.413090	0.028612

Excitation functions

The excitation functions for ^{127}I(p, 6n)^{122}Xe and ^{124}Xe(p, x)^{122}Xe are shown in Figs 2.43.1 and 2.43.2, respectively.

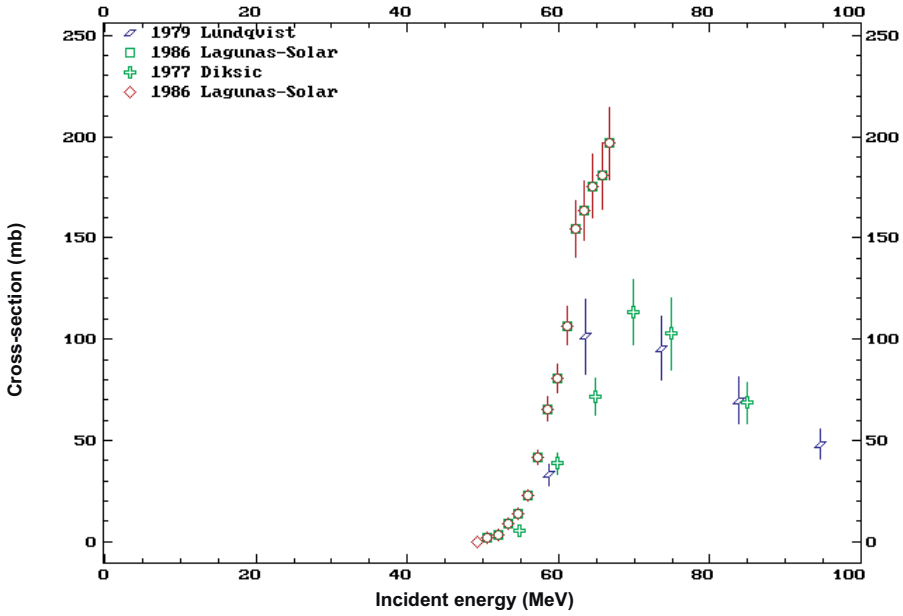

FIG. 2.43.1. Excitation function for the ^{127}I(p, 6n)^{122}Xe reaction.

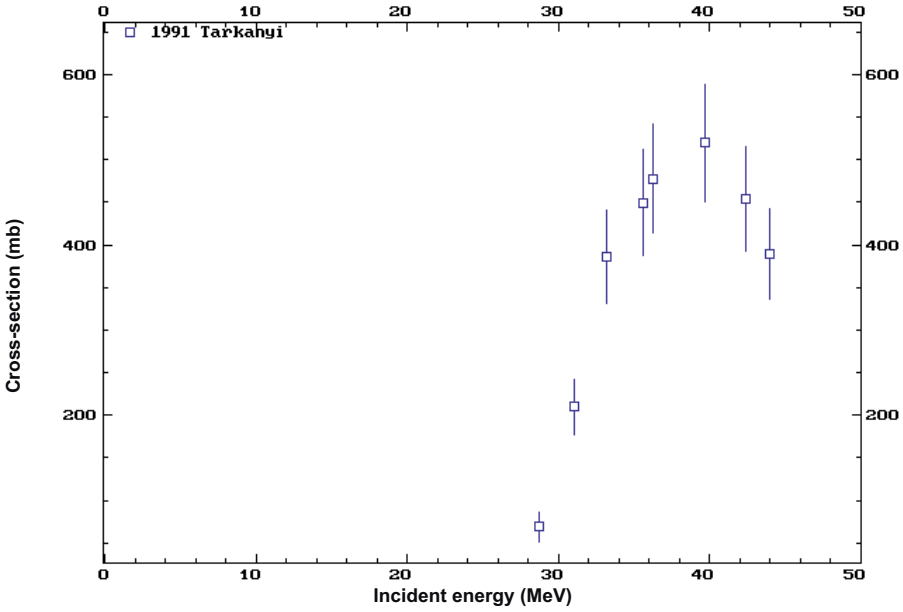

FIG. 2.43.2. Excitation function for the $^{124}Xe(p, x)^{122}Xe$ reaction.

BIBLIOGRAPHY TO SECTION 2.43

ADILBISH, M., et al., I-123 production from radioxenon formed in spallation reactions by 660 MeV protons for medical research, Int. J. Appl. Radiat. Isot. **31** (1980) 163.

DIKSIC, M., YAFFE, L., A study of I-127(p, xn) and I-127(p, pxn) reactions with special emphasis on production of Xe-123, J. Inorg. Nucl. Chem. **39** (1977) 1299.

LAGUNAS-SOLAR, M.C., CARAVACHO, O.F., HARRIS, L.J., MATHIS, C.A., Cyclotron production of ^{122}Xe (20.1 h) $\rightarrow$ ^{122}I (beta+ 77%; EC 23%; 3.6 min) for positron emission tomography: Current methods and potential developments, Appl. Radiat. Isot. **37** (1986) 835.

TÁRKÁNYI, F., QAIM, S.M., STÖCKLIN, G., SAJJAD, M., LAMBRECHT, R., Nuclear reaction cross sections relevant to the production of the Xe-122 $\rightarrow$ I-122 generator system using highly enriched Xe-124 and a medium-sized cyclotron, Appl. Radiat. Isot. **42** (1991) 229.

2.44. XENON-127

Half-life: 34.4 d.

Parent nucleus	Parent energy level	Parent half-life (d)	Decay mode	Daughter nucleus
Xe-127	0.0	36.4	EC: 100%	I-127

Electron emission products of ^{127}Xe

Fraction	Energy (keV)
0.962	3.31
0.118	23.6
0.0392	24.441
0.0154	112.083
0.0365	138.963
0.0663	169.691
0.0098	197.672

Photon emission products of ^{127}Xe

Fraction	Energy (keV)
0.097	3.94
0.251	28.317
0.462	28.612
0.0431	32.239
0.0831	32.295
0.0246	33.047
0.0122	57.61
0.0429	145.252
0.255	172.132
0.683	202.86
0.172	374.991

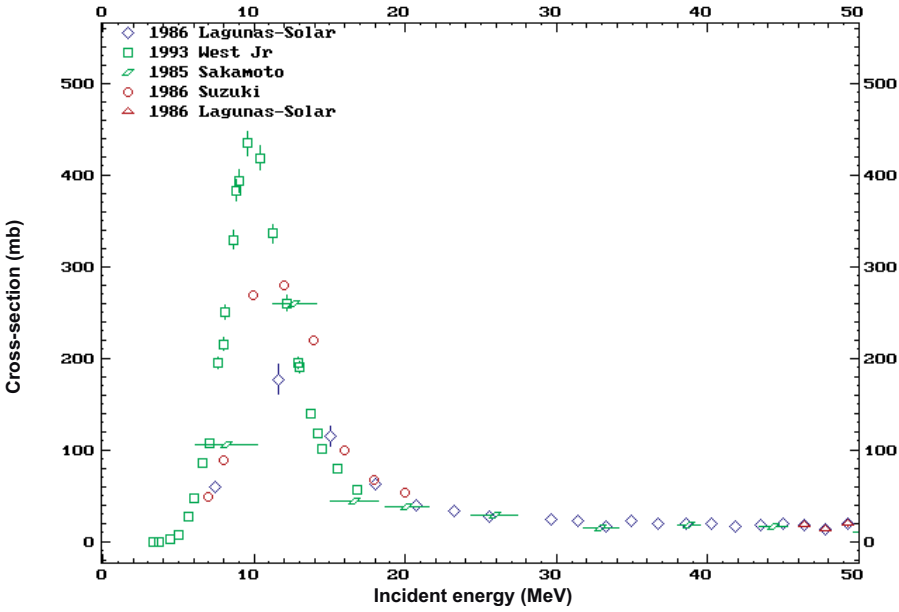

FIG. 2.44.1. Excitation function for the $^{127}I(p, n)^{127}Xe$ reaction.

Excitation function

The excitation function for $^{127}I(p, n)^{127}Xe$ is shown in Fig. 2.44.1.

BIBLIOGRAPHY TO SECTION 2.44

LAGUNAS-SOLAR, M.C., et al., Cyclotron production of high-purity ^{123}I: A revision of excitation functions, thin-target and cumulative yields for $^{127}I(p, xn)$ reactions, J. Radioanal. Chem. **65** (1986) 31.

LAGUNAS-SOLAR, M.C., CARAVACHO, O.F., HARRIS, L.J., MATHIS, C.A., Cyclotron production of ^{122}Xe (20.1 h) $\rightarrow$ ^{122}I (beta+ 77%; EC 23%; 3.6 min) for positron emission tomography: Current methods and potential developments, Appl. Radiat. Isot. **37** (1986) 835.

SAKAMOTO, K., DOHNIWA, M., OKADA, K., Excitation functions for (p, xn) and (p, pxn) reactions on natural $^{79+81}Br$, $^{85+87}Rb$, ^{127}I and ^{133}Cs up to E_p = 52 MeV, Appl. Radiat. Isot. **36** (1985) 481.

SUZUKI, K., Production of pure ^{123}I by the ^{127}I(p, 5n)^{123}Xe $\rightarrow$ ^{123}I reaction, Radioisotopes **35** (1986) 235.

WEST, H.I., Jr., et al., Bromine and iodine excitation-function measurements with protons and deuterons at 3–17 MeV, Phys. Rev. C **47** (1993) 248–259.

2.45. YTTRIUM-86

Half-life: 14.7 h.

Uses

The main use of this isotope is to quantitatively track the progress of the bone pain palliation agent ^{90}Y [2.45.1, 2.45.2].

Decay characteristics

Yttrium-86 decays 66% by electron capture and 34% by positron emission. The end point energy of the positron ranges from 3.2 to 0.4 MeV, depending on the decay mode, and several high energy gamma rays are associated with electron capture.

Positron emission products of ^{86}Y

This table is also continued on the next page.

Fraction	Maximum energy (MeV)	Average energy (MeV)
0.001980	0.888830	0.389000
0.002659	0.791000	0.355030
0.003100	0.419830	0.187000
0.003300	0.485190	0.215000
0.003710	0.605950	0.267000
0.007200	1.372600	0.603000
0.010000	2.396700	1.093000
0.012800	0.933260	0.408000
0.014100	1.195100	0.524000
0.017000	1.769000	0.783000

Fraction	Maximum energy (MeV)	Average energy (MeV)
0.020000	1.065700	0.467000
0.020000	3.174200	1.452000
0.036000	2.021100	0.899000
0.056000	1.578000	0.696000
0.124000	1.253500	0.550000

Electron emission products of ^{86}Y

Fraction	Energy (MeV)
0.180620	0.012100
0.700590	0.001790

Photon emission products of ^{86}Y (abundance >5%)

Fraction	Energy (MeV)
0.060741	0.015800
0.091575	0.645870
0.117100	0.014098
0.154280	0.703330
0.169130	0.443130
0.171600	1.854400
0.207900	1.920700
0.224400	0.777370
0.226070	0.014165
0.305250	1.153100
0.325880	0.627720
0.663700	0.511000
0.825000	1.076600

Nuclear reactions for production of ^{86}Y

The main production reactions for ^{86}Y are the proton reaction on enriched ^{86}Sr, ^{86}Sr(p, n)^{86}Y, and the ^{3}He reaction on natural rubidium, ^{nat}Rb(^{3}He, 2n)^{86}Y [2.45.3, 2.45.4]. The proton reaction can be carried out at relatively low energies (10–15 MeV). The impurity level is also lower for the proton reaction than for the ^{3}He reaction. Higher energy accelerators have another possibility available, i.e. the ^{88}Sr(p, 3n)^{86}Y reaction, which becomes important above 30 MeV [2.45.5]. If there are high energy deuterons available, the ^{nat}Sr(d, x)^{86}Y reaction is also possible [2.45.6] and gives relatively good yields at energies above 30 MeV.

Nuclear reaction	Useful energy range (MeV)	Natural abundance (%)	References
^{86}Sr(p, n)^{86}Y	6–17	9.9	[2.45.3, 2.45.4]
^{nat}Rb(^{3}He, 2n)^{86}Y	15–25	Natural	[2.45.3, 2.45.4]
^{88}Sr(p, 3n)^{86}Y	30–55	82.6	[2.45.5]
^{nat}Zr(d, x)^{86}Y	30–50	Natural	[2.45.6]

In most facilities, the low energy proton reaction will be the preferred reaction for production. The yield is higher and the impurities are lower than with some of the other possible production reactions.

Cross-sections for the ^{86}Sr(p, n)^{86}Y reaction

This table is also continued on the next page.

Energy (MeV)	Cross-section (mb)			
	Y-(86m+g)	Y-86m	Y-85g	Y-85m
6.6	6	–	–	–
7.9	323	25	–	–
8	231	25	–	–
9.2	922	133	–	–
9.2	701	139	–	–
10.3	820	171	–	–

Energy (MeV)	Cross-section (mb)			
	Y-(86m+g)	Y-86m	Y-85g	Y-85m
10.4	1016	220	–	–
11.4	814	183	–	–
11.4	930	214	–	–
12.4	778	185	–	–
12.6	1081	280	–	–
13.3	998	254	–	–
13.5	932	255	–	–
14.4	1297	324	–	28
15.3	1119	333	19	106
16.2	931	277	133	401
17	580	188	147	669

Excitation functions

The excitation functions for ^{86}Y are shown in Figs 2.45.1–2.45.3.

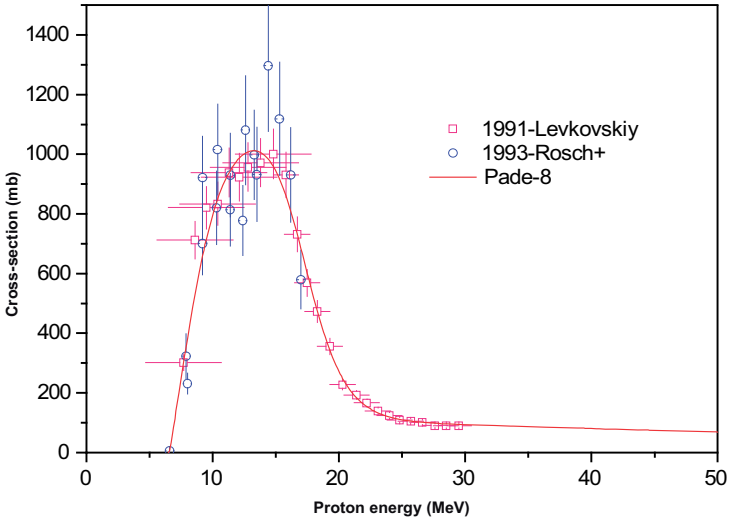

FIG. 2.45.1. Excitation function for the ^{86}Sr(p, n)^{86}Y reaction.

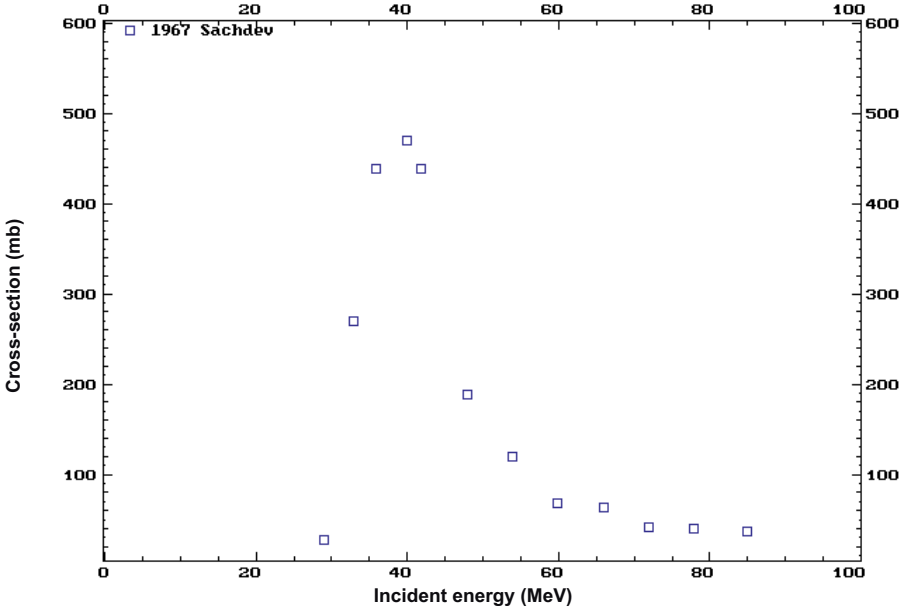

FIG. 2.45.2. Excitation function for the $^{88}Sr(p, 3n)^{86}Y$ reaction.

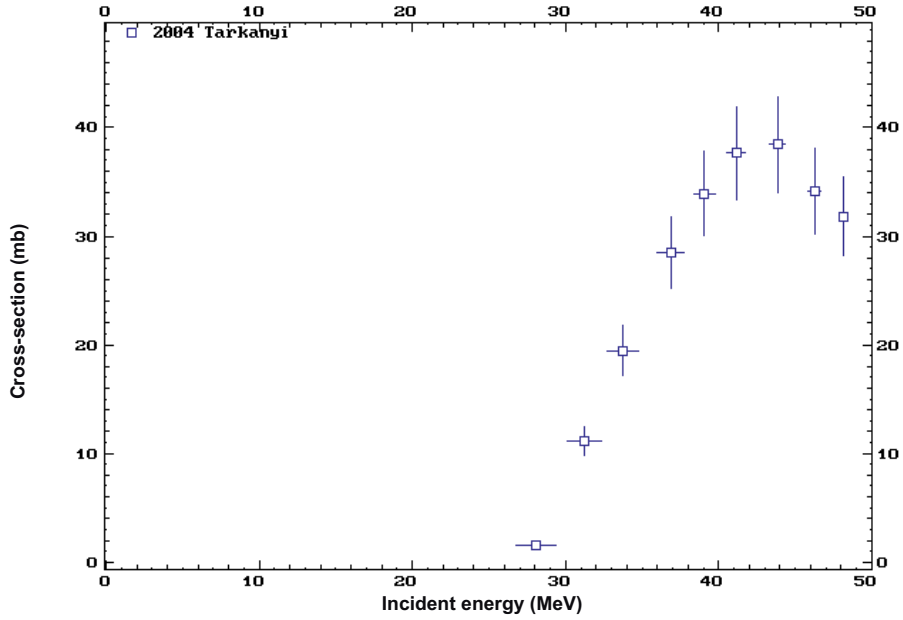

FIG. 2.45.3. Excitation function for the $^{nat}Zr(d, x)^{86}Y$ reaction.

Thick target yields

For the $^{86}Sr(p, n)^{86}Y$ reaction involving 22 MeV protons, the yield is 2.7 mCi/(μA·h) (99.9 MBq/(μA·h)).

Target materials

There are two targets that are used for production of ^{86}Y. The first is an enriched ^{86}Sr target, usually irradiated as the carbonate salt [2.45.3]. The second is a natural rubidium target using the ^{3}He reaction. This is a much less common reaction due to the requirement for a ^{3}He accelerator [2.45.3, 2.45.4].

Another method for production of ^{86}Y involves the use of a small amount of [^{86}Sr]SrO as the target material. SrO was a more effective target than the commonly used $SrCO_3$ because of its thermal stability. The method of Yoo et al. [2.45.7] shows that enriched SrO is a preferable target material, and that electrolysis can efficiently collect ^{86}Y after it has been released from the target.

Target preparation

The powder is pressed into a pellet and then placed into a target holder. In general, the target is similar to that used for the production of ^{123}I from tellurium oxide. The target material is covered with an aluminium cover foil to prevent loss of material during irradiation. A similar target is used when rubidium carbonate is the target material.

Another type of target holder is a platinum disc with a 6.4 mm diameter depression containing a grid to hold 50 mg of [^{86}Sr]SrO. The [^{86}Sr]SrO is pressed into the platinum disc at 600 lbf/in^2 (4.14 MPa) for 30 s. The disc is held in place by the cooling system vacuum. During irradiation, the disc is actively cooled by water flowing in direct contact with the back of the disc, thus allowing efficient heat removal from the substrate. When SrO is used as target material, the prepared target is kept in a vacuum desiccator until the target is placed into the target holder, because SrO is very sensitive to carbon dioxide [2.45.7].

Target processing

Separation of ^{86}Y from the target matrix can be carried out by dissolving the salt in acidic solution and then co-precipitating it with lanthanum by adding ammonia. The precipitate is dissolved and then separated on a cation exchange column [2.45.3]. The procedure has been modified by Garmestania et al. [2.45.8], as will now be described.

The target delivered from the cyclotron facility was dissolved in 3M HNO_3 (150 μL) plus 8M HNO_3 (one to two drops) and loaded on to a column (1 cm × 10 cm) of Sr(II) selective resin (strontium resin from Eichrom Technologies Inc., Darien, Illinois) pre-equilibrated with 3M HNO_3 (1 g of resin was used for each 10 mg of Sr(II) irradiated). The target holder was then washed with 3M HNO_3 (2 × 150 μL), to ensure that the radioactivity was all transferred and that this washing solution was also loaded on to the column. The ^{86}Y was eluted from the resin with 3M HNO_3 (2 mL). The eluted solution was then heated to dryness on a hot plate and under a heat lamp. The residue was dissolved in 2M HNO_3 (3 × 150 μL) and loaded on to a column (0.6 cm × 10 cm) of RE-SPEC resin (with a bed volume of 1 mL). The column was eluted with 2M HNO_3, and ^{86}Y was routinely obtained within the 2.5–5.5 mL fraction. The eluted ^{86}Y solution was then heated to dryness on a hot plate and under a heating lamp, and then dissolved in 0.1M HNO_3 (3 × 150 μL) for use in radiolabelling. Routinely, 18–20 mCi of ^{86}Y were recovered from such an irradiation cycle for use in the procedures to be described in the following paragraphs.

For the electrodeposition process, ^{86}Y was separated with a high collection yield by using two platinum plates and one platinum wire. The use of NH_4NO_3 as the electrolyte during the first electrolysis stabilized the pH of the electrocell. The ^{86}Y activity was adsorbed on the platinum wire and collected with a high yield using a mixture of 2.8M HNO_3 and EtOH. Target materials were recovered as $SrCO_3$ and converted to SrO by thermal decomposition.

Yttrium-86 can be separated from irradiated enriched ^{86}Sr target material using a modification of Machulla's methods that has been previously reported [2.45.9]. For [^{86}Sr]SrO, the entire platinum disc (including the target material) is transferred to a 20 mL beaker, and 3 mL of 2.8M HNO_3 is added slowly. The clear target solution is then diluted with 10 mL of Milli-Q water (Millipore, Billerica, Massachusetts) and decanted into the first electrocell. The beaker (and platinum disc if applicable) is rinsed twice with water (8 mL each). While stirring, the pH of the clear solution is adjusted to pH2.5–3 by adding dropwise 3% ammonium hydroxide, confirmed by pH paper. The Teflon cap in which the two platinum plates are embedded is inserted into the electrocell, and the argon gas is connected and bubbled through the solution for 10–15 min prior to electrolysis. The first electrolysis is performed galvanostatically at 2000 mA for 40 min with no stirring. Argon gas is bubbled through the solution during the electrolysis. After the first electrodeposition has been completed, the Teflon cap and electrodes are removed from the cell and moved to the second glass vial that is filled with freshly prepared 3mM nitric acid (36 mL). The power is turned off, and argon gas is bubbled through again for 10–15 min. The third electrode (platinum wire) is then inserted into the Teflon cap. The cathode is

connected to the platinum wire, and the previous cathode (the platinum plate) is connected to the anode. Electrolysis is performed for 20 min with a constant current of 230 mA, while argon gas is constantly bubbled through the solution. Upon completion, the platinum wire is removed from the second electrocell and is washed with a small amount of acetone (<100 μL) with the voltage on. After the voltage has been turned off, the ^{86}Y is collected by washing the electrode with 2 mL of a 1:3 ethanol–nitric acid mixture. The collected solution is evaporated to dryness at 130°C under a gentle stream of argon gas. The final ^{86}Y is reconstituted with 100 μL of 0.1M HCl [2.45.7].

Recovery of enriched materials

The Sr(II) selective resin column used to separate the ^{86}Y was washed with 0.05M HNO_3 to elute ^{86}Sr in the form of $^{86}Sr(NO_3)_2$. For each 3 g of resin, 20 mL of 0.05M HNO_3 were used as eluent. In the first 5 mL of eluent no ^{86}Sr was present and it was discarded. The remainder of the eluent was heated to dryness to recover the ^{86}Sr. The enriched Sr(II) was recovered for irradiation to produce additional ^{86}Y [2.45.8].

Isotopically enriched target material $[^{86}Sr]SrCO_3$ can be recovered by methods previously reported in Refs [2.45.3] and [2.45.9] from the first electrolysis solution. The combined electrolysis solutions are neutralized with 3% NH_4OH solution and then treated with saturated ammonium carbonate solution to precipitate strontium carbonate. The precipitated white solid is collected, rinsed with dilute ammonium carbonate solution and water, and dried at 130°C. The $[^{86}Sr]SrCO_3$ collected is converted to $[^{86}Sr]SrO$ by thermal decomposition [2.45.7].

Specifications for purity of ^{86}Y

The purity of the ^{86}Y obtained by this method is routinely determined by gamma spectroscopy using a Ge(Li) detector. The nuclides present are reported as relative activity to ^{86}Y at EOB normalized to the ^{86}Y activity, and are as follows: 100% ^{86}Y, 1.09% ^{87m}Y, 0.34% ^{87}Y, 0.02% ^{88}Y, 90.25% ^{86m}Y and 28.9% ^{87m}Sr. Strontium-85 and ^{83}Rb are found to be less than 0.01% at EOB, and no other isotopes have been identified [2.45.8]. The SA of ^{86}Y separated by electrolysis was determined by titration of $^{86}Y(OAc)_3$ with DOTA or DTPA in order to check its chemical purity. Even although yttrium ions form metal complexes with DTPA more easily than with DOTA, both ligands gave similar values for the SA. The effective SA of ^{86}Y was calculated to be 29 ± 19 mCi/μg (1.07 ± 0.70 GBq/μg). When the same methods were employed for commercially available ^{90}Y (MDS Nordion, Ottawa), the SA of ^{90}Y was 16 mCi/μg

(0.59 GBq/μg). These assays indicate that the chemical purity of ^{86}Y is comparable with, or slightly higher than, that of ^{90}Y. To place this into context with other values in the literature, reactions with a 1×10^4 molecular excess of DOTA resulted in quantitative labelling [2.45.9]. The same group reported similar specific activities of the ^{86}Y produced to that obtained for ^{90}Y purchased from Pacific Northwest National Laboratory, Richland, Washington [2.45.9].

REFERENCES TO SECTION 2.45

[2.45.1] HERZOG, H., et al., Measurement of pharmacokinetics of yttrium-86 radiopharmaceuticals with PET and radiation dose calculation of analogous yttrium-90 radiotherapeutics, J. Nucl. Med. **34** (1993) 2222–2226.

[2.45.2] PAGANI, M., STONE-ELANDER, S., LARSSON, S.A., Alternative positron emission tomography with non-conventional positron emitters: Effects of their physical properties on image quality and potential clinical applications, Eur. J. Nucl. Med. **24** (1997) 1301–1327.

[2.45.3] RÖSCH, F., QAIM, S.M., STÖCKLIN, G., Nuclear data relevant to the production of the positron emitting radioisotope ^{86}Y via the ^{86}Sr(p, n)- and the ^{nat}Rb(^{3}He, 2n)-processes, Radiochim. Acta **61** (1993) 1–8.

[2.45.4] RÖSCH, F., QAIM, S.M., STÖCKLIN, G., Production of the positron emitting radionuclide ^{86}Y for nuclear medical applications, Int. J. Appl. Radiat. Isot. **44** (1993) 677–681.

[2.45.5] SACHDEV, D.R., PORILE, N.T., YAFFE, L., Reactions of Sr-88 with protons of energies 7–85 MeV, Can. J. Chem. **45** (1967) 1149.

[2.45.6] TÁRKÁNYI, F., et al., Excitation functions for production of radioisotopes of niobium, zirconium and yttrium by irradiation of zirconium with deuterons, Nucl. Instrum. Methods Phys. Res. B **217** (2004) 373–388.

[2.45.7] YOO, J., et al., Preparation of high specific activity ^{86}Y using a small biomedical cyclotron, Nucl. Med. Biol. **32** (2005) 891–897.

[2.45.8] GARMESTANIA, K., MILENICA, D.E., PLASCJAK, P.S., BRECHBIELA, M.W., A new and convenient method for purification of ^{86}Y using a Sr(II) selective resin and comparison of biodistribution of ^{86}Y and ^{111}In labeled HerceptinTM, Nucl. Med. Biol. **29** (2002) 599–606.

[2.45.9] REISCHL, G., RÖSCH, F., MACHULLA, H.J., Electrochemical separation and purification of yttrium-86, Radiochim. Acta **90** (2002) 225–228.

BIBLIOGRAPHY TO SECTION 2.45

FINN, R.D., et al., "Low energy cyclotron production and separation of yttrium-86 for evaluation of monoclonal antibody pharmacokinetics and dosimetry", Application of Accelerators in Research and Industry (DUGGAN, J.L., MORGAN, I.L., Eds), American Institute of Physics, Woodbury, New York (1999) 991–993.

INTERNATIONAL ATOMIC ENERGY AGENCY, Charged Particle Cross-section Database for Medical Radioisotope Production: Diagnostic Radioisotopes and Monitor Reactions, IAEA-TECDOC-1211, IAEA, Vienna (2001).

MICHEL, R., et al., Cross sections for the production of residual nuclides by low- and medium-energy protons from the target elements C, N, O, Mg, Al, Si, Ca, Ti, V, Mn, Fe, Co, Ni, Cu, Sr, Y, Zr, Nb, Ba and Au, Nucl. Instrum. Methods Phys. Res. B **129** (1997) 153–193.

2.46. YTTRIUM-88

Half-life: 106 d.

Positron emission products of ^{88}Y

Fraction	Maximum energy (MeV)	Average energy (MeV)
0.002170	0.754760	0.355200

Electron emission products of ^{88}Y

Fraction	Energy (MeV)
0.268990	0.012100
1.045100	0.001790

Photon emission products of ^{88}Y

Fraction	Energy (MeV)
0.000955	1.188300
0.004340	0.511000
0.005963	2.734000
0.016994	0.001810
0.090460	0.015800
0.174400	0.014098
0.336680	0.014165
0.934170	0.898020
0.993800	1.836000

Excitation function

The excitation function for ^{88}Sr(p, n)^{88}Y is shown in Fig. 2.46.1.

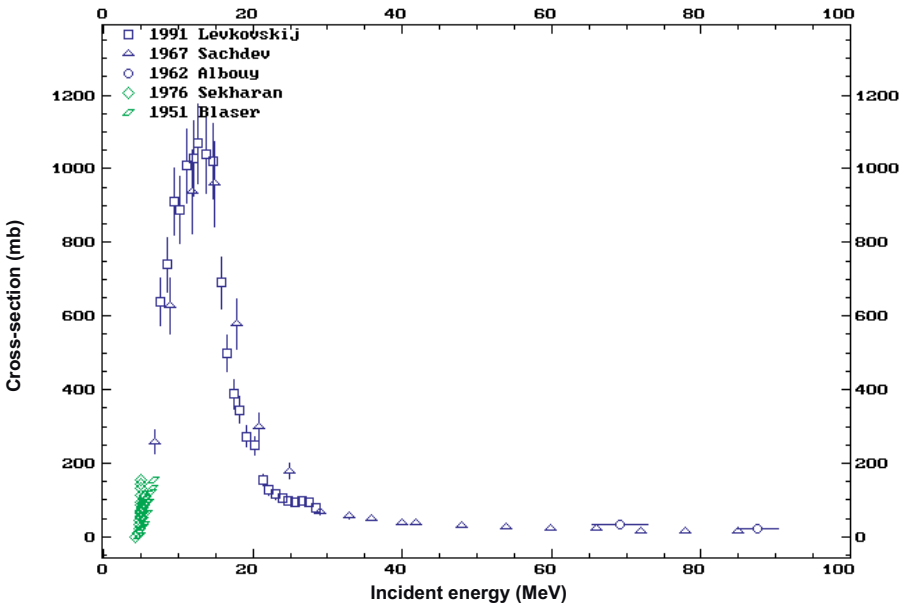

FIG. 2.46.1. Excitation function for the ^{88}Sr(p, n)^{88}Y reaction.

BIBLIOGRAPHY TO SECTION 2.46

ALBOUY, G., GUSAKOW, M., POFFE, N., SERGOLLE, H., VALENTIN, L., (p, n)-Reactions at medium energy, J. Physique **23** (1962) 1000.

BLASER, J.P., BOEHM, F., MARMIER, P., SCHERRER, P., Anregungsfunktionen und Wirkungsquerschnitte der (p, n)-Reaktion (II), Helv. Phys. Acta **24** (1951) 441.

LEVKOVSKIJ, V.N., Activation Cross Sections for the Nuclides of Medium Mass Region (A = 40–100) with Medium Energy (E = 10–50 MeV) Protons and Alpha-particles: Experiment and Systematics, Inter-Vesi, Moscow (1991).

SACHDEV, D.R., PORILE, N.T., YAFFE, L., Reactions of Sr-88 with protons of energies 7–85 MeV, Can. J. Chem. **45** (1967) 1149.

SEKHARAN, K.K., LAUMER, H., KERN, B.D., GABBARD, F., A neutron detector for measurement of total neutron production cross sections, Nucl. Instrum. Methods Phys. Res. **133** (1976) 253–257.

2.47. ZINC-62

Half-life

Zinc-62 has a 9.22 h half-life, and 7% of the decay is by a low energy positron (0.66 MeV end point energy) and 93% by electron capture with several gamma rays in the 500 keV range. Zinc-62 can be used by itself or it can be incorporated into several biomolecules.

Positron emission products of ^{62}Zn

Fraction	Maximum energy (MeV)	Average energy (MeV)
0.076000	0.605000	0.258600

Electron emission products of ^{62}Zn

Fraction	Energy (MeV)
0.005525	0.040720
0.016736	0.039743
0.156850	0.031861
0.542960	0.007030
1.421500	0.000920

Photon emission products

Gamma rays with less than 1% abundance are not shown in the following table.

Fraction	Energy (MeV)
0.014300	0.260500
0.020075	0.247040
0.023650	0.394060
0.026675	0.243440
0.051781	0.008910
0.129380	0.008028
0.152000	0.511000
0.156750	0.507600
0.162250	0.548410
0.254180	0.008048
0.269500	0.040840
0.275000	0.596650

Nuclear reactions

Zinc-62 is produced mainly by the proton reaction on natural copper, ^{nat}Cu(p, x)^{62}Zn.

Excitation function

The excitation function for ^{nat}Cu(p, x)^{62}Zn is shown in Fig. 2.47.1.

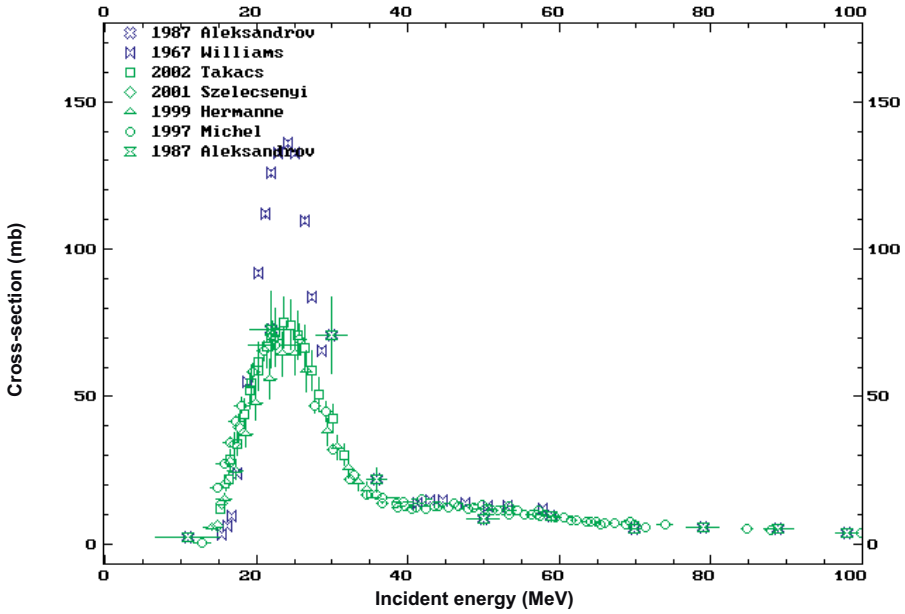

FIG. 2.47.1. Excitation function for the $^{nat}Cu(p, x)^{62}Zn$ reaction.

BIBILIOGRAPHY TO SECTION 2.47

FUJIBAYASHI, Y., MATSUMOTO, K., YONEKURA, Y., KONISHI, J., YOKOHAMA, A., A new zinc-62/copper-62 generator as a copper-62 source for PET radiopharmaceuticals, J. Nucl. Med. **30** (1989) 1838–1842.

MATHIAS, C.J., MARGENAU, W.H., BRODACK, J.W., WELCH, M.J., GREEN, M.A., A remote system for the synthesis of copper-62 labeled Cu(PTSM), Int. J. Radiat. Appl. Instrum. A **42** (1991) 317–320.

RAMAMOORTHY, N., PAO, P.J., WATSON, I.A., Preparation of a ^{62}Zn–^{62}Cu generator and of ^{61}Cu following alpha particle irradiation of a nickel target, Radiochem. Radioanal. Lett. **46** (1989) 371–380.

ROBINSON, G.D., ZIELINSKI, F.W., LEE, A.W., The zinc-62/copper-62 generator: A convenient source of copper-62 for radiopharmaceuticals, Int. J. Appl. Radiat. Isot. **31** (1980) 111–116.

TAKÁCS, S., TÁRKÁNYI, F., SONCK, M., HERMANNE, A., New cross-sections and intercomparison of proton monitor reactions on Ti, Ni and Cu, Nucl. Instrum. Methods Phys. Res. B **174** (2001) 47–64.

SZELECSÉNYI, F., et al., Excitation function for the ^{nat}Ti(p, x)^{48}V nuclear process: Evaluation and new measurements for practical applications, Nucl. Instrum. Meth. Phys. Res. B **188** (2002) 106–111.

YAGI, M., KONDO, K.A., A ^{62}Cu generator, Int. J. Appl. Radiat. Isot. **30** (1979) 569–570.

2.48. ZINC-63

Half-life

Zinc-63 has a 38 min half-life and decays 93% by positron emission and 7% by electron capture.

Parent nucleus	Parent energy level	Parent half-life (min)	Decay mode	Daughter nucleus
Zn-63	0.0	38.47	EC	Cu-63

Positron emission products of ^{63}Zn

Fraction	Energy (keV)	End point energy (keV)
3.2E–6	115.4	263.4
0.000025	123.5	282.7
3.9E–6	144.7	333.8
0.0004	341.4	797.9
0.005	400.1	932.9
0.049	599.9	1382.8
0.07	732.5	1675.3
0.803	1042.3	2344.9

Note: Mean β^+ energy: 992 keV; total β^+ intensity: 92.7%.

Electron emission products of ^{63}Zn

Fraction	Energy (keV)
0.0927	0.92
0.0348	7.03

Photon emission products

Gamma rays with less than 1% abundance are not shown in the following table.

Fraction	Energy (keV)
0.0166	8.048
1.855	511
0.082	669.62
0.065	962.06

Nuclear reactions

The primary reaction for production of ^{63}Zn is through the ^{63}Cu(p, n)^{63}Zn reaction on natural copper. The targetry consists of a simple copper foil or an electroplated copper layer on a backing plate of nickel or other inert material.

Excitation functions

The excitation functions for ^{63}Cu(p, n)^{63}Zn and ^{nat}Cu(p, x)^{63}Zn are shown in Figs 2.48.1 and 2.48.2, respectively.

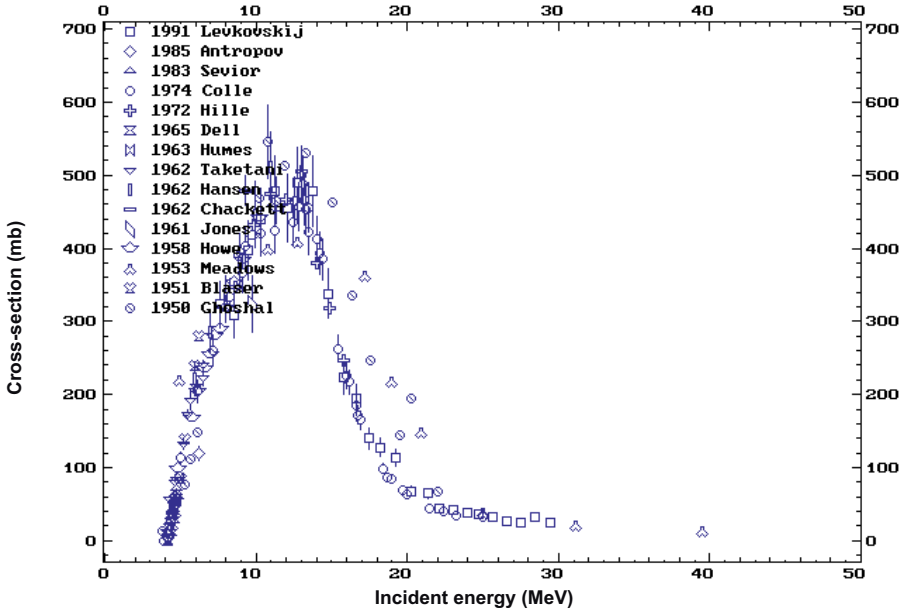

FIG. 2.48.1. Excitation function for the $^{63}Cu(p, n)^{63}Zn$ reaction.

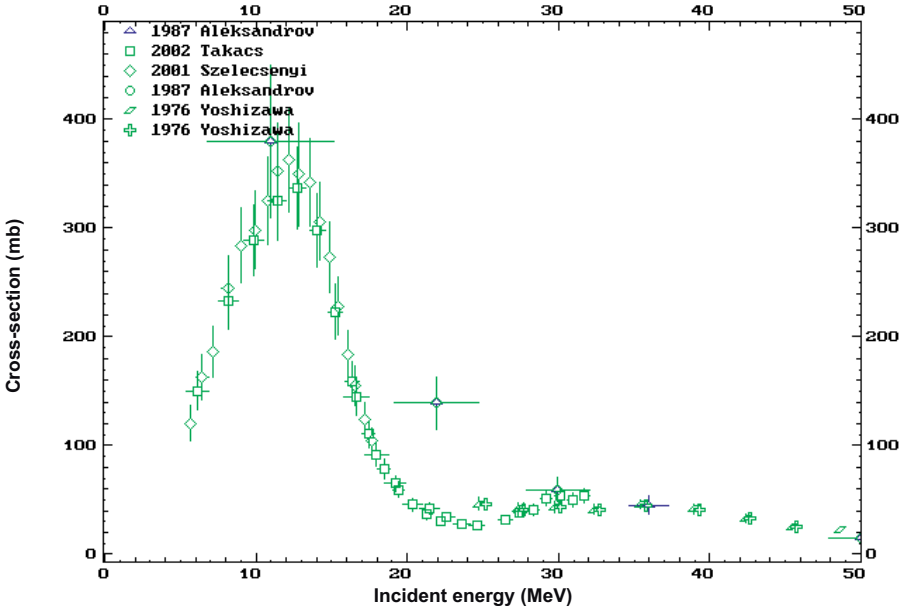

FIG. 2.48.2. Excitation function for the $^{nat}Cu(p, x)^{63}Zn$ reaction.

BIBLIOGRAPHY TO SECTION 2.48

ALEKSANDROV, V.N., SEMYONOVA, M.P., SEMYONOV, V.G., Excitation functions for radionuclides produced by (p, x)-reactions of copper and nickel, Atomnaya Energ. **62** (1987) 411–413.

COLLÉ, R., KISHORE, R., CUMMING, J.B., Excitation functions for (p, n) reactions to 25 MeV on ^{63}Cu, ^{65}Cu, and ^{107}Ag, Phys. Rev. C **9** (1974) 1819–1830.

GRUTTER, A., Excitation functions for radioactive isotopes produced by proton bombardment of Cu and Al in the energy range of 16 to 70 MeV, Nucl. Phys. A **383** (1982) 98–108.

HILLE, M., HILLE, P., UHL, M., WEISZ, W., Excitation functions of (p, n) and (α, n) reactions on Ni, Cu and Zn, Nucl. Phys. A **198** (1972) 625–640.

SEVIOR, M.E., MITCHELL, L.W., ANDERSON, M.R., TINGWELL, C.W., SARGOOD, D.G., Absolute cross sections of proton induced reactions on Cu-65, Ni-64, Cu-63, Austral. J. Phys. **36** (1983) 463–471.

SZELECSÉNYI, F., et al., Excitation function for the ^{nat}Ti(p, x)^{48}V nuclear process: Evaluation and new measurements for practical applications, Nucl. Instrum. Methods Phys. Res. B **188** (2002) 106–111.

TAKÁCS, S., TÁRKÁNYI, F., SONCK, M., HERMANNE, A., New cross-sections and intercomparison of proton monitor reactions on Ti, Ni and Cu, Nucl. Instrum. Methods Phys. Res. B **188** (2002) 106–111.

WING, J., HUIZENG, J.R., (p, n) Cross sections of V-51, Cr-52, Cu-63, Cu-65, Ag-107, Ag-109, Cd-111, Cd-114, and La-139 from 5 to 10.5 MeV, Phys. Rev. **128** (1962) 280.

2.49. ZIRCONIUM-89

Half-life

Zirconium-89 has a relatively long half-life (3.3 d) and decays 23% by positron emission and 77% by electron capture. The end point energy of the positron is 0.9 MeV.

Parent nucleus	Parent energy level	Parent half-life (h)	Decay mode	Daughter nucleus
Zr-89	0.0	78.41	EC: 100%	Y-89

Positron emission products of ^{89}Zr

Fraction	Energy (keV)	End point energy (keV)
0.2274	395.5	902

Electron emission products of ^{89}Zr

Fraction	Energy (keV)
0.786	1.91
0.192	12.7

Photon emission products of ^{89}Zr

Gamma rays with less than 1% abundance are not shown in the following table.

Fraction	Energy (keV)
0.0234	1.92
0.141	14.883
0.27	14.958
0.0205	16.726
0.0397	16.738
0.455	511
0.9904	909.15

Nuclear reactions for production of ^{89}Zr

There are only two nuclear reactions that have been explored for the production of ^{89}Zr. The first, and most commonly used, is the ^{89}Y(p, n)^{89}Zr reaction [2.49.1, 2.49.2]. Since yttrium has only one stable isotope and the product can be made relatively pure at low energy, this is an ideal reaction for production of ^{89}Zr. The other reaction that has been used is the ^{89}Y(d, 2n)^{89}Zr reaction [2.49.3].

Excitation functions

The excitation functions for $^{89}Y(p, n)^{89}Zr$ and $^{89}Y(d, 2n)^{89}Zr$ are shown in Figs 2.49.1 and 2.49.2, respectively.

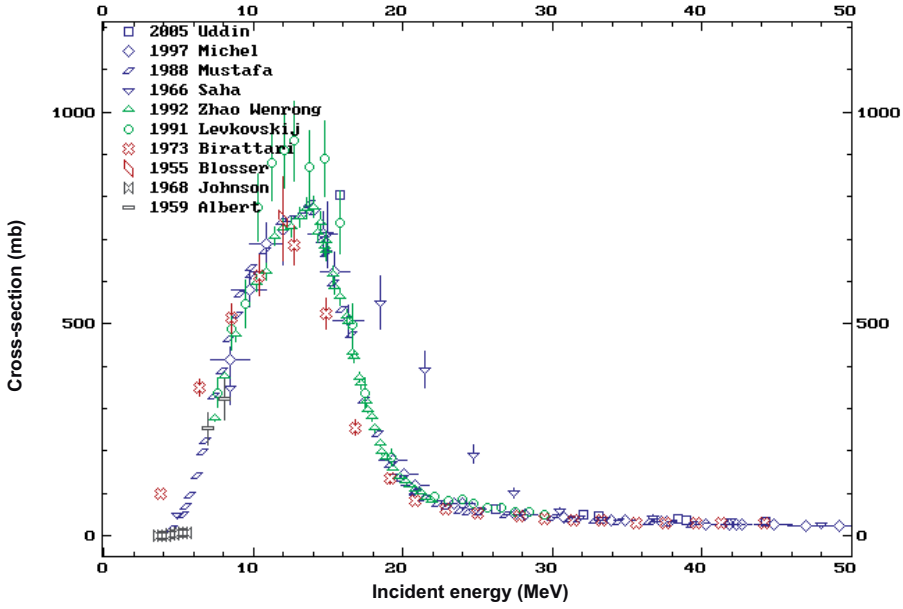

FIG. 2.49.1. Excitation function for the $^{89}Y(p, n)^{89}Zr$ reaction.

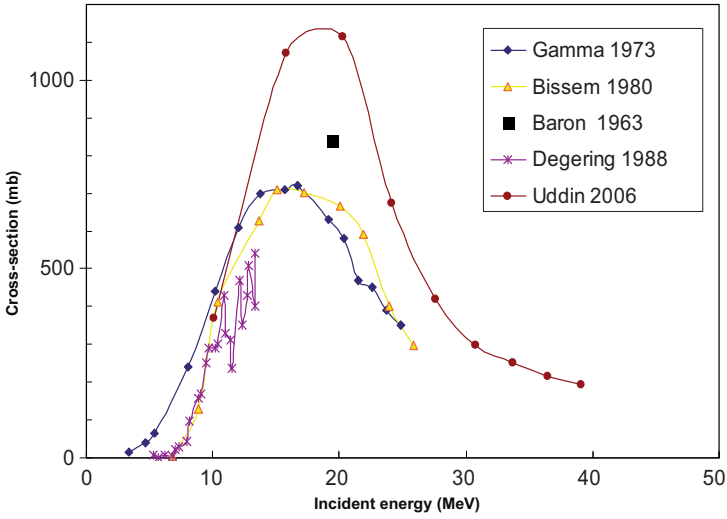

FIG. 2.49.2. Excitation function for the $^{89}Y(d, 2n)^{89}Zr$ reaction.

REFERENCES TO SECTION 2.49

[2.49.1] DE JESUS, O.T., NICKLES, R.J., Production of ^{89}Zr, a potential PET antibody label, Int. J. Radiat. Appl. Instrum. A **41** (1990) 789–790.
[2.49.2] SAHA, G., PORILE, N.T., YAFFLE, L., (p, xn) and (p, pxn) Reactions of yttrium-89 with 5–85 MeV protons, Phys. Rev. **144** (1966) 962–971.
[2.49.3] ZWEIT, J., SHARMA, H., DOWNEY, S., Production of no-carrier added zirconium-89 for positron emission tomography, Int. J. Radiat. Appl. Instrum. A **42** (1991) 199–201.

BIBLIOGRAPHY TO SECTION 2.49

BARON, N., COHEN B.L., Activation cross-section survey of deuteron-induced reactions, Phys. Rev. **129** (1963) 2636.

BISSEM, H.H., et al., Entrance and exit channel phenomena in d- and He-3-induced preequilibrium decay, Phys. Rev. C **22** (1980) 1468.

DEGERING, D., UNTERRICKER, S., STOLZ, W., Excitation function of the ^{89}Y(d, 2n)^{89}Zr reaction, J. Radioanal. Nucl. Chem. Lett. **127** (1988) 7–11.

GAMMA, A.M.L., NASSIFF, S.J., Excitation functions for deuteron-induced reactions on ^{89}Y, Radiochim. Acta **19** (1973) 161–162.

LINK, J.M., et al., ^{89}Zr for antibody labelling and positron emission tomography, J. Labelled Compd. Radiopharm. **23** (1986) 1297.

MEIJS, W.E., HERSCHEID, J.D., HAISMA, H.J., PINEDO, H.M., Evaluation of desferal as a bifunctional chelating agent for labeling antibodies with Zr-89, Int. J. Radiat. Appl. Instrum. A **43** (1992) 1443–1447.

MEIJS, W.E., HERSCHEID, J.D., HAISMA, H.J., VAN LEUFFEN, P.J., High yield production of pure ^{89}Zr: A positron emitter for labeling proteins, J. Labelled Compd. Radiopharm. **35** (1994) 264–266.

CONTRIBUTORS TO DRAFTING AND REVIEW

DRAFTING

Haji-Saeid, M.	International Atomic Energy Agency
Pillai, M.R.A.	International Atomic Energy Agency
Ruth, T.J.	Tri University Meson Facility (TRIUMF), Canada
Schlyer, D.J. (Chair)	Brookhaven National Laboratory, United States of America
Van den Winkel, P.	Cyclotron Laboratory, Vrieje Universiteit Brussel (VUB), Belgium
Vora, M.M.	King Faisal Specialist Hospital and Research Centre, Saudi Arabia

REVIEW

Capote Noy, R.	International Atomic Energy Agency
Carroll, L.	Carroll & Ramsey Associates, United States of America
Clark, J.C.	Wolfson Brain Imaging Center, United Kingdom
Čomor, J.	Vinča Institute of Nuclear Sciences, Serbia
Dehnel, M.	D-Pace, Canada
Ferrieri, R.	Brookhaven National Laboratory, United States of America
Finn, R.D.	Memorial Sloan-Kettering Cancer Center, United States of America
Fowler, J.S.	Brookhaven National Laboratory, United States of America
Schueller, M.J.	Brookhaven National Laboratory, United States of America

Tárkányi, F. Institute of Nuclear Research of the Hungarian Academy of Sciences (ATOMKI), Hungary

MANUAL FOR REACTOR PRODUCED RADIOISOTOPES
IAEA TECDOC Series No. 1340
IAEA-TECDOC-1340 (258 pp.; 2003)
ISBN 92–0–101103–2 Price: €15.00

STANDARDIZED HIGH CURRENT SOLID TARGETS FOR CYCLOTRON PRODUCTION OF DIAGNOSTIC AND THERAPEUTIC RADIONUCLIDES
Technical Reports Series No. 432
STI/DOC/010/432 (71 pp.; 2004)
ISBN 92–0–109304–7 Price: €40.00

CYCLOTRON PRODUCED RADIONUCLIDES: PRINCIPLES AND PRACTICE
Technical Reports Series No. 465
STI/DOC/010/465 (217 pp.; 2008)
ISBN 978–92–0–1002 Price: €45.00

DIRECTORY OF CYCLOTRONS USED FOR RADIONUCLIDE PRODUCTION IN MEMBER STATES
2006 UPDATE
Non-serial Publication
IAEA-DCRP/CD/2006 (538 pp.; 2006)
ISBN 92–0–111506–7 Price: €15.00

This publication contains radioisotope decay and production details of 49 isotopes that can be prepared using cyclotrons. The introductory chapter discusses the principles of radioisotope production using cyclotrons, while Chapter 2 contains data on nuclear decay characteristics such as half-life, mode of decay, energy and abundance, nuclear reactions and excitation functions of the selected isotopes. This publication will be of interest to scientists and engineers working in radioisotope production using cyclotrons.

INTERNATIONAL ATOMIC ENERGY AGENCY
VIENNA
ISBN 978–92–0–106908–5
ISSN 0074–1914